



**THE *EX VIVO* AND *IN VITRO*
TRANSCRIPTOMIC PROFILES OF
EQUINE ENDOMETRIUM USING AN
EXPLANT MODEL TO FURTHER
STUDY ENDOMETRITIS**

Maithê Rocha Monteiro de Barros
(DVM)

A thesis submitted in Full Candidature for the
Degree of Doctor of Philosophy

Institute of Biological, Environmental and Rural Sciences
Aberystwyth University

May 2019

ABSTRACT

Equine endometritis is one of the most common and important reproductive conditions causing infertility in mares. After mating there is a normal, transient inflammation in response to sperm, seminal plasma and bacteria in the uterus, termed mating-induced endometritis (MIE). Mares are classified as susceptible to persistent mating-induced endometritis (PMIE) when they fail to clear the uterus from MIE within 36-48 hours post mating. PMIE creates an adverse uterine environment, resulting in subfertility due to inflammation and disruption of the endocrine maintenance of pregnancy. An equine endometrial explant system was previously established to measure uterine inflammation via Prostaglandin $F_{2\alpha}$ as a biomarker. However, it was not determined if the transcriptome from explants was altered once in culture.

The aim of this study was to characterise the genetic profiles of equine endometritis *in vitro* to better understand the transition from MIE to PMIE. The objectives were 1) to determine if the transcriptome of cultured endometrial explants collected from native pony mares represent the transcriptome of the whole mare in the pre-breeding, non-inflammatory state and thus, determine how the transcriptome of explants is modulated once in culture; 2) compare the transcriptome profiles from unchallenged cultured explants from the follicular, luteal and anoestrous phases to characterise the global uterine transcriptomic changes throughout the oestrous cycle and anoestrous; 3) determine the RNA-Sequencing (RNA-Seq) changes in cultured explants after challenge with *E. coli* lipopolysaccharide (LPS) to better understand transcriptome modulation during inflammation; 4) compare the transcriptome profiles of mares resistant and susceptible to PMIE before breeding.

Endometrium was collected from mares sent to a commercial abattoir, during different stages of the oestrous cycle or anoestrous, and explants established as appropriate to address each objective. RNA-Seq was performed for all experiments and differentially expressed genes (DEGs) were investigated in terms of significantly enriched biological pathways. *In vitro* explants cultured for 24 hours demonstrated significant transcriptomic changes compared to the *ex vivo* 0 hours biopsies, but thereafter remained similar up to 48 hours in culture. DEGs related to inflammation differing between 0 and 24 hours were set as the baseline changes between the *ex vivo* biopsies and the *in vitro* explants. The gene expression of innate immunity genes was greatest during the follicular phase of the oestrous cycle, followed by the anoestrous period and lower during the luteal phase in accordance with the endocrine milieu. Cultured explants did not exhibit large scale gene expression changes in response to LPS challenge and it was not in agreement with other studies. In addition, the transcriptome of resistant and susceptible mares showed different expression profiles of immune genes even before breeding.

The thesis investigated the use of an explant tissue culture system as a future model for studies of equine endometritis at the level of the transcriptome. Innate immune-associated genes exhibited increased expression during the follicular phase compared to the luteal phase of the oestrous cycle and anoestrous period. Furthermore, four genes were suggested to have the potential of distinguishing mares likely to be resistant or susceptible to PMIE, which may be identified in practice at pre-breeding examination.

DECLARATION

This work has not previously been accepted in substance for any degree and is not being concurrently submitted in candidature for any degree.

Candidate name:

Signature: _____

Date: __ / __ / ____

STATEMENT 1

This thesis is the result of my own investigations, except where otherwise stated. Where correction services have been used, the extent and nature of the correction is clearly marked in a footnote(s). Other sources are acknowledged by footnotes giving explicit references. A bibliography is appended.

Signature: _____

Date: __ / __ / ____

STATEMENT 2

I hereby give consent for my thesis, if accepted, to be available for photocopying and for inter-library loan, and for the title and summary to be made available to outside organisations.

Signature: _____

Date: __ / __ / ____

Word Count of Thesis: 70928

ACKNOWLEDGMENTS

I am profoundly grateful to my enthusiastic supervisors, Debbie Nash and Mina Davies-Morel. My research would have been impossible without their aid and support. My PhD has been an amazing experience and I thank Debbie and Mina wholeheartedly, not only for their tremendous academic support, but also for giving me so many opportunities. I am grateful for the positive learning environment they provided me with, for their guidance and support. Similar, profound gratitude goes to David Wilcockson for being so dedicated to his role as my supervisor when Debbie was away.

I am hugely appreciative to Gareth Owen, Mike Holland, Richard Huxley, Rory Geoghegan, Ruth Wonfor and Vasilis Lenis for sharing their laboratory expertise so willingly and for their support and patience in helping me out throughout the PhD. I am also appreciative to F. Drury and Sons for allowing sample collection and of Deborah White for her help and for kindly letting me use her office during sample collection. Special thanks go to Matt Hegarty for performing the RNA-Sequencing for this project, and to Chris Creevey for kindly sharing his knowledge about transcriptomic and gene expression analysis with me. Special thanks to Rosa Soto, for her endless support and kindness. Thanks to Julia Kydd from Nottingham University for lending us the biopsy instrument to collect samples, as well as for her enthusiasm and willingness to help me.

I am deeply grateful to the close friends I made during this journey, that have been there for me during the good and the bad times. To Alessandra Crusco, Ana Carrelhas, Annika Steibel, Caio Dutra, Emma Davies, Daniel Alati, Denisa Asandei, Desiree Poets, Diana Valverde, Gabriela Bittencourt, Gilda Padalino, Holly Craven,

Jorge Martinez, Lina Avila, Luís Silva, Luke Dearden, Marcello De Souza, Mariya Marinova, Rafael Baptista, Rachel Paes, Simão Gustavo de Abreu, Sumana Bhowmick and Thomer Durman. Many thanks for being my family here in Wales. I am thankful to you for being true friends, for helping me stay strong and focused, for supporting me and keeping me sane throughout this journey. You have been by my side through the hard times and the good and I will always cherish the moments we shared together.

To my best friends over in Brazil, Luisa Passos and Pedro Trebilcock, for the psychological support and for making themselves present in my life regardless the distance. To Javier Barrios, for all the support he has given me throughout my life, but especially for supporting my decision to come to Aberystwyth and for always being there for me when I needed.

Finally, but by no means least, my heartfelt thanks to my parents, Marta Cristina Rocha Aguiar Monteiro de Barros and Evandro Castro Monteiro de Barros, for being the best parents someone could have asked for. Thanks for making yourselves present in my life during these four long years and thanks for all the support you have given me. Thanks for believing in me even when I was about to lose faith. Also, my most sincere thanks go to my beloved brother, Matheus Rocha Monteiro de Barros. If it was not for you I would not have continued down this very lonely road that is a PhD study. Thank you for continuously reminding me to enjoy life and to take it easy, and thanks for always helping me out when I most needed you. Also, thanks to my niece and god-daughter Giovanna. Being away from you during these four years was one of the hardest parts of this PhD. You are not aware of it, but you have been a great source of strength to help keep me going.

This thesis is dedicated to my mum, dad and brother, the most important people in my world. I love you three so much. I am and will always be grateful to you and grateful for having you in my life.

CONTENTS

Abstract	ii
Declaration	iii
Acknowledgments	iv
Contents	vii
List of Figures	xii
List of Tables	xv
List of Appendices	xviii
List of Abbreviations	xx
Abstracts Presented at Conferences	xxii
CHAPTER 1 Introduction	23
CHAPTER 2 Literature Review	28
2.1 Introduction	29
2.2 Female Reproductive System	30
2.2.1 Reproductive Anatomy	30
2.2.2 Reproductive Cycle of the Mare	35
2.3 Mare Infertility	38
2.4 Endometritis	39
2.5 Persistent Mating-induced Endometritis	43
2.5.1 Physical Clearance	44
2.5.2 Immune System	47
2.5.2.1 Innate Immunity	47
2.5.2.2 Adaptive Immunity	54
2.5.3 Markers of Uterine Inflammation	57
2.6 Equine Tissue Culture Model	58

2.7 RNA-Sequencing	60
2.8 Aims and Objectives	64
CHAPTER 3 General Material and Methods	66
3.1 Animals	67
3.2 Blood Sampling and Tissue Collection	67
3.3 Endometrial Cytology	69
3.4 RNA-Sequencing Biopsy	71
3.5 Histology	71
3.6 Endometrial Explant Culture	74
3.7 Prostaglandin F _{2α} Radioimmunoassay	78
3.8 RNA Extraction and RNA-Sequencing	80
3.9 Data Processing and Gene Expression Analysis	83
CHAPTER 4 Characterization of Cultured Equine Endometrial Transcriptome at Different Time Points to Study Explant Tissue Culture	87
4.1 Introduction	88
4.2 Material and Methods	90
4.2.1 Animals	90
4.2.2 Sample Collection	90
4.2.3 Endometrial Tissue Culture	93
4.2.4 RNA Extraction and RNA-Sequencing	93
4.2.5 Data Processing and Gene Expression Analysis	94
4.2.6 Statistical Analysis	96
4.3 Results	97
4.3.1 Cuffdiff	97
4.3.2 DESeq2	100

4.4 Discussion	112
4.4.1 Cuffdiff	113
4.4.2 DESeq2	114
4.5 Conclusion	117
 CHAPTER 5 A Comparison of the <i>Ex vivo</i> and <i>In vitro</i> Equine Endometrial Transcriptomic Profiles at the Follicular, Luteal and Anoestrous Phases	119
5.1 Introduction	120
5.2 Material and Methods	122
5.2.1 Animals	122
5.2.2 Sample Collection	123
5.2.3 Endometrial Tissue Culture	124
5.2.4 RNA Extraction and RNA-Sequencing	129
5.2.5 Data Processing and Gene Expression Analysis	130
5.2.6 Statistical Analysis	132
5.3 Results	133
5.3.1 Follicular vs Luteal	135
5.3.2 Follicular vs Anoestrous	139
5.3.3 Luteal vs Anoestrous	142
5.4 Discussion	146
5.4.1 Follicular vs Luteal	147
5.4.2 Follicular vs Anoestrous	151
5.4.3 Luteal vs Anoestrous	153
5.5 Conclusion	156

CHAPTER 6 Effects of LPS on the Equine Endometrium Transcriptome at the Follicular Phase of the Oestrous Cycle	159
6.1 Introduction	160
6.2 Material and Methods	163
6.2.1 Animals	163
6.2.2 Sample Collection	163
6.2.3 Endometrial Tissue Culture	166
6.2.4 Prostaglandin F _{2α} Radioimmunoassays	169
6.2.5 Endometrial Expression of IL-10	170
6.2.6 RNA Extraction and RNA-Sequencing	171
6.2.7 Data Processing and Gene Expression Analysis	172
6.2.8 Statistical Analysis	174
6.3 Results	176
6.3.1 Prostaglandin F _{2α} Secretion by Challenged Explants	176
6.3.2 Endometrial Expression of IL-10 After LPS Inoculation	176
6.3.3 Gene Expression	177
6.4 Discussion	183
6.4.1 Prostaglandin F _{2α} Secretion by Challenged Explants	183
6.4.2 Endometrial Expression of IL-10 After LPS Inoculation	184
6.4.3 Gene Expression	185
6.5 Conclusion	191
 CHAPTER 7 Characterization of Transcriptomic Profiles of Mares Resistant and Susceptible to PMIE <i>In vivo</i> and <i>Ex vivo</i>	 194
7.1 Introduction	195
7.2 Material and Methods	196

7.2.1 Animals	196
7.2.2 Sample Collection	197
7.2.3 RNA Extraction and RNA-Sequencing	201
7.2.4 Data Processing and Gene Expression Analysis	201
7.2.5 Statistical Analysis	202
7.3 Results	203
7.4 Discussion	206
7.5 Conclusion	209
 CHAPTER 8 General Discussion	 212
 CHAPTER 9 References	 229
 Appendices	 245

LIST OF FIGURES

CHAPTER 1 | Introduction

Figure 1.1 Pathophysiology of Mating-induced endometritis (MIE) and Persistent mating-induced endometritis (PMIE).	25
--	----

CHAPTER 2 | Literature Review

Figure 2.1 Dorsal view of the mare's reproductive tract.	31
Figure 2.2 Equine uterine wall diagram.	34

CHAPTER 3 | General Material and Methods

Figure 3.1 Endometrial cytological smear.	71
Figure 3.2 Preparation of equine endometrial explants for the tissue culture.	76
Figure 3.3 Preparation of each well for tissue culture.	77
Figure 3.4 Agarose gel electrophoresis (1% agarose) of RNA extracted samples.	81
Figure 3.5 Shrinkage estimation of dispersion.	85

CHAPTER 4 | Characterization of Cultured Equine Endometrial Transcriptome at Different Time Points to Study Explant Tissue Culture

Figure 4.1 Cuffdiff sample-to-sample distances.	98
Figure 4.2 DESeq2 sample-to-sample distances.	101
Figure 4.3 PCA plot of the gene expression profiles for the eight horses.	102
Figure 4.4 PCA plot of the gene expression profiles for the seven mares included in the analysis.	102
Figure 4.5 DEGs in the KEGG Complement and coagulation cascade between 0 hours (control) and 24 hours.	105

Figure 4.6 | DEGs in the KEGG Cytokine-cytokine receptor interaction between 0 hours (control) and 24 hours. 106

Figure 4.7 | STRING predicted PPI network of the DEGs related to immune response and inflammation GO terms between the 0 hours (control) and 24 hours. 109

Figure 4.8 | STRING predicted PPI network of the DEGs related GO terms and KEGG pathways related to immune response and inflammation between 0 hours (control) and 24 hours. 110

CHAPTER 5 | A Comparison of the *Ex vivo* and *In vitro* Equine Endometrial Transcriptomic Profiles at the Follicular, Luteal and Anoestrous Phases

Figure 5.1 | PCA plot of the gene expression profiles for the eighteen mares. 134

Figure 5.2 | PCA plot of the gene expression profiles for the seventeen mares included in the analysis. 135

Figure 5.3 | STRING predicted PPI network of the DEGs related to immune response and inflammation between the follicular and luteal phases at 24 hours. 138

Figure 5.4 | STRING predicted PPI network of the DEGs related to immune response and inflammation between the follicular phase and the anoestrous period at 24 hours. 141

Figure 5.5 | STRING predicted PPI network of the DEGs related to immune response and inflammation between the luteal phase and the anoestrous period at 24 hours. 144

CHAPTER 6 | Effects of LPS on the Equine Endometrium Transcriptome at the Follicular Phase of the Oestrous Cycle

Figure 6.1 | Tissue culture design for each mare. 167

Figure 6.2 | Time scale demonstrating the medium collection for the IL-10 investigation. 169

Figure 6.3 | Secretion of PGF_{2α} (Mean ± SEM) from equine endometrial explants challenged with LPS. 176

Figure 6.4 | Interleukin-10 concentration (Mean ± SEM) of explants cultured in control media, challenged with LPS and pre-treated with *M. ilicifolia*. 177

Figure 6.5 | PCA plot of the RNA-Seq data. 178

Figure 6.6 | STRING predicted PPI network of the DEGs between 24 and 48 181
hours post LPS challenge in the tissue culture media

Figure 6.7 | DEGs in the KEGG Cell cycle pathway between 24 and 48 hours 182
after LPS challenge in the tissue culture media.

CHAPTER 7 | Characterization of Transcriptomic Profiles of Mares Resistant and Susceptible to PMIE *In vivo* and *Ex vivo*

Figure 7.1 | PCA plot of the gene expression profiles for the six mares analysed. 203

LIST OF TABLES

CHAPTER 3 | General Material and Methods

Table 3.1 Characterization of the phase of the oestrous cycle.	69
Table 3.2 Kenney classification of the endometrium.	73

CHAPTER 4 | Characterization of Cultured Equine Endometrial Transcriptome at Different Time Points to Study Explant Tissue Culture

Table 4.1 Summary of mares sampled at the abattoir.	92
Table 4.2 Summary of the 32 RNA-Sequencing samples.	95
Table 4.3 Summary of the 5 most enriched GO terms between 0 hours (control) and 72 hours sorted.	99
Table 4.4 First most enriched cluster between 0 hours (control) and 72 hours.	100
Table 4.5 Second most enriched cluster between 0 hours (control) and 72 hours.	100
Table 4.6 Summary of the 5 most enriched KEGG pathways when comparing the transcriptome at 0 hours relative to the transcriptome at 24 hours.	104
Table 4.7 Summary of the 5 most enriched GO terms when comparing the transcriptome at 0 hours relative to the transcriptome at 24 hours.	107
Table 4.8 Summary of the 4 enriched GO terms related to inflammation when comparing the transcriptome at 0 hours relative to the transcriptome at 24 hours.	108
Table 4.9 Summary of the 2 enriched KEGG pathways when comparing the transcriptome at 24 hours relative to the transcriptome at 48 hours.	111

CHAPTER 5 | A Comparison of the *Ex vivo* and *In vitro* Equine Endometrial Transcriptomic Profiles at the Follicular, Luteal and Anoestrous Phases

Table 5.1 Summary of mares sampled at the abattoir at the follicular phase of the oestrus cycle.	126
Table 5.2 Summary of mares sampled at the abattoir at the luteal phase of the oestrus cycle.	127

Table 5.3 Summary of mares sampled at the abattoir during the anoestrous period.	128
Table 5.4 Summary of the 54 RNA-sequencing samples.	131
Table 5.5 Summary of the 7 enriched KEGG pathways when comparing the follicular transcriptome relative to the luteal transcriptome at 24 hours.	136
Table 5.6 Summary of the 10 most enriched GO terms when comparing the follicular transcriptome relative to the luteal transcriptome at 24 hours.	137
Table 5.7 Summary of the 6 enriched KEGG pathways when comparing the follicular transcriptome relative to the anoestrous transcriptome at 24 hours.	140
Table 5.8 Summary of the 10 most enriched GO terms when comparing the follicular transcriptome relative to the anoestrous transcriptome at 24 hours.	140
Table 5.9 Summary of the 7 enriched KEGG pathways when comparing the follicular transcriptome relative to the anoestrous transcriptome at 48 hours.	142
Table 5.10 Summary of the 5 enriched GO terms when comparing the follicular transcriptome relative to the anoestrous transcriptome at 48 hours.	142
Table 5.11 Summary of the 2 enriched KEGG pathways when comparing the luteal transcriptome relative to the anoestrous transcriptome at 24 hours.	143
Table 5.12 Summary of the 3 enriched GO terms when comparing the luteal transcriptome relative to the anoestrous transcriptome at 24 hours.	143
Table 5.13 Summary of the 2 enriched KEGG pathways when comparing the luteal transcriptome relative to the anoestrous transcriptome at 48 hours.	145
Table 5.14 Summary of the 10 most enriched GO terms when comparing the luteal transcriptome relative to the anoestrous transcriptome at 48 hours.	146

CHAPTER 6 | Effects of LPS on the Equine Endometrium Transcriptome at the Follicular Phase of the Oestrous Cycle

Table 6.1 Characteristics of uteri from mares sampled at the abattoir used to determine the follicular phase of the oestrous cycle.	165
Table 6.2 Summary of the 25 RNA-Sequencing samples.	174
Table 6.3 Summary of the differentially expressed genes between control and LPS challenged explants cultured for 24 hours sorted by p-value.	179
Table 6.4 Summary of the functional enrichments in the network retrieved by STRING between 24 and 48 hours after LPS challenge sorted by p-value.	180

CHAPTER 7 | Characterization of Transcriptomic Profiles of Mares Resistant and Susceptible to PMIE *In vivo* and *Ex vivo*

Table 7.1 Summary of resistant mares sampled at the abattoir.	199
Table 7.2 Clinical history of susceptible mares.	200
Table 7.3 Summary of the 6 RNA-sequencing samples.	202
Table 7.4 Summary of the 10 most enriched GO terms.	202
Table 7.5 Summary of the 6 enriched KEGG pathways.	205

LIST OF APPENDICES

CHAPTER 3 | General Material and Methods

Appendix 3.1 Progesterone ELISA	245
Appendix 3.2 Buffers and Reagents for Histology and Tissue Culture	246
Appendix 3.3 Prostaglandin F2 α Radioimmunoassay	247
Appendix 3.4 RNA Extraction	250
Appendix 3.5 Computer codes	252

CHAPTER 4 | Characterization of Cultured Equine Endometrial Transcriptome at Different Time Points to Study Explant Tissue Culture

Appendix 4.1 Kenney Classification of Mares Providing Endometrial Explants in Chapter 4	253
Appendix 4.2 Computer Code Used in Chapter 4	254
Appendix 4.3 List of all significantly enriched GO terms in Chapter 4 between 0 hours (control) and 72 hours – Cuffdiff results	258
Appendix 4.4 Clusters between 0 hours (control) and 72 hours	260
Appendix 4.5 List of all significantly enriched KEGG pathways and GO terms in Chapter 4 when comparing the 0 hours (control) relative to 24 hours associated with Log2FC ≥ 2 at an FDR of 0.05 sorted by p-value – DESeq2 results	264

CHAPTER 5 | A Comparison of the *Ex vivo* and *In vitro* Equine Endometrial Transcriptomic Profiles at the Follicular, Luteal and Anoestrous Phases

Appendix 5.1 Kenney Classification of Mares Providing Endometrial Explants in Chapter 5	267
Appendix 5.2 Computer Code Used in Chapter 5	269

Appendix 5.3 | List of all significantly enriched GO terms in Chapter 5 when comparing the follicular and luteal phase groups at 24 hours associated with $\text{Log}_2\text{FC} \geq 2$ at an FDR of 0.05 sorted by p-value 272

Appendix 5.4 | List of all significantly enriched GO terms in Chapter 5 when comparing the follicular and anoestrous phase groups at 24 hours associated with $\text{Log}_2\text{FC} \geq 2$ at an FDR of 0.05 sorted by p-value 273

Appendix 5.5 | List of all significantly enriched GO terms in Chapter 5 when comparing the luteal and anoestrous phase groups at 48 hours associated with $\text{Log}_2\text{FC} \geq 2$ at an FDR of 0.05 sorted by p-value 274

CHAPTER 6 | Effects of LPS on the Equine Endometrium Transcriptome at the Follicular Phase of the Oestrous Cycle

Appendix 6.1 | Kenney Classification of Mares Providing Endometrial Explants in Chapter 6 275

Appendix 6.2 | Computer Code Used in Chapter 6 276

CHAPTER 7 | Characterization of Transcriptomic Profiles of Mares Resistant and Susceptible to PMIE *Ex vivo* and *In vivo*

Appendix 7.1 | Kenney Classification of Mares Providing Biopsies in Chapter 7 278

Appendix 7.2 | Computer Code Used in Chapter 7 279

Appendix 7.3 | List of all significantly enriched GO terms in Chapter 7 when comparing the transcriptome of resistant mares relative to the transcriptome of susceptible mares at an FDR of 0.05 sorted by p-value 281

LIST OF ABBREVIATIONS

Abbreviations used throughout this body of work are given here in alphabetical order. Within each chapter the abbreviation is defined at its first appearance.

AI	Artificial insemination
APP	Acute phase protein
APR	Acute phase response
BAM	Binary format file
BH	Benjamini-Hochberg
bp	Base pairs
CCL	C-C motif chemokine ligand
cDNA	Complimentary DNA
CFU	Colony-forming unit
CL	Corpus luteum
CLR	C-type lectin receptor
CO₂	Carbon dioxide
CPM	Counts per minute
CSF	Colony-stimulating factor
CV	Coefficient of variation
CX3CL	C-X3-C motif chemokine ligand
CXCL	C-X-C motif chemokine ligand
CXCR	C-X-C chemokine receptor type
°C	Degrees Celsius
DAMP	Damage-associated molecular pattern
DARC	Duffy antigen/chemokine receptor
DAVID	Database for annotation, visualization and integrated discovery
DEG	Differentially expressed genes
<i>E.coli</i>	<i>Escherichia coli</i>
eCG	Equine chorionic gonadotropin
EGF	Epidermal growth factor
ELISA	Enzyme-linked immunosorbent assay
FBS	Foetal bovine serum
FCS	Foetal calf serum
FDR	False discovery rate
FSH	Follicle stimulating hormone
GnRH	Gonadotropin-releasing hormone
GO	Gene ontology
HBSS	Hank's balanced salt solution
HPC	High performance computing
hpf	High power field
IFN	Interferon
Ig	Immunoglobulin
IL	Interleukin
IL-1ra	Interleukin-1 receptor antagonist
IMS	Industrial methylated spirit
IRAK	Interleukin 1-associated kinase

ITS	Insulin-transferrin-selenium
KEGG	Kyoto encyclopedia of genes and genomes
LH	Luteinizing hormone
Log₂FC	Logarithmic fold change
LPS	Lipopolysaccharide
M	Molar
<i>M. ilicifolia</i>	<i>Maytenus ilicifolia</i>
MCWE	<i>Mycobacterium phlei</i> cell wall extract
mg	Miligram
MIE	Mating-induced endometritis
mL	Millilitre
mRNA	Messenger RNA
NF-κB	Nuclear factor-κB
ng	Nanogram
NGS	Next-generation sequencing
NLR	NOD-like receptor
nM	NanoMolar
mM	MiliMolar
NOD	Nucleotide-binding oligomerization
P4	Progesterone
PAMP	Pathogen-associated molecular pattern
PC1	First component
PC2	Second component
PCA	Principal component analysis
PCR	Polymerase chain reaction
PFAM	Database of protein families
PGF_{2α}	Prostaglandin F _{2α}
PGN	Peptidoglycan
pM	Picomolar
PMIE	Persistent mating-induced endometritis
PMN	Polymorph nuclear neutrophils
PPI	Protein-protein interaction
PRP	Pattern-recognition receptor
RIA	Radioimmunoassay
RLR	Retinoic acid-inducible gene-1-like receptor
RNA-Seq	RNA-Sequencing
rpm	Revolutions per minute
<i>S. zooepidemicus</i>	<i>Streptococcus equi subspecies zooepidemicus</i>
SAA	Serum amyloid A
SEM	Standard error of the mean
STRING	Search tool for the retrieval of interacting genes/proteins
TB	Thoroughbred
TLR	Toll-like receptor
TNF	Tumour necrosis factor
TRAF	Tumour necrosis factor associated factor
mg	Microgram
μL	Microliter

ABSTRACTS PRESENTED AT CONFERENCES

ORAL COMMUNICATIONS

M Monteiro de Barros *et al.* Characterisation of transcriptome profiles of fresh or cultured *ex vivo* equine endometrial explants at different time points. British Society of Animal Science (BSAS) Annual Conference. University of Chester, Chester, England, United Kingdom. April, 2017.

M Monteiro de Barros *et al.* Characterisation of transcriptome profiles of fresh or cultured *ex vivo* equine endometrial explants at different time points. Endometritis as a cause of infertility in domestic animals International Conference. September, 2017. Olsztyn, Poland.

M Monteiro de Barros *et al.* Characterisation of cultured *ex vivo* genetic profiles of the equine endometrial transcriptome at different time points. Brazilian Association of Postgraduate Students and Researchers in the UK (ABEP-UK) Conference. University College London (UCL), London, United Kingdom. March, 2018.

PRIZES

Highly Commended Presentation – BSAS Conference 2017, University of Chester

Best Presentation of the Conference – ABEP-UK Conference 2018, University College London

CHAPTER 1

INTRODUCTION

Pregnancy rates in broodmares have remained low, between 50-65 % per cycle, for many years, notwithstanding extensive research into fertility problems (Ball *et al.*, 1986; Allen *et al.*, 2007). Of the nearly 24,000 Thoroughbred (TB) mares sent to the stud in Great Britain and Northern Ireland in 2017, only 61 % produced a live foal (www.weatherbys.co.uk). The equine industry is a financially lucrative business worldwide, however persistence of uterine inflammation (endometritis) is one of the main causes of infertility in mares and the third most important clinical problem affecting adult horses according to equine practitioners in the USA (Traub-Dargatz *et al.*, 1991; Watson, 2000). It has been reported that 15-40 % of a normal population of TB mares suffer from persistent endometritis, reducing pregnancy rates by 13 % (Pycock and Newcombe, 1996; Zent *et al.*, 1998).

Mating-induced endometritis, also known as MIE, is a normal physiological endometrial inflammation that occurs in response to a variety of stimuli such as spermatozoa, seminal plasma, debris and bacteria introduced in the uterine lumen during breeding (Troedsson, 1999; Watson, 2000; Katila, 2001). Mating-induced endometritis eliminates the excess of semen and bacteria from the uterine lumen after breeding, leaving the uterus in a sterile and non-inflamed condition to receive the embryo 5-6 days after fertilization through immune responses and mechanical clearance of fluid (Betteridge *et al.*, 1982; Troedsson, 2006). Nonetheless, some mares fail to clear this transient normal inflammation, which then becomes persistent, known as persistent mating-induced endometritis or PMIE (Watson, 2000; Troedsson, 2006). Mares that clear their uteri from the normal transient MIE within 36-48 hours after breeding are considered resistant to PMIE, while mares that fail to clear inflammation within this time are classified as susceptible to PMIE (Katila,

1995; Troedsson, 1999). Figure 1.1 demonstrates the major differences between MIE and PMIE.

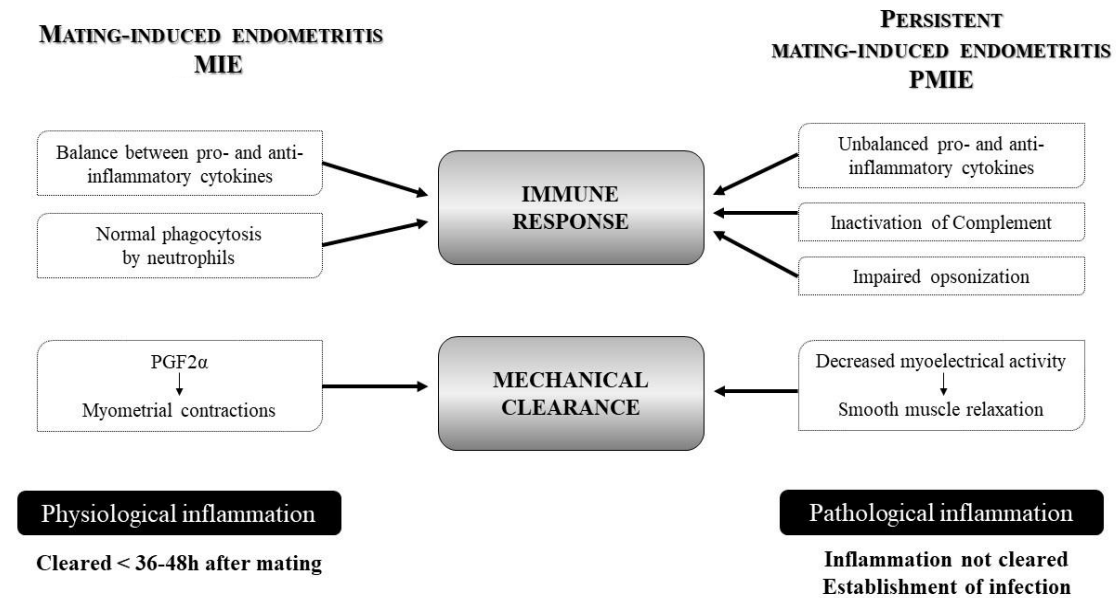


Figure 1.1 – Pathophysiology of Mating-induced endometritis (MIE) and Persistent mating-induced endometritis (PMIE).

Early identification of mares susceptible to PMIE is critical for appropriate breeding management. Research has demonstrated that cytokines contribute to the pathogenesis of persistent endometritis induced by semen and/or bacteria, focusing on the factors associated with resistance and susceptibility in mares (Fumuso *et al.*, 2003; Christoffersen *et al.*, 2010; Christoffersen *et al.*, 2012; Woodward and Troedsson, 2013). Nonetheless, the mechanisms linking the progression of MIE to PMIE are not well elucidated, and the endometrial global gene expression in resistant and susceptible mares before challenge is still unclear. Once the mechanisms underlying uterine inflammation are better understood at the transcriptomic and gene expression levels, identification of mares likely to be susceptible to PMIE at the pre-breeding examination will lead to appropriate management and an increase in fertility.

It is known that the steroid hormone changes within the oestrous cycle affect the efficiency of the uterine immune response. Depending on the stage of the oestrous cycle, the uterine environment faces challenges differently. During the luteal phase progesterone effects predominate over those of oestrogens in the uterus. Linked to these the proliferation of bacteria, accumulation of uterine fluid and accumulation of neutrophils is significantly greater when compared to the follicular phase of the oestrous cycle (Evans *et al.*, 1986a; LeBlanc *et al.*, 1994). However, there is a lack of knowledge regarding the change in global gene expression of the endometrium throughout the oestrous cycle and anoestrous period. Elucidating the changes in gene expression between phases will improve the understanding of the influence of hormones in resistance and susceptibility to PMIE.

An endometrial explant culture system composed of epithelial and stromal cells and resident leukocytes has already been used in previous research, and it responds to inflammatory stimuli by secreting markers of inflammation such as prostaglandin $F_{2\alpha}$ ($PGF_{2\alpha}$) synonymous to that of the whole animal (Nash *et al.*, 2008; Nash *et al.*, 2010b; Nash *et al.*, 2018). However, it has not been determined whether the transcriptome of cultured endometrial explants is altered once in culture. The use of abattoir-derived tissue negates the need to collect numerous uterine biopsies from living mares, and it also allows the entire surface of the endometrium to be used in laboratory experiments with different treatments. An *in vitro* system is needed to further study the equine endometrium and to better understand the global gene expression changes related to endometrial inflammation. Following successful analysis of the explant system at the transcriptomic level, this endometrial model presents a promising means by which PMIE may be explored further.

The aim of this thesis was to first investigate the use of an *ex vivo* endometrial explant tissue culture system at the level of gene expression as a baseline transcriptome for future studies, reducing the need for whole-animal research. Establishing an in culture model is important for studying the endometrial innate immune system as a baseline for future studies analysing equine endometritis. The second aim was to characterise the global gene expression in the equine endometrium and generate transcriptomic profiles of unchallenged endometrial cultured biopsies during the follicular and luteal phases of the oestrous phase, as well as during the anoestrous period. These findings will provide an innovative and significant insight into the understanding of physiological variation due to hormonal changes during the different phases of the oestrous cycle. The third aim of this thesis was to investigate the mechanisms underlying inflammation at different time points to understand the link between MIE and PMIE in mares. By using the explant tissue model, the innate immunity gene expression during challenge with *Escherichia coli* (*E. coli*) lipopolysaccharide (LPS) was characterized. The fourth and final aim was to determine the differences in global gene expression between resistant and susceptible mares before breeding. Identifying genes linked to both MIE and PMIE before the endometrium faces a challenge with semen and/or bacteria will improve the understanding of the delicate balance between resistance and susceptibility to PMIE in mares.

CHAPTER 2

LITERATURE REVIEW

2.1 | Introduction

The equine sector is of significant economic importance worldwide. It is worth approximately 73 billion pounds annually with around 7 million horses in the European Union (BETA, 2015). In Europe horses have historically been widely used in the military, industry, agriculture and for transportation. In modern times, horses perform sports activities and are extensively used for leisure. It is projected that horses will be no longer used for agricultural work. Instead, they will increasingly be used in sports and for recreation, due to the great popularity of such activities (Aurich and Aurich, 2006).

Investments in equine-related research worldwide are closely related to the increasing growth and development of the equine industry. Due to constant progress in animal genetics producing high commercial value horses, the equine industry is a financially lucrative, global business (Coelho and Oliveira, 2008). To capitalise on this, equine reproductive management aims to achieve the highest percentage possible of mares producing live foals per mating. However, it is not guaranteed the mare will deliver a live foal as a consequence of mating. The costs associated with producing a foal are high, such as investment in the mare, mating costs, nutrition and management costs. A study looking at the financial value of mares and the impact of reproductive efficiency over time indicated that mares are long-term investments and for them to be financially viable they need to produce at least six foals over a 7 year period (Bosh *et al.*, 2009). Therefore, mare fertility in the equine industry needs to be constantly optimised so that the aim of one foal per mare per mating per year is achieved in order to minimise costs. Understanding the mechanisms involved in low fertility rates is strategic to maximising breeding efficiency and, consequently,

profitability (Bosh *et al.*, 2009). Reproductive efficiency, in the mare, is associated with a series of different events such as puberty, ovulation, oestrous cycles, age at first conception and first parturition, birth intervals, easy of parturition, the number of live foals delivered, and longevity (Gonçalves *et al.*, 2009). Amongst these, one of the most important is the ability to conceive after mating. This is governed by amongst other things the ability of the uterus to accept a pregnancy and so can be adversely affected by conditions such as endometrial inflammation, known as endometritis. In order for the mechanism of endometritis to be understood, knowledge of the mare's reproductive tract is required.

2.2 | Female Reproductive System

2.2.1 | Reproductive Anatomy

Female reproductive anatomy is critical to the breeding value and success of the mare (Jones and Troxel, 2006). The mare's reproductive tract lies horizontally with 50 % in the abdominal and 50 % in pelvic cavity. It is composed of the perineum, vulva, vestibule, vagina, cervix, uterus, oviducts, and ovaries (Figure 2.1). Abnormalities and/or lack of function in any portion of the reproductive tract can be partly responsible for reproductive problems (Jones and Troxel, 2006; Dascanio, 2011).

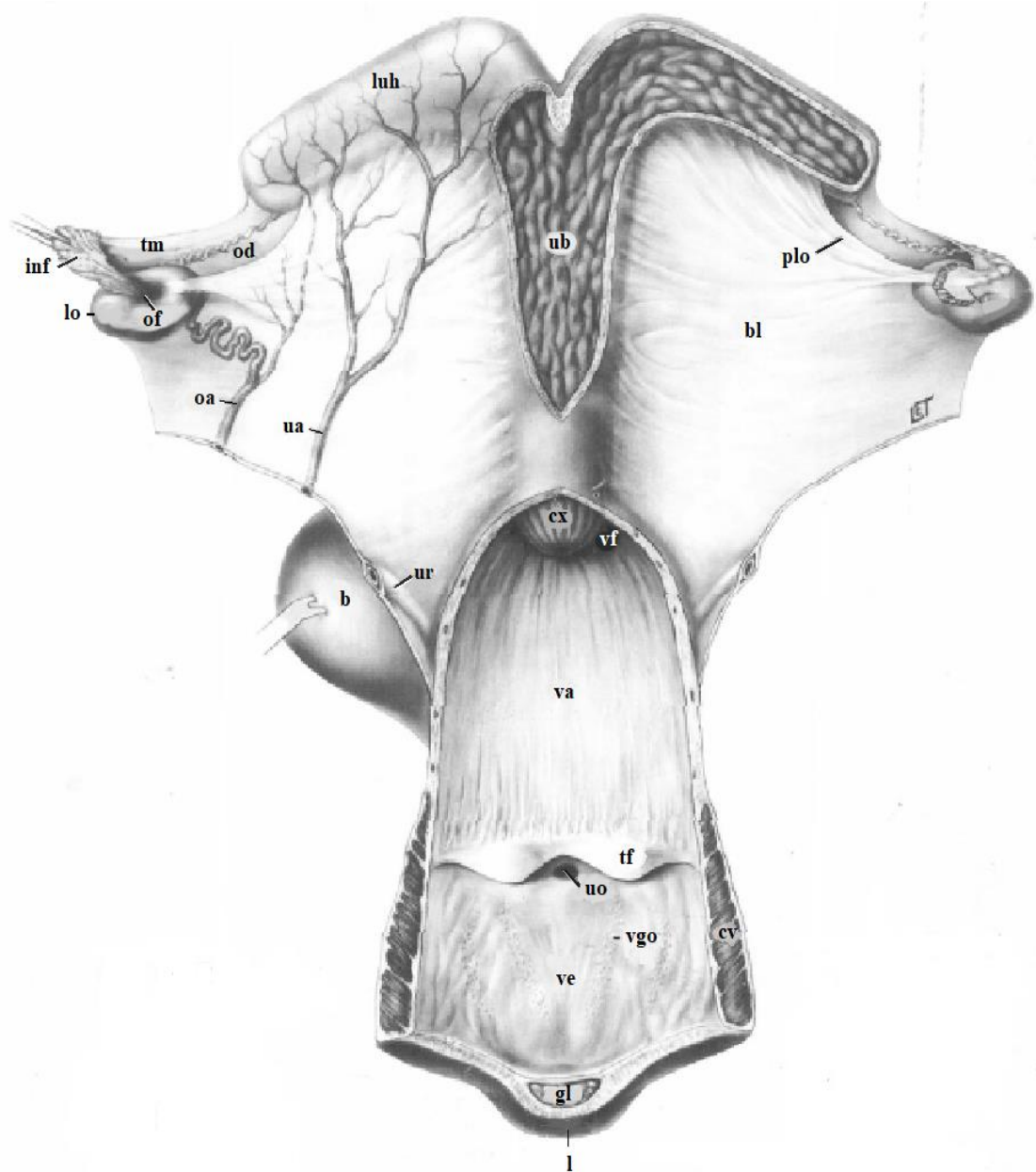


Figure 2.1 – Dorsal view of the mare’s reproductive tract. The left infundibulum is retracted to expose the ovulation fossa. The urethral orifice is shown by retraction of the transverse fold. Structures shown: bladder (b), broad ligament (bl), constrictor vestibuli and vulvae (cv), cervix (cx), glans clitoridis (gc), infundibulum (inf), labia (l), left ovary (lo), left uterine horn (luh), ovarian artery (oa), oviduct (od), ovulation fossa (of), proper ligament of ovary (plo), transverse fold (tf), tubal membrane (tm), uterine artery (ua), uterine body (ub), urethral orifice (uo), ureter (ur), vagina (va), vestibule (ve), vaginal fornix (vf) and vestibular gland openings (vgo). From Ginther (1992).

The perineum and the labia of the vulva constitute the external genitalia. The perineum comprises the outer vulva, anus, caudal rectum, vestibule, and the body wall surrounding the urogenital tract outlet (Ley, 2004). The vulva is the exterior opening to the reproductive tract. It is composed by two labia, clitoris, and the

vestibule, and it is also part of the urinary system. The labia enclose the external opening of the vulva and prevent the entrance of air and contaminants into the vagina. The labia have a dorsal and ventral commissure; located at the junction near the anal sphincter and at the rounded confluence surrounding the clitoris, respectively. The clitoris is situated at the ventral commissure. The vulva should be upright, vertically orientated, dorsal to the pelvic floor and ventral to the rectum and anus (Jones and Troxel, 2006; Dascanio, 2011). A section of the vulva called vestibule connects the vagina to the vulvar lips. When mechanically separating the vulvar lips, the vestibule and the vestibulovaginal fold are exposed and this is known as the “Windsucker test”. No inrush of air into the vagina should occur, indicating a good seal by the vulvovaginal fold. If there is any inrush of air a condition called pneumovagina occurs where air and debris enter the tract, leading to inflammation (Dascanio, 2011).

The vagina is an elastic muscular tube, with a mucous aglandular membrane that connects the vulvar vestibule to the cervix. The cranial vaginal walls and the vaginal portion of the cervix join together and form the vaginal fornix. Major stretching occurs during parturition allowing the passage of the foal (Ley, 2004). The vagina has acidic bacterial and spermicidal secretions. Consequently, it protects and cleans the reproductive tract. Sperm are deposited into the cervix and/or bottom of the uterus at mating in order to avoid the acidic spermicidal condition (Davies Morel, 2015).

The cervix is located between the uterus and the vagina. It is a tight, constricted thick-walled muscular sphincter and it is the final physical barrier defending the reproductive system against contamination and infection during the luteal phase of

the oestrous cycle and pregnancy. The cervix is a highly vascularized structure characterized by a folded muscular, collagenous connective tissue wall, which is lined by longitudinally folded columnar epithelium containing mucous-secreting cells. Its shape and colour vary and adapt to suit different patterns of reproduction depending on hormones. During parturition, it dilates to allow foal's passage. During the follicular phase of the oestrous cycle it is pink and relaxed, lying on the vaginal floor and secreting mucus to lubricate the passage of the penis and to allow the entry of semen into the uterus. During the luteal phase of the oestrous cycle the cervix is white, toned, does not lie on the vaginal floor and its secretion is thick and minimal (Jones and Troxel, 2006; Davies Morel, 2015).

The "Y" shaped uterus is divided into two uterine horns and the uterine body and it is located in the abdominal cavity, supported and suspended by the mesometrium. The uterine horns approach the fallopian tubes, and the uterine body joins the cervix. The uterus is divided into three different layers: the perimetrium, the myometrium, and the endometrium (Figure 2.2). The perimetrium is the outermost serosa layer, which is continuous with the broad ligaments. The myometrium is the middle muscular layer, composed of an outer longitudinal layer of smooth muscle, an inner circular layer of smooth muscle and a middle vascular layer. The myometrium is responsible for elasticity, expansion of the uterus and contractions during parturition. The endometrium is the inner layer of the uterus, characterized by longitudinal folds similar to the cervix. It is composed by an inner submucosa containing endometrial glands, ducts, stromal cells and connective tissue, and an outer layer of epithelial cells. Hormonal changes ruled by the oestrous cycle influence the appearance and activity of these epithelial cells and endometrial glands (Dascanio, 2011; Davies Morel, 2015).

Oviducts are also called Fallopian tubes or uterine tubes. Each mare has two oviducts, which are tortuous tubes continuous with the uterine horns that connect to the ovaries. The oviducts are thin structures of 20-30 cm long each when extended. They are divided into three parts from the ovary to the horn: infundibulum, ampulla, and isthmus. The oviducts are located in peritoneal folds, in the mesosalpinx part of the broad ligaments. The infundibulum has a slightly funnel-shaped form with hair-like projections called *fimbriae*. The infundibulum covers the ovulation fossa in the ovary, the only site where ova are released. The *fimbriae* catch and guide the ova released into the oviduct. The ampulla is an expanded part of the oviducts, and where fertilization occurs. The isthmus is a narrow structure that connects the ampulla to the uterine horn. It has a thicker myometrial layer when compared to the other two structures to push the fertilized ova from the ampulla into the uterus by contractions. The uterotubal junction is the site where the lumen of the uterus and the lumen of the oviduct connect together (Ginther, 1992; Davies Morel, 2015).

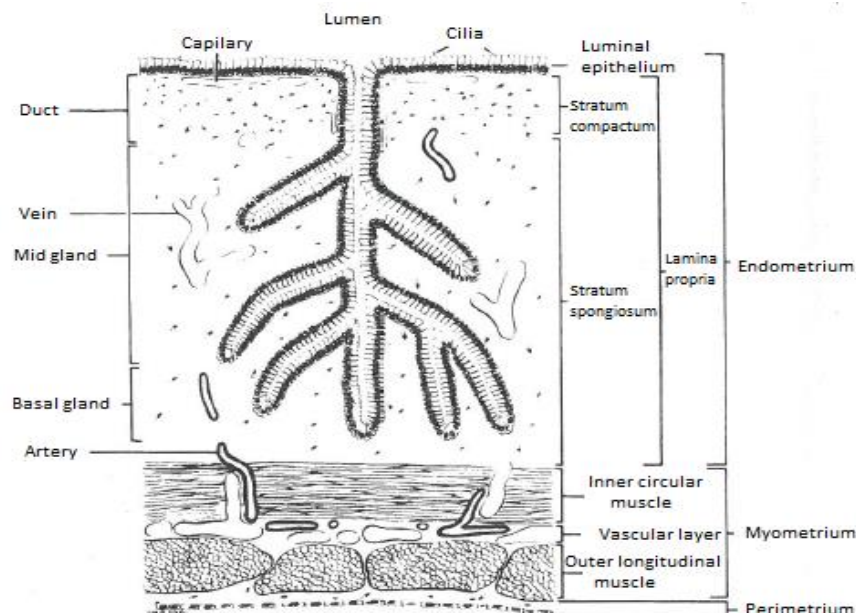


Figure 2.2 – Equine uterine wall diagram. The relative myometrium thickness is reduced in this diagram for illustrative purpose. Made by Kenney (1978), from Ginther (1992).

Ovaries in mares are kidney/bean-shaped with a noticeable depression, the ovulation fossa. Its size and texture vary according to the phase of the oestrous cycle. During the breeding season, the ovaries are fully functional, exhibiting many soft follicles filled with fluid. Different from other mammals, the supporting tissue called medulla is the outer part of the ovaries while the inner part is the cortex. The ovaries produce the female gametes and hormones, and the follicles and *corpus luteum* (CL) grow within the cortex. A thick layer known as tunica albuginea protects the whole surface of the ovary, except for the ovulation fossa through which ovulation can occur (Ginther, 1992; Davies Morel, 2015).

2.2.2 | Reproductive Cycle of the Mare

Within the breeding season, independent of mating, mares present multiple spontaneous oestrous cycles and because of this are termed seasonal polyoestrous spontaneous ovulators (Davies Morel, 2015). Mares are classified as seasonal breeders as their reproductive cycle and sexual activity occur during the spring, summer and autumn months when the length of the daylight is longer (Allen, 1977). The non-breeding season takes place during the winter months and it is known as anoestrus. The oestrous cycle of 21 days (± 3 days) is a period characterized by physiological and behavioural events controlled by specific hormones, which is divided into follicular (or oestrus) and luteal (or dioestrus) phases. The follicular phase lasts 4-6 days normally and it is when the follicles mature in the ovary and ovulate, oestrogen is secreted and consequently the mare is sexually receptive to the stallion (Ginther, 1992; Watson, 1998). Ovulation occurs normally in the last 24-48 hours of the follicular phase and it is known as day 0 (Ginther, 1992; Watson, 1998).

The luteal phase lasts 15-16 days and the mare shows no sexual receptiveness to the stallion (Aurich, 2011; Davies Morel, 2015).

The hypothalamic-pituitary-gonadal axis is the endocrine control of the oestrous cycle. Artificial and/or natural light reduces the melatonin secretion by the pineal gland, removing inhibition of the hypothalamus and allowing gonadotropin releasing hormone (GnRH) to be released (Snyder *et al.*, 1979; Sharp, 2011; Davies Morel, 2015). It is released through pulsatile secretions and reaches the anterior pituitary via the hypophyseal portal vessels, stimulating the production and secretion of luteinising hormone (LH) and follicle stimulating hormone (FSH) into the general circulatory system (Irvine and Alexander, 1997; Elhay *et al.*, 2007; Alexander and Irvine, 2011). GnRH may have a bigger effect on LH than it has on FSH, where they predominate at the follicular phase and mid- to late-luteal phase respectively (Watson *et al.*, 2000; Ginther *et al.*, 2004; Elhay *et al.*, 2007). However, GnRH is also controlled by an LH, FSH, and oestrogen feedback system. Furthermore, sexual stimulation may increase GnRH concentration, and other situations such as stress, nutrition and body condition can affect the production of GnRH (Alexander and Irvine, 2011). During the anoestrous period, low frequency pulses of GnRH are associated with a basal production of LH from the pituitary gland, to inhibit ovulation (Snyder *et al.*, 1979).

FSH is responsible for stimulating follicle development, growth and maturation, and its secretion begins to increase slowly after ovulation. The FSH concentration rates during the oestrous cycle in mares are still unclear, and different concentration peaks have been reported (Alexander and Irvine, 2011; Davies Morel, 2015). Preliminary studies measured FSH concentrations in mare's serum and indicated that FSH

concentration peaks occurred at 10-11 days intervals. The first peak usually appeared within 24 hours of ovulation, whereas the second one occurred mid cycle normally 10 days before the next ovulation (Evans and Irvine, 1975). It is now suggested by recent studies that during the luteal phase there is actually only one elongated FSH peak with elevated levels observed around ovulation, FSH episodic release slowing rising throughout the 21-day cycle. Inaccurately and non-continuous sampling of episodic hormone release may be the cause of previous errors when describing FSH concentration (Davies Morel, 2015).

The developing follicles then secrete oestrogen into the blood stream. Oestrogen prepares the equine reproductive tract for pregnancy by acting on the oviducts, uterus and cervix. At this stage the cervix is characterized by a pink colour, it is relaxed, opened, oedematous and mucus producing, whereas the uterus is flaccid and oedematous. Oestrogens are also responsible for the behavioural signs of the follicular phase, when mares show sexual receptiveness to stallions. This includes standing to be mounted, seeking stallion's attention, raising the tail, urination, clitoris exposure by everting the vulva, and absence of kicks or flatter ears (Watson, 1998; Jones and Troxel, 2006).

When blood oestrogen reaches a certain level, the pituitary gland releases LH into the blood stream stimulated by high frequency pulses of GnRH from the hypothalamus. LH is the hormone responsible for oocyte maturation, ovulation, luteinizing the dominant follicle and transforming it into a CL. During the follicular phase, its secretion is tonic and pulsatile. LH concentration begins to increase days before the follicular phase starts and there is a prolonged peak shortly after ovulation.

In the middle of the luteal phase (between days 6 and 15) the concentration of LH is low (Ginther, 1992; Alexander and Irvine, 2011).

Progesterone is the steroid hormone produced primarily by the CL to prepare the uterine environment for pregnancy. It inhibits the release of GnRH and hence LH and FSH and, therefore it suppresses follicular development and follicular phase behaviour. It also regulates the uterine and cervical tone and secretions in the tubular genitalia. Under the influence of progesterone, mares enter the luteal phase of the oestrous cycle. The principal function of progesterone is to maintain pregnancy by sustaining a uterine environment conducive to foetal development (Aurich, 2011; Vanderwall, 2011). Oxytocin is a neuropeptide secreted by the posterior pituitary and by the endometrium in order to stimulate smooth muscle contraction in the uterus. If the mare is not pregnant, the CL remains functional for around 12-14 days. Then, oxytocin stimulates the production of Prostaglandin $F_{2\alpha}$ ($PGF_{2\alpha}$) by the endometrium, which induces the luteolysis of the CL, allowing the onset of another follicular phase and ovulation. Much higher concentrations of oxytocin also cause smooth muscle contraction within the uterus post coitum as a means to help eliminate debris deposited at mating and so ensure the uterus is fit to accept a pregnancy (Morresey, 2011; Stout, 2011; Davies Morel, 2015). Understanding the oestrous cycle is important as breeding takes place during the follicular phase of the cycle. Therefore, this is the relevant time to study uterine inflammation.

2.3 | Mare Infertility

Fertility is the competence of a mare to deliver a live foal in the year following mating, and it may be expressed as the percentage of mares pregnant per mating/per oestrous cycle/at the end of the season or the percentage of mares producing live

offspring (Davies Morel, 2015). Infertility is characterised by a mare's transitory failure/incompetence to conceive a foal. Sterility, on the other hand, is a permanent inability to reproduce, often associated with anatomy defects of the reproductive tract. Mares with good reproductive history but that are not pregnant at the end of a breeding season are classified as barren, regardless the reason underlying it (Troedsson and Ricketts, 2007; Davies Morel, 2015). In the UK, the percentage of mares delivering a live foal varies hugely from 40 % to 80 %, mainly due to different management procedures (Osborne, 1975; Sullivan and Pickett, 1975; Baker *et al.*, 1993). More recent studies carried out among well-managed Thoroughbred (TB) showed percentages between 78-83 % of mares producing a live foal after mating (Morris and Allen, 2002; Hemberg *et al.*, 2004; Bosh *et al.*, 2009). Furthermore, of the nearly 24,000 Thoroughbred mares sent to the stud in Great Britain and Northern Ireland in 2017, 39 % failed to produce a live foal (www.weatherbys.co.uk).

Some pathogenic causes of low pregnancy rates and high levels of embryonic loss are related, even partially, with diminished uterine contractility, decreased uterine clearance of external/foreign material, including bacteria, high endometritis rates, large amounts of intrauterine inflammatory exudate, and elevated spermicidal and embryocidal effects (Carnevale and Ginther, 1992; LeBlanc and Causey, 2009; Woodward *et al.*, 2012).

2.4 | Endometritis

Endometritis is an inflammatory condition of the endometrium, mainly caused by opportunistic or sexually transmitted bacterial infections but may also be caused by fungi and yeasts (Watson, 1998; Albiñ *et al.*, 2003b; Hurtgen, 2006; Troedsson and Woodward, 2016). Different species of microorganisms can be found and linked to

fertility problems, as stud farm management and the breeding system used can influence this. *Escherichia coli* (*E. coli*), and *Streptococcus zooepidemicus* (*S. zooepidemicus*) are common pathogens cultured from the uterus of mares, but also the ones regularly isolated from mares with bacterial endometritis (Albihn *et al.*, 2003a; Frontoso *et al.*, 2008; Rasmussen *et al.*, 2015; Christoffersen and Troedsson, 2017). Endometritis in mares is considered one of the most common pathogenic causes of infertility (Bennett, 1987; Card, 2005; Hurtgen, 2006; Liu and Troedsson, 2008; Troedsson and Woodward, 2016). It creates an adverse and unfavourable uterine environment, resulting in early embryonic loss and abortion due to the difficulty of embryo survival and implantation. It is characterized by large amounts of fluid accumulation and occasionally mucus exuding the vulva, uterine increased blood flow and high leukocyte count (Troedsson, 2006; Davies Morel, 2015; Troedsson and Woodward, 2016). The uterus is often large and flaccid, and oedema and fluid retention may be evidenced by ultrasound scanning. In some instances, irritation to the uterine wall results in prostaglandin production which causes premature CL regression; therefore, the oestrous cycle may be shortened and pregnancy loss (Neely *et al.*, 1979; Troedsson *et al.*, 2001b).

During natural mating and artificial insemination (AI), semen is deposited into the uterus. It carries spermatozoa, seminal components, debris, and bacteria, that contaminate the uterus causing a normal, transient uterine inflammation (Troedsson, 1999; Watson, 2000; Katila, 2001; Troedsson *et al.*, 2001a). This inflammation is required for uterine cleaning of bacteria and excess spermatozoa. This normal response is called mating-induced endometritis (MIE) and it is occasionally clinically noticeable as a vaginal discharge of purulent fluid during the first hours after breeding. Efficient reproductive management is important: no mare presenting this

normal inflammatory response must undergo treatments as these may affect embryo survival and may even bring more contamination (Troedsson, 2006; Christoffersen and Troedsson, 2017).

After breeding only a small part of the ejaculated or inseminated sperm are transported from the uterus to the oviduct, within a period of 4 hours. This rapid transport of sperm coincides with increased myometrial contractions, which are also responsible for the elimination of non-viable sperm through the cervix. The myometrial contractions are not enough to eliminate the excess of spermatozoa from the uterus after breeding. Therefore, a combination of innate immune reactions characteristic of MIE and mechanical cleaning occur (Troedsson, 2006; Woodward and Troedsson, 2015). The uterus uses combined defence mechanisms to combat endometritis, which include physical clearance of bacteria and inflammatory products (Evans *et al.*, 1986a; Evans *et al.*, 1986b; Troedsson and Liu, 1991), phagocytosis (Liu *et al.*, 1986) and local uterine antibody-mediated immunity (Williamson *et al.*, 1983).

About 10-15 % of broodmares present failure of uterine defence mechanisms, being unable to effectively eliminate antigens and/or inflammatory products from the uterus after breeding (Pycock and Newcombe, 1996; Zent *et al.*, 1998). Consequently, the inflammation that was previously physiological becomes persistent known as persistent mating-induced endometritis (PMIE), bringing detrimental effects on uterine environment, and therefore on embryo survival and sperm motility (Troedsson, 1997, 2006; Woodward and Troedsson, 2015). Studies suggest that mares considered normal must be able to spontaneously clear the inflammation within a period of up to five days after breeding, which is the period of

time that the fertilized oocyte remains in the oviduct before descending into the uterine lumen (Betteridge *et al.*, 1982; Troedsson, 1999, 2006). However, the inflammatory response in most mares disappears within a period of 36-48 hours after breeding and these mares are classified as resistant to PMIE. Mares are classified as susceptible to PMIE when they fail to clear the uterus from the normal transient inflammatory response within 48 hours post mating (Hughes and Loy, 1975; Katila, 1995; Troedsson, 1999, 2006; Woodward and Troedsson, 2013).

MIE and its persistence, PMIE, seem to be particular to the mare. Cows, for example, do not show persistent inflammation after mating, but do suffer from subclinical endometritis and persistent endometritis after parturition (Bretzlaff, 1987; Wagener *et al.*, 2017). Postpartum endometritis impacts the fertility in dairy cows by increasing the days to conception as well as increasing the number of services and maintenance for conception, consequently increasing the risk of culling (LeBlanc *et al.*, 2002; Ghanem *et al.*, 2015). It has been shown that persistent endometritis after parturition is correlated with the presence of *Trueperella pyogenes* in the uterus of cows, which can prolong the luteal phase and decrease ovarian activity between weeks 3 and 5 post-partum (Ghanem *et al.*, 2015). Since the pathophysiology of persistent mating-induced endometritis in mares and persistent post-partum endometritis in cows is different and associated with distinct bacteria, results from cows cannot be extrapolated to mares. For this reason, research on equine MIE and PMIE is required to better understand these conditions and improve the mare's breeding management and efficiency.

2.5 | Persistent Mating-induced Endometritis

The persistence of MIE can be facilitated by predisposing factors such as stress, impaired general health, and malconformation or abnormalities in the reproductive tract (Davies Morel, 2015; Woodward and Troedsson, 2015). Reduced closure of the vulvar lips (Hemberg *et al.*, 2005) and pneumovagina (Caslick, 1937) may also predispose uterine infection, for example. Mares are more predisposed to retain uterine fluid as the uterus is more ventrally located in the abdomen, below the pelvic brim (LeBlanc *et al.*, 1998). This is exacerbated by age; the uterus of young mares shows a greater ability to eliminate infectious organisms, while older mares and multiparous mares display lower defence response against harmful organisms (Hughes and Loy, 1975; Evans *et al.*, 1986a; Ley, 2004). In studies conducted by Carnevale and Ginther (1992), old mares had reduced contractility and tone, demonstrating uterine physical impairment, increased intrauterine fluid accumulation and inflammation as indicated by endometrial biopsy. Physical clearance of intrauterine material was poorer with or without the presence of bacteria (antigenic stimulus) in older compared to young mares. Semen is a possible source of uterine contamination; however mares in good reproductive health are able to effectively clear the uterus and are not affected by exposure to bacteria. Therefore, there is a fine line between bacterial pathogenicity and mare's ability to tackle the inflammation (Hughes and Loy, 1975; Watson, 1998). It is known that each mare has differences in its susceptibility to persistent uterine infection, and it is also known that the bacteria recovery from the uterus or the cervix is not always synonymous of a diseased mare (Hughes and Loy, 1975; Hughes, 1980).

During the luteal phase of the oestrous cycle the mare is under the influence of progesterone, during this stage uterine infections occur more easily than in the follicular phase of the cycle, when the uterus is under the influence of oestrogens and consequently more resistant (Hughes, 1980; Evans *et al.*, 1986a; Katila, 2001). This happens due to the immune suppression, reduced uterine oedema and diminished myometrial contractility caused by high concentrations of progesterone during the luteal phase of the oestrous cycle (Hughes, 1980; Evans *et al.*, 1986a; Battut *et al.*, 1997; Katila, 2001). During the follicular phase of the oestrous cycle, the high oestrogen level provides a more resistant uterine environment, enhancing the immunological response to infection (Marth *et al.*, 2015a).

Hughes and Loy (1975) and studies revised by Evans *et al.* (1986a) propose that mares become susceptible to uterine infections when their normal immunological and cellular defence mechanisms are disrupted. However, much research is still needed to discover the precise cause of PMIE (Watson, 2000).

2.5.1 | Physical Clearance

The physical clearance mechanism is the result of a combination of different factors such as cervical relaxation and dilation, fluid secretion from the endometrium and from the cervix under the influence of oestrogen, rhythmical and coordinated myometrial contractions to expel uterine contents through the relaxed cervix. It has been shown that the uterine physical clearance is an important defence mechanism; therefore, its impairment or dysfunction is the major problem contributing to chronic or recurrent endometritis (Troedsson and Liu, 1991; Nikolakopoulos and Watson, 1999; Troedsson, 1999; Ley, 2004; Troedsson, 2006).

Part of the physical uterine defence mechanism is affected by the contractile activity of the myometrium. When susceptible mares are challenged with bacteria their electrical myometrial activity is lower than that found in normal mares (Troedsson *et al.*, 1993a). LeBlanc *et al.* (1989) measured the uterine clearance through scintigraphy, during the follicular phase and within 48 hours of ovulation. Multiparous mares considered reproductively normal cleared the radiocolloids consistently. However, mares susceptible to endometritis and nulliparous mares with poor cervical dilation showed a delay in the mechanical clearing of the uterus. This study suggests that a delay in the mechanical cleaning of the uterus is a factor that contributes to susceptibility in some mares. However, mares susceptible to endometritis may not always demonstrate a delay in uterine clearance. For this reason, further research is needed to clarify the factors underlying resistance and susceptibility to PMIE.

In mares considered susceptible to PMIE, uterine clearance can be stimulated through a sterile saline lavage or/and through the administration of uterotonic drugs such as oxytocin or PGF_{2α} (Troedsson, 1999). Lavage promotes artificial uterine clearance and stimulates lymphatic and uterine blood flow to trigger polymorphonuclear neutrophils (PMN) migration into the endometrial lumen and into endometrial tissues for cellular defence response. It reduces the number of bacteria/fungi/yeast and mitigates their toxicity. Fluids used for uterine lavage include sterile saline (0.9 % NaCl), lactated ringers solution, hypertonic saline (9 % NaCl), or povidone-iodine solution (0.05-1 % v : v). The temperature of these liquids can vary between room temperature (25 °C), body temperature (37 °C) or 42-45 °C, higher temperatures are aimed at boosting uterine tone, increase uterine blood flow and aid clearance (Ley, 2004). Uterine lavage should be performed from 6 to 24

hours after breeding in order not to interfere with fertility, as the sperm transportation into the oviduct takes 4 hours to be completed (Troedsson, 2006).

Spermatozoa placed in an inflamed uterine environment present diminished motility and mean path velocity. However, seminal plasma is reported to protect sperm when in the presence of inflammation by suppressing complement activation, PMN binding and phagocytosis (Troedsson *et al.*, 2001a; Troedsson *et al.*, 2002; Alghamdi *et al.*, 2004; Troedsson, 2006). Cryopreserved semen is made by removing the seminal plasma (Graham, 1996). Therefore, there is a greater duration of uterine inflammation after breeding with frozen/thawed semen. Thus, some mares may develop PMIE with frozen/thawed semen; when they do not if mated through natural covering or fresh/cooled semen. Mares inseminated with frozen semen have very low pregnancy rates because the sperm motility is decreased due to changes to the plasma membrane and because there is no suppression of their phagocytosis (Katila, 2001). The protection offered by seminal plasma is important when the insemination is repeated in the same mare within a 24-hour period, as an MIE environment is created for sperm inseminated last (Dahms and Troedsson, 2002). The immunosuppressive effect of seminal plasma that protects the sperm from phagocytosis can provide the bacteria with a favourable environment for adhesion and growth. Studies suggest that bacterial endometritis can contribute to a more aggressive PMIE in mares inseminated with frozen-thawed semen (Troedsson, 2006).

2.5.2 | Immune System

2.5.2.1 | Innate Immunity

The innate immune system is the first line of defence against invading microorganisms. This quick-response system is characterized by a group of subsystems working through different mechanisms to assure the homeostasis of the organism. Inflammation is the most important subsystem of the innate immune system (Tizard, 2013). It is important to fully understand the mechanisms underlying endometrial inflammation in order to better understand the characteristics involved in persistent inflammation and, in the future, develop treatments for PMIE.

During inflammation, white blood cells and proteins are recruited to the site of microbial invasion to destroy them and promote tissue repair. The innate immune system is activated either by exogenous or endogenous signals. Pathogen-associated molecular patterns (PAMPs) are the exogenous molecules produced by invading microorganisms. Damage-associated molecular patterns (DAMPs) are molecules produced endogenously by damaged, dying or dead cells. Pattern-recognition receptors (PRRs) throughout the body recognize PAMPs and DAMPs and consequently, the immune system is activated. Toll-like receptors (TLRs), the retinoic acid-inducible gene 1-like receptors (RLRs), nucleotide-binding oligomerization domain (NOD)-like receptors (NLRs) and the C-type lectin receptors (CLRs) are examples of PRRs. PRRs are located on phagocytic cells such as the white blood cells (Medzhitov and Janeway, 1997; Schnare *et al.*, 2001; Tizard, 2013). However, both endometrial epithelial and stromal cells play roles in the innate immunity response by recognizing invaders (Silva *et al.*, 2010; Cronin *et al.*, 2012; Marth *et al.*, 2015a).

The white blood cells, or leukocytes, are the defensive circulating cells in the bloodstream. The PMN is the most predominant type, constituting around 50 % of the white blood cells in the horse. PMNs are responsible for the phagocytosis of invading microorganisms and for this reason they are the first cells to be attracted to inflammation sites by cytokines. Phagocytosis is the continuous process by which a PMN engulfs and destroys an invading microorganism, the process of which involves PMN activation, chemotaxis, adherence, ingestion, and destruction (Underhill and Ozinsky, 2002; Tizard, 2013). PMNs are developed from bone marrow stem cells, and move into the bloodstream for a period of 12 hours, after which they migrate into the liver, spleen, lungs and bone marrow capillaries. PMN have a short life (few days), therefore, they are continuously produced. In the presence of infection, PMNs migrate into the bloodstream again and go directly towards the site of microbial invasion and damaged tissue, guided by chemoattractants (Nathan, 2006; Tizard, 2013). Uterine inflammation is indicated by an influx of PMN into the uterine lumen. PMNs aim to clear the contaminants, dead and/or defective spermatozoa via phagocytes (Kotilainen *et al.*, 1994; Troedsson, 1999). The number of uterine luminal PMNs peaks at 8 hours after insemination but after 48 hours the numbers are extremely low (Katila, 1995).

Previous studies attested that PMN activation and functionality indicate uterine responses to insemination (Katila *et al.*, 1990; Kotilainen *et al.*, 1994). Nash *et al.* (2010a) conducted an experiment where ponies were intra-uterine treated with frozen/thawed semen to induce MIE. At the beginning of the MIE cytological PMN numbers varied widely, reaching a peak 8 hours after inflammatory induction. However, mares showed decreased PMN count in periods of 16, 24, 48 and 72 hours after treatment. Further, uterine luminal PGF_{2α} concentrations increased 16 hours

after treatment with sperm and returned to basal concentration 72 hours after challenge. Therefore, PMN cytology count might be a valid marker of MIE (Nash *et al.*, 2010a).

Seminal plasma modulates the inflammatory response caused by sperm as it reduces the complement activation, PMN-chemotaxis, and phagocytosis in the mare's uterus (Dahms and Troedsson, 2002; Troedsson, 2006). When seminal plasma is included in the insemination, the intensity of inflammation is the same but the duration of MIE can be shorter. Fiala Rechsteiner *et al.* (2002) compared the number of leukocytes in uterine flushings after inseminating follicular phase mares with seminal plasma or skim milk extender. The inflammatory response after seminal plasma inoculation increased progressively up to 4 hours, while the inflammatory response showed continuous increase up to 24 hours after milk extender inoculation (Fiala Rechsteiner *et al.*, 2002). Therefore, it is believed that seminal plasma has an important role in modulating post-breeding inflammation (Troedsson, 1999; Katila, 2001; Troedsson, 2006). Other studies suggest that seminal plasma provides sperm protection by blocking binding and phagocytosis by PMNs (Dahms and Troedsson, 2002; Alghamdi *et al.*, 2004; Troedsson, 2006). This selective protection allows a greater survival rate of viable sperm, increasing the quantity reaching the oviduct where fertilization occurs (Troedsson, 2006). However, the number of PMNs recovered from the equine uterus 6 hours after insemination did not decrease when seminal plasma was present (Kotilainen *et al.*, 1994).

Liu *et al.* (1986) induced uterine infection by inoculating *S. zooepidemicus* in mares susceptible and resistant to chronic uterine infection. A functional disorder of uterine-derived PMNs 12 hours after induction was reported only in susceptible

mares. It was thought that this may occur because uterine PMNs from susceptible mares show a compromised ability to migrate, facilitating the spread of bacterial agents that are already within the uterine lumen. On the other hand, uterine PMNs from resistant mares demonstrated significant migration during the same period, moving continuously, phagocytising and killing microbes. Resistant mares, 15-25 hours after bacterial inoculation, showed a decrease in the number of PMNs and a reduction in the functional activity of cells obtained from uterine flushings. This suggests that there was no continuous recruitment of new PMNs in the peripheral circulation in resistant mares, as it is known that peripheral blood PMNs are able to maintain their migration activity only for 12-15 hours after venipuncture. PMNs in uterine flushings obtained 15 hours after bacterial inoculation in resistant mares only corresponded to the initial population of PMNs migrating to the lumen in response to the induced infection. Conversely, continuous recruitment of PMNs was seen in susceptible mares in response to continuous bacteria presence in the uterus. However, circulating PMNs obtained from resistant and susceptible mares and uterine-derived PMNs in resistant mares are all equally able to migrate and to remain viable. Therefore, the migration dysfunction found in uterine-derived PMNs in susceptible mares can be related to the luminal environment inside the uterus (Liu *et al.*, 1986).

Another study suggested by Troedsson *et al.* (1993a) establishes that uterine PMNs from mares susceptible to PMIE are indeed functional when the uterine environment is adequate. In reality, PMNs from susceptible mares, when assessing phagocytosis and chemotaxis using a standardized chemoattractant, performed better than those in resistant mares in the experiment of Troedsson *et al.* (1993a). On the other hand, uterine secretions in susceptible mares were a significantly worse opsonin source

when compared to resistant mares. As a result it is believed that the defective phagocytosis of uterine-PMNs in susceptible mares correlates not with a PMNs dysfunction, but with an altered opsonisation as a result of a non-adequate uterine environment. This is thought to be caused by an accumulation of inflammatory products in the uterus. In summary, PMNs have an important role in the uterus' immune response, however, they are fully operational both in resistant and susceptible mares. It is the uterine secretion in susceptible mares that impairs PMN phagocytosis (Troedsson *et al.*, 1993b).

Cytokines are signalling proteins synthesized and secreted by immune system cells. They regulate the immune reaction by communicating between cells, and there are many different types of cytokines. Interleukins (IL) control the interaction between lymphocytes and other white blood cells. IL-1 is a pro-inflammatory cytokine that triggers innate immune reactions and inflammatory responses (Dunne and O'Neill, 2003; Subramaniam *et al.*, 2004; Weber *et al.*, 2010; Boraschi and Tagliabue, 2013). The IL-1 receptor (IL-1R) mediates the effects of IL-1 and it is part of the interleukin-1 receptor/toll-like receptor (IL-1R/TLR) superfamily (Dunne and O'Neill, 2003). The members of the IL-1R/TLR family are receptors involved in inflammatory responses and host defence, including receptors for lipopolysaccharide (LPS) derived from gram-negative bacteria (O'Neill and Greene, 1998; Poltorak *et al.*, 1998). The protein motifs shared by the IL-1R/TLR family are called toll-interleukin receptor (TIR) motifs (Kimbrell and Beutler, 2001; Dunne and O'Neill, 2003).

Macrophages are also part of the innate immune response acting in the first line of defence in the host defence, but they also take part in the adaptive immune response

as accessory cells (Ma *et al.*, 2003). They become activated by LPS stimulation from gram-negative bacteria such as *E. coli*, by recognizing the LPS' PAMPs by PRRs called CD14. To signal, CD14 acts together with MD-2, cooperating with a PRR co-receptor, TLR4 (Akira, 2003; Beutler *et al.*, 2003). Following TLR4 activation MyD88 protein is recruited. The TIR domain of MyD88 signals by recruitment of IL 1-associated kinase (IRAK1) and tumour necrosis factor receptor associated factor-6 (TRAF-6), inducing nuclear factor- κ B (NF- κ B) activation (Muzio *et al.*, 1997; Beutler *et al.*, 2003; Warner and Nunez, 2013; Hayden and Ghosh, 2014).

Endometrial mRNA expression of the pro-inflammatory cytokines IL-1 β , IL-6, TNF- α and IL-8, and the anti-inflammatory cytokine IL-10 was previously analysed in PMIE susceptible and resistant mares (Fumuso *et al.*, 2003; Fumuso *et al.*, 2006). Twenty-four hours after AI with killed sperm, the endometrial expression of IL-1 β , IL-6, TNF- α was increased in both resistant and susceptible mares, but the basal levels of these pro-inflammatory cytokines during the follicular phase of the oestrous cycle was higher in susceptible mares (Fumuso *et al.*, 2003). On the other hand, susceptible mares had higher rates of IL-8 and lower rates of IL-10 when compared to resistant mares after AI. The large increase in the pro-inflammatory cytokine IL-8 after AI is considered normal because spermatozoa can produce an inflammatory reaction, and its concentration falls in the luteal phase of normal mares (7 ± 1 days after ovulation), but in susceptible mares IL-8 concentrations remain high. Thus, susceptible and resistant mares have different IL-8 and IL-10 transcription profiles during the untreated oestrous cycle. In basal conditions (control, no AI) and after insemination, susceptible mares have higher IL-8 expression during the follicular phase, and that may explain their susceptibility (Fumuso *et al.*, 2006).

Studies analysed IL-8 expression changes in normal pony mares and in cultured endometrial explants and TLR4 in normal pony mares free from acute or persistent inflammation (Nash *et al.*, 2010a; Nash *et al.*, 2010b). TLR4 recognizes LPS on the surface of *E. coli*, a commonly isolated bacterium from PMIE cases (Hughes and Loy, 1975). However, it was not possible to find a significant IL8 and TLR4 response 24 hours after insemination with frozen/thawed semen in reproductive normal pony mares (Nash *et al.*, 2010a). Also, cultured endometrial explants expressed IL-8 and expression did not change after challenge with washed sperm or seminal plasma (Nash *et al.*, 2010b). These studies (Nash *et al.*, 2010a; Nash *et al.*, 2010b) were based on selected mares and uteri free of acute or persistent inflammation. These observations align with previously mentioned studies (Fumuso *et al.*, 2003; Fumuso *et al.*, 2006) and taken together attest that susceptible but not resistant mares expressed greater IL-8 levels. Thus, it is reasonable that explants from normal mares did not show any variation in IL-8 expression but explants collected from susceptible mares may present gene expression changes (Nash *et al.*, 2010b).

Christoffersen *et al.* (2012) inoculated the uteri of PMIE resistant and susceptible mares with 10^5 colony-forming units (CFU) of *E. coli* and evaluated the inflammatory cytokines response in endometrial tissue and circulating white blood cells. The cytokines measured were IL-1 β , IL-6, IL-8, IL-10, TNF- α , IL-1 receptor antagonist [ra] (IL-1ra) and serum amyloid A (SAA). Immediately after bacterial infusion, resistant mares showed increased expression of these cytokines. However, within a short period of time (12-24 hours) they returned to baseline expression levels. In contrast, susceptible mares expressed these cytokines for 72 hours, perhaps because of the imbalance between IL-1 β and IL-1ra, pro-inflammatory and anti-inflammatory cytokines respectively. This study suggests that imbalanced endometrial expression of pro and anti-inflammatory cytokines may be involved in the pathogenesis of persistent endometritis (Christoffersen *et al.*, 2012). Further, it may be that systemic Acute Phase Response (APR) depends on the number of bacteria inoculated. In this experiment, a very small dose of bacteria (10^5 CFU) was inoculated and consequently no APR was detected, in contrast to another study (Christoffersen *et al.*, 2010) where a higher dose of *E. coli* was inoculated and APR was detected. It was suggested that the expression of inflammatory cytokines in the endometrium occurs in a time-related manner, and that peak expression occurs immediately after uterine bacteria infusion. Nevertheless, more extensive research is required to better understand cytokine expressions in resistant and susceptible mares undergoing both MIE and PMIE. **2.5.2.2 | Adaptive Immunity**

Chemoattractants in the uterine fluid such as complement products, prostaglandin E (PGE) and PGF_{2 α} allow PMN migration, phagocytosis and subsequent bactericidal activity (Liu *et al.*, 1986; Troedsson, 1999). Inflammatory reactions start when the sperm enters the uterus, activating complement in the uterine secretion. The

chemotactic signal to PMNs occurs when the complement C5 factor is cleaved into C5a and C5b, resulting in a PMN influx into the uterine lumen. In the presence of C3b complement factor, and other independent complement mechanisms, activated PMNs bind to sperm and phagocytose it (Troedsson, 2006). Some chemoattractants generated by damaged tissue and microorganisms, are the C5a peptide derived from complement activation, hydrogen peroxide and a fibrinogen derived peptide, fibrinopeptide B. Opsonisation is the process where the electrostatic charge of a microorganism is neutralized, so the PMN can adhere and phagocytose it. Complement and antibodies are examples of opsonins (Nathan, 2006; Tizard, 2013).

Immunoglobulins (Ig) are glycoprotein molecules commonly known as antibodies. Immunoglobulins A (IgA), D (IgD), E (IgE), G (IgG), and M (IgM) are the five different isotypes found in mammal body fluids, especially blood serum. Their role in the immune system is to mark foreign antigens that should be destroyed and eliminated, by binding to them (Wagner, 2006; Tizard, 2013). Plasma cells in the lymph nodes and spleen produce IgG and IgM. IgG is also produced by the bone marrow and it is responsible for the systemic defence, while IgM participates mainly in the primary immune response. IgA and IgE are produced by plasma cells situated under body surfaces (intestine, respiratory tract, urinary system, skin, mammary gland). IgA protects the intestinal, respiratory and urogenital tracts and in non-ruminant animals, it is the dominant immunoglobulin in the external secretions. Acute inflammation is triggered by IgE and it is also responsible for immunity against parasitic worms and allergies. IgD is an immunoglobulin found attached to B cells and its function is still unclear in animals (Wagner, 2006; Tizard, 2013). Immunoglobulins have subclasses that differ among species. Horses, specifically,

express different subclasses of IgG such as IgGa, IgGb, IgGc, IgGt and IgGb based on their electrophoretical and serological properties (Wagner, 2006).

Williamson *et al.* (1983) compared immunoglobulins levels in uterine flushings from mares with and without current uterine inflammation. Immunoglobulins of classes IgA, IgG and IgGt were found, of which IgA was predominant. A higher proportion of mares with inflammation showed a measurable amount of IgA than mares with no current inflammation. This higher IgA concentration in the uterine washings of mares with uterine inflammation in this experiment (Williamson *et al.*, 1983), and also in the experiments of Asbury *et al.* (1980), brought into question the IgA role in the uterine defence system. Elevated IgA concentrations indicate that inflammation is established, but the presence of such immunoglobulins does not give the assurance that the infection will be tackled. The conclusion of this experiment, as well as the experiment conducted by Asbury *et al.* (1980), was that mares with no current inflammation have lower levels of IgA in their uterine washings.

Liu *et al.* (1986) compared several articles investigating the role of immunoglobulins in addressing bacterial invasion in the endometrium. IgA, IgG, IgGt, and IgM were found free in the mare's uterus. The locations from which these immunoglobulins were derived confirm the ability of the uterus to locally produce and secrete into the endometrial lumen specific classes of immunoglobulins. These studies emphasize the preferential production of IgA and the role of the endometrium as a mucosal immune system in mares. Troedsson (1999) also compared various immunohistochemical endometrial studies showing that different classes of immunoglobulins (IgGa, IgGb, IgGc, IgGt, IgA, and IgM) were isolated from the uterus, and the number of free immunoglobulins and immunoglobulin containing cells in susceptible mares was

equal to, or sometimes greater than, the amount found in resistant mares. Thus, the antibody-mediated uterine defence in susceptible mares is indeed functional. The pathophysiology involved in the transition from a susceptible to a resistant condition is not therefore associated with lack or deficiency of immunoglobulins (Troedsson *et al.*, 1993c; Katila, 1996; Troedsson, 1999).

2.5.3 | Markers of Uterine Inflammation

PMIE is usually diagnosed late, and prediction of susceptibility is subjected only to the mare's poor reproductive clinical histories and prolonged veterinary assessments of reproductive tract over many oestrous cycles. Being able to identify mares susceptible to persistent endometritis in advance is critical to increasing pregnancy rates.

Prostaglandins are pro-inflammatory mediators associated to mare endometritis, and quantifying its production is of major importance. During the process of PMN activation, $\text{PGF}_{2\alpha}$ is released from the endometrium as an inflammatory mediator. It causes mild myometrial contractions and subsequent removal of accumulated fluid and harmful inflammatory products inside the uterus (Troedsson, 1999, 2006). $\text{PGF}_{2\alpha}$ also initiates a premature luteolysis of the CL, leading to an early embryonic loss (Adams *et al.*, 1986). During a live animal experiment conducted by Nash *et al.* (2010a) ponies were evaluated before treatment and at strategic periods of time after treatment to test possible cellular and molecular markers of MIE. Among all parameters analysed it was concluded that uterine cytology and analysis of $\text{PGF}_{2\alpha}$ secreted by the uterus of a mare are the most accurate markers of uterine inflammation during induced MIE. Therefore utilization of $\text{PGF}_{2\alpha}$ as uterine inflammation marker both *in vivo* and *in vitro* is particularly important as it can be

analysed through uterine lavage samples, a clinical routine procedure in mares used for reproduction (Nash *et al.*, 2010a; Nash *et al.*, 2010b).

Endometrial cytology is also a diagnostic method for retrospective assessment of presence or absence of active uterine inflammation based on the presence of PMN cells, which are the prevailing and most important cells during acute endometritis (LeBlanc, 2011; Diel de Amorim *et al.*, 2016). Epithelial cells are the prevalent ones in an endometrial cytology, varying from tall columnar during the oestrous cycle to cuboidal during the anoestrous season (LeBlanc, 2011).

Endometrial biopsy quality is an accepted marker for uterine health and endometrial pathologies are linked to PMIE (Woodward and Troedsson, 2013). Assessment of endometrial quality has been a standard procedure for more than 35 years by taking endometrial biopsies for histopathological analysis (Schlafer, 2007). Yet the primary method of endometrial assessment is still histopathology of endometrial sections stained with haematoxylin and eosin (Brandt and Manning, 1969; Kenney, 1978). Depending on intensity and/or severity of uterine inflammation, fibrosis and glandular degeneration mares are classified as I, II and III (Kenney, 1978).

Nevertheless, information retrieved from endometrial histopathology is limited. Thus, newer procedures to diagnose endometritis can generate quantitative data, removing some subjective aspects of histopathology. Gene expression in the endometrium has been analysed by RT-PCR and more detailed information about uterine inflammation and health is being studied (Schlafer, 2007). The use of transcriptomic analysis such as RNA-Sequencing (RNA-Seq) will allow better and fuller understanding of the mechanisms underlying resistance and susceptibility to PMIE in mares.

2.6 | Equine Tissue Culture Model

An endometrial explant culture model was developed to analyse prostaglandin production by the uterus in response to a physiological challenge with oxytocin, spermatozoa, bacteria and/or bacterial LPS (Nash *et al.*, 2008). This explant culture endometrial model was conducted by collecting uteri of mares presented for euthanasia at a slaughterhouse where uteri with no visual indications of inflammation were collected. Explants taken from the uterine horns and histological analysis were performed to confirm that there was no current inflammation since it is known that pathological degenerative changes caused by an inflammation would hinder the *in vitro* PGF_{2α} secretion. Endometrial explants were viable throughout the experiment period. Analyses were conducted in periods of 24 and 72 hours after the explant culture was begun, wherein the first period corresponds to the analysis of acute inflammation and the second analysis refers to the period where persistent inflammation may occur. Also, 24 and 72 hours after oxytocin treatment explants showed a PGF_{2α} response, proposing the existence of functional cells. On the other hand, during the follicular phase, there was no PGF_{2α} response after treatment with extended semen, killed *S. zooepidemicus* (10, 10³ or 10⁵ CFU/mL) or *E. coli* LPS (0.03 and 3 µg/mL) (Nash *et al.*, 2008).

Nash *et al.* (2010b) conducted another experiment utilizing the existing endometrial explant culture model (Nash *et al.*, 2008) as an *in vitro* imitation of sperm induced-induced PMIE. The markers of inflammation chosen were PGF_{2α} and IL-8. The explant cultures, 24 and 72 hours after inoculation of 1 or 10 x 10⁶ frozen/thawed semen, frozen/thawed extender, chilled semen and washed sperm per ml, did not show PGF_{2α} secretion different from the secretion found in the control tissue. Only explants challenged with seminal plasma had a higher secretion of PGF_{2α} compared

to the control, during the acute inflammation (24 hours) but not at 72 hours. It was possible to measure IL-8 expression, even though the expression after challenge with washed sperm or seminal plasma was not different from the controls (Nash *et al.*, 2010b).

Using abattoir tissues negates the need to collect multiple uteri biopsies from living mares, and the entire surface of the uterine horn can be used for in vitro culture, allowing the use of different treatments on the same animal (Nash *et al.*, 2010b). Tissue culture of intact explants have distinct advantages over isolated cell cultures, since the extracellular matrix is not disrupted which may affect cell differentiation and function and time is saved because cell culture requires several days or weeks for cells to reach confluence (Borges *et al.*, 2012). The equine endometrial explant culture model is representative of the functional endometrium of a live mare, composed of epithelial, stromal and resident leukocytes (Nash *et al.*, 2008). It is also possible to harvest mRNA from cultured explants to measure gene expression. Explants were tested in this current study as a model for transcriptomic changes synonymous with MIE and PMIE in the whole animal.

2.7 | RNA-Sequencing

Next-generation sequencing (NGS) produces a substantial amount of genomic or transcriptomic sequence data. NGS may be broadly used to better understand genetic changes associated with health and disease by resequencing genomes. All sequencing technologies are divided into template preparation, sequencing and imaging, and data analysis. Different technologies use specific protocols and, therefore, produce distinct types of data (Metzker, 2010).

RNA-Seq, or whole transcriptome sequencing, is an NGS technology used to catalogue the transcriptome of cells, tissues and organisms (Metzker, 2010; Roberts *et al.*, 2011). The transcriptome represents the entire set of transcripts in a cell, tissue or organisms. Messenger RNA (mRNA), non-coding RNAs and small RNAs are species of transcripts (Wang *et al.*, 2009). RNA-Seq allows the catalogue of transcripts, determination of the 5' start and 3' end sites of genes, analysis of splicing patterns, quantification of gene expression levels and identification of expression changes at different development stages and during various other conditions (Wang *et al.*, 2009). RNA-Seq is a valuable tool to understand transcriptomic transitions and biological dynamics during normal developmental changes in an organism. Biomedical samples can be analysed, and changes in the transcriptome between healthy and unhealthy tissue can also be contrasted and studied. The understanding of transcriptomics is applied to sub classify illness and disease states, and RNA assessments may be used for clinical diagnosis (Wang *et al.*, 2009; Ozsolak and Milos, 2011).

RNA-Seq requires an RNA population to be converted into cDNA fragments containing adaptors attached to its ends. These fragments constitute the library. Molecules are then amplified to be sequenced in a high-throughput manner. The results are single-end sequencing (short reads from one end) or paired-end sequencing (short reads from both ends). The sequencing results should be aligned to a previously published reference genome or to reference transcripts. In the absence of a reference, results are assembled *de novo* to generate a transcriptional map including gene expression levels and/or gene transcriptional structure (Wang *et al.*, 2009). When aligned to a reference genome, the gene expression level is calculated, as well as the number of mapped reads. Using statistical analysis the differential gene

expression is determined. Depending on the requirements for each experiment a range of bioinformatics tools are available, with different and specific applications (Mutz *et al.*, 2013). Data generated is immense, and presents a bioinformatic challenge. Efficient processing, storing and retrieval methods minimise imaging analysis errors and removal of low-quality reads (Wang *et al.*, 2009).

A previous study conducted by Christoffersen *et al.* (2012) investigated the expression of a few inflammatory and immune endometrial genes that have a role in the process of endometritis in resistant and susceptible mares. Considering that the inflammatory and immune responses are multifaceted, analysing only a group of genes is not enough for a complex and meaningful analysis of the disease. Thus, using new technologies to perform endometrium genome-wide profiling is necessary. Then it will be possible to characterise the interactions and changes occurring in the genes during uterine inflammation to advance the understanding of the underlying mechanisms involved in the progression from normal MIE to clinically important PMIE.

Recently Marth *et al.* (2015b) analysed the global gene expression of the healthy equine uterus of resistant mares under the normal effect of ovarian hormones. Global uterine profiles during the follicular and luteal phases were created using RNA-Seq and the differential gene expression between these two stages of oestrous cycle was investigated. Results revealed that mRNA expression profiles between the follicular and luteal phases were significantly different. Genes involved in the immune response were highly expressed during the follicular phase while those related to metabolic functions predominated during the luteal phase. During follicular phase a total of 1577 genes from immune system, cellular metabolism and extracellular

matrix complex were upregulated. Toll-like receptor 1 (TLR1), chemokines such as C-X-C motif chemokine ligands 6 (CXCL6), 10 (CXCL10), 16 (CXCL16), 17 (CXCL17), C-C motif chemokine ligand 5 (CCL5) and C-X3-C motif chemokine ligand 1 (CX3CL1), chemokine receptors such as C-X-C chemokine receptor type 4 (CXCR4) and type 7 (CXCR7), antigen/chemokine receptor (DARC), interleukins such as IL-8, IL-15 and IL-34, interleukins receptors for IL-1 and IL-17, and the TNF family were significantly upregulated during the follicular phase. High regulation of immune pathways during the follicular phase is correlated with the physiological uterine preparation for breeding, where foreign material may enter the uterus. This study is one of the first analysing equine endometrial gene expressions by using RNA-Seq and it supplies a baseline of endometrial immune regulation during the follicular phase in resistant mares free of inflammation, and it may be used as a reference transcript for future studies. Additionally, Marth *et al.* (2015a) focused on the immune response and characterized endometrial gene expression changes by using RNA-Seq in PMIE resistant mares in follicular and luteal phases. Uterine health was confirmed at the first oestrous cycle by bacteriological culture and animals were randomised into two groups. Experiments were done in a crossover design and endometrial inflammation was induced by *E. coli* inoculation in both groups. At the second oestrous cycle, bacterial inoculation took place during the follicular phase in group 1, and during the luteal phase in group 2. During the third and last oestrous cycle, bacterial inoculation for groups 1 and 2 were done during the luteal and follicular phases respectively. Uterine biopsies were taken 0 hours and 3 hours post-inoculation in all animals. RNA-Seq was performed using Illumina HiSeq sequencing, generating paired-end sequencings. It was found that 2422 genes were upregulated and 2191 genes were down-expressed in response to *E. coli* inoculation,

and similar to that found before (Marth *et al.*, 2015a) it was shown that most of the up-regulated genes relate to the immune response.

After *E. coli* inoculation genes from the Toll-like receptors and NOD-like receptors (TLR2, TLR4, NLRC4, NLRC5, NLRP3 and NLRP12) were significantly up-expressed in the follicular and luteal phases (Marth *et al.*, 2015a). TLR4 is important as it recognizes LPS produced by gram-negative bacteria (Chow *et al.*, 1999), explaining the relationship between its high expression when inflammation is induced by bacteria inoculation. Observations emphasize the complexity involved in the balance between pro- and anti-inflammatory factors when there is current uterine inflammation. Therefore, more complex studies in endometrial gene expression are required to identify genes involved in the process of physiological and persistent endometritis (Marth *et al.*, 2015a).

2.8 | Aims and Objectives

The aim of this study is to use transcriptome technology to better understand the mechanisms of resistance and susceptibility to PMIE. The identification of susceptible mares at the earliest possible stage ie. at pre-breeding examination will improve clinical management of equine endometritis. Therapies and prophylaxis may be improved and investigated once the underlying cause of susceptibility is better understood at the transcriptome level. New endometritis treatments that seek to immuno-modulate uterine response to the challenge may be tested by analysing their ability to restore the transcriptome of an inflamed uterus to the “base profile” transcriptome.

To achieve this, the first aim of this project was to establish whether an endometrial *ex vivo* tissue culture system has the potential to be used as a model to study the equine endometrium, negating the need for whole-animal research. Biopsies were taken from resistant pony mares in the follicular phase of the oestrous cycle at an abattoir for immediate analysis of RNA-Seq (0 hours), and cultured explants were harvested at 24, 48 and 72 hours and subjected to RNA-Seq. It was determined whether the transcriptome profiles of cultured explants were altered once in culture and whether they were representative of the *in vivo* scenario for native ponies free from uterine inflammation. The second aim was to characterise and compare the global gene expression profiles of unchallenged endometrial cultured explants from the follicular and luteal and anoestrous period to better understand the differences in transcriptome profiles due to hormonal changes throughout the oestrous cycle in mares. The third aim was to challenge cultured explants with inflammatory uterine stimulants, use RNA-Seq to determine the changes in transcriptome profiles during inflammation and investigate expression changes that might be linked with the progression of MIE to PMIE. Thereafter, the fourth aim was to compare the transcriptome of pony mares known to be resistant to PMIE with the transcriptome of mares thought to be susceptible to PMIE before breeding, enabling the analysis of genes involved in susceptibility and resistance to PMIE.

CHAPTER 3

GENERAL MATERIALS AND METHODS

3.1 | Animals

Uteri from native pony mares presented for euthanasia were collected at a commercial abattoir (F. Drury & Sons Ltd, Swindon, United Kingdom). Mares were slaughtered by free bullet. Management of the animals, age or reproductive history were unknown. Collection of blood and uteri from mares during the follicular and the luteal phase of the oestrous cycle was carried out between June and August, while collection of samples during the anoestrous phase was carried out in January.

3.2 | Blood Sampling and Tissue Collection

Blood from all native pony mares was collected immediately after death from the jugular vein into a plain vacutainer (367895, BD Vacutainer, Plymouth, UK), kept at room temperature for 1 hour and subsequently kept on ice. Uteri from the same mares were collected and stored on ice along with its corresponding blood tube. In order to predict which mares were in the follicular or luteal phase of the oestrous cycle, as well as during anoestrous period before blood hormone analyses were complete, uteri and ovaries were examined at the abattoir. Uteri and cervix were physically and visually assessed. Ovaries were immersed in a bucket with water and were analysed using an ultrasound scanner (Concept M6, Digital Ultrasound Diagnostic Imaging System, Livingston, UK) for assessment of ovarian structures and follicle measurements. The stage of the oestrous cycle was determined based on the number of fingers passed through the cervical os, the colour and appearance of the cervix, presence/absence of corpus luteum and follicle size (Table 3.1) as previously described (Nash *et al.*, 2008).

Uteri with typical characteristics relating to the appropriate phase of the oestrous cycle required for specific experiments were selected. Blood and uteri were kept on ice and transported back to the laboratory in Aberystwyth within 7 hours. Immediately after arriving at the laboratory, the blood samples were stored at 4 degrees Celsius (°C) for 24 hours and then centrifuged for 10 minutes at 700 x g. Serum was pipetted to 1.5 mL tubes (11926955, Fisherbrand, UK) and frozen at -20 °C until analysis. Serum progesterone (P4) concentration was measured by an enzyme-linked immunosorbent assay (ELISA) kit (EIA 1561, DRG Diagnostics, Germany) following the manufacturer's instructions (Appendix 3.1) to retrospectively confirm the phase of the oestrous cycle for each animal at the time of death.

For uteri collected during the summer months (June-August), which is the period of the year when mares are cycling, P4 concentrations lower than 2 ng/mL indicated that the mare was in the follicular phase and concentrations higher than 2 ng/mL indicated that the mare was in the luteal phase. For uteri collected during the winter (January), a P4 concentration lower than 1 ng/mL indicated that the mare was in anoestrous (Ginther *et al.*, 2006; Nash *et al.*, 2008); (Table 3.1). Equine male serum and female equine serum from a pregnant mare were used as negative and positive controls respectively. The mean intra (n = 3) and inter-assay coefficients of variation (CV) for a low (0.3 ng/mL), medium (2.5 ng/mL) and high (15 ng/mL) were 2.99 % and 10.1 %; 5.25 % and 13.9 %; and 3.21 % and 15.5 % respectively.

Table 3.1. Characterization of the phase of the oestrous cycle. Based on an ultrasonic view of ovaries and physical aspect of the cervix (Addapted from Ginther and Pierson, 1984; Squires *et al.*, 1988; Nash *et al.*, 2008; Miro, 2012).

Stage of the cycle	Ovaries	Cervix	Progesterone concentration
Follicular	One or occasionally two dominant follicles (>35 mm in diameter), absence of corpus luteum, follicle wall increasingly echogenic and follicle changing from spherical to irregular shape before ovulation.	Cervix is red in colour, soft, open and with a 'rose flower' characteristic. Two to three fingers can be passed through the cervix.	< 2 ng/mL
Luteal	Follicles between 5 to 25 mm in diameter, increasing in size as luteal phase progresses. Presence of corpus luteum.	Cervix is pale, closed and with a 'close bud' characteristic. No finger can be passed through cervix at early luteal phase, whereas one to two fingers can be passed through at late luteal phase.	> 2 ng/mL
Anoestrous	Few small follicles (<15 mm). Absence of corpus luteum.	Cervix is pale in colour. Little cervical tone, one finger can be passed through the cervical os.	<1 ng/mL

3.3 | Endometrial Cytology

At the abattoir, endometrial samples for cytology were collected from each uteri using a sterile cytobrush (Cytobrush plus GT, C0112, Carefusion, UK). To avoid contamination that is normally found in the cervix, a sterile plastic pipette (10732742, 25 mL, Corning, Fisher, UK) cut in half was introduced into the cervix to serve as a channel to guide the cytobrush. If the brush contacts the cervix a false-

positive result may appear, given that the amount of bacteria isolated from the cervix is three times higher than that isolated from the uterus (Baker and Kenney, 2007). The cytobrush was inserted into the cervix, cells were harvested from the uterine body and the uterine secretion smeared onto a microscope slide (S8902, Sigma, UK) and left to air dry before transporting back to the laboratory.

In the laboratory, slides were fixed and stained with eosin and methylene blue (Shandon Kwik-Diff Kit, 9990700, ThermoFisher Scientific, UK) by dipping the slide five times (1 second per dip) into the fixative liquid, six times into eosin, and five times into methylene blue. Slides were rinsed by dipping in distilled water. Excess solution was allowed to dry and edges blotted on absorbent paper after every solution. Once dried, the slides were mounted with Canada balsam (C1795, Sigma, UK) and a coverslip (12323138, Fisher, UK) and stored at room temperature.

The cytology slides were evaluated by recording the number of neutrophils per high power field (hpf) (400x) across 10 fields (Diel de Amorim et al., 2016; Leblanc, 2011). Findings were classified as: normal (0 to 2 neutrophils/hpf), moderate inflammation (2 to 5 neutrophils/hpf) and severe inflammation (>5 neutrophils/hpf) (Knudsen, 1964; Brook, 1984; Riddle *et al.*, 2007). Uteri showing moderate to severe inflammation were discarded from the explant culture experiments.

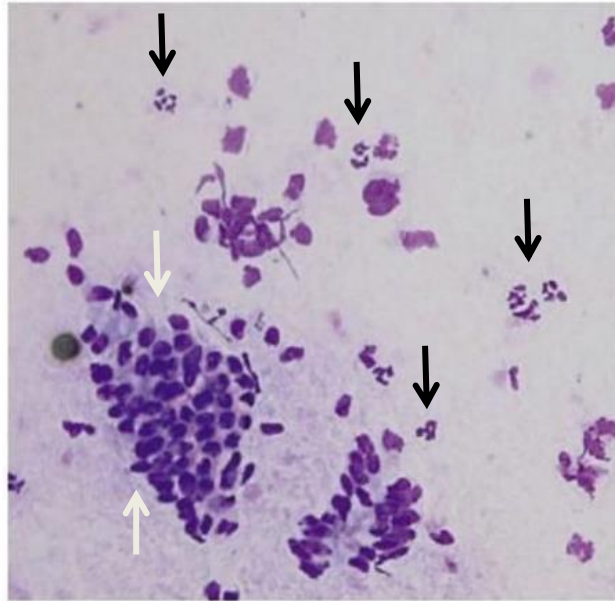


Figure 3.1. Endometrial cytological smear (LeBlanc, 2011). Epithelial cells are marked by white arrows and neutrophils marked by black arrows.

3.4 | RNA-Sequencing Biopsy

At the abattoir, biopsies were taken from the uterine horn bifurcation with the aid of a sterilized biopsy instrument (Equivet uterine biopsy forceps 62cm, 141965, Kruuse, UK). Duplicated biopsies from each uterus were collected and placed into 1.5 mL of RNALater (10437114, Fisher, UK) in RNase/DNase free 2 mL tubes (11598252, Fisher, UK), and kept at 4 °C for 24 hours. RNALater was removed from the tubes and tissues were stored at -80 °C until RNA extraction and retrospective RNA sequencing. These were termed the “0 hours” endometrial biopsies, best representing the whole mare, for RNA-Sequencing (RNA-Seq) analysis.

3.5 | Histology

Immediately after arriving at the laboratory the uteri were dissected. The bench used for dissection was cleaned with 70 % industrial methylated spirit (IMS) twice, aluminium foil was placed on the bench and 70 % IMS was used to clean the coated

bench top. One uterus was then placed on top of aluminium foil. With the aid of a surgical blade, a biopsy of approximately $1 \times 1 \text{ cm}^2$ was taken from the uterine body including the three layers of the uterus (endometrium, myometrium and perimetrium) and immediately placed in a 15 mL tube (525-0400, VWR, UK) containing 10 mL of Bouin's Fixative Fluid (10821910, Fisher, UK). Biopsies were stored for a maximum period of 6 months at room temperature until used for histological assessment.

After fixation with Bouin's liquid, tissues were subjected to several changes of 70 % ethanol until the yellow colour disappeared. Then, tissues were sectioned and placed into histological cassettes (U4635-1CS, Sigma Aldrich, UK) and subjected to dehydration: 1 hour in 70 % ethanol, 1 hour in 95 % ethanol, 2 hours in a change of 100 % ethanol, another 2 hours in a new change of 100 % ethanol and 2 hours in a final change of 100 % ethanol. Following dehydration, tissues were subjected to 3 different changes of fresh xylene (10588070, Fisher, UK) for 2 hours each (total of 6 hours). Cassettes were then submerged in molten wax at 60 to 65 °C overnight, followed by 3 hours in a change of molten wax and then a final and fresh change of molten wax for 3 more hours. Tissues were embedded into wax moulds using the cassettes as mounts for the blocks and transferred to a container filled with cold water to float and harden. Each block was trimmed using a blade to ensure a clear surface of the tissue and placed on the microtome. Blocks were cut upon a microtome (Minot 1212 rotary microtome, Leitz Wetzlar) into sections of 8 μm , floated out on a water bath at 50 °C, placed onto a microscope slide (10149870, Fisher, UK) and placed on a hot plate at 40 °C to stretch the section. Slides were left to drain for at least 30 min.

Sections were placed in a glass slide holder and de-waxed by immersing in two changes of xylene for 4 min each, followed by rehydration in descending concentrations of ethanol (5 min in absolute ethanol, 2 min in 90 % ethanol, 2 min in 70 % ethanol), and then rinsed in distilled water (4 dips). Sections were stained with Harris haematoxylin (Appendix 3.2) for 15 min, washed in tap water (4 dips) and differentiated in 1 % acid alcohol for 5 sec. Slides were washed in tap water for 10 min and rinsed (4 dips) with absolute alcohol before staining with alcoholic 1 % eosin (Appendix 3.2) for 5 min. Slides were subjected to three changes of 100 % ethanol for 1 minute each. Slides were then cleared in xylene three times (3 min each) and mounted with a Histomount solution (008030, Life Technologies, UK) and a coverslip. Slides were left to dry and analysed under a light microscope.

Histology slides were assessed by a Board Certified Veterinary Pathologist (Roger Alison) following the Kenney classification (Kenney, 1978); (Table 3.2) to indicate pathological or degenerative endometrial changes.

Table 3.2. Kenney classification of the endometrium (Kenney, 1978).

Category ^a	Endometrial findings
I	Endometrium is considered normal, with no pathological changes and absence of atrophy and/or hypoplasia; or pathologic changes are slight and scattered.
II	Light to moderate diffuse infiltrations, or scattered but frequent foci in the stratum compactum and the stratum spongiosum. Fibrotic changes such as frequent scattered involvement of individual gland branches or nests of branches (average of 3 fibrotic gland nests per 5.5 mm in 4 linear fields). Scattered lymphatic lacunae.
III	Widespread periglandular fibrosis (average of 5 or more fibrotic gland nests per 5.5 mm in 4 linear fields). Widespread inflammatory changes (continuous infiltration). Infiltration of plasmocytes if moderate or heavy. Endometrial hypoplasia. Extensive lymphatic lacunae.

^a Grading/categorical system for equine endometrial biopsies

As a result of the histological assessment, mares showing pathological or degenerative endometrial changes correspondent to category III (as described in Table 3.2), were discarded from tissue culture.

3.6 | Endometrial Explant Culture

Supplemented William's Medium

William's Liquid E Medium (William's phenol red free, 500 mL, A12176-01, Life Technologies, UK) was supplemented with 0.01 µg/mL epidermal growth factor (EGF) (Recombinant Human Protein, 10605-HNAE-250, Life Technologies, UK) (Appendix 3.2), 0.1 mg/mL neomycin (N6386, Sigma, UK) and streptomycin (S6501, Sigma, UK) solution (Appendix 3.2), 2 miliMolar (mM) of L-Glutamine (25030-032, Life Technologies, UK), 2.5 µg/mL amphotericin B (A2942-20ML, Sigma, UK), 5 mL of insulin-transferrin-selenium (ITS) (Gibco, 100X, 10524233, Fisher, UK) and 50 mL of batch tested foetal bovine serum (FBS) (Invitrogen FBS Heat Inactivated 500 mL, 10695023, Fisher, UK). The supplemented medium was stored at 4 °C for a maximum period of 7 days.

Supplemented Hank's Balanced Salt Solution

A volume of 100 mL of Hank's Balanced Salt Solution (HBSS) (1X, 500 mL, no calcium no phenol red, 14175053, Life Technologies, UK) was supplemented with 0.1 µg/mL EGF, 1 mL of 10 mg/mL neomycin and streptomycin solution (Appendix 3.2), 2 mM of L-Glutamine, 2.5 µg/mL Amphotericin B, 1 mL of ITS and 10 mL of FBS. Supplemented HBSS was stored at 4 °C for a maximum period of 2 days.

Endometrial culture procedure

With a surgical blade, the uterine horns were dissected and endometrium was exposed. With the aid of a sterile biopsy punch (8 mm Kai Biopsy punch, BP-80F, Northumbrian Medical Supplies, UK), sterile scissors and tweezers, endometrial biopsies were collected (Figure 3.2., A). Punch biopsies were immediately placed in a 50 mL sterile tube (525-0402, VWR, UK) containing 20 mL of warm supplemented HBSS. Each uterus was processed using a different sterile set of punch biopsies, scissors and tweezers. Tubes containing biopsies in supplemented HBSS were left in the incubator (5 % CO₂, 38 °C) while biopsies from other uterus were being collected. Once biopsies had been collected from all uteri, the tissue culture was assembled in a laminar flow hood (Microflow Biological, Bioquell, Hampshire, UK). Tubes containing endometrial punch biopsies were removed one mare at the time and taken to the hood, while the other tubes of the remaining mares were kept in the incubator. Once in the flow hood, the supplemented HBSS in the tube was discarded and the biopsies were washed twice with 20 mL of un-supplemented HBSS. With the help of a sterile pipette tip, the punch biopsies were individually placed in a sterile petri dish (11329283, Fisher, UK; Figure 3.2 B), weighed and the weight recorded.

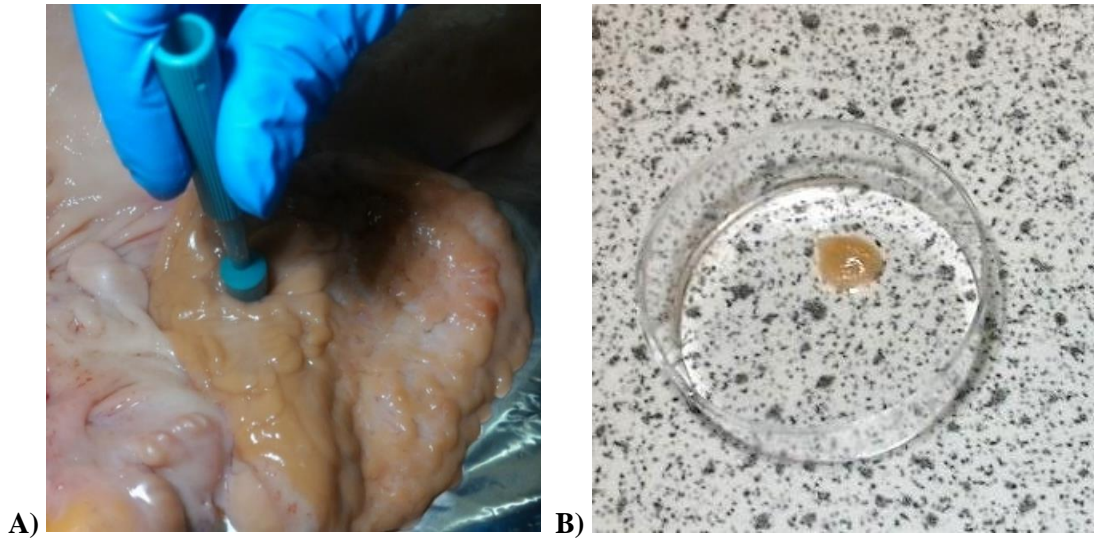


Figure 3.2. Preparation of equine endometrial explants for the tissue culture. (A) Collection of endometrial explants using a sterile punch biopsy and (B) An intact endometrial explant in a sterile petri dish after being washed with HBSS ready to be weighed and placed in the culture medium.

During the initial experiments of the tissue culture model (Chapter 4), the protocol previously described by Nash *et al.* (2008) was followed. Briefly, sterile wire gauze platforms were placed into each well of the culture plate and onto it a piece of sterile lens cleaning tissue (11769994, Fisher, UK) was added, as shown in Figure 3.3 (A). To accomplish this, an aluminium mesh and lens cleaning tissue were cut into squares that could fit within the wells. All aluminium squares had their top and bottom edges folded inwardly so that they formed a platform. Both wire gauze platforms and lens cleaning tissue were autoclaved at 121 °C for 20 minutes before use. Each biopsy was placed individually into one well of a six-well culture plate (10578911, Fisher, UK), on top of the lens-tissue lined wire platform. Into each well 4.25 mL of supplemented William's medium was added. However, after a preliminary radioimmunoassay (RIA) analysis of Prostaglandin $F_{2\alpha}$ ($PGF_{2\alpha}$) production as a marker of inflammation after *Escherichia coli* (*E. coli*) lipopolysaccharide (LPS) challenge, it was determined that the greater volume of medium might be diluting the production of $PGF_{2\alpha}$ by the explants (data not shown).

Therefore, the volume of supplemented William's medium added to each well was decreased to 3 mL. Furthermore, following the decrease in media volume, the wire platforms and the lens tissue were removed, following the protocol described by Borges *et al.* (2012) as also shown in Figure 3.3 (B). Due to the difficulty in collecting samples at the correct stage of the oestrous cycle, especially those at follicular phase, explants cultured in both volumes of supplemented William's media were used in this study.

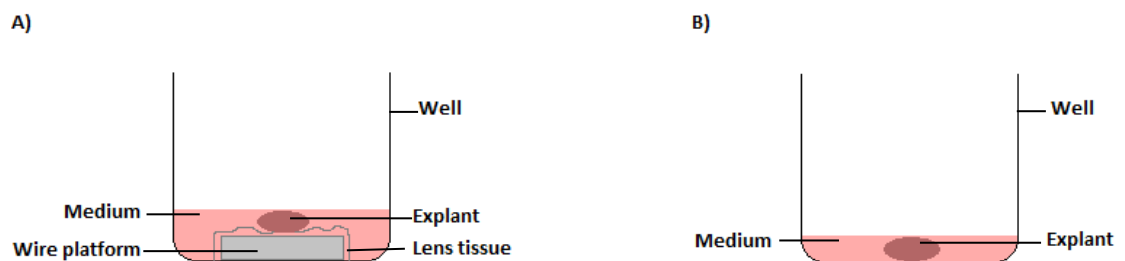


Figure 3.3. Preparation of each well for tissue culture. (A) Individual well with 4.25 mL of supplemented William's medium and explant placed on top of a wire platform covered with lens tissue and (B) Individual well with 3 mL of supplemented William's medium and explant placed directly on the bottom of the well.

Uterine inflammation was induced in the laboratory by challenging the explants with different concentrations of LPS (LPS-EB ultrapure tlr1-3pepls, *E.coli* 0111:B4 strain, Invivogen, UK). A 5 mg/mL stock solution of LPS was prepared by adding 1 mL of endotoxin-free water to the lyophilized LPS vial and mixing by pipetting followed by gentle vortexing. Upon resuspension, aliquots were prepared and stored at -20 °C for a maximum period of 6 months.

The explant culture was performed in triplicate for group/treatment per animal. For all experiments, the tissue explants were incubated at 38 °C in 5 % CO₂ in air, in a humidified incubator. After periods of 24, 48 and 72 hours the explants appropriate to treatments and the specific experiment were removed from the well and stored in

1.5 mL of RNALater for a 24 hour period at 4 °C. After that, the RNALater was removed and the tissue was stored at -80 °C for future RNA extraction. Depending on the experiment, 1 mL of the medium from each well was also removed in duplicate at each time point using a Pasteur pipette (BR747775, Sigma, UK), stored in 2 mL tubes (11598254, Fisher, UK) and frozen at -20 °C. Culture medium was subjected to RIA for retrospective analysis of PGF_{2α} concentration.

3.7 | Prostaglandin F_{2α} Radioimmunoassay

Radioimmunoassays were performed to quantify PGF_{2α} production by the cultured explants in the medium (Cheng *et al.*, 2001); (Appendix 3.3). The standard curve for the assay was prepared in 0.05 molar (M) tris buffer containing 1 g gelatin (440454B, BDH), 0.2 g sodium azide (S-8032, Sigma, UK), 6.61 g tris HCl (T-3253, Sigma, UK) and 0.97 g tris base (T-1503, Sigma, UK) in 1 L of distilled water at 7.4 pH. Samples of cultured medium were diluted in Tris buffer in a 1:50 dilution.

Briefly, PGF_{2α} tracer (NET433250UC, Perkin Elmer, UK) was used in a working concentration of 10000-12000 counts per minute (cpm)/mL and the chosen dilution for PGF_{2α} antiserum was 1:1000. A stock solution of 1 mg/mL of PGF_{2α} standard (P0314-1MG, Sigma, UK) was made up by adding 1 mL absolute ethanol to a 1 mg vial of PGF_{2α} (P0314-1MG, Sigma, UK). Eight standard concentrations were made up (0.025, 0.05, 0.10, 0.25, 0.5, 1, 2.5 and 5 ng/mL) by dissolving the stock solution in Tris buffer. Each standard was run in triplicate and samples were run in duplicate. The assay procedure included tubes (11778908, Fisher, UK) allocated for Buffer blanks (NSB), standards (Std), total binding (TB), total counts (TC), quality controls (QC) and test samples. Reagents were added as follows: 100 µL of tracer to all tubes; 100 µL of antiserum to all tubes except TC and NSB; 500 µL of buffer to TC, 300

μL of buffer, 200 μL of buffer to TB and 100 μL of buffer to Std, QC and tests; 100 μL of sample to QC and tests and 100 μL of standards to Std.

Tubes were vortexed and incubated at 4 °C for 16-24 hours. Two hundred microliters of charcoal dextran solution containing 0.4 % dextran (3190, Sigma, UK) and 2 % activated charcoal (C404053, Fisher, UK) were added to each tube except TC. Tubes were vortexed, incubated for 10 min at 4 °C and centrifuged at 1000-1500 x g at 4 °C. The supernatant was decanted into labelled 6 mL scintillation tubes (E1412-7000, Star Lab, UK). Four millilitres of scintillation liquid (1200-436, Perkin Elmer, UK) were added to each tube. Tubes were counted as cpm for 2 min. Normalised percent bound for each standard/sample was gained with the following equation:

$$\%B/B0 = \frac{(standard\ or\ sample\ cpm - NSB\ cpm)}{(B0\ cpm - NSB\ cpm)} \times 100\%$$

A standard curve was generated by plotting the normalised percent bound as a function of the log₁₀ PGF_{2α} concentrations. The mean intra-assay (n=2) and inter-assay CV for a low (0.05 ng/mL), medium (0.50 ng/mL) and high (5.00 ng/mL) samples were 2.29 % and 8.66 % (low), 3.87 % and 15.6 % (medium) and 4.92 % and 9.56 % (high), respectively.

3.8 | RNA Extraction and RNA-Sequencing

Total RNA was extracted from endometrial samples using an RNA purification kit (GeneJET RNA Purification Kit, Thermo Scientific, UK) following the manufacturer's instructions (Appendix 3.4). Briefly, frozen endometrial tissue was placed in a safe lock tube (0030123328, Fisher, UK) containing 300 μL of supplemented lysis buffer and a stainless-steel bead (69989, 5mm, Qiagen, UK). The

tissue was disrupted using a rotor-stator homogenizer (TissueLyser LT, 85600, Qiagen, UK) and centrifuged for 2 minutes at 12000 x g to pellet any cell debris. The supernatant was transferred to a RNA/DNase free tube (11598252, Fisher, UK) containing 600 μ L of diluted Proteinase K and incubated at 15-25 °C for 10 minutes. Tubes were centrifuged for 10 min at 12000 x g, the supernatant was transferred into a new RNase-free tube and 400 μ L of 100% ethanol was added to each tube. The lysate was transferred to a purification column inserted in a collection tube, centrifuged for 1 min at 12000 x g, the flow-through was discarded and the purification column was placed back in the collection tube. When all lysate was transferred and centrifuged, the collection tube was discarded. The purification column was placed into a new collection tube, 700 μ L of supplemented wash buffer 1 were added to the RNA purification column and centrifuged for 1 min at 12000 x g. The flow-through was discarded, the purification column was placed back into the collection tube, 600 μ L of supplemented wash buffer 2 were added into the purification column and centrifuged for 1 min at 12000 x g. The flow-through was discarded, the purification column was placed back into the collection tube, 250 μ L of supplemented wash buffer 2 were added to the purification column and centrifuged for 2 min at 12000 x g. Finally, the collection tube containing the flow-through solution was discarded and the purification column was transferred to a sterile tube, where 100 μ L nuclease/RNase-free water was added to the purification column membrane and centrifuged for 1 min at 12000 x g to elute RNA.

The kit produced a final volume of 100 μ L purified RNA for each sample. The NanoDrop 1000 Spectrophotometer (Thermo Scientific, UK) was used to check RNA concentration and purity by pipetting 1 μ L of total RNA sample onto the measurement pedestal. In addition, RNA samples were subjected to gel

electrophoresis to assess RNA integrity before gene expression analysis. A 1 % agarose gel was prepared by dissolving 1.5 g of agarose (16500100, Life Technologies, UK) in 150 mL of Tris base, acetic acid and EDTA (TAE) buffer (B49, Life Technologies, UK) by heating in a microwave, the solution was allowed to cool down and 1.5 μ L of gel red (41003, VWR, UK) was added. The gel and the tray were set inside the electrophoresis chamber, sufficient TAE was added to cover the entire gel and the comb was removed. Six microliters of RNA sample was mixed with 6 μ L of loading dye (R0641, Life Technologies, UK), incubated for 10 minutes at 4 °C and loaded into the gel. Four microliters of RNA Ladder were mixed with 4 μ L of loading dye and loaded in the gel. Gel electrophoresis was run at 100 volts and 3.00 amperes for 75 minutes. Gels were imaged using the U: Genius Syngene machine (12814068, Fisher, UK). Integrity of RNA samples was confirmed through visualization of distinct 28S and 18S ribosomal RNA bands as shown in Figure 3.4. RNA samples were stored at -80 °C until used for RNA seq.

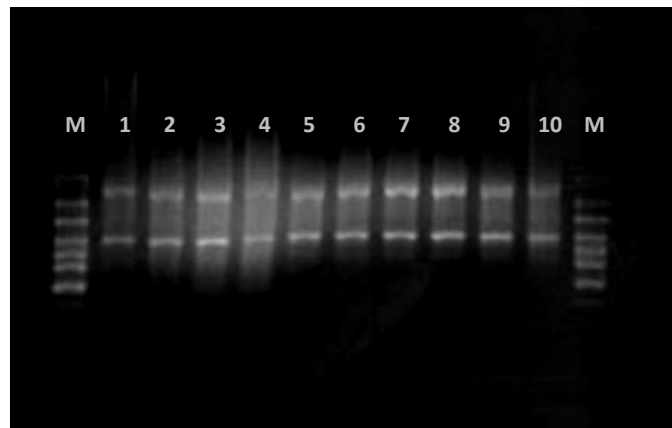


Figure 3.4. Agarose gel electrophoresis (1% agarose) of RNA extracted samples. Lanes 1-10 represent the RNA extracted from 10 different samples. The 18S and 28S ribosomal RNA bands indicate the RNA samples were intact. Lane M, RNA loading dye + ladder marker.

Preparation of RNA samples was performed by Dr Matt Hegarty at the Translational Genomics facility based at the Gogerddan Campus, Aberystwyth University. According to the manufacturer's instructions, the Illumina TruSeq Stranded mRNA

kit (20020594, Illumina) was used to prepare the dual-indexed next-generation sequencing libraries. Briefly, from each sample poly-A messenger RNA (mRNA) was purified, fragmented and reversed transcribed into complementary DNA (cDNA). The cDNA was end-repaired and connected to adaptors that contained unique indexes for each sample. The connected products were amplified by a polymerase chain reaction (PCR) for approximately 15 cycles, followed by purification with AMPure (A63882, Beckman Coulter, UK) to remove PCR reagents and adaptor dimers. Product quantity in ng/ μ L was assessed using a Qubit fluorescence spectrophotometer (Thermo Fisher Ltd). After calculation of the molarity, each sample was diluted in Tris buffer to 10 nanomolar (nM) and equally pooled to obtain a 10 nM pool. Another dilution to 1 nM was made with additional buffer and also 0.1 M NaOH to denature DNA and, to consequently make it single-stranded. Following denaturation, Illumina hybridisation buffer was added to dilute to 20 picomolar (pM) and from there a final dilution based on the type of library was chosen for each experiment.

RNA-Seq was performed at the Translational Genomics facility (Gogerddan Campus, Aberystwyth University, Aberystwyth, Wales, UK) and also at the Wales Gene Park Institute (Institute of Medical Genetics, Cardiff University, Cardiff, Wales, UK). The diluted library was loaded, bound and amplified onto a flowcell using an Illumina cBOT platform. The flowcell was then transferred to the HiSeq2500 or HiSeq4000 sequencer platform for sequencing, depending on the experiment. Paired-end sequencing runs in the 2x75 bp format or in the 2x216 bp format were performed. Raw reads retrieved from RNA-Seq were stored as FASTQ files in the High Performance Computing (HPC) at Aberystwyth University.

3.9 | Data Processing and Gene Expression Analysis

The following steps of the analysis were operated through the UNIX shell; no graphical user interface was included. Raw reads were subjected to quality analysis using FastQC software (version 0.11.2) and filtering using Trimmomatic software (version 0.33) when needed. After trimming, filtered reads were assessed using FastQC one more time. Reads were mapped to the *Equus caballus* reference genome (Ensembl, EquCab2; GCA_000002305.1) using Bowtie software (version 2.2.3) and TopHat software (version 2.0.14), resulting in a binary format (BAM) alignment file for each read. The number of reads/fragments assigned to genomic features for each sample were counted using the BAM files and the *Equus caballus* annotation file available from Ensembl website (version EquCab2.89) using the FeatureCounts software (version 1.5.2). The computer codes used are described in Appendix 3.5.

At first, the RNA-Seq analysis for differentially expressed genes (DEG) was carried out following the Tuxedo Protocol (Trapnell *et al.*, 2012). The workflow aimed to compare the transcriptome profiles of two or more biological conditions. Cufflinks assembled the reads into transcripts for each condition by using the reference genome. These assemblies were then merged together and used to calculate the expression levels for all samples. Cuffdiff then tested the statistical significance of each change in expression between all samples. Genes with fragments per kilobase million (FPKM) values smaller than 1.0 were removed, as well as genes not mapped to the genome. DEGs were then submitted to the Database for Annotation, Visualization and Integrated Discovery (DAVID) website (Huang *et al.*, 2009) (<https://david.ncifcrf.gov>).

However, after analysing the RNA-Seq data from the first experiment, it was noted that Cuffdiff was not the best statistical package to analyse the data for this study. It models the length of the fragments created from each transcript across samples and it is also excessively conservative by over controlling the false positive rate of the algorithms (Trapnell *et al.*, 2012; Love *et al.*, 2014). Therefore, DEGs were identified using the DESeq2 R/Bioconductor version 1.16.1 (Anders and Huber, 2010; Love *et al.*, 2014).

DESeq2 uses raw RNA-Seq counts to identify DEG (Gentleman *et al.*, 2004). Based on the data of each individual gene the gene-wise dispersion is estimated, modelling the variability between replicates (Love *et al.*, 2014). The estimation assumes that genes have similar dispersion if they show similar average expression strength, and a precise estimation of gene dispersion is crucial for the analysis of differential expression. Figure 3.5 represents the shrinkage for dispersion estimation, where the black dots represent the gene-wise dispersion estimates of individual genes, with a red curve fitted to it to capture the overall trend of the dispersion and blue dots representing the shrinkage of the gene-wise estimates towards the red line (Love *et al.*, 2014).

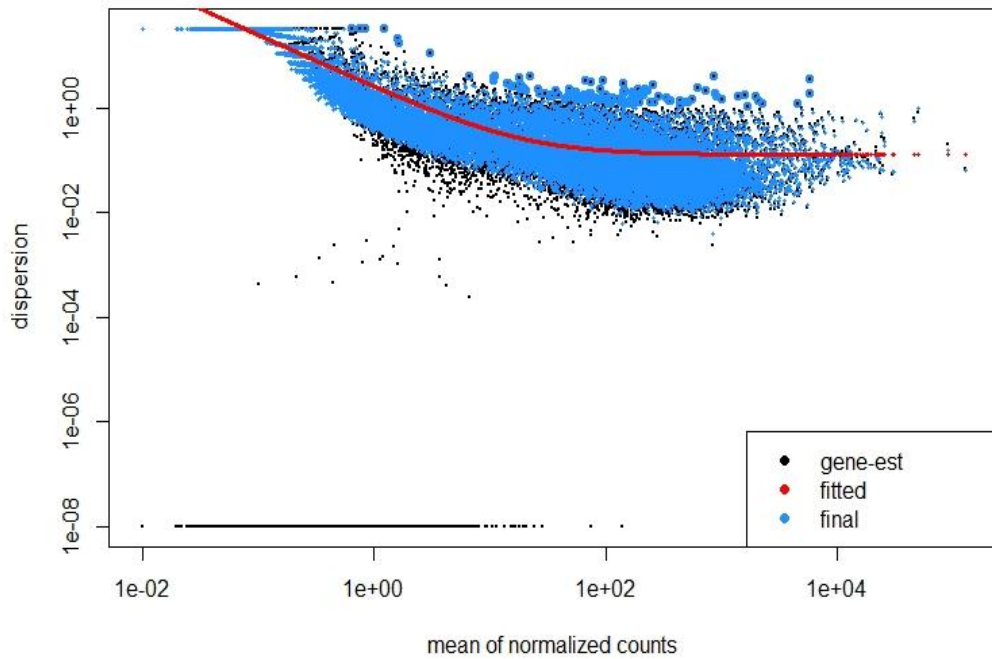


Figure 3.5. Shrinkage estimation of dispersion. Black dots represent gene dispersion of each gene. The red line represents the overall trend of dispersion-mean dependence. Blue dots represent the shrinkage gene-wise final dispersion values based on the red line.

The null hypothesis used by DESeq2 is that there is no effect of the different time points on the genes and that the observed difference between time points is random or due to experimental variability. For each gene, DESeq2 performs a hypothesis test to decide against the null hypothesis or not. The result of the statistical test is reported as a P value. DESeq2 uses the log fold change to estimate the gene's expression changes between time points, which is a value reported on a logarithmic scale to base 2 (Log_2FC). The P value expresses the probability that the observed fold change for each gene is observed under the situation described by the null hypothesis (Gentleman *et al.*, 2004). The Benjamini-Hochberg (BH) false discovery rate (FDR) method (Benjamini and Hochberg, 1995) was performed in R (version 3.4.1) to correct for multiple testing. Genes were considered differentially expressed at an FDR of 0.05 with a Log_2FC greater or equal to 2.

The principal component analysis (PCA) plot is an effective tool for RNA-Seq quality control and outlier sample removal (Gabriela *et al.*, 2016). Using the R “ggplot” visualization package (version 2.2.1) PCA plots were created, displaying each sample in the data set and visually representing the overall effects of experimental conditions and individuals (mares) for each experiment.

Genes with reading count lower than 1000 across all samples were removed from the enrichment analysis. DEGs were then submitted to the Search Tool for the Retrieval of Interacting Genes/Proteins (STRING) database (Szklarczyk *et al.*, 2015) (<http://string-db.org>) for retrieval of protein-protein interactions (PPI), network analysis and gene associations discovery. Also, KEGG (Kyoto Encyclopedia of Genes and Genomes;) (Kanehisa and Goto, 2000) (<http://www.genome.jp/kegg>) pathways retrieved from STRING were listed for each experiment, as well as submitted to the advanced KEGG pathway mapping tool “Search&Color Pathway” to produce graphical images of the differentially expressed genes within the pathways. Furthermore, the Gene Ontology (GO) (Ashburner *et al.*, 2000) terms retrieved from STRING were discussed for each experiment.

CHAPTER 4

CHARACTERIZATION OF CULTURED EQUINE ENDOMETRIAL TRANSCRIPTOME AT DIFFERENT TIME POINTS TO STUDY THE EXPLANT TISSUE CULTURE

4.1 | Introduction

Endometritis is one of the most common and important reproductive conditions causing infertility in mares (Watson, 2000; Troedsson and Woodward, 2016). After natural mating or artificial insemination, a normal and transient endometrial inflammation takes place in response to the presence of bacteria and semen in the uterus, which is resolved within 36-48 hours post-mating. However, persistent endometritis causes infertility in mares unable to resolve inflammation within this time (Kotilainen *et al.*, 1994; Troedsson, 1999; Watson, 2000). The mechanisms underlying the transition of normal mating-induced endometritis (MIE) to the pathological persistent post-mating induced endometritis (PMIE) are still not well elucidated. Depending on each individual susceptible mare, many different variables can be associated with endometritis (Hurtgen, 2006).

An *ex vivo* equine endometrial explant system has been used previously to measure endometritis via biomarker secretion such as Prostaglandin $F_{2\alpha}$ ($PGF_{2\alpha}$). It has been proven that endometrial explants maintained their colour and appearance throughout the 72 hours culture period. It has also been observed that explants from the uterine horns tend to be more responsive to biomarkers of inflammation than explants from the uterine body (Nash *et al.*, 2008). It is proposed that the equine explant system is representative of the whole endometrium considering that tissues are composed of epithelial, stromal and resident leukocytes (Nash *et al.*, 2008). Nonetheless, it was not known how the transcriptome from explants is modified once in culture. Establishing an *ex vivo* cultured explant model at the transcriptomic level is crucial for studying the equine endometrial innate immunity as a baseline for future studies studying inflammation in the endometrium using this model.

Alternative model systems include epithelial and stromal cell culture, yet as a model, these do not necessarily represent the whole animal because of disruption of the endometrial architecture and also cell damage. Additionally, most tissue explant models mechanically chop the tissue aiming for better oxygenation and perfusion of nutrients, which also leads to damage and disruption of tissue architecture (Borges *et al.*, 2012). Damage-associated molecular patterns (DAMPs) are intracellular and extracellular molecules typically released by the extracellular matrix after cell death and/or injury. DAMPs therefore modulate the innate immune system, triggering inflammation even under sterile conditions (Chen and Nuñez, 2010; Krysko *et al.*, 2011). Previous *ex vivo* bovine studies have adopted an intact biopsy endometrium model that better mimics the whole cow (Borges *et al.*, 2012; Saut *et al.*, 2014). Thus, it was proposed that a similar *ex vivo* equine endometrial explant model may act in a similar way in the equine endometrium. The present study used such an equine endometrial explant culture, proposed by Nash *et al.* (2008), but substituting the mechanical tissue chopper for sterile punch biopsies, used by Borges *et al.* (2012), to tackle the issues described above.

Therefore, the aim of the present study was to determine whether *ex vivo* endometrial explants collected from native pony mares cultured over a period of 72 hours were representative of the *in vivo* scenario for native ponies in the pre-breeding, non-inflammatory state on the transcriptome level. If cultured explants provide a true baseline transcriptome before challenge, they have potential application for future study of endometritis.

4.2 | Materials and Methods

4.2.1 | Animals

Uteri from native mares (n=8) presented for euthanasia at an abattoir were collected during the follicular phase of the oestrous cycle and transported back to the laboratory on ice. The population sampled represented a random selection of native mares available at the abattoir and information regarding these animals was unknown.

4.2.2 | Sample Collection

Sample collection was performed as described in Chapter 3. Briefly, blood for all the native pony mares was collected from the jugular vein immediately after death, except for mare number 7. At the abattoir, ovaries were scanned and the cervix physically examined to assess the phase of the oestrous cycle. Blood samples were stored at 4 °C for 24 hours, centrifuged and blood serum used to analyse progesterone concentration to confirm the phase of the oestrous cycle retrospectively. Records of criteria used in the abattoir to predict the stage of the oestrous cycle and serum progesterone concentrations are described in Table 4 1.

Endometrial smears for cytology were collected using a cytobrush and microscope slides, fixed and stained as previously described (Chapter 3). Neutrophil counts for the eight mares were < 2 per high power field (400x), therefore endometrium was classified as normal (non-inflamed). Based on these criteria all uteri collected were included in the experiment. At the abattoir, endometrial biopsies from the uterine bifurcation were collected in duplicate with the aid of a sterile biopsy instrument and stored in 1.5 mL of RNALater at 4 °C for 24 hours. After a period of 24 hours,

RNALater was removed and samples stored at -80 °C until RNA extraction. These biopsies represent the “0 hours” samples, representing the whole mare. Uteri and blood samples were placed on ice and transported back to the laboratory within 7 hours.

After transportation to the laboratory, from each uteri a 1x1 cm² biopsy was taken from the uterine body and stored in 10 mL of Bouin’s fixative liquid for a period of 2-6 months for posterior histological analysis of pathological or degenerative endometrial changes. The histology report of mares providing endometrial explants for this experiment is summarised in Appendix 4.1.

Table 4.1. Summary of mares sampled at the abattoir. Information regarding ovarian structures, cervical analysis and serum progesterone concentration.

Mare	Ovaries ^a	Cervix ^b	Progesterone Concentration (ng/mL) ^c
1	One 41 mm x 32 mm follicle on left ovary. Small follicles (around 7 mm in diameter) on right ovary.	Cervix pale in colour. Two fingers were passed through cervix	1.95
2	One small (10 mm in diameter) follicle on left ovary. One 33 mm x 37 mm on right ovary.	Cervix pale in colour. Three fingers were passed through cervix.	0.16
3	Two follicles (42 mm x 48 mm ; 39mm x 39 mm) on left ovary. Small follicles (around 15 mm in diameter) and a regressing CL on right ovary.	Cervix pale in colour. One to two fingers were passed through the cervix.	Undetectable
4	One 38 mm x 45 mm follicle on left ovary. Regressing CL on right ovary.	Cervix pink in colour, soft and open. Two to three fingers were passed through the cervical os.	0.32
5	One 39 mm x 49 mm follicle on left ovary. Regressing CL on right ovary.	Cervix had a colour that varied from pale to light pink. Three fingers were passed through the cervical os.	0.47
6	One 30 mm x 30 mm and a few small follicles on the left ovary. Regressing CL on left ovary. One 30 mm x 25 mm follicle on right ovary.	Cervix was becoming red. One to two fingers were passed through the cervical os.	0.64
7	Two follicles (52 mm x 39 mm ; 50 mm x 30 mm) on left ovary. Regressing CL on left ovary. Small follicles (10 mm in diameter) on right ovary.	Cervix pale in colour. One finger was passed through the cervical os.	No blood
8	Small follicles on left ovary. One 42 mm x 36 mm follicle on right ovary.	Cervix pink in colour. Four fingers were passed through the cervical os.	0.05

^a Ultrasonographic measurements of ovaries.

^b Physical examination of cervix.

^c ELISA serum progesterone analysis for confirmation of stage of the oestrous cycle.

4.2.3 | Endometrial Tissue Culture

Following the protocol described in Chapter 3, endometrial punch biopsies were collected from each uterus and placed into warm supplemented HBSS and left in the incubator (5% CO₂, 38 °C) while the other uteri were being processed and before tissue culture began. Biopsies were washed twice with unsupplemented HBSS before tissue culture was initiated. Each punch biopsy was weighed in a sterile petri dish and individually placed into a different well of the 6-well culture plate, on top of the lens tissue-lined wire platform. To each well, a volume of 4.25 mL of supplemented William's medium was added. All explants were cultured in triplicate.

Plates were incubated in a humidified incubator at 38 °C in 5 % CO₂ for 24, 48 and 72 hours. At each time point, the three explants from each mare were removed from their respective well and individually stored in 1.5 mL of RNALater for 24 hours at 4 °C, after which RNALater was removed and samples were frozen at -80 °C until RNA-extraction.

4.2.4 | RNA Extraction and RNA-Sequencing

Total RNA was extracted from all samples resulting in a total of 32 RNA samples. The Nanodrop machine was used to check RNA concentration and quality. In addition, RNA samples were subjected to electrophoresis gel to assess RNA integrity before gene expression analysis. Samples were diluted in DNase/RNase free water to the final concentration of 30 ng/μL in a total volume of 50 μL and sent to RNA-Sequencing (RNA-Seq).

RNA-Seq was performed by Dr Matt Hegarty at the Translational Genomics facility based at the Gogerddan Campus, IBERS, Aberystwyth University. Each sample of total RNA was reverse transcribed into a cDNA sequencing library using the TrueSeq RNA sample

preparation kit and paired-end sequences were created using the Illumina HiSeq 2500 machine. For this experiment, the final library dilution was 8 pM.

4.2.5 | Data Processing and Gene Expression Analysis

The pair-end sequencing produced forward and reverse reads for each sample, totalling 64 raw reads. The quality of each raw read was checked as previously described in Chapter 3, using the FasQC software. Reads were then filtered by the following Trimmomatic (version 0.33) steps: sequencing adapters were removed (i.e. ILLUMINACLIP), bases off the start of a read were removed if the quality was below 30 (i.e. LEADING = 30), bases off the end of a read were removed if the quality was below 30 (i.e. TRAILING = 30), a sliding window trimming approach was performed once the average quality within the window fell below 30 (i.e. SLIDINGWINDOW 4:30), reads were dropped if they were below a specific length of 100bp (i.e. MINLEN = 100), and a specified number of 10 bases from the start of the read were removed (i.e. HEADCROP = 10). The quality of the trimmed reads was assessed by FASTQ. The 32 reads were mapped to the *Equus caballus* reference genome (Ensembl, EquCab2; GCA_000002305.1) using TopHat software (version 2.0.14) as described in Chapter 3, resulting in 32 BAM alignment files. Total count of reads assigned to genomic features for each sample was retrieved from both the BAM files and the equine annotation file (Ensembl website, EquCab2.89) using FeatureCounts software (version 1.5.2). Computer codes used in this chapter are shown in Appendix 4.2 and Table 4.2 compares information about each sample.

Table 4.2. Summary of the 32 RNA-Sequencing samples.

Sample	Mare	Time point ^a	Total sequences Raw reads ^b	Sequences after trimming ^c	Mapped reads ^d	Alignment rate ^e	Total count ^f
1	1	0h	19717258	8502094	7038297	82.5%	4935705
2	1	24h	67308470	32342562	27290172	84.1%	20643708
3	1	48h	19839515	9954298	8415638	84.3%	6389708
4	1	72h	14432128	7358130	6262279	84.7%	4618836
5	2	0h	18178744	9085634	7476789	82.1%	5301029
6	2	24h	12681202	6069612	5153439	84.6%	3966757
7	2	48h	30143876	15499068	13394112	86%	10212117
8	2	72h	12826353	6530807	5634759	85.9%	4232183
9	3	0h	20960250	10117417	8728814	86.0%	5970499
10	3	24h	15509308	7851773	6745965	85.7%	5082456
11	3	48h	16948027	8578848	7405235	86%	5642663
12	3	72h	25647761	13313650	11604766	86.8%	8782806
13	4	0h	28670134	13715002	11290844	82.0%	8083377
14	4	24h	20422712	10795659	9354169	86.4%	7080569
15	4	48h	15788862	8014918	6990433	86.9%	5260783
16	4	72h	18383955	9131700	7871686	85.9%	6013728
17	5	0h	22947695	9857331	8497119	85.9%	6103661
18	5	24h	21849937	10419618	8921018	85.4%	6717715
19	5	48h	24772671	12453536	10832088	86.7%	8256983
20	5	72h	23018161	11156075	9762271	87.2%	7511617
21	6	0h	18112353	9450237	8129631	85.8%	5743608
22	6	24h	18419612	10260890	8858564	86.1%	6704169
23	6	48h	19130571	10543071	9249797	87.4%	6885048
24	6	72h	18810862	10857330	9744804	89.4%	7217846
25	7	0h	18438679	8526023	7439831	86.9%	5339891
26	7	24h	20176785	10709870	9454038	87.9%	7122759
27	7	48h	25947827	14121856	12386310	87.4%	9565446
28	7	72h	21821418	11656927	10321964	88.2%	8111957
29	8	0h	24180545	13500189	11858759	87.5%	8700692
30	8	24h	18784516	9993324	8813179	87.8%	6835047
31	8	48h	22175150	11562073	10131838	87.3%	7462079
32	8	72h	19340153	9988254	8757692	87.3%	6209711

^a Specific time-points when explants were removed from culture.^b A count of the total number of sequences processed.^c Number of sequences actually used for the rest of the analysis after quality filtering.^d Number of reads mapped to the annotated equine genome.^e Percentage of reads mapped to the annotated equine genome.^f Counts of reads assigned to genomic features.

Firstly, RNA-Seq analysis was carried out following the Tuxedo Protocol (Trapnell *et al.*, 2012). Two different approaches for analysis of differentially expressed genes (DEGs) were performed by executing two different Cuffdiff scripts (Appendix 4.2). The first approach analysed the DEGs sample by sample, whereas the second approach analysed DEGs at each of the four different time points (0, 24, 48 and 72 hours), using the samples from each animal as replicates. DEGs were submitted to the Database for Annotation, Visualization and Integrated Discovery (DAVID) website (Huang *et al.*, 2009) (<https://david.ncifcrf.gov>) for investigation, functional annotation and enrichment analysis of genes of interest.

DEGs were also identified using the DESeq2 package (version 0.11.2) (Appendix 4.2) to enable comparison of results. Three tests were performed in total: between the 0 and 24 hours, between 24 and 48 hours and between 48 and 72 hours. DEGs from DESeq2 were submitted to the Search Tool for the Retrieval of Interacting Genes/Proteins (STRING) database (Szklarczyk *et al.*, 2015) (<http://string-db.org>) for the discovery of functional gene associations and protein-protein interaction (PPI) networks.

The Kyoto Encyclopedia of Genes and Genomes (KEGG) pathways (Kanehisa and Goto, 2000; Kanehisa *et al.*, 2016; Kanehisa *et al.*, 2017) (<http://www.genome.jp/kegg>) and Gene Ontology terms (GO) terms (Ashburner *et al.*, 2000) were used to identify significantly enriched pathways.

4.2.6 | Statistical Analysis

Cuffdiff package

Reads mapped to each transcript were calculated and normalized by the length of each transcript to calculate the transcripts' individual expression level. The linear statistical model with maximum likelihood estimated transcripts abundance was performed by Cuffdiff

(Trapnell *et al.*, 2010; Trapnell *et al.*, 2012). Cuffdiff revealed DEGs at the default false discovery rate (FDR) of 0.05 (Benjamini and Hochberg, 1995). Significance was assumed where $P < 0.05$.

DESeq2 package

The negative binomial distribution was used to perform statistical inference on differences. The P value for multiple tests was corrected using the FDR method (Benjamini and Hochberg, 1995). Genes with a reading count lower than 1000 across all samples were removed from the differential analysis. Genes were considered differentially expressed at an FDR of 0.05 with a logarithmic fold change (Log_2FC) greater or equal to ± 2 .

4.3 | Results

4.3.1 | Cuffdiff

Sample to sample analysis

Sample by sample results were analysed and from a total of 13212 genes found to be expressed, none were statistically significantly differentially expressed. A heat map was created (Figure 4.1) for the gene expression data, displaying a cluster analysis to illustrate the association between experimental conditions. The highest value was 1.0 where the association between conditions was identical (colour red) and the lowest value was 0.5 (colour green). Mid-range values were correlations of 0.7 and 0.8, which correspond to transition between these two extremes. The gene expression in unstimulated explants at 0 hours (expressing the gene expression for mares at a time as close as possible post-mortem) was characterized by the red area in the left corner. The correlation was high (between 0.8 and 1); showing that the *ex vivo* 0 hours samples are similar to each other (Figure 4.1).

Similarly, the gene expression of cultured explants (24, 48 and 72 hours) is shown in the red area on the top right-hand side. Likewise, the correlation between the *in vitro* cultured explants was high (between 0.8 and 1; Figure 4.1).

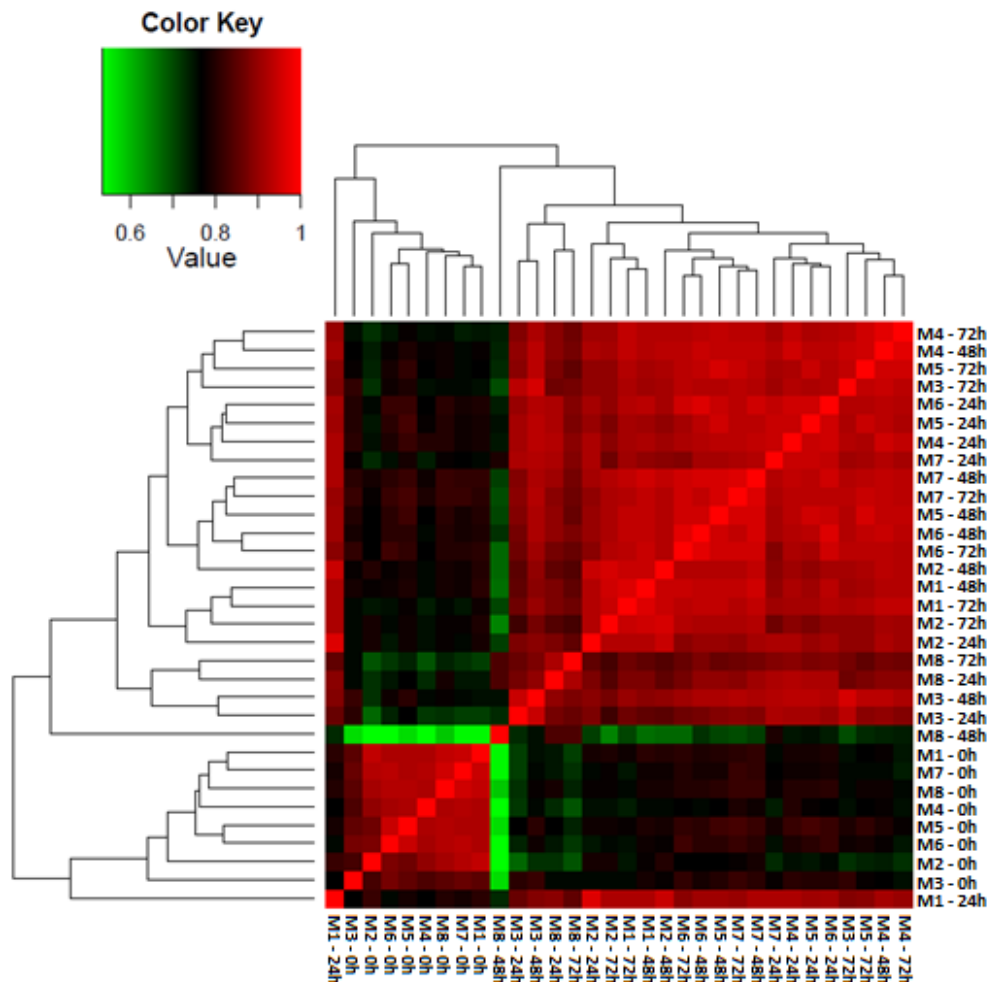


Figure 4.1. Cuffdiff sample-to-sample distances. Sample-to-sample gene expression variation calculated from fragments per kilobase of exon per million reads (FPKM) in eight horses from which equine endometrial explants were sampled at 0 hours then cultured for 24, 48, and 72 hours. Samples identity are as follow: “M” – Mare, numbers “1” to “8” refers to mares’ numbers (Table 4.1).

When comparing the three-time points (either 24, 48 or 72 hours) to samples at 0 hours a correlation can also be seen. The most predominant colour was black, indicating that the correlation is around 0.8 (between 0.7 and 0.9). From a total of 13212 genes found to be expressed, none was statistically significantly differentially expressed ($P < 0.05$) when comparing the 32 samples at the four-time points between themselves.

Time point analysis

From the Cuffdiff output, the pairwise comparisons between 0 and 72 hours were retrieved. A list containing 3523 unique DEGs ($P < 0.05$) when comparing the 0 hours (control) to the 72 hours transcriptome was created and fed into DAVID. The Functional Annotation Chart from DAVID reported 46 significantly enriched GO terms ($P < 0.05$) (Appendix 4.3). The majority of genes were enriched for cellular component terms such as extracellular exosome, cytoplasm, focal adhesion, external side of plasma membrane correlated with biological processes such as cell adhesion (Table 4.3).

Table 4.3. Summary of the 5 most enriched GO terms between 0 hours (control) and 72 hours sorted. Table created using the “Functional Annotation Chart” from DAVID website. Results sorted by p-value.

GO Category ^a	Term name ^b	Description ^c	Count ^d	FDR p-value ^e
GO Component	GO.0070062	Extracellular exosome	644	2.06×10^{-41}
GO Component	GO.0005925	Focal adhesion	130	2.71×10^{-19}
GO Component	GO.0005737	Cytoplasm	598	9.30×10^{-12}
GO Component	GO.0009897	External side of plasma membrane	68	3.37×10^{-10}
Go Biological Process	GO.0007155	Cell adhesion	56	1.12×10^{-07}

^a GO domains (cellular component, biological process and molecular function).

^b Term associated with gene ontology biological processes.

^c Description of each GO category.

^d The number of genes involved in each biological process term.

^e Over-represented p-value with false discovery rate statistical correction for multiple comparisons.

Genes were also clustered by DAVID into smaller biological annotation modules, organizing redundant terms within the cluster groups based on the enrichment score. Enrichment scores categorize the overall importance of genes clusters, therefore a high score (> 1.3) indicates that genes in the clusters perform an important role in the study (Huang *et al.*, 2009). A total of 19 high score (> 1.3) clusters were retrieved (Appendix 4.4), however only two of them were significant ($P < 0.05$) as shown in Tables 4.4 and 4.5.

Table 4.4. First most enriched cluster between 0 hours (control) and 72 hours. Table created using the “Functional Annotation Clustering” from DAVID website.

Annotation Cluster 1 - Enrichment Score: 5.99			
Category ^a	Term ^b	Count ^c	FDR p-value ^d
UP_KEYWORDS	Integrin	19	0.000
INTERPRO	IPR013649:Integrin alpha-2	14	0.001
INTERPRO	IPR000413:Integrin alpha chain	14	0.001
INTERPRO	IPR018184:Integrin alpha chain, C-terminal cytoplasmic region, conserved site	13	0.002
INTERPRO	IPR013519:Integrin alpha beta-propellor	14	0.004
INTERPRO	IPR013517:FG-GAP repeat	13	0.014
SMART	SM00191:Int_alpha	14	0.020

^a Gene functional categories.

^b Term associated with each category.

^c The number of genes involved in each biological process term.

^d Over-represented p-value with false discovery rate statistical correction for multiple comparisons.

Table 4.5. Second most enriched cluster between 0 hours (control) and 72 hours. Table created using the “Functional Annotation Clustering” from DAVID website.

Annotation Cluster 2 - Enrichment Score: 4.06			
Category ^a	Term ^b	Count ^c	FDR p-value ^d
UP_KEYWORDS	EGF-like domain	38	0.026
INTERPRO	IPR001881:EGF-like calcium-binding	37	0.075
INTERPRO	IPR000152:EGF-type aspartate/asparagine hydroxylation site	31	0.099
SMART	SM00179:EGF_CA	37	1.731

^a Gene functional categories.

^b Term associated with each category.

^c The number of genes involved in each biological process term.

^d Over-represented p-value with false discovery rate statistical correction for multiple comparisons.

4.3.2 | DESeq2

Analysis was carried out using DESeq2 (Anders and Huber, 2010; Love *et al.*, 2014) to identify significantly DEGs and associated over-represented biological pathways across the endometrial transcriptome. Based on the data of each individual gene the gene-wise dispersion was estimated, modelling the variability between replicates (Love *et al.*, 2014). Figure 4.2 shows the distance between samples' matrix. The dark navy blue colour is set for

distance 0, meaning that the samples being compared are identical. The blue colour fades as the distance between samples increase.

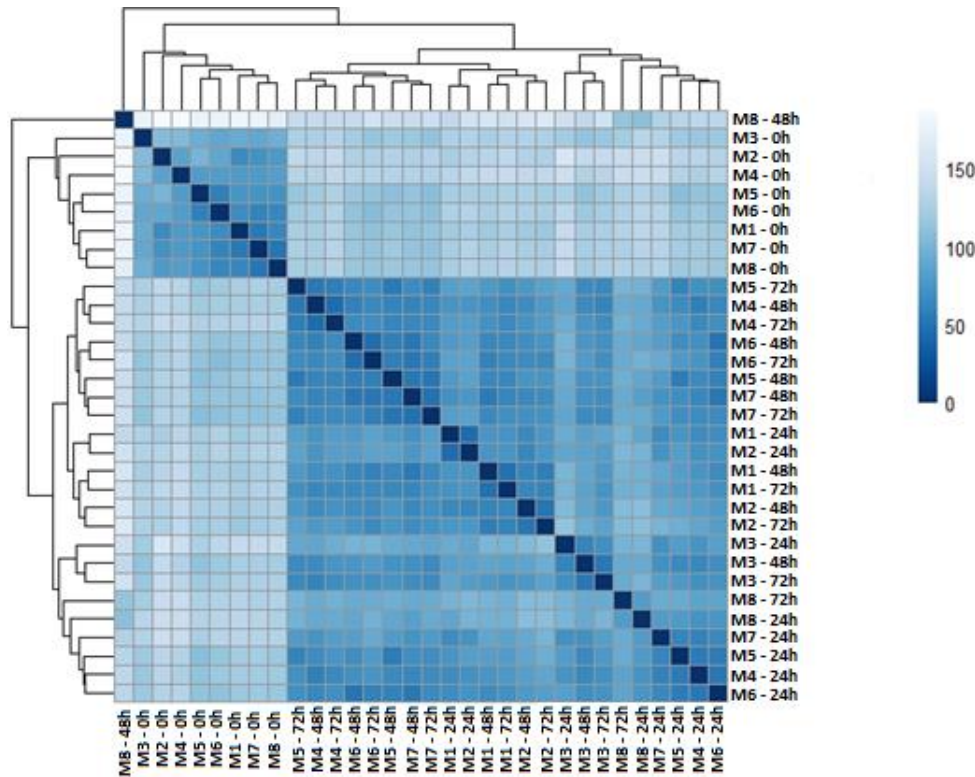


Figure 4.2. DESeq2 sample-to-sample distances. The Euclidean distances between samples calculated from the regularized log transformation of the count reads in eight horses from which equine endometrial explants were sampled across the 4-time points (0, 24, 48 and 72 hours). Samples identity are as follow: “M” – Mare, numbers “1” to “8” refers to mares’ numbers (Table 4.1).

The PCA plots (Figures 4.3 and 4.4) display each sample in the data set, visually representing the overall effect of experimental conditions and mares on the count matrix. In both figures there is a clear separation of control (0 hours) groups and cultured samples by the first component (PC1). However, from Figure 4.3 it can be seen that there is an outlier.

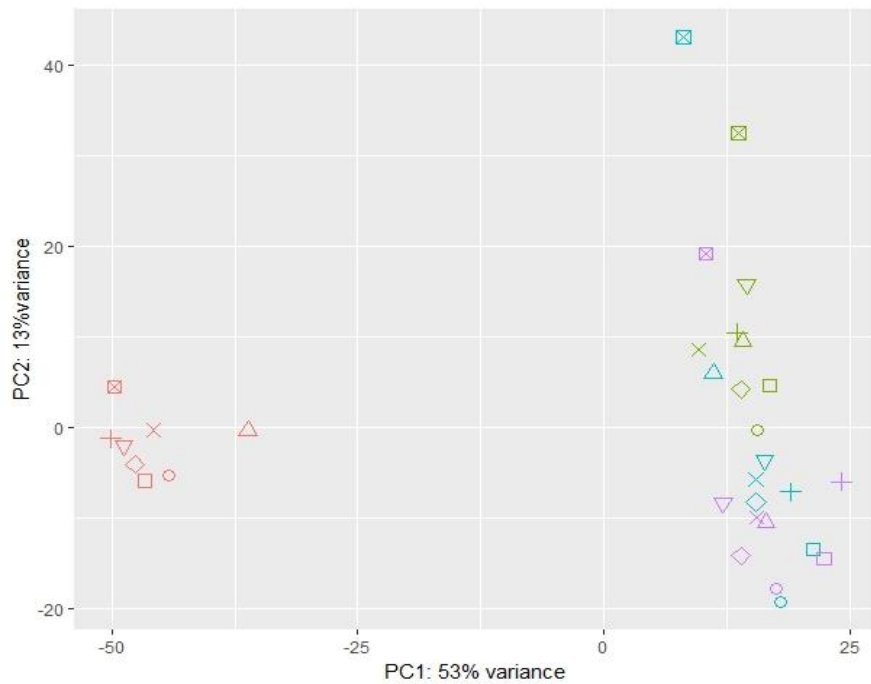


Figure 4.3. PCA plot of the gene expression profiles for the eight horses. Biopsies taken at **0 hours** and explants cultured up to **24, 48** and **72 hours** (n=8). The plot displays each sample in the dataset, where each horse is represented by a unique shape: Mare 1 (\square), mare 2 (\circ), mare 3 (\triangle), mare 4 ($+$), mare 5 (\times), mare 6 (\diamond), mare 7 (∇) and mare 8 (\boxtimes). The analysis clearly demonstrates clustering for the 0h (control, representing the whole mare) and another cluster for the cultured samples (24, 48 and 72 hour time points). Horse 8 (\boxtimes) is clearly an outlier, not clustering well with the other seven horses across all time points.

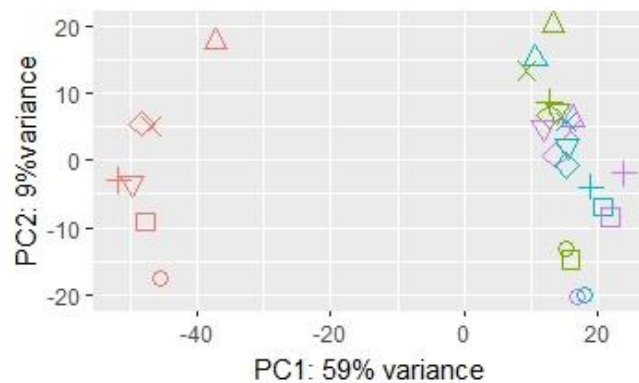


Figure 4.4. PCA plot of the gene expression profiles for the seven mares included in the analysis. Biopsies taken at **0 hours** and explants cultured up to **24, 48** and **72 hours** excluding Mare number 8 (\boxtimes) (n=7). The plot displays each sample in the dataset, where each time point is represented by a unique colour and each horse by a unique shape: Mare 1 (\square), mare 2 (\circ), mare 3 (\triangle), mare 4 ($+$), mare 5 (\times), mare 6 (\diamond), mare 7 (∇). Analysis still demonstrates clusters for 0h and for cultured samples (24, 48 and 72 hours). Variance is lower after removal of the outlier horse.

Mare number 8 was responsible for the majority of variance when comparing Figures 4.3 and 4.4. Maintaining this horse in the differential expression analysis could bias the results, leading to unreliable analysis (Gabriela *et al.*, 2016). For this reason, horse 8 was removed and analysis for DEGs was performed with DESeq2.

Differential gene expression analysis between time points was performed (n=7). The null hypothesis for each gene tested using DESeq2 was that there was no difference in its expression between time points. The null hypothesis was rejected when the observed difference in expression of a gene was greater than expected by random chance (using an adjusted p-value of 0.05).

When comparing control (0 hours) to 24 hours a total of 11266 genes were found to be expressed, 385 of which were shown to be statistically significantly differentially up-regulated and 589 shown to be statistically significantly differentially down-regulated, both at a FDR of 0.05 and $\text{Log}_2\text{FC} \geq \pm 2$. Similarly, when comparing the gene expression between 24 and 48 hours, 11266 genes were found to be expressed. At FDR of 0.05 and $\text{Log}_2\text{FC} \geq \pm 2$, only 17 genes were significantly differentially up-regulated while 50 genes were significantly down-regulated. Again, 11266 genes were found to be expressed between 48 hours and 72 hours, however not even one gene was shown to be statistically significantly up-regulated, and only 1 gene was down-regulated at an FDR of 0.05 and $\geq \pm 2 \text{Log}_2\text{FC}$.

The STRING functional enrichment analysis of DEGs between 0 hours (control) and 24 hours using the 11266 total expressed genes as the statistical background was performed. A PPI (protein-protein interaction) p-value of 1.0^{-16} was retrieved, meaning that the genes/proteins show more interactions between themselves than that evident in a similar size of random genes. The predicted STRING network was composed of 924 nodes and 792 edges. The STRING enrichment analysis returned a total of 45 KEGG pathways associated with $\text{Log}_2\text{FC} \geq \pm 2$ at an FDR of 0.05 when comparing the transcriptome of 0 relative to 24 hours (Appendix 4.5). The five most statistically significant KEGG terms were “Complement and coagulation cascades”, “Hematopoietic cell lineage”, “Cytokine-cytokine

receptor interaction”, “PI3K-Akt signalling pathway” and “ECM-receptor interaction” which are shown in more detail in Table 4.6.

Table 4.6. Summary of the 5 most enriched KEGG pathways when comparing the transcriptome at 0 hours relative to the transcriptome at 24 hours. Associated with $\text{Log}_2\text{FC} \geq \pm 2$ and sorted by p-value. Table created using the STRING website.

Pathway code ^a	Description ^b	Count ^c	FDR p-value ^d
04610	Complement and coagulation cascades	26	6.33×10^{-15}
04640	Hematopoietic cell lineage	49	4.8×10^{-11}
04060	Cytokine-cytokine receptor interaction	24	1.01×10^{-9}
04151	PI3K-Akt signalling pathway	18	1.51×10^{-9}
04512	ECM-receptor interaction	22	2.69×10^{-9}

^a KEGG pathway identification code.

^b Description of each KEGG pathway.

^c The number of genes involved in each pathway.

^d Over-represented p-value with false discovery rate statistical correction for multiple comparisons.

DEGs linked to the “Complement and coagulation cascades” and in the “Cytokine-cytokine receptor interaction” were fed to the “KEGG Color and Pathway Search” (Figure 4.5 and 4.6 respectively).

[illegible]

105

A total of 71 redundant GO terms (Appendix 4.5) were retrieved from the enrichment analysis between 0 (control) and 24 hours. The five GO terms with the highest enrichment were “Extracellular region”, “Extracellular region part”, “Cellular component”, “Biological process” and “Single-organism process” (Table 4.7).

Table 4.7. Summary of the 5 most enriched GO terms when comparing the transcriptome at 0 hours relative to the transcriptome at 24 hours. Associated with $\text{Log}_2\text{FC} \geq \pm 2$ sorted by p-value. Table created using the STRING website.

GO Category ^a	Term name ^b	Description ^c	Count ^d	FDR p-value ^e
Cellular component	GO.0005576	Extracellular region	24	5.94×10^{-11}
Cellular component	GO.0044421	Extracellular region part	20	1.33×10^{-9}
Cellular component	GO.0005575	Cellular component	33	2.65×10^{-9}
Biological process	GO.0008150	Biological process	33	2.10×10^{-8}
Biological process	GO.0044699	Single-organism process	29	6.84×10^{-8}

^a GO domains (cellular component, biological process and molecular function).

^b Term associated with gene ontology biological processes.

^c Description of each GO category.

^d The number of genes involved in each biological process term.

^e Over-represented p-value with false discovery rate statistical correction for multiple comparisons.

With respect to extracellular matrix (ECM) and extracellular region, collagen coding genes such as COL1A2, COL12A1, COL14A1, COL17A1, COL21A1 and COL4A6 and laminin coding genes such as LAMA2 and LAMA4 were shown to be up- and down-regulated when comparing the transcriptome at 0 hours (control) relative to the transcriptome of 24 hours, with Log_2FC between -2.6 and 4.3.

Pathways related to inflammation and immune system were also reported in the GO enrichment analysis, despite not being in the top 5 most enriched GO terms identified in Table 4.7. The aim is to use the explant model as a baseline for further studies into endometritis, therefore the inflammatory and immune genes and pathways are the most relevant for the assessment of the culture model, validating its suitability for future challenges with bacteria to begin modelling endometritis. Table 4.8 presents an overview of GO biological processes related to inflammation and immune system from the STRING

enrichment analysis. The “Genes” column of the table shows the list of genes related to each GO term. From table 4.8, it can be seen that genes overlap within the four described GO terms, and they are more comprehensively illustrated in Figure 4.7. Closer inspection of table 4.8 shows that most genes were also involved in the KEGG Cytokine-cytokine receptor interaction (Figure 4.6).

Table 4.8. Summary of the 4 enriched GO terms related to inflammation when comparing the transcriptome at 0 hours relative to the transcriptome at 24 hours. Associated with $\text{Log}_2\text{FC} \geq \pm 2$ and sorted by p-value. Table created using the STRING website.

GO Category ^a	Term name ^b	Description ^c	Genes	Count ^d	FDR p-value ^e
Biological process	GO.0006954	Inflammatory response	CCL2, IL1B, IL1A, IL1RN, IL23A, IL4R, IL6, IL8, PTGS2, SPI2, Spi2-8	11	2.04×10^{-6}
Biological process	GO.0002376	Immune system process	CCL2, CD40, CXCL6, IL1B, IL1A, IL23A, IL6, IL8, LTF, PLG, TFRC	11	2.59×10^{-4}
Biological process	GO.0006953	Acute-phase response	IL1B, IL1A, IL1RN, IL6, SPI2, Spi2-8	6	3.83×10^{-4}
Biological process	GO.0006955	Immune response	CCL2, CXCL6, IL1B, IL1A, IL23A, IL6, IL8, LTF	8	0.002

^a GO domains (cellular component, biological process and molecular function).

^b Term associated with gene ontology biological processes.

^c Description of each GO category.

^d The number of genes involved in each biological process term.

^e Over-represented p-value with false discovery rate statistical correction for multiple comparisons.

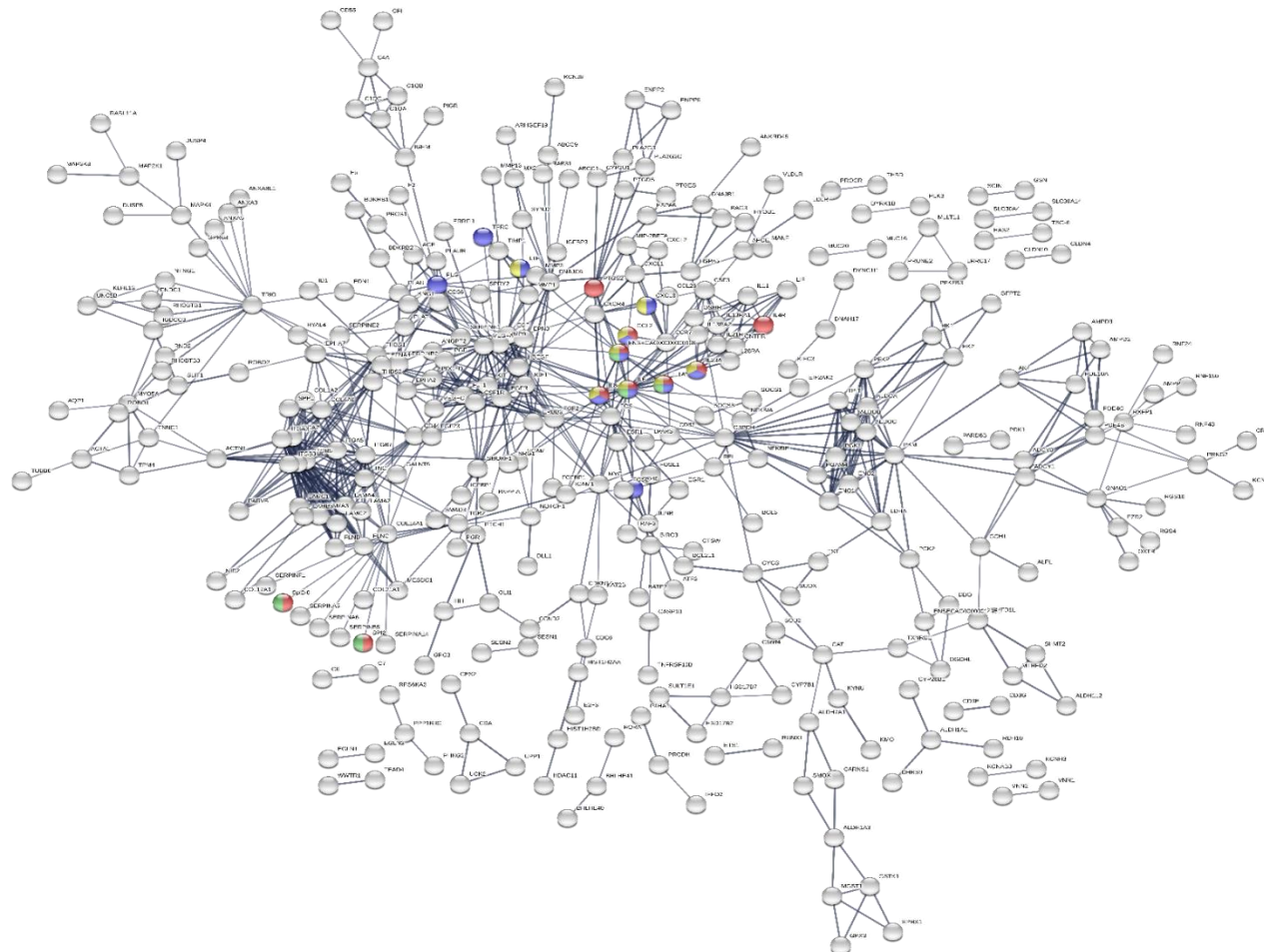


Figure 4.7. STRING predicted PPI network of the DEGs related to immune response and inflammation GO terms between the 0 hours (control) and 24 hours. **Red** nodes represent genes that belong to “Inflammatory response” (GO Biological Process), **blue** nodes represent genes that belong to the “Immune system process” (GO Biological Process), **green** nodes represent genes that belong to the “Acute-phase response” (GO Biological Process) and **yellow** nodes represent genes that belong to the “Immune response” (GO Biological Process). The interaction score between nodes was set to high confidence (0.7), where the thickness of the lines between nodes indicate the degree of confidence prediction of the interaction. Disconnected nodes are hidden in the network. Image created using the STRING website.

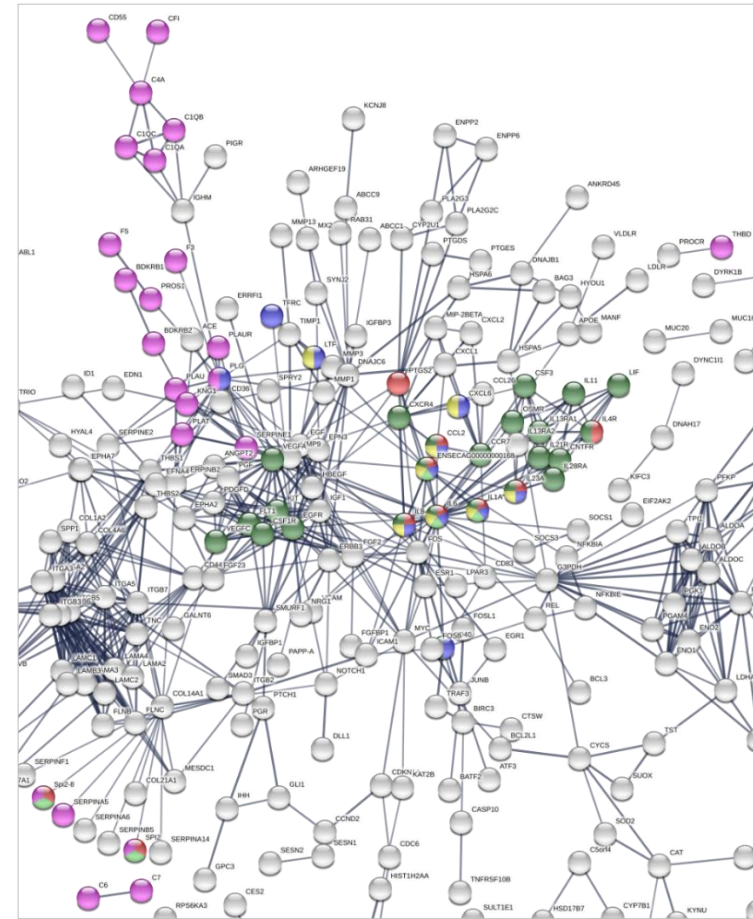
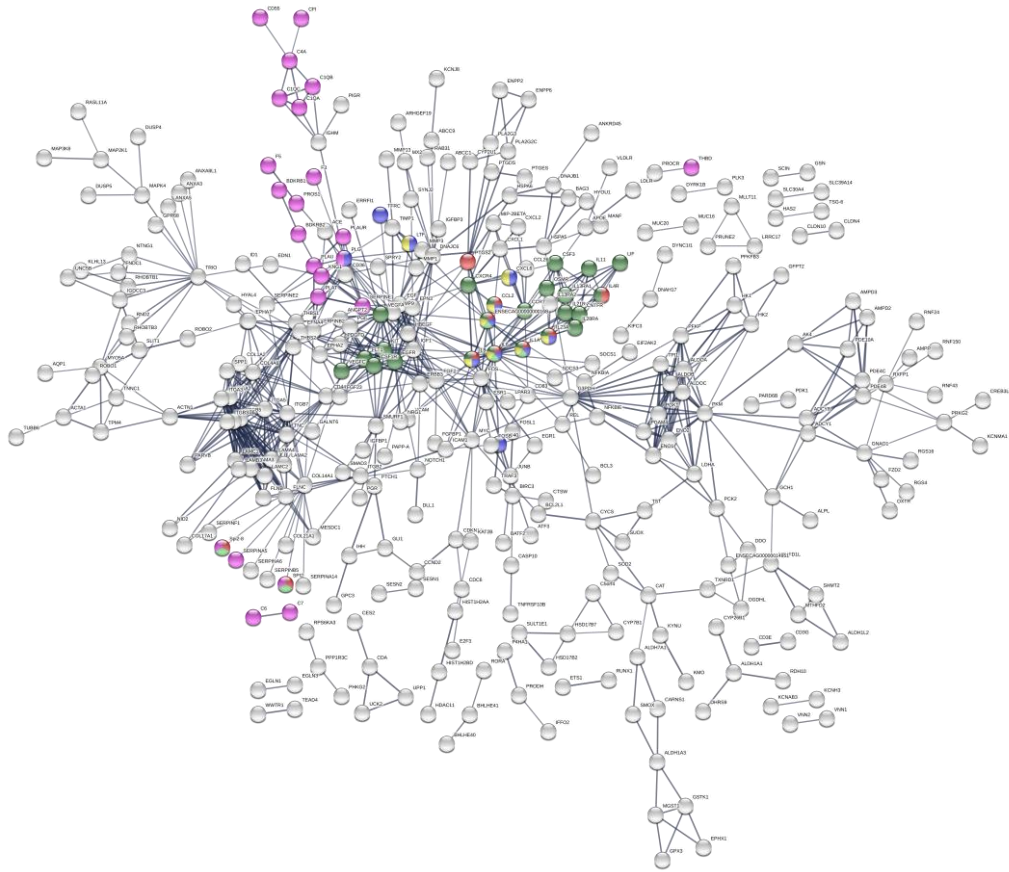


Figure 4.8. STRING predicted PPI network of the DEGs related GO terms and KEGG pathways related to immune response and inflammation between 0 hours (control) and 24 hours. **Red** nodes represent genes the “Inflammatory response” (GO Biological Process), **blue** nodes represent the “Immune system process” (GO Biological Process), **light-green** nodes represent the “Acute-phase response” (GO Biological Process) and **yellow** nodes represent the “Immune response” GO terms. **Pink** nodes represent the “Complement and coagulation cascades” (KEGG) and **dark-green** nodes the “Cytokine-cytokine receptor interaction” (KEGG). The interaction score between nodes was set to high confidence (0.7), where the thickness of the lines between nodes indicates the degree of confidence prediction of the interaction. Disconnected nodes are hidden in the network. The network is zoomed-in for better visualization of target genes.

The genes overlapping between the “Complement and coagulation cascade” KEGG pathway (Figure 4.5), the “Cytokine-cytokine receptor” KEGG pathway (Figure 4.6) and the GO terms in Table 4.8 are considered DEGs relate to innate immunity when comparing the transcriptome of 0 hours relative to the 24 hours. Overlapping genes are CCL2, CD40, IL1A, IL1B, IL23A, IL4R and IL6, showing a Log₂FC down-regulation between -2.7 and -6.10.

The STRING enrichment analysis of DEGs when analysing the transcriptome at 24 hours relative to the transcriptome at 48 hours was performed using the same statistical background. A PPI p-value of 1.0^{-16} was retrieved, indicating that the network had significantly more interactions than expected. There were 63 nodes and 66 edges in the PPI network. Only 2 KEGG pathways were significantly enriched in this network (Table 4.9) and no GO terms were retrieved from the enrichment analysis.

Table 4.9. Summary of the 2 enriched KEGG pathways when comparing the transcriptome at 24 hours relative to the transcriptome at 48 hours. Associated with Log₂FC $\geq \pm 2$ sorted by p-value. Table created using the STRING website.

Pathway code ^a	Description ^b	Count ^c	FDR p-value ^d
05134	Legionellosis	4	0.0248
04110	Cell cycle	5	0.049

^a KEGG pathway identification code.

^b Description of each KEGG pathway.

^c The number of genes involved in each pathway.

^d Over-represented p-value with false discovery rate statistical correction for multiple comparisons.

Analysis of 48 hours relative to 72 hours returned only one down-regulated gene called Collagenase 3 Precursor or MMP13. The PPI p-value was 1, indicating that the predicted network did not have more expected and no enrichment for this gene was retrieved.

4.4 | Discussion

As described in Table 4.1, blood from mare number 7 was not collected and consequently the progesterone concentration at the time of the death was unknown. However, this mare was selected at the abattoir based on the criteria to predict the follicular stage of the oestrous cycle (Table 4.1). Also, based on the PCA plots (Figures 4.3 and 4.4) mare number 7 clustered together with the other mares, demonstrating that it was in the follicular phase of the oestrous cycle. Therefore, mare number 7 was kept in this study.

RNA-Seq analysis has been proven to be challenging mainly because there is a variety of different pipelines for different cases, and none of them are considered optimal overall. The heat maps from the Cuffdiff (Figure 4.1) and the DESeq2 (Figure 4.2) analysis can be compared. The similarity between the heat maps shows the consistency of gene expression from Cufflinks and DESeq2 packages (but not the consistency between differential expression). Analysis of DEGs were carried out using Cuffdiff (Trapnell *et al.*, 2012) and DESeq2 (Anders and Huber, 2010; Love *et al.*, 2014). The discrepancy between the Cuffdiff and the DESeq2 differential analysis results can be attributed to how they deal with the analysis of differential expression genes. In the current experiment, a major problem with Cuffdiff was that it modelled the length of the fragments created from each transcript across all replicates, therefore it normalized fragment counts by transcript length and did not account for differences in coverage (Trapnell *et al.*, 2013). It has also been reported that Cuffdiff over controls the false positive rate of the algorithms, making the analysis excessively conservative (Love *et al.*, 2014). Results for DEGs between Cuffdiff and DESeq2 were compared and DESeq2 seemed to be the most suitable

package for the discovery and analysis of DEGs. Therefore, this discussion will focus mainly on DESeq2 results.

4.4.1 | Cuffdiff

From the DEGs retrieved when comparing the 0 hours (control) transcriptome relative to the transcriptome cultured for 72 hours, ‘Extracellular exosome’, ‘Cytoplasm’, ‘Nucleus’, ‘Signalling pathways’ and ‘Nucleoplasm’ were the five most enriched terms, suggesting that at the level of transcription in the endometrium the explant model was subjected to changes mostly related to cell component.

In this study, genes were also functionally clustered in smaller groups, ranked by enrichment scores (Tables 4.4 and 4.5). Clustering is excellent to highlight important gene groups by functionality based on their annotation terms instead of on individual gene names. This condenses the analysis and results in a more comprehensive understanding of gene association, overcoming the difficulty of analysing many redundant/similar terms within the group (Huang *et al.*, 2009). Between 0 hours (control) and 72 hours, the five most enriched gene groups were ‘Integrin’, ‘Epidermal growth factor’, ‘Tyrosine-protein domains’, ‘Immunoglobulin-like domains’ and ‘Rho GTPase-activating proteins’.

Regarding the clusters represented in Table 4.4, all biological terms retrieved from DAVID were related to integrins. Integrins are transmembrane receptors that regulate cell adhesion, usually binding extracellular matrix (ECM) glycoproteins and connective tissue (Hynes and Zhao, 2000). It has been demonstrated that there is an overexpression of genes linked to ECM in the equine endometrium during the

follicular phase of the oestrous cycle (Marth *et al.*, 2015b), therefore expression of integrins might be expected in this study.

Epidermal growth factors domains mediate intercellular signalling of growth and development (Wouters *et al.*, 2005). Addition of EGF to the culture media may have contributed to the increase of significant expression genes related to the ‘Epidermal Growth Factor’ cluster, suggesting that this cluster may be already expected when analysing the transcriptome of cultured explants. Immunoglobulin-like domains are involved in cell-cell recognition, cell-surface receptors and the immune system, and are found in various protein families (Teichmann and Chothia, 2000). Tyrosine-protein domains relate to cell cycle control regulation such as growth, proliferation, differentiation and transformation (Denu and Dixon, 1998). The Rho GTPase-activating proteins regulate the Rho GTPases that are involved in cellular functions regulations such as gene transcription (Moon and Zheng, 2003).

4.4.2 | DESeq2

Over 1000 genes were observed to be differentially expressed across all time points (0 to 72 hours). In order to better understand these results, enrichment analysis using the GO categories and KEGG pathways were performed between time points. Normally, many gene products were associated with more than one GO category. Table 4.7 presented the most enriched GO terms between 0 and 24 hours, which included “extracellular region part”, “cellular component”, “biological process” and “single-organism process”. These enrichment terms are GO “cellular component” and “biological process” terms, which involve processes relevant to the functioning of cells or specific parts such as the extracellular environment, and processes involving only one organism. The explant tissues need to adapt and maintain their

homeostasis after removal from the mares' uterus, therefore it is not surprising that genes related to biological processes and cell components are differentially expressed between 0 and 24 hours, allowing the explant tissues to remain viable even with a limited availability of nutrients in the culture compared to the whole mare.

On the other hand, the aim of this study was to investigate whether the tissue culture system has the potential to be used for future studies into equine endometritis by challenging the culture with bacterial inoculation. Inflammation is an important portion of the innate immune system, characterizing the first line of defence against attacking microorganisms. Consequently, part of the analysis was focused on genes related to immune system and inflammatory responses (Table 4.8). It is apparent from Figure 4.8 that only a few genes in the network are related to immune system and inflammation.

A study using RNA-Seq to target the global gene expression of the equine uterus under the normal effect of ovarian hormones has already been performed, in which over 1500 genes from the immune system, cellular metabolism and extra cellular matrix were up-regulated during the follicular phase of the oestrous cycle (Marth *et al.*, 2015b). Toll-like receptor 1 (TLR1), chemokines (CXCL6, CXCL10, CXCL16, CXCL17, CCL5 and CX3CL1), chemokine receptors (CXCR4, CXCR7 and DARC), interleukins (IL-8, IL-15 and IL-34), interleukins receptors for IL-1 and IL-17, and the TNF family are examples of significantly up-regulated genes during the follicular phase (Marth *et al.*, 2015b). The results between 0 and 24 hours in the current study are comparable with the results reported in live mares by Marth *et al.* (2015b) in regards to ECM receptor-interaction (Table 4.6), immune system (Tables 4.6 and 4.8; Figures 4.5 and 4.6) and cell function (Table 4.7).

Despite this, little has changed in terms of transcriptome between 24 and 48 hours as shown in Table 4.9. “Legionellosis” was the most enriched KEGG pathway, but only the CXCL1, HSPA1A, HSPA6 and MIP-2BETA genes were related to this pathway. This is an unexpected pathway that is part of the bacterial infectious diseases under the KEGG human disease. However, the four genes can also be found in the “Antigen processing and presentation” KEGG pathway, as well as in the “Estrogen signalling pathway”. Pathways summarised in Table 4.9 were not discussed in more detail as the aim of this study was to focus mainly on the immune and inflammatory responses.

Interestingly, MMP13 was the only down-regulated gene when analysing the transcriptome at 48 hours relative to 72 hours, suggesting that at 48 hours its expression is lower than at 72 hours. Furthermore, it did not show any significant enrichment analysis. MMP13 is a matrix metalloproteinases’ enzyme known to take part in the remodelling of connective tissue during normal or pathological conditions (Woessner, 1991; Murphy and Docherty, 1992). Notwithstanding, there is some evidence to suggest that collagenase-3 transcripts could be associated with malignancy since there was no significant expression of collagenase-3 reported in normal tissue (Freije *et al.*, 1994). It has also been reported that expression of MMP13 is a possible marker of compromised uterine environment in cows (Wathes *et al.*, 2011; Forde and Lonergan, 2012). This finding is somewhat surprising, and it indicates that relevant changes might happen in the endometrial tissue once in culture between 48 and 72 hours. One implication of this is that the explant tissue might not be viable after 48 hours of culture, even though its colour and appearance continued the same.

4.5 | Conclusion

The findings in this chapter indicate that there are significant differences when comparing the transcriptome at 0 hours to the transcriptome of cultured samples. Indeed, some degree of transcriptional changes was expected, considering that it is not possible to perfectly mimic the complex *in vivo* uterine system in an *ex vivo* tissue culture. Interestingly, following culture the transcriptome of explants showed only relatively minor variations as demonstrated in the time point analysis performed by DESeq2. Tissues cultured for up to 48 hours were still viable and interesting results can be withdrawn from studies using the explant system. It is important to bear in mind the possible bias in the responses after 48 hours of culture due to the possible interference of MMP13.

Notwithstanding the fact that the *ex vivo* explant cannot perfectly mimic the endometrium of a live mare since there are significant transcriptomic changes between 0 and 24 hours, the explant model is still useful as a baseline for future studies. Knowing exactly which genes and pathways differ between 0 and 24 hours that are related to inflammation and uterine global function provides the means to set these changes as a baseline. Accordingly, when challenging the explant model with bacteria, inflammatory responses that differ from this ‘baseline’ can be determined and pathways truly related to endometrial inflammation can be further studied. The genes overlapping between the “Cytokine-cytokine receptor” KEGG pathway (Figure 4.6) and the GO terms in Table 4.6 are considered the baseline genes when utilising the explant model to modulate and study endometritis. The baseline is composed of the following overlapping genes: CCL2, CD40, IL1A, IL1B, IL23A, IL4R, IL6 and IL8 (Figure 4.8).

In general, this study provides the first comprehensive assessment of the pre-breeding, non-inflammatory global gene expression analysis for the explant culture model, highlighting the use of abattoir-derived samples to better understand the physiology of the uterus to further study endometritis. It can be concluded that the unchallenged explants are suitable to begin modelling endometritis. The next chapter, therefore, moves on to discuss the differences in gene expression at the level of transcriptome across the different phases of the oestrous cycle.

CHAPTER 5

A COMPARISON OF THE *EX VIVO* AND *IN VITRO* EQUINE ENDOMETRIAL TRANSCRIPTOMIC PROFILES AT THE FOLLICULAR, LUTEAL AND ANOESTROUS PHASES

5.1 | Introduction

The 21-day equine oestrous cycle is divided into the follicular and luteal phase, which last approximately 4-6 days and 15-16 respectively. The anoestrous phase is the non-breeding season and it takes place during the winter (Watson, 1998; Aurich, 2011). Throughout the oestrous cycle, specific physiological and behavioural events are controlled by particular hormones (Aurich, 2011). During the follicular phase, oestrogen is secreted by the developing follicles causing the mare to be sexually receptive to the stallion. Also, during this phase secretory and ciliary endometrial activities are part of the uterine clearance mechanism, enhancing the ability of the uterus to eliminate foreign material introduction during mating (Tunon *et al.*, 1995; Aurich, 2011; Marth *et al.*, 2015b).

The high oestrogen and low progesterone concentrations during the follicular phase also provide a more resistant uterine environment against foreign material introduction during breeding, enhancing immunological response to infection (Marth *et al.*, 2015a). Progesterone levels rise after ovulation (day 0) reaching peak levels on days 6-8 in mares (Ginther *et al.*, 2006; Aurich, 2011). The combination of high progesterone and low oestrogen levels during the luteal phase of the oestrous cycles reduce the uterine oedema and diminish the uterine immune response and the myometrial contractility to prepare the uterine environment for the potential arrival of a conceptus at 5-7 days after ovulation (Evans *et al.*, 1986a; Battut *et al.*, 1997; Cannon, 1998).

Furthermore, during the luteal phase of the oestrous cycle, if challenge occurs, uterine infections tend to develop more easily due to the immune suppression effect of high concentrations of progesterone (Hughes, 1980; Katila, 2001). A study

investigated the effects of steroid hormone on bacterial clearance after intra-uterine inoculation with bacteria, and the presence of progesterone can significantly slower uterine clearance (Evans *et al.*, 1986a). Marth *et al.* (2015a) reviewed many studies (Nishikawa *et al.*, 1984; Evans *et al.*, 1986a; de Winter *et al.*, 1992; Battut *et al.*, 1997; Ramadan *et al.*, 1997) attesting that a higher progesterone concentration is indeed correlated with bacterial growth and inflammatory cell migration in the uterus. It has been suggested that during the follicular phase the equine uterus triggers a more efficient immune response than during the luteal phase of the oestrous cycle (Marth *et al.*, 2015a).

Microarray work has been carried out to explore the *in vivo* gene expression changes during the follicular and luteal phases of the equine oestrous cycle at specific days after ovulation (Days 0, 3, 8, 12 and 16) (Gebhardt *et al.*, 2012). Genes with greatest messenger RNA (mRNA) expression during the follicular phase of the oestrous cycle were associated with the extracellular matrix, focal adhesion process and immune system functions. With regard to the luteal phase, gene expression was linked to protein secretion, signalling processes and metabolic processes (Gebhardt *et al.*, 2012).

One study has used RNA-Sequencing (RNA-Seq) technology to investigate how the ovarian hormones change between the follicular phase and the luteal phase at the level of endometrial gene expression (Marth *et al.*, 2015b). Consistent with the literature, Marth *et al.* (2015b) showed that during the follicular phase of the oestrous cycle the expression of genes related to the innate immune response was up-regulated whereas during the luteal phase the higher expressed genes were mainly associated with metabolic functions.

Nonetheless, little is known about changes in the global gene expression in the equine endometrium throughout the oestrous cycle. The majority of studies have focused on specific genes pertinent to inflammation such as interleukins (IL1, IL1RN, IL6, IL8 and IL10) after uterine challenge with bacteria or semen instead of looking at the global endometrial gene expression during the different phases of the oestrous cycle (Fumuso *et al.*, 2003; Fumuso *et al.*, 2006; Nash *et al.*, 2010a). Moreover, there is a dearth of research that has characterised global gene expression during the anoestrous period.

Understanding differences between each phase of the oestrous cycle at the level of transcriptome will improve the understanding of physiological cyclic variation, thus improving the understanding of pathologies of the reproductive tract in mares such as endometritis. Therefore, the aim of this study was to generate transcriptomic profiles of unchallenged endometrial biopsies at the follicular phase, luteal phase and anoestrous period at three different time points (0, 24 and 48 hours). This research provides an innovative insight into the physiological changes across each stage of the equine reproductive cycle, improving the current understanding of this matter at the level of gene expression.

5.2 | Materials and Methods

5.2.1 | Animals

Uteri from 18 native mares were collected during the follicular phase of the oestrous cycle (n=6), the luteal phase (n=6), and during the anoestrous period (n=6). Tissue collection from the abattoir were carried out between June-August for the follicular and luteal phases experiments, and in January for the anoestrous period. The

population represents a random selection of mares presented for euthanasia (Robertson *et al.*, 2007).

5.2.2 | Sample Collection

Sample collection from native pony mares was accomplished following the previously described protocol (Chapter 3). Briefly, blood was collected directly from the jugular vein and stored at 4 °C for 24 hours, followed by blood serum separation by centrifugation. To confirm the phase of the oestrous cycle at the time of the death the blood serum progesterone concentration was analysed. Records of criteria used in the abattoir to predict the stage of the oestrous cycle and serum progesterone concentrations for each animal are described in Tables 5.1, 5.2 and 5.3.

At the abattoir, cytology samples were collected with the aid of a cytobrush as previously described (Chapter 3). The neutrophil count for endometrium collected from all mares was < 2 per high power field (400x), classifying the uterine tissue as normal. Blood samples and uteri were stored on ice and transported back to the laboratory within 7 hours. From each uterus, endometrial biopsies were taken in duplicate and stored in 1.5 mL of RNALater at 4 °C for a period of 24 hours, followed by RNALater removal and sample storage at -80 °C until RNA extraction. These represent the “0 hours” samples.

At the laboratory, an additional 1x1 cm² endometrial biopsy from the uterine body was collected and stored in 10 mL of Bouin’s fixative liquid for a period of up to 6 months. Histology procedure was carried out as previously described (Chapter 3) and analysed by a Bored Pathologist for pathological and/or degenerative endometrial changes (Appendix 5.1).

5.2.3 | Endometrial Tissue Culture

Following the protocol described in Chapter 3, biopsies were collected from each uterus and stored in the incubator (5% CO₂, 38 °C) immersed in supplemented Hanks' Balanced Salt Solution (HBSS) until all biopsies were harvested for the tissue culture. Before initiating the tissue culture, all biopsies were washed twice in unsupplemented HBSS, individually weighed and individually placed into each well of a 6-well culture plate. During the preliminary stages of the explant tissue culture, there was a development in protocol regarding the volume of media added to each well in the 6-well plate, which is detailed in the General Material and Methods chapter (Chapter 3). Explants from mares 1-7 at the follicular phase of the oestrous cycle (Table 5.1) were collected during the preliminary stages of this project, therefore the tissue culture was carried out using 4.25 mL of supplemented William's medium as described by Nash *et al.* (2008), with the aid of the wire platforms and lens cleaning tissue. However, biopsies taken from mares at the anoestrous phase (Table 5.3; Mares 13-18) were cultured in 3 mL of supplemented William's medium direct in the well, excluding the use of the wire platform and the lens tissue, following the protocol described by Borges *et al.* (2012), also described in detail in Chapter 3. Due to the change in the protocol, mares at the luteal phase of the oestrous cycle (Table 5.2) were cultured in 3 mL of medium (mares 9-12) and also in 4.25 mL of medium (mares 7 and 8).

All explants were cultured in triplicate for each time point and each phase of the oestrous cycle. The culture plates were stored in an incubator at 38 °C in 5 % CO₂. At 24 hours and at 48 hours the explants were removed from the wells and

individually stored in 1.5 mL of RNALater at 4 °C. After a period of 24 hours the RNALater was removed and explants frozen at -20 °C until RNA extraction.

Table 5.1. Summary of mares sampled at the abattoir at the follicular phase of the oestrus cycle. Information regarding ovarian structures, cervical analysis and serum progesterone concentration.

Mares	Month of collection	Ovaries ^a	Cervix ^b	Progesterone Concentration (ng/mL) ^c
1	July	One 41 mm x 32 mm follicle on left ovary. Small follicles (around 7mm in diameter) on right ovary.	Cervix pale in colour. Two fingers were passed through cervix	1.95
2	July	One small (10 mm in diameter) follicle on left ovary. One 33 mm x 37 mm on right ovary.	Cervix pale in colour. Three fingers were passed through cervix.	0.16
3	July	One 38 mm x 45 mm follicle on left ovary. Regressing CL on right ovary.	Cervix pink in colour, soft and open. Two to three fingers were passed through the cervical os.	0.32
4	July	One 30 mm x 30 mm and a few small follicles on the left ovary. Regressing CL on left ovary. One 30mm x 25mm follicle on right ovary.	Cervix becoming red. One to two fingers were passed through the cervical os.	0.64
5	July	Two follicles (52 mm x 39 mm ; 50 mm x 30 mm) on left ovary. Regressing CL on left ovary. Small follicles (10 mm in diameter) on right ovary.	Cervix pale in colour. One finger was passed through the cervical os.	No blood
6	July	One 40 mm in diameter follicle on right ovary. Smaller follicles (around 20 mm in diameter) on left ovary.	Cervix had a pink-pale colour and an open appearance. Three fingers were passed through the cervix	0.21

^a Ultrasonographic measurements of ovaries.

^b Physical examination of cervix.

^c ELISA serum progesterone analysis for confirmation of stage of the oestrous cycle.

Table 5.2. Summary of mares sampled at the abattoir at the luteal phase of the oestrus cycle. Information regarding ovarian structures, cervical analysis and serum progesterone concentration.

Mares	Month of collection	Ovaries ^a	Cervix ^b	Progesterone Concentration (ng/mL) ^c
7	June	One small (20 mm x 15 mm) follicle on the left ovary. One follicle (40 mm x 38 mm) on the right ovary.	Cervix was pale in colour, becoming red. One and a half finger can be passed through the cervical os.	8.44
8	June	One small (10 mm in diameter) follicle and a CL on left ovary. Two follicles (30 mm in diameter) on right follicle.	Cervix was pale in colour, becoming red. One finger was passed through cervix.	20
9	June	One follicle (30 mm in diameter) on left ovary. One follicle (also 30 mm in diameter) on right ovary.	Cervix pale in colour and it was closed.	4.08
10	July	One small follicle on left ovary (20 mm in diameter). One follicle (24 mm x 34 mm) on right ovary.	Cervix was pale, and only one finger was passed through cervix.	36.62
11	August	Small follicles on the left ovary. One follicle (40 mm in diameter) on the left ovary.	Cervix was becoming red. One and a half fingers were passed through the cervical os.	5.82
12	August	Small follicles (smaller than 10 mm in diameter) on left ovary. One follicle 40 mm x 35 mm on right ovary.	Cervix pale in colour. One and half a finger were passed through the cervical os.	5.23

^a Ultrasonographic measurements of ovaries.

^b Physical examination of cervix.

^c ELISA serum progesterone analysis for confirmation of stage of the oestrous cycle.

Table 5.3. Summary of mares sampled at the abattoir during the anoestrous period. Information regarding ovarian structures, cervical analysis and serum progesterone concentration.

Mares	Month of collection	Ovaries ^a	Cervix ^b	Progesterone Concentration (ng/mL) ^c
13	January	Small follicles smaller than 10 mm in diameter.	Cervix pale in colour and tight. One finger was passed through cervix.	Undetectable
14	January	Follicles smaller than 10 mm in diameter found on both ovaries.	Cervix was pale and with a tight appearance. One finger was passed through the cervical os.	0.16
15	January	Follicles smaller than 10 mm in diameter found on both ovaries.	Cervix was tight and pale in colour. One finger was passed through the cervix.	1.00
16	January	Follicles smaller than 10 mm in diameter found on both ovaries.	Cervix was pale and closed. Only half a finger was passed through the cervical os.	0.11
17	January	Small follicles smaller than 10 mm in diameter.	Cervix pale in colour. One finger was passed through cervix.	0.09
18	January	Small follicles smaller than 10 mm in diameter.	Cervix pale and one and a half fingers were passed through the cervical os.	0.05

^a Ultrasonographic measurements of ovaries.

^b Physical examination of cervix.

^c ELISA serum progesterone analysis for confirmation of stage of the oestrous cycle.

5.2.4 | RNA Extraction and RNA-Sequencing

As described in Chapter 3, total RNA was extracted from each technical replicate at the three time points resulting in a total of 144 RNA samples. The quality and concentration of each RNA sample were checked by Nanodrop 1000 Spectrophotometer (Thermo Scientific, UK), and RNA integrity was assessed by agarose gel electrophoresis.

Equivalent concentrations of RNA from each technical replicate (duplicates for the “0 hours” samples and triplicates for the cultured “24 hours” and “48 hours” samples) were pooled into a single library to mitigate oddities in a single replicate. The pooled samples had a final concentration of 1500 ng of RNA in a total volume of 50 μ L and were used to prepare dual-indexed next-generation sequencing libraries via the Illumina TruSeq Stranded mRNA kit, according to the manufacturer's instructions (Chapter 3). Following library construction, individual libraries were quantified using an Epoch spectrophotometer (BioTek Ltd) and pooled at equal concentrations. The pooled DNA was quantified again using Qubit fluorometer (Thermo Fischer Ltd) and size determined via agarose gel electrophoresis, with an average size of 300 base pairs (bp). The pooled library was then diluted to 10 nM and sent to the Wales Gene Park (Institute of Medical Genetics, Cardiff University) for sequencing in the 2x75 bp format on an Illumina HiSeq4000 platform at a final dilution of 8 pM. After an initial run of one sequencing lane to determine read counts for each sample, the original pool was adjusted by spiking in more of any underperforming samples, re-quantified and diluted to 10 nM for transport to Cardiff.

5.2.5 | Data Processing and Gene Expression Analysis

Following RNA-Seq, a total of 54 pair-end raw reads were generated. As previously described in Chapter 3, the FastQC software (version 0.11.2) was used to check the quality of each read, followed by the TopHat software (version 2.0.14) that was used to map the read to the equine reference genome (*Equus caballus*, EquCab2; GCA_000002305.1, Ensembl website). In order to summarize the number of aligned reads per exon, the FeatureCounts package (version 1.5.2) was used using the equine annotation file (Ensembl website, version EquCab2.89). Information regarding all RNA-Seq samples is shown in Table 5.4. Sample number 5 (Table 5.4) was excluded from the differential analysis due to its low sequence reads.

To perform the differential gene expression the R/Bioconductor DESeq2 package was used. Pairwise analysis between the follicular, luteal and anoestrous phases were performed at 24 and 48 hours, while the 0 hours samples were used as a baseline for all comparisons. Computer codes used in this chapter are shown in Appendix 5.2. The Ensembl gene ID's from the differentially expressed genes (DEGs) were submitted to the Search Tool for the Retrieval of Interacting Genes/Proteins (STRING) database (Szklarczyk *et al.*, 2015) for retrieval of protein-protein interactions (PPI), network analysis and gene associations discovery. The Kyoto Encyclopedia of Genes and Genomes (KEGG) pathways (Kanehisa and Goto, 2000) and the Gene Ontology (GO) terms (Ashburner *et al.*, 2000) retrieved from STRING were discussed in more detail.

Table 5.4. Summary of the 54 RNA-sequencing samples.

Sample	Mare	Time point ^a	Total sequences ^b	Mapped reads ^c	Alignment ^d	Total count ^e
1	1	0h	14732999	13093630	88.0%	8189448
2	1	24h	14413060	12851895	88.2%	9089595
3	1	48h	14478404	12388732	82.7%	9164680
4	2	0h	20944446	18583416	87.8%	12011433
5	2	24h	51908	-	-	-
6	2	48h	18426338	16460869	88.5%	11751541
7	3	0h	20676567	18713941	89.6%	11677948
8	3	24h	17025391	15344289	89.3%	10509216
9	3	48h	10176691	9064388	88.2%	6518790
10	4	0h	25755178	22889123	88.0%	15379136
11	4	24h	13825435	12385346	88.8%	8865615
12	4	48h	15265076	13562712	88.1%	10063029
13	5	0h	15271868	13766764	89.3%	8800428
14	5	24h	16545945	14801063	88.7%	10454711
15	5	48h	21623764	19162433	87.8%	14019493
16	6	0h	17701562	16121060	90.2%	10141641
17	6	24h	24846417	16743308	66.8%	15154964
18	6	48h	13704434	12424768	89.7%	9032012
19	9	0h	15837921	14198656	88.8%	8528780
20	9	24h	16801565	14870710	87.8%	10533817
21	9	48h	21894316	12286341	87.7%	8717409
22	10	0h	15640508	14114175	89.5%	8348050
23	10	24h	14858665	13344364	89.0%	8954146
24	10	48h	21421597	19469935	90.1%	13390511
25	11	0h	18187487	12480734	87.3%	9552985
26	11	24h	17030297	4560948	86.3%	9929801
27	11	48h	16955601	4644608	87.0%	9862552
28	12	0h	8588873	7576298	85.7%	5019375
29	12	24h	30704205	27406716	86.8%	19331141
30	12	48h	14546852	13012189	86.5%	9130360
31	13	0h	17092428	15259118	85.4%	9504581
32	13	24h	16675863	15074768	88.7%	10823555
33	13	48h	17559191	15783230	89.2%	10835122
34	14	0h	13009074	8965623	89.2%	6786842
35	14	24h	14567503	13105169	89.2%	8283221
36	14	48h	16831156	3149852	88.9%	9142764
37	15	0h	16058695	14188031	87.6%	8202444
38	15	24h	16822769	19736480	88.7%	13323753
39	15	48h	19567236	17537222	88.7%	12196475
40	16	0h	18087681	15121438	82.7%	8912819
41	16	24h	19114852	16766789	86.9%	10986930
42	16	48h	11933812	10568219	87.7%	7282826
43	17	0h	13425144	11973270	88.4%	7556195
44	17	24h	14682843	13038782	87.9%	9024019
45	17	48h	13115579	11688883	88.3%	8131313
46	18	0h	15593019	13905005	88.2%	8674913
47	18	24h	14437386	12823612	87.9%	8809986
48	18	48h	14545972	12861753	87.6%	8442258
49	19	0h	22527362	20371381	89.6%	12732723
50	19	24h	10566912	9542369	89.5%	6549129
51	19	48h	16112922	14471574	88.8%	10092367
52	20	0h	19575797	17636602	89.2%	10757896
53	20	24h	15628899	14103747	89.5%	9640596
54	20	48h	14577396	13294564	90.3%	8845260

^a Specific time-points when explants were removed from culture.^b A count of the total number of sequences processed.^c Number of reads mapped to the annotated equine genome.^d Percentage of reads mapped to the annotated equine genome.^e Counts of reads assigned to genomic features.

5.2.6 | Statistical analysis

The negative binominal distribution was used to model the data for the statistical analysis of DEGs on the RNA-Seq data, performed by the R/Bioconductor DESeq2 package (Love *et al.*, 2014). The Benjamini-Hochberg (BH) false discovery rate (FDR) (Benjamini and Hochberg, 1995) method was used to determine differential gene expression with an adjusted $P < 0.05$ along with a \log_2 fold change (Log_2FC) equal or greater than ± 2 . Six tests were performed in total: between the follicular and luteal phases at 24 and at 48 hours, between the follicular and anoestrous phases at 24 and 48 hours and between the luteal and anoestrous phases at 24 and 48 hours, while the 0 hours samples were used as a baseline for all comparisons. It was tested whether the 24 hours or whether the 48 hours effect over the fresh 0h baseline transcriptome was different across the follicular and luteal phase groups, across the follicular and anoestrous phase groups and across the luteal and anoestrous phase groups while controlling for individuals. Genes featuring less than 1000 reads across all samples were excluded from the enrichment analysis. DEGs were analysed with respect to KEGG pathways and GO terms.

The formulas indicated below express the six different comparisons performed:

$$\begin{aligned} &(\text{Follicular}_{24\text{h}} - \text{Follicular}_{0\text{h}}) - (\text{Luteal}_{24\text{h}} - \text{Luteal}_{0\text{h}}) \\ &(\text{Follicular}_{48\text{h}} - \text{Follicular}_{0\text{h}}) - (\text{Luteal}_{48\text{h}} - \text{Luteal}_{0\text{h}}) \\ &(\text{Follicular}_{24\text{h}} - \text{Follicular}_{0\text{h}}) - (\text{Anoestrous}_{24\text{h}} - \text{Anoestrous}_{0\text{h}}) \\ &(\text{Follicular}_{48\text{h}} - \text{Follicular}_{0\text{h}}) - (\text{Anoestrous}_{48\text{h}} - \text{Anoestrous}_{0\text{h}}) \\ &(\text{Luteal}_{24\text{h}} - \text{Luteal}_{0\text{h}}) - (\text{Anoestrous}_{24\text{h}} - \text{Anoestrous}_{0\text{h}}) \\ &(\text{Luteal}_{48\text{h}} - \text{Luteal}_{0\text{h}}) - (\text{Anoestrous}_{48\text{h}} - \text{Anoestrous}_{0\text{h}}) \end{aligned}$$

5.3 | Results

Based on PCA, the expression profile variation between and within the follicular, luteal and anoestrous groups was determined to allow a visual inspection of the samples based on their gene expression profiles. Similar expression profiles cluster together, as can be seen from Figure 5.1. The PCA analysis confirmed the presence of three subgroups; distinct clusters of follicular, luteal or anoestrous tissues. The clear distinction between follicular and anoestrous tissue clusters, represented by the green and red colours respectively, suggest that the collection of tissue at the follicular and anoestrous phase of the oestrous cycle was correct, taking into consideration that during these phases there is a low progesterone serum concentration in the mares' blood. On the other hand, the cluster of luteal tissue, represented by the blue colour, was identified as the major component for sample distances. This was expected since the progesterone serum concentration at this phase of the oestrous cycle is much higher.

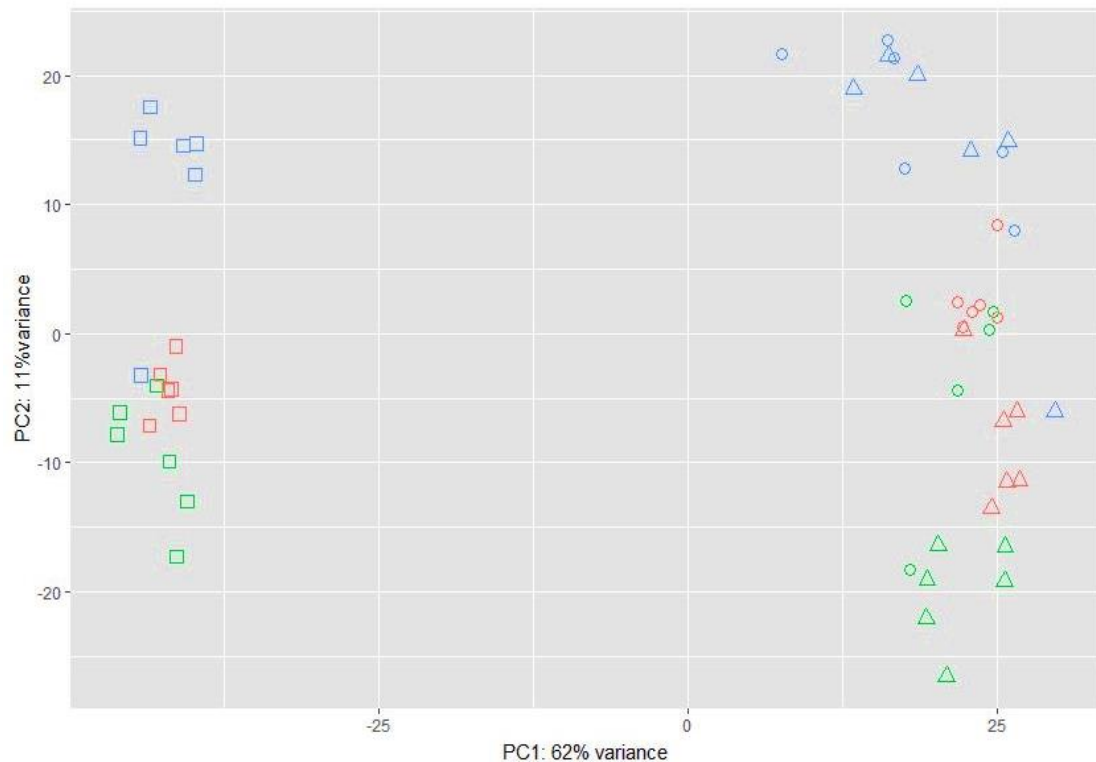


Figure 5.1. PCA plot of the gene expression profiles for the eighteen mares. The different colours show the biopsies taken at the **anoestrous**, **follicular** and **luteal** phases, while the different shapes demonstrate the different time points: 0h (□), 24h (○) and 48h (△). The analysis clearly demonstrates one outlier from the **luteal** phase. The **anoestrous** and **follicular** mares cluster together, as expected. The **luteal** mares are shown in a separate cluster, as expected, based on the difference in progesterone concentrations.

However, it can be seen from Figure 5.1 that the luteal cluster represented by the blue colour has one outlier. From further analysis, mare number 7 (Table 5.2) was identified as the outlier. Therefore, this mare was removed from the analysis for DEGs to avoid biased and unreliable results. Hence, another PCA plot was produced to confirm that the outlier was indeed removed. Figure 5.2 shows the gene expression profiles for the seventeen mares used in the final differential analysis. From the PCA plots, it is also possible to visualise that the transcriptome profiles were not affected by the volume of supplemented William's media used to culture each explant tissue as previously described in the Materials and Methods.

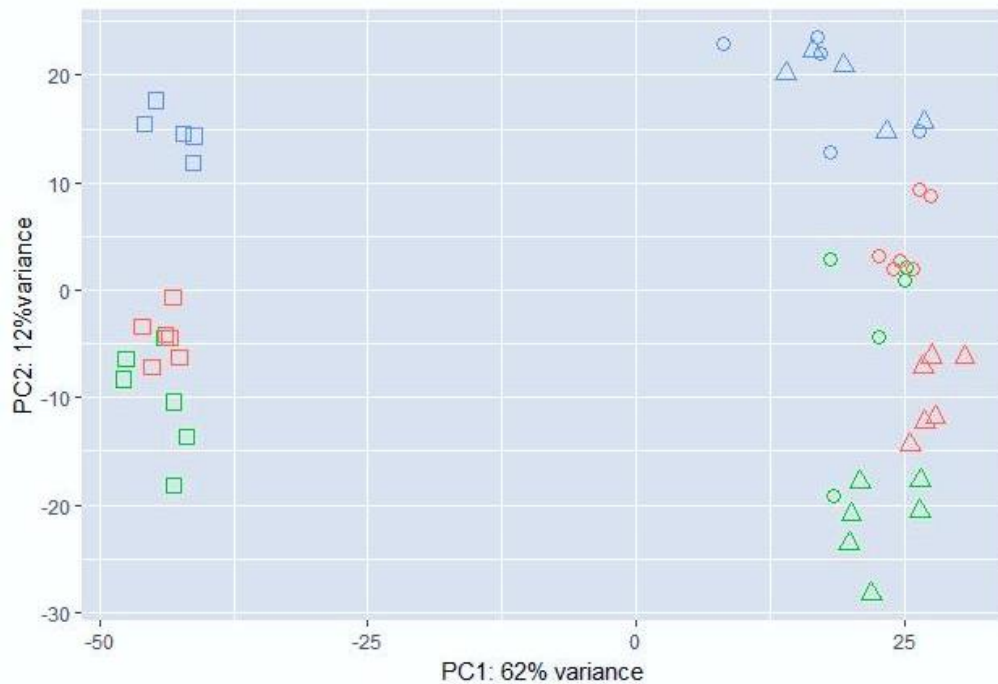


Figure 5.2. PCA plot of the gene expression profiles for the seventeen mares included in the analysis. The different colours show the biopsies taken at the **anoestrous**, **follicular** and **luteal** phases, while the different shapes demonstrate the different time points: 0h (□), 24h (○) and 48h (△).

The null hypothesis for each gene tested using DESeq2 was that there was no difference in its expression between the phase of the oestrous cycle groups at 24 or at 48 hours using the 0 hours samples as a baseline. The null hypothesis was rejected when the observed difference in expression of a gene was greater than expected by random chance (using an adjusted p-value of 0.05).

5.3.1 | Follicular vs Luteal

At 24 hours, 12834 genes were found to be expressed, 125 of which were shown to be statistically significantly differentially up-regulated and 58 shown to be statistically significantly differentially down-regulated in the follicular relative to the luteal phase groups, at an FDR of 0.05 and $\text{Log}_2\text{FC} \geq \pm 2$.

The STRING functional enrichment analysis of the DEGs identified at 24 hours was performed using the 12834 total expressed genes as the statistical background. The

protein-protein interaction (PPI) p-value was 1.0^{-16} , indicating that the genes are biologically connected as a group since the list of genes showed more interactions between themselves than what was expected when a similar size of random genes is analysed. The predicted STRING network was composed of 181 nodes and 35 edges. The STRING enrichment analysis of all DEGs when comparing the follicular transcriptome relative to the luteal transcriptome at 24 hours returned a total of 7 enriched KEGG pathways which are shown in more detail in Table 5.5. Furthermore, 48 GO terms (Appendix 5.3) were enriched and the 10 most enriched terms are listed in Table 5.6.

Table 5.5. Summary of the 7 enriched KEGG pathways when comparing the follicular transcriptome relative to the luteal transcriptome at 24 hours. Associated with $\text{Log}_2\text{FC} \geq \pm 2$ and sorted by p-value. Table created using the STRING website.

Pathway code ^a	Description ^b	Count ^c	FDR p-value ^d
04060	Cytokine-cytokine receptor interaction	12	1.49^{-5}
05164	Influenza A	10	0.002
05134	Legionellosis	6	0.003
04668	TNF signalling pathway	8	0.005
04630	Jak-STAT signalling pathway	7	0.022
05162	Measles	7	0.022
05140	Leishmaniasis	5	0.035

^a KEGG pathway identification code.

^b Description of each KEGG pathway.

^c The number of genes involved in each pathway.

^d Over-represented p-value with false discovery rate statistical correction for multiple comparisons.

Table 5.6. Summary of the 10 most enriched GO terms when comparing the follicular transcriptome relative to the luteal transcriptome at 24 hours. Associated with $\text{Log}_2\text{FC} \geq \pm 2$ and sorted by p-value. Table created using the STRING website.

GO Category ^a	Term name ^b	Description ^c	Count ^d	FDR p-value ^e
Cellular component	GO.0005575	Cellular component	13	4.10×10^{-6}
Biological process	GO.0044707	Single-multicellular organism process	8	8.04×10^{-5}
Cellular component	GO.0005576	Extracellular region	8	1.49×10^{-4}
Molecular function	GO.0003674	Molecular function	11	2.37×10^{-4}
Molecular function	GO.0005488	Binding	9	2.37×10^{-4}
Molecular function	GO.0046914	Transition metal ion binding	5	2.37×10^{-4}
Biological process	GO.0044699	Single-organism process	10	7.80×10^{-4}
Biological process	GO.0050794	Regulation of cellular process	8	7.80×10^{-4}
Molecular function	GO.0046872	Metal ion binding	6	8.51×10^{-4}
Biological process	GO.0008150	Biological process	10	0.002

^a GO domain (cellular component, biological process or molecular function).

^b Term associated with gene ontology biological processes.

^c Description of each GO category.

^d The number of genes involved in each biological process term.

^e Over-represented p-value with false discovery rate statistical correction for multiple comparisons.

The “Immune system process” (GO:0002376) and the “Inflammatory response” (GO:0006954) biological process GO terms were also enriched (FDR = 0.005 and FDR = 0.009 respectively), despite not being listed in the top 10 enriched GO terms featured in Table 5.6. However, the DEGs part of these GO terms are illustrated in Figure 5.3 along with the “Cytokine-cytokine receptor interaction”, the “TNF signalling pathway” and the “Jak-STAT signalling pathway” KEGG pathways related to inflammation and immune system response (Table 5.5). With regard to immune gene expression, several chemokines such as CXCL1, CXCL10, CXCL14, interleukin (IL)-1 α , IL-7 receptor (IL7R) and the NF- κ B inhibitor alpha (NFKBIA) are examples of significantly differentially expressed genes up-regulated when comparing the follicular transcriptome relative to the luteal transcriptome at 24 hours.

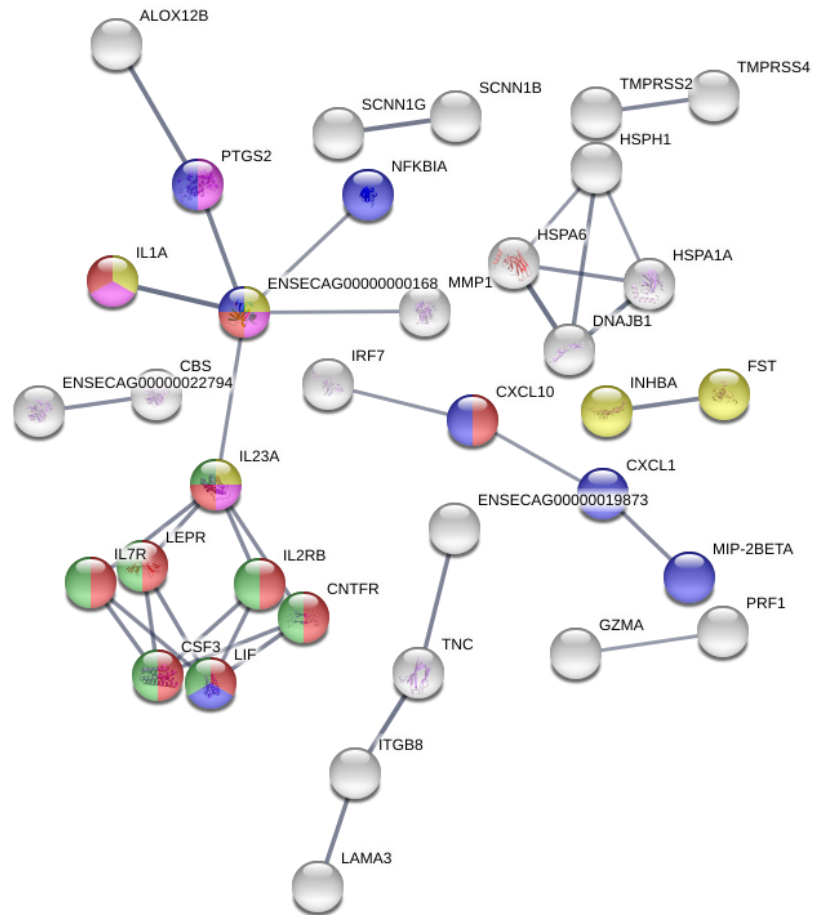


Figure 5.3. STRING predicted PPI network of the DEGs related to immune response and inflammation between the follicular and luteal phases at 24 hours. Red nodes represent genes that belong to “Cytokine-cytokine receptor interaction” (KEGG pathway), blue nodes represent genes that belong to the “TNF signalling pathway” (KEGG pathway), green nodes represent genes that belong to the “Jak-STAT signalling pathway” (KEGG pathway), yellow nodes represent genes that belong to the “Immune system process” (GO biological process terms) and pink nodes represent genes that belong to the “Inflammatory response” (GO biological process terms). The interaction score between nodes was set to high confidence (0.7). Disconnected nodes are hidden in the network. Image created using the STRING website.

A total of 12834 genes were also found to be expressed at 48 hours, 401 of which were statistically significantly differentially up-regulated and 155 genes were shown to be statistically significantly differentially down-regulated in the follicular relative to the luteal phase groups at an FDR of 0.05 and $\text{Log}_2\text{FC} \geq \pm 2$.

The STRING functional enrichment analysis of the DEGs identified at 48 hours was performed using the 12834 total expressed genes as the statistical background. The protein-protein interaction (PPI) p-value was 1.0^{-16} , indicating that the genes are biologically connected as a group since the list of genes showed more interactions

between themselves than what was expected when a similar size of random genes is analysed. The predicted STRING network was composed of 547 nodes and 472 edges. When comparing the follicular transcriptome relative to the luteal transcriptome, no GO terms were significantly enriched. The “Chemical carcinogenesis” (05204 pathway code) was the only KEGG pathway significantly enriched (FDR = 0.014).

5.3.2 | Follicular vs Anoestrous

At 24 hours 12834 genes were found to be expressed, 14 of which were shown to be statistically significantly differentially up-regulated and 76 shown to be statistically significantly differentially down-regulated in the follicular relative to the luteal phase group, at an FDR of 0.05 and $\text{Log}_2\text{FC} \geq \pm 2$.

The STRING functional enrichment analysis of DEGs at 24 hours was performed using the 12834 total expressed genes as the statistical background. The protein-protein interaction (PPI) p-value was 0.008, indicating that the genes are biologically connected as a group since the list of genes showed more interactions between themselves than what was expected when a similar size of random genes is analysed. The predicted STRING network was composed of 88 nodes and 10 edges.

The STRING enrichment analysis when comparing the follicular transcriptome relative to the anoestrous transcriptome at 24 hours returned a total of 6 enriched KEGG pathways which are shown in more detail in Table 5.7. Furthermore, 30 GO terms (Appendix 5.4) were enriched and 10 most enriched terms are listed in Table 5.8. The “Immune response” biological process GO term (GO:0006955) was also enriched (FDR = 0.0235), despite no presence in the top 10 list of GO enriched

terms featured in Table 5.8. However, the genes related to the “immune response” GO term are shown in Figure 5.4 along with the “Cytokine-cytokine receptor interaction” and the “Complement and coagulation cascades” KEGG pathways related to inflammation and immune system response.

Table 5.7. Summary of the 6 enriched KEGG pathways when comparing the follicular transcriptome relative to the anoestrous transcriptome at 24 hours. Associated with $\text{Log}_2\text{FC} \geq \pm 2$ and sorted by p-value. Table created using the STRING website.

Pathway code ^a	Description ^b	Count ^c	FDR p-value ^d
4640	Hematopoietic cell lineage	5	0.004
5144	Malaria	4	0.008
4060	Cytokine-cytokine receptor interaction	6	0.011
4610	Complement and coagulation cascades	4	0.013
5133	Pertussis	4	0.032
5323	Rheumatoid arthritis	4	0.042

^a KEGG pathway identification code.

^b Description of each KEGG pathway.

^c The number of genes involved in each pathway.

^d Over-represented p-value with false discovery rate statistical correction for multiple comparisons.

Table 5.8. Summary of the 10 most enriched GO terms when comparing the follicular transcriptome relative to the anoestrous transcriptome at 24 hours. Associated with $\text{Log}_2\text{FC} \geq \pm 2$ and sorted by p-value. Table created using the STRING website.

GO Category ^a	Term name ^b	Description ^c	Count ^d	FDR p-value ^e
Biological process	GO.0044699	Single organism process	9	5.70×10^{-5}
Biological process	GO.0008150	Biological process	9	1.12×10^{-4}
Molecular function	GO.0003674	Molecular function	8	2.29×10^{-4}
Molecular function	GO.0005488	Binding	7	2.29×10^{-4}
Cellular component	GO.0005575	Cellular component	8	4.80×10^{-4}
Biological process	GO.0042221	Response to chemical	5	9.52×10^{-4}
Biological process	GO.0048871	Multicellular organismal homeostasis	3	9.52×10^{-4}
Biological process	GO.0050794	Regulation of cellular process	6	9.52×10^{-4}
Biological process	GO.0050896	Response to stimulus	6	9.52×10^{-4}
Cellular component	GO.0044421	Extracellular region part	5	0.001

^a GO domain (cellular component, biological process and molecular function).

^b Term associated with gene ontology biological processes.

^c Description of each GO category.

^d The number of genes involved in each biological process term.

^e Over-represented p-value with false discovery rate statistical correction for multiple comparisons.

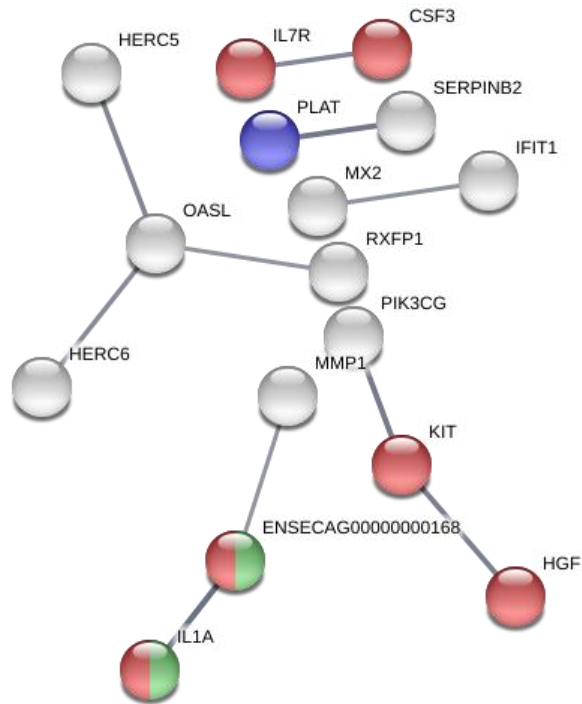


Figure 5.4. STRING predicted PPI network of the DEGs related to immune response and inflammation between the follicular phase and the anoestrous period at 24 hours. Red nodes represent genes that belong to the “Cytokine-cytokine receptor interaction” (KEGG pathway), blue nodes represent genes that belong to the “Complement and coagulation cascades” (KEGG pathway), and green nodes represent genes that belong to the “Immune response” term (GO biological process term). The interaction score between nodes was set to high confidence (0.7). Disconnected nodes are hidden in the network. Image created using the STRING website.

A total of 12834 genes were also found to be expressed at 48 hours, 104 of which were statistically significantly differentially up-regulated and 42 shown to be statistically significantly differentially down-regulated in the follicular relative to the anoestrous phase group at an FDR of 0.05 and $\text{Log}_2\text{FC} \geq \pm 2$.

At 48 hours, the protein-protein interaction (PPI) p-value was 3.6×10^{-06} , indicating that the genes are biologically connected as a group since the predicted network has significantly more interactions than expected. The predicted STRING network was composed of 137 nodes and 23 edges composed the network. Table 5.9 provides information about the 7 enriched KEGG pathways and Table 5.10 shows the 5 enriched GO terms.

Table 5.9. Summary of the 7 enriched KEGG pathways when comparing the follicular transcriptome relative to the anoestrous transcriptome at 48 hours. Associated with $\text{Log}_2\text{FC} \geq \pm 2$ and sorted by p-value. Table created using the STRING website.

Pathway code ^a	Description ^b	Count ^c	FDR p-value ^d
5133	Pertussis	6	0.008
5162	Measles	7	0.008
5164	Influenza A	8	0.008
4640	Hematopoietic cell lineage	5	0.009
4144	Endocytosis	8	0.035
4610	Complement and coagulation cascades	4	0.045
4974	Protein digestion and absorption	4	0.045

^a KEGG pathway identification code.

^b Description of each KEGG pathway.

^c The number of genes involved in each pathway.

^d Over-represented p-value with false discovery rate statistical correction for multiple comparisons.

Table 5.10. Summary of the 5 enriched GO terms when comparing the follicular transcriptome relative to the anoestrous transcriptome at 48 hours. Associated with $\text{Log}_2\text{FC} \geq \pm 2$ and sorted by p-value. Table created using the STRING website.

GO Category ^a	Term name ^b	Description ^c	Count ^d	FDR p-value ^e
Biological process	GO.0006952	Defense response	5	0.010
Biological process	GO.0048871	Multicellular organismal homeostasis	3	0.010
Biological process	GO.0006955	Immune response	4	0.023
Biological process	GO.0006953	Acute-phase response	3	0.024
Biological process	GO.0001660	Fever generation	2	0.041

^a GO domain (cellular component, biological process and molecular function).

^b Term associated with gene ontology biological processes.

^c Description of each GO category.

^d The number of genes involved in each biological process term.

^e Over-represented p-value with false discovery rate statistical correction for multiple comparisons.

5.3.3 | Luteal vs Anoestrous

A total of 12834 genes were found to be expressed where 83 genes were shown to be significantly up-regulated while 103 were shown to be down-regulated in the luteal relative to the anoestrous phase group at an FDR of 0.05 and $\text{Log}_2\text{FC} \geq \pm 2$. The STRING functional enrichment analysis of differentially expressed genes at 24 hours was performed using the 12834 total expressed genes as the statistical background. According to STRING, the list of genes/proteins showed statistically more interactions between themselves than what was expected when a similar size of

random genes/proteins is analysed for both time points indicating that genes are biologically connected as a group ($P=0.002$).

The predicted STRING network was composed of 180 nodes and 20 edges. The STRING enrichment analysis of all DEGs when comparing the luteal transcriptome relative to the anoestrous transcriptome at 24 hours returned a total of 2 enriched KEGG pathways which are shown in Table 5.11 while the total of 3 enriched GO terms is listed in table 5.12. DEGs part of the “Cytokine-cytokine receptor interaction” pathway are shown in Figure 5.5.

Table 5.11. Summary of the 2 enriched KEGG pathways when comparing the luteal transcriptome relative to the anoestrous transcriptome at 24 hours. Associated with $\text{Log}_2\text{FC} \geq \pm 2$ and sorted by p-value. Table created using the STRING website.

Pathway code ^a	Description ^b	Count ^c	FDR p-value ^d
04060	Cytokine-cytokine receptor interaction	8	0.024
04972	Pancreatic secretion	6	0.024

^a KEGG pathway identification code.

^b Description of each KEGG pathway.

^c The number of genes involved in each pathway.

^d Over-represented p-value with false discovery rate statistical correction for multiple comparisons.

Table 5.12. Summary of the 3 enriched GO terms when comparing the luteal transcriptome relative to the anoestrous transcriptome at 24 hours. Associated with $\text{Log}_2\text{FC} \geq \pm 2$ and sorted by p-value. Table created using the STRING website.

GO Category ^a	Term name ^b	Description ^c	Count ^d	FDR p-value ^e
Biological process	GO.0050896	Response to stimulus	7	0.023
Molecular function	GO.0003674	Molecular function	8	0.043
Molecular function	GO.0005102	Receptor binding	3	0.043

^a GO domain (cellular component, biological process and molecular function).

^b Term associated with gene ontology biological processes.

^c Description of each GO category.

^d The number of genes involved in each biological process term.

^e Over-represented p-value with false discovery rate statistical correction for multiple comparisons.

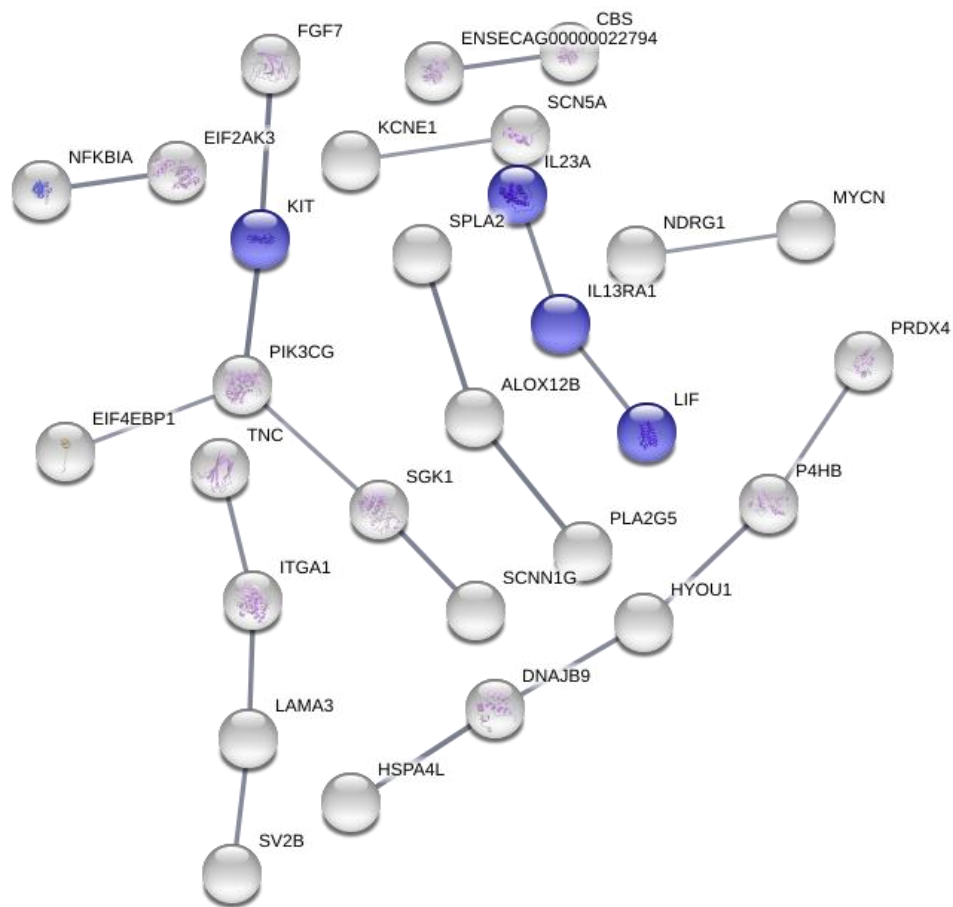


Figure 5.5. STRING predicted PPI network of the DEGs related to immune response and inflammation between the luteal phase and the anoestrous period at 24 hours. Blue nodes represent genes that belong to the “Complement and coagulation cascades” (KEGG pathway). The interaction score between nodes was set to high confidence (0.7). Disconnected nodes are hidden in the network. Image created using the STRING website.

At 48 hours, 12834 genes were found to be expressed, 165 of which were shown to be statistically significantly differentially up-regulated and 272 shown to be statistically significantly differentially down-regulated in the luteal relative to the anoestrous phase group, both at an FDR of 0.05 and $\text{Log}_2\text{FC} \geq \pm 2$.

The STRING functional enrichment analysis of DEGs at 48 hours was performed using the 12834 total expressed genes as the statistical background. The STRING PPI p-value was $< 1 \times 10^{-16}$, indicating that the genes are biologically connected as a group since the predicted network has significantly more interactions than expected. The predicted STRING network was composed of 422 nodes and 246 edges. The

STRING enrichment analysis of all DEGs when comparing the luteal transcriptome relative to the anoestrous transcriptome at 48 hours returned a total of 2 significantly enriched KEGG pathways as shown in Table 5.13. Also, a total of 31 GO terms (Appendix 5.5) were shown to be significantly enriched at 48 hours and Table 5.14 lists the 10 most enriched sorted by p-value.

Table 5.13. Summary of the 2 enriched KEGG pathways when comparing the luteal transcriptome relative to the anoestrous transcriptome at 48 hours. Associated with Log₂FC $\geq \pm 2$ and sorted by p-value. Table created using the STRING website.

Pathway code ^a	Description ^b	Count ^c	FDR p-value ^d
4974	Protein digestion and absorption	9	0.003
4512	ECM-receptor interaction	10	0.010

^a KEGG pathway identification code.

^b Description of each KEGG pathway.

^c The number of genes involved in each pathway.

^d Over-represented p-value with false discovery rate statistical correction for multiple comparisons.

Table 5.14. Summary of the 10 most enriched GO terms when comparing the luteal transcriptome relative to the anoestrous transcriptome at 48 hours. Associated with $\text{Log}_2\text{FC} \geq \pm 2$ and sorted by p-value. Table created using the STRING website.

GO Category ^a	Term name ^b	Description ^c	Count ^d	FDR p-value ^e
Biological process	GO.0051716	Cellular response to stimulus	9	0.005
Cellular component	GO.0005615	Extracellular space	7	0.005
Cellular component	GO.0012505	Endomembrane system	6	0.005
Cellular component	GO.0005576	Extracellular region	9	0.006
Cellular component	GO.0044421	Extracellular region part	8	0.006
Biological process	GO.0006508	Proteolysis	4	0.022
Biological process	GO.0009887	Organ morphogenesis	4	0.022
Biological process	GO.0009987	Cellular process	12	0.022
Biological process	GO.0032501	Multicellular organismal process	8	0.022
Biological process	GO.0044767	Single-organism developmental process	7	0.022

^a GO domain (cellular component, biological process and molecular function).

^b Term associated with gene ontology biological processes.

^c Description of each GO category.

^d The number of genes involved in each biological process term.

^e Over-represented p-value with false discovery rate statistical correction for multiple comparisons.

5.4 | Discussion

In the present experiment, RNA-Seq was used to further investigate the gene expression profiles in the equine endometrial environment throughout the oestrous cycle and anoestrous period to identify the key significant changes associated with the different phases using the explant tissue culture. Analysis of RNA-Seq data generated gene expression profiles when comparing the follicular and luteal phases, the follicular and anoestrous phases, and the luteal and anoestrous phases. After performing the general KEGG/GO enrichment analysis of all DEGs, genes related to the immune system, to uterine function and to cellular processes were selected as important target genes to be discussed herein. Results from this study will improve the understanding of the physiological uterine changes in response to different pituitary and ovarian hormone concentrations and also serve as a baseline for future studies in mares that develop uterine pathological changes and diseases, especially endometrial inflammation.

5.4.1 | Follicular vs Luteal

When comparing how the 24 hours effect over the fresh 0 hours transcriptome is different across the follicular and the luteal phase a total of 183 genes were significantly differentially expressed. The two biological processes retrieved from the enrichment analysis were the immune system and cellular processes.

The DEGs related to the immune function were linked to the “cytokine-cytokine receptor interaction”, “TNF signalling pathway” and “Jak-STAT signalling pathway” KEGG pathways and with the GO biological processes “immune system” and “inflammatory response”. These categories comprised genes coding for interleukin family and receptors (IL1A, IL23A, IL2RB and IL7R), chemokine (C-X-C motif) ligand family (CXCL1, CXCL10 and CXCL14), the tumour necrosis factor (TNF) receptor superfamily member 4 (TNFRSF4), the NF- κ B Inhibitor Alpha (NFKBIA), showing an Log_2FC up-regulation between 2.1 and 5.3 in follicular relative to luteal samples. Furthermore, the LEPR gene ($\text{Log}_2\text{FC} = -2.4$) encodes a leptin receptor that is known to be expressed in the uterus with higher expressions observed during the luteal phase of the oestrous cycle in heifers (Sosa *et al.*, 2010). Leptin is usually found in adipose tissue with an important role on appetite regulation; however, its presence in the uterus has hypothesised its relation in reproductive function as well as in the metabolic status (Chilliard *et al.*, 2001; Chelikani *et al.*, 2003). The down-regulation of LEPR during the follicular relative to the luteal phase agrees with these findings, indicating that the leptin receptor is more expressed during the luteal phase of the oestrous cycle also in mares.

There is a relatively small body of literature that focuses on the equine endometrial gene expression profiles throughout the oestrous cycle, however the current result

agrees with the findings from an RNA-Seq study conducted by Marth *et al.* (2015b) when investigating the endometrial global gene expression profiles during the follicular and the luteal phases of the oestrous cycle. It also agrees with the first microarray analysis of the genes involved in the follicular and luteal phases carried out by Gebhardt *et al.* (2012), where expression profiles related to inflammatory responses were up-regulated during the follicular phase. Genes related to the immune system, when comparing the follicular transcriptome relative to the luteal transcriptome, were expected to be up-regulated, since the innate immune system is responsible for tackling the intrusion of foreign material into the uterus, specially pathogens, that is more likely to occur during the follicular phase when the cervix is open (Troedsson *et al.*, 2001a). Furthermore, the INHBA gene and the FST genes coding the inhibin beta A and follistatin respectively, which are proteins linked to the immune system and related to hormonal changes during the oestrous cycle (Ueno *et al.*, 1987; Walton *et al.*, 2012) were up-regulated (Log_2FC of 2.2 and 2.0 respectively). It has already been described that progesterone decreases the expression of steroidogenic factors such as INHBA and FST in rats (Tebar *et al.*, 2000; Zheng *et al.*, 2007). Therefore it is indeed expected the INHBA and FST expression would be up-regulated in follicular relative to luteal phase also in mares.

The PTGS2 gene ($\text{Log}_2\text{FC} = 2.2$) encodes a cyclooxygenase that plays a role in prostaglandin biosynthesis which can be induced in different tissues by cytokines, growth factor and inflammatory stimuli (Jones *et al.*, 1993; Cabrera *et al.*, 2006). In mammals, the expression of PTGS2 is induced by the ovulatory gonadotropin surge in granulosa cells, producing prostaglandins which are suggested to be mediators of the ovulatory process (Sirois, 1994; Sirois and Doré, 1997). It has also been reported that the expression of PTGS2 was upregulated in the equine

endometrium when luteolysis had already started (day 15-15.5) and when progesterone concentration declined (Atli *et al.*, 2010). However, the up-regulation of PTGS2 during the follicular phase shown in the current study might be later than expected as PGF_{2α} increases around day 14-16 of the oestrous cycle in mares and induces luteolysis, allowing the onset of another follicular phase and ovulation (Zavy *et al.*, 1978; Morrese, 2011; Stout, 2011). On the other hand, if PTGS2 also regulates prostaglandin E (PGE) which is known to have anti-inflammatory properties (Harris *et al.*, 2002; Ricciotti and FitzGerald, 2011), an up-regulation of PTGS2 during the follicular phase of the oestrous cycle is indeed expected.

The ESR1 and the FGFR genes, coding an oestrogen receptor and a fibroblast growth factor protein respectively, were also differentially expressed when comparing the transcriptome across follicular and luteal phase (Log₂FC of -2.0 and 4.4 respectively). Gebhardt *et al.* (2012) reported the expression of ESR1 to start increasing at the beginning of the follicular phase with a peak during the early luteal phase, therefore it is expected ESR1 to be down-regulated comparing the follicular transcriptome relative to the luteal transcriptome in the current study. Similarly, the up-regulation of FGFR described in the current study agrees with Gebhardt *et al.* (2012) where it was found that a fibroblast growth factor (FGF), which acts as one of the mediators in the endometrial oestrogen signalling, is up-regulated during the early follicular phase with a peak at ovulation.

The results at 48 hours compared the differences between the follicular and the luteal transcriptomes using the 0 hours transcriptome as a baseline. Since the explants have been in culture for a total period of 48 hours it is expected the changes in gene expression to be greater when comparing the 48 hours' time point to the 0 hours

baseline over the 24 hours' time point to the 0 hours baseline. Indeed, at 48 hours a total of 556 genes were differentially expressed, in contrast to only 183 genes at 24 hours. However, the enrichment analysis at 48 hours only retrieved one enriched KEGG pathway that is not related to the immune function or with the endometrial environment. The “chemical carcinogenesis” KEGG pathway was the only enriched pathway (FDR = 0.0137). This is a rather unexpected outcome related to environmental chemical carcinogens that can contribute to genomic instability. This might be explained because the genes are overly general or because many gene sets participating in different pathways and processes overlapped (Simillion *et al.*, 2017). However, this might be also a factor of the biases in the databases. Results that do not make much sense to other systems can be retrieved since many pathway studies have been done on diseases in humans. Therefore, this result might represent a set of genes that are involved in another process that is not yet annotated in horses. As described before, the predicted STRING protein-protein interaction network generated significantly more connections than expected, suggesting that the genes are functionally interacting units, like pathways. Therefore, it can be suggested the possibility of unannotated processes that are being up or down regulated.

Individual genes related to immune function such as CXCL14 ($\text{Log}_2\text{FC} = 2.7$) and TNFRSF4 ($\text{Log}_2\text{FC} = 2.9$) were differentially expressed, meaning that the immune response is also up-regulated during the follicular transcriptome relative to the luteal transcriptome at 48 hours. The ESR1 gene was again found to be down-regulated ($\text{Log}_2\text{FC} = -2.5$) during the follicular relative to the luteal phase at 48 hours. However, it has been suggested that it is more reliable to concentrate on trends indicated by grouped genes rather than on specific isolated genes in order to interpret the biological changes throughout the oestrous cycle (Marth *et al.*, 2015b).

5.4.2 | Follicular vs Anoestrous

When comparing how the 24 hours effect over the fresh 0 hours transcriptome is different across the follicular and the anoestrous phase a total of 90 genes were significantly differentially expressed. The biological processes retrieved from the enrichment analysis were mainly related to the immune system.

The “cytokine-cytokine receptor interaction” and the “complement and coagulation cascades” were the significantly enriched KEGG pathways with genes related to the immune function, along with the GO biological processes “immune response”. Enriched genes from these categories encode for IL family and receptors (IL1A, IL1B, IL33, IL7R and IL1RN), chemokine ligand family (CXCL6), complement factors and proteins (CFB, C4BPA), toll-like receptor (TLR3) showing a Log₂FC up-regulation between 2.2 and 5.9 in the follicular phase group relative to the anoestrous group. The hepatocyte growth factor (HGF) gene was also over expressed (Log₂FC = 2.7) and it encodes a protein that is secreted by mesenchymal cells and acts as a cytokine on epithelial cells (Niranjan *et al.*, 1995). The colony stimulating factor 3 (CSF3) gene encodes a cytokine that controls the production, differentiation and function of granulocytes (Raposo *et al.*, 2006; Liu *et al.*, 2016). As discussed before, genes linked to the immune response are expected to be up-regulated during the follicular phase, which is the period of the oestrous cycle when foreign material might enter the uterus and contact the endometrium during natural mating or artificial insemination.

Furthermore, genes related to cellular processes were also differentially expressed. The tyrosine-protein kinase (KIT) is a protein coding gene that plays a role in the regulation of cell survival and proliferation and gametogenesis, as well as acting as a

cell-surface receptor for specific cytokines (Blume-Jensen *et al.*, 1994; Roskoski, 2005). The plasminogen activator tissue type (PLAT) gene encodes an enzyme that plays a role in cell migration and tissue remodelling (Green and Lund, 2005). Thus a higher expression of KIT and PLAT ($\text{Log}_2\text{FC} = 2.2$ and 2.1 respectively) evident in the follicular phase, might be expected as this is the stage of the cycle where there is glandular hyperplasia and increased stromal extracellular matrix compared to the anoestrous phase.

Genes related to the extracellular matrix (ECM) were also found to be up-regulated in the follicular transcriptome relative to the anoestrous transcriptome at 24 hours. The TNC gene encodes Tenascin C, an extracellular matrix protein that is known to be expressed in the endometrium (Midwood *et al.*, 2011) was up regulated with a Log_2FC of 3.1 . Matrix metalloproteinases (MMPs) are proteolytic enzymes known to play an important role in follicular development in mammals by breaking down ECM and facilitating tissue remodelling (Curry and Osteen, 2003). In the present study, the MMP1 gene was found to be up-regulated with a Log_2FC of 2.8 .

When comparing how the 48 hours effect over the fresh 0 hours transcriptome is different across the follicular and the anoestrous phase, 146 genes were significantly differentially expressed. Even though a higher number of genes were significantly differentially expressed at 48 hours when compared to the analysis at 24 hours, the DEGs were linked to a smaller number of GO categories and KEGG pathways, as was the case when comparing the follicular transcriptome to the luteal transcriptome at 48 hours. The principal biological process retrieved from the enrichment analysis as previously was again, the immune system. Similarly, genes involved in the “complement and coagulation cascades” KEGG pathway and GO biological

processes “defense response”, “immune response” and “acute-phase response” encode IL family and receptors (IL1A, IL1B and IL1RN), chemokine ligand family (CXCL6), and complement component/protein (C1QC and C4BPA), with a Log₂FC up-regulation between 2.2 and 3.8 in follicular compared to anoestrous samples.

Collagen genes (COL1A1, COL21A1 and COL3A1) were down regulated (Log₂FC = -2.2, -3.1 and -2.4 respectively) in the follicular transcriptome compared to anoestrous transcriptome. However, this finding contrasts to that of others, where an upregulation of collagen genes occurred during the follicular phase, where it was hypothesised that collagen provides structural strength to help stabilise the oedematous uterus during the follicular phase (Marth *et al.*, 2015b). However, it has been demonstrated that collagen levels decline during the ovine follicular phase while MMP activity increased, and it has been suggested that cervix relaxation during the follicular phase might be due to collagen fibre degradation (Rodriguez-Pinon *et al.*, 2015). Thus, it could be proposed that collagen down-regulation during the follicular phase compared to the anoestrous period might be related to cervix relation.

5.4.3 | Luteal vs Anoestrous

When comparing how the 24-hour effect over the fresh 0 hours transcriptome is different across the luteal and the anoestrous phase, a total of 186 genes were significantly differentially expressed. The significant enrichments observed in the GO categories (Table 5.12) were “molecular function”, “receptor binding” and “response to stimulus”.

From the genes linked to the GO categories, the INHBA gene was also down-regulated in the luteal relative to the anoestrous period, with a Log₂FC of -2.1, which agrees with previous research demonstrating that high progesterone concentrations diminish its endometrial expression (Tebar *et al.*, 2000). The PTHLH gene that encodes the parathyroid hormone-related protein, which is involved in the regulation of cellular and organ growth and development, especially in epithelial-mesenchymal interactions (Foley *et al.*, 2001; Hens and Wysolmerski, 2005), was also down-regulated with a Log₂FC of -4.3. These results agree with bovine work where the uterine expression of both PTHLH and INHBA genes is diminished in the luteal phase of the oestrous cycle (Bauersachs *et al.*, 2005). The EDNRB gene (Log₂FC = 3.1) encodes the endothelin B receptor. It has been suggested that endothelin participates in the luteal regression induced by prostaglandin F_{2α} in cows (Meidan *et al.*, 1999; Levy *et al.*, 2000; Wright *et al.*, 2001). Therefore, an up-expression of EDNRB during the luteal phase relative to the anoestrous phase in mares might suggest a stimulatory activity in luteolysis that occurs at the very end of the luteal phase in mares.

Genes related to the “cytokine-cytokine receptor interaction” KEGG pathway (Table 5.11) encode proteins for IL family and receptors (IL23A and IL12RA1), chemokine ligand family (CXCL10 and CXCL14), and a TNF-receptor superfamily (TNFRSF4), showing a Log₂FC down-regulation between -2.3 and -3.6 in luteal relative to anoestrous samples at 24 hours. This result agrees with the hypothesis that high progesterone concentrations during the luteal phase reduce the efficiency of endometrial bacteria elimination by neutrophils, leading to a lower uterine clearance (Evans *et al.*, 1986a; Watson *et al.*, 1987; Reiswig *et al.*, 1993). It can also be

deduced that the immune system during the anoestrous period is more active than during the luteal phase of the oestrus cycle in mares.

When comparing how the 48 hours effect over the fresh 0 hours transcriptome is different across the luteal and the anoestrous phase, 437 genes were significantly differentially expressed. Genes related to the “protein digestion and absorption” and “ECM-receptor interaction” KEGG pathways encode proteins for collagen such as COL1A1, COL1A2, COL22A1, COL3A1 and COL5A3, with a Log₂FC down-regulation between -2.2 to -4.4. Since genes encoding collagen proteins were also found to be down-regulated when comparing the follicular relative to the anoestrous transcriptome at 48 hours, they might be associated with the anoestrous period itself rather than with the follicular or luteal phases. These results lead to the hypothesis that collagen genes are more expressed during the anoestrous period than during the oestrous cycle, and this might be the reason why genes encoding collagens are down-regulated at both follicular and luteal phases relative to anoestrous. There is a lack of information on the collagen content of the endometrium during the anoestrous period in mares and in other mammals, making it difficult to theorise the reasons for the down-regulation of collagen coding genes when comparing the follicular and luteal transcriptome to the anoestrous transcriptome.

The 10 most enriched GO terms described in Table 5.14 when comparing the luteal transcriptome relative to the anoestrous transcriptome at 48 hours were related to biological processes and cellular components. The GO terms are mostly related to the extracellular space/region and cellular processes and cellular responses. As previously mentioned, the endometrial expression of ESR1 changes throughout the oestrous cycle in mares, increasing at the beginning of the follicular phase and

reaching its peak during the early luteal phase (3 days after ovulation) (Gebhardt *et al.*, 2012). Therefore, the up-regulation of the ESR1 gene ($\text{Log}_2\text{FC} = 2.2$) during the luteal relative to the anoestrous phase in the current study agrees with previous findings. The INHBA and PTHLH genes were again down-regulated showing Log_2FC of -2.9 and -5.2 respectively, while the EDNRB gene was up-regulated with Log_2FC of 3.1. These results agree with the previous discussion when comparing the luteal transcriptome relative to the anoestrous transcriptome at 24 hours where a down-regulation of INHBA and PTHLH and an up-regulation of EDNRB are expected during the luteal phase.

5.5 | Conclusion

One of the current limitations of global gene expression study during the oestrous cycle in mares is that all studies consider the follicular and luteal phases only, leading to a lack of information related to the anoestrous period. This might be justified if the focus on the follicular phase is in order to better understand the mechanisms underlying equine fertility problems. However, it is important to determine the global gene expression changes throughout the equine breeding season to improve understanding of the physiological cyclic changes by comparing and contrasting the findings at the follicular and luteal phases with the anoestrous period. This may lead to a better understanding of how pituitary and ovarian hormones shape the morphological and functional characteristics of the endometrium throughout the oestrous cycle and shed light on how uterine pathologies disrupt the endometrial physiological equilibria.

The RNA-Seq data analysis provided a snapshot of gene expression levels of follicular phase, luteal phase and anoestrous period in the equine endometrium. At

the follicular phase, the gene expression is mainly related to immune pathways, while the gene expression at the luteal phase is mainly related to molecular functions and biological processes. This might be the first RNA-Seq analysis of the equine endometrium during the anoestrous period, suggesting the collagen genes are more expressed during the anoestrous period than during the oestrous cycle.

For all comparisons (follicular relative to luteal, follicular relative to anoestrous and luteal relative to anoestrous) the results of the differences between the different transcriptomes at 48 hours using the 0 hours transcriptome as a baseline, retrieved a higher number of DEGs in contrast to the DEGs retrieved at 24 hours. However, the enrichment analysis at 48 hours did not retrieve many KEGG pathways and/or GO terms, or the terms were too generic. This might be due to a great number of genes sets taking in part in different pathways that somehow overlapped. Therefore, the findings at 24 hours might be the most reliable and biologically trustworthy.

The most important limitation of this study lies in the fact that handling high throughput data such as RNA-Seq is still incredibly challenging. There is no gold-standard protocol to analyse transcriptomic data and the application of rigorous statistical methods to target significant effects and potential candidate genes is complex and time-consuming. This stated bioinformatics research is still developing, and the biological accuracy of results is continually being improved. The data presented in this chapter must be interpreted with caution because the effect of cultivating the explants was a larger source of variation than the effect of oestrous cycle stage. Another point to consider is that there is a possibility of tissues collected at different stages of the oestrous cycle have different “sensibilities” to the tissue culture. In the future, more research needs to focus on which stage of the oestrous

cycle is the most sensitive to the culture to account for gene expression variations related to the culture itself. This way, it will be possible to investigate the modulation in gene expression based on the phase of the oestrous cycle and based on the effect of culture upon the explants.

CHAPTER 6

EFFECTS OF LPS ON THE EQUINE ENDOMETRIUM TRANSCRIPTOME AT THE FOLLICULAR PHASE OF THE OESTROUS CYCLE

6.1 | Introduction

It is established that uterine infections are substantial cause of low fertility in mares (Asbury, 1986). As a consequence, horse breeding industries are affected by significant financial losses (Riddle *et al.*, 2007; Marth *et al.*, 2015a). A normal, transient uterine inflammation known as mating-induced endometritis (MIE) takes place after breeding due to the introduction of semen, seminal plasma, debris and bacteria (Watson, 2000; Katila, 2001; Troedsson *et al.*, 2001a). Nonetheless, in some mares the physiological inflammation develops into a persistent endometritis known as persistent mating-induced endometritis (PMIE), causing early embryonic loss and infertility (Troedsson, 1997, 2006). It has been observed that the three most common bacterial species isolated in uterine samples collected from mares with fertility problems were *Escherichia coli* (*E. coli*), *Streptococcus* β -haemolytic and *Streptococcus equi subspecies zooepidemicus* (*S. zooepidemicus*) respectively (Albihn *et al.*, 2003a). *E. coli* has been associated with repeat breeding, while β -haemolytic streptococci were related to clinical endometritis (Albihn *et al.*, 2003a).

Being the first line of defence against invading microorganisms, the innate immune system produces a rapid response to maintain the homeostasis of the organism. The most important subsystem of the innate immune system is inflammation, responsible for recruiting white blood cells and immune proteins to destroy invading microbes and promote tissue repair (Tizard, 2013). Cytokines are important signalling proteins secreted by immune system cells responsible for regulating the immune reaction. Interleukins (IL), interferons, tumour necrosis factors (TNF) and chemokines are examples of cytokines that are involved in immune regulation and inflammation (Tizard, 2013).

Most studies in the field of equine endometritis have only focused on specific genes hypothesised to be involved in uterine inflammation. Detailed examination of mRNA expression of pro-inflammatory cytokines IL-1 β , IL-6, TNF- α and IL-8, and the anti-inflammatory cytokine IL-10 showed that the endometrial expression of IL-1 β , IL-6, TNF- α was increased in both resistant and susceptible mares 24 hours after artificial insemination with killed sperm (Fumuso *et al.*, 2003). Similarly, previous research carried out by Christoffersen *et al.*, (2012) found that mares showed increased gene expression of IL-1 β , IL-6, IL-8, IL-10, TNF- α , IL-1 receptor antagonist (IL-1ra) and serum amyloid A (SAA) after bacterial infusion. The expression levels of these cytokines returned to normal within a period of 12 to 24 hours after infusion in resistant mares, whilst susceptible mares expressed the cytokines for up to 72 hours.

Furthermore, it has been reported that *Maytenus ilicifolia* (*M. ilicifolia*) can modulate a range of inflammatory responses (Souza-Formigoni *et al.*, 1991; Jorge *et al.*, 2004; Wonfor *et al.*, 2017). *M. ilicifolia*, a plant of the family Celastrace, is native to the Tropical Atlantic Forest and it has been used in traditional medicine in South America in cases of inflammation and gastric ulcer due to its analgesic, anti-inflammatory and antiulcerogenic activities (Balbach, 1980; Born, 2000; Jorge *et al.*, 2004). The usage of *Maytenus* species on inflammation and ulcers can be justified by the presence of metabolites such as flavonoids (Leite *et al.*, 2001), condensed tannins (Gonzalez and Di Stasi, 2002), triterpenes (Itokawa *et al.*, 1991; Shirota *et al.*, 1994) and sesquiterpenes (Itokawa *et al.*, 1991) in *Maytenus* leaves. It has been demonstrated that no apparent toxicity was induced by an acute and chronic administration of *M. ilicifolia* and *M. aquifolium* in rats and mice (Oliveira *et al.*, 1991). To date, little research has been carried out to examine the effects of *Maytenus* species in humans and animals and little is known about it. More studies

are still needed to confirm the effectiveness of this plant extract to treat and/or prevent inflammation and gastric ulcers. Based on other exploratory studies, it is hypothesised that they are safe for human and animal use (Oliveira *et al.*, 1991; Jorge *et al.*, 2004). Therefore, the effectiveness of *M. ilicifolia* plant extract as a preventative treatment for equine uterine inflammation was assessed in the current study as a preliminary pilot study.

Studies in equine endometritis remain narrow in focus dealing only with a limited number of genes. In order to better understand the factors underlying endometritis at the level of gene expression, a more extensive transcriptomics research is required. Emerging transcriptomic technology offers the opportunity to investigate global gene expression in resistant and susceptible mares. Consequently, it will be possible to characterize most genes involved in PMIE. The purpose of this investigation was to improve the understanding of the mechanisms underlying uterine inflammation, examining the development of PMIE at the level of global gene expression. Understanding the link between MIE and PMIE at the broadest level will contribute to an early identification of mares susceptible to PMIE, leading to appropriate breeding management. Therefore, the objectives were 1) challenge equine endometrial explants (n=5) with *E. coli* lipopolysaccharide (LPS) and 2) preliminary investigate the potential anti-inflammatory effect of *M. ilicifolia* in potentially abrogating these responses (n=3).

6.2 | Materials and Methods

6.2.1 | Animals

Uteri from five native mares in the follicular phase of the oestrous cycle presented for euthanasia at an abattoir were collected, as they are known to be resistant to PMIE. The age and reproductive history of each mare were unknown. Collection at the abattoir were carried out between June and August, which is also the period of the year in which mating occurs and, potentially, MIE/PMIE occurs.

6.2.2 | Sample Collection

Blood was collected from the jugular vein immediately after death into plain vacutainer tubes. Blood samples were stored at 4 °C for a period of 24 hours and blood serum was used to confirm the phase of the oestrous cycle by measuring progesterone concentration. Uteri were collected as soon as possible post mortem and stored on ice. Uteri undergoing the follicular phase of the oestrous cycle was initially identified by examination at the abattoir as previously described (Chapter 3). Briefly, the cervix was physically examined for morphology and the ovaries were ultrasonographically assessed for the presence of a dominant follicle and absence of a corpus luteum. Records of criteria used in the abattoir to predict the stage of the oestrous cycle and serum progesterone concentrations are described in Table 6.1.

Endometrial smears were collected from each uteri with the aid of a cytobrush and rolled onto microscope slides, following the fixation and staining protocols previously described. Cytology slides were prepared and assessed for neutrophil counts as previously described in Chapter 3. Mares demonstrated neutrophil counts < 2 per high power field (400x), and therefore all uteri were included in the

experiment. Furthermore, two endometrial biopsies were taken from the uterine horn bifurcation using a sterile biopsy instrument. Biopsies were stored in 1.5 mL of RNALater for a period of 24 hours at 4 °C. Thereafter, RNALater was then removed and the biopsies were frozen at -80 °C until RNA extraction.

Blood samples and uteri were transported on ice back to the laboratory within 7 hours of collection. At the laboratory, an additional 1x1 cm² biopsy was carefully excised from the uterine body of each uterus and stored in 10 mL of Bouin's fixative liquid for subsequent histology. The summary of the pathological and degenerative endometrial changes of mares providing endometrial explants for this experiment can be found in Appendix 6.1. All mares were kept in the study following the histopathological assessment.

Table 6.1. Characteristics of uteri from mares sampled at the abattoir used to determine the follicular phase of the oestrous cycle. Information regarding ovarian structures, cervical analysis and serum progesterone concentration measured retrospectively.

Mares	Ovaries ^a	Cervix ^b	Progesterone Concentration (ng/mL) ^c
1	One 40 mm in diameter follicle on right ovary. Smaller follicles (around 20 mm in diameter) on left ovary.	Cervix pink-pale in colour and open appearance. Three fingers were passed through the cervix	0.21
2	One 47 mm x 37 mm follicle on left ovary. Small follicles on right ovary.	Cervix red in colour, soft and open. Three fingers were passed through the cervix.	0.43
3	One 30 mm x 41 mm follicle on left ovary. Small follicles (around 10mm in diameter) on right ovary.	Cervix becoming pink, but three fingers were passed through the cervix.	0.54
4	One 30 mm x 30 mm follicle on left ovary.	Cervix was becoming pink. Two to three fingers were passed through the cervical os.	0.45
5	One 25 mm in diameter follicle on left ovary.	Cervix was becoming red. Two fingers were passed through the cervical os.	0.86

^a Ultrasonographic measurements of ovaries.

^b Physical examination of the cervix.

^c ELISA serum progesterone analysis for confirmation of stage of the oestrous cycle.

6.2.3 | Endometrial Tissue Culture

At the laboratory, the uterine horns were dissected and the endometrium was exposed. Numerous punch biopsies were collected from each uterus, placed into warm supplemented Hank's Balanced Salt Solution (HBSS) and incubated (5 % CO₂, 38 °C) until cultured, as described in Chapter 3. Immediately after biopsies had been collected from all uteri, the samples were removed from the incubator, washed twice with unsupplemented HBSS and the tissue culture was initiated. Before placing each punch biopsy into a separate well of the 6-well culture plate, biopsies were individually weighed in a Petri dish and the weights were recorded to allow prostaglandin F_{2α} (PGF_{2α}) production to be expressed as per mg of tissue. The hexane extract from dried ground *M. ilicifolia* leaves was prepared at Bangor University (Dr Vera Thoss and Dr Marc Bouillon) following methods previously described (Jorge *et al.*, 2004). Briefly, pulverized *M. ilicifolia* leaves (1000 g) were extracted with n-hexane (4 L) in two batches (500 g/ 2 L) via stirring at room temperature for 24 hours. The solid leaf material was then filtered off and air-dried overnight. The green filtrate was concentrated under reduced pressure affording the n-hexane extract as a dark green brown sticky solid. The hexane extract was then diluted in absolute ethanol to a stock solution of 1 mg/mL.

The tissue culture was performed in triplicate for each treatment as shown in Figure 6.1, and plates were incubated at 38 °C in 5 % CO₂ for 24 and 48 hours. To induce inflammation and address objective 1, *E. coli* LPS was added to the supplemented William's medium used in the explant tissue culture. Three different concentrations of LPS were used: 0.3 µg/mL, 1.0 µg/mL and 3.0 µg/mL. The concentrations of LPS

for this experiment were chosen based on previously published explant models of uterine inflammation (Nash *et al.*, 2008; Herath *et al.*, 2009; Penrod *et al.*, 2013).

Explants from mares 2, 3, 4 and 5 were cultured in a total of 3 mL supplemented William's medium without the wire platforms and lens cleaning tissue. As described in Chapter 3, some explants were cultured in 4.25 mL of supplemented William's medium on top of a wire platform covered with a lens cleaning tissue during the first trial of the tissue culture set up. Mare 1 was one of these animals and due to the difficulty of finding mares at the follicular phase of the oestrous cycle, it had to be included in the current study. Nonetheless, the concentration of LPS per millilitre of medium and the proportion of supplements in William's medium were identical to the cultured explants provided by mares 2, 3, 4 and 5.

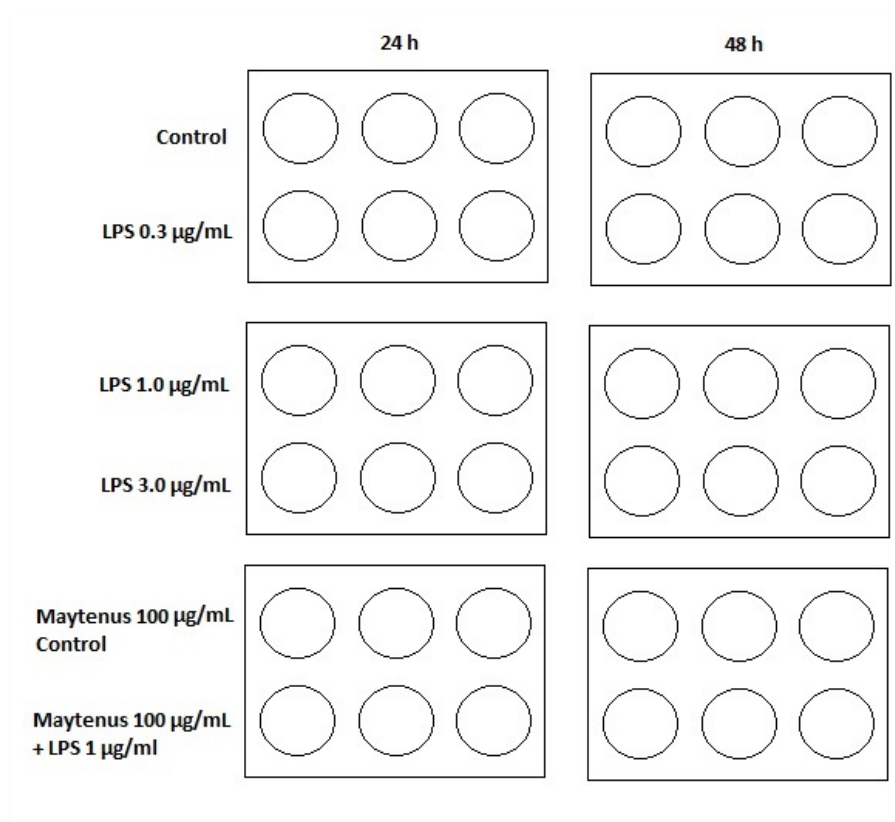


Figure 6.1. Tissue culture design for each mare. Samples were cultured in triplicate for each treatment for 24 and 48 hours. Samples were challenged with three different concentrations of LPS (0.3 µg/mL, 1.0 µg/mL and 3.0 µg/mL). *M. ilicifolia* was used as a pre-treatment before LPS inoculation.

For the objective two, a prophylactic pre-treatment using *M. ilicifolia*, the culture plates had a different time course than that of objective 1: all explants were immersed in supplemented William's medium containing *M. ilicifolia* alone (100 µg/mL) for a period of 24 hours. Following the pre-treatment, the medium was changed and replaced with fresh new medium containing *M. ilicifolia* (100 µg/mL) alone for the control group, *M. ilicifolia* (100 µg/mL) or LPS (1.0 µg/mL) for the *M. ilicifolia* and LPS group. The medium was assessed to investigate the endometrial secretion of interleukin-10 after challenge with LPS as well as after a 24 hours pre-treatment with the plant extract *M. ilicifolia* to inspect its potential anti-inflammatory compounds. A sample volume of 200 µL of the control culture medium was aseptically collected at 6 hours as well as the medium from explants treated only with 1.0 µg/mL LPS and stored at -80 °C until assayed. Six hours after the end of the 24-hour pre-treatment 200 µL of the *M. ilicifolia* control medium and 200 µL of the *M. ilicifolia* + LPS medium were also collected and stored at -80 °C (Figure 6.2). The culture time of 6 hours after LPS inoculation was chosen based on another study for the investigation of inflammatory cytokine response (Woodward *et al.*, 2013), while the *M. ilicifolia* concentrations were chosen based on previous work (Wonfor *et al.*, 2017).

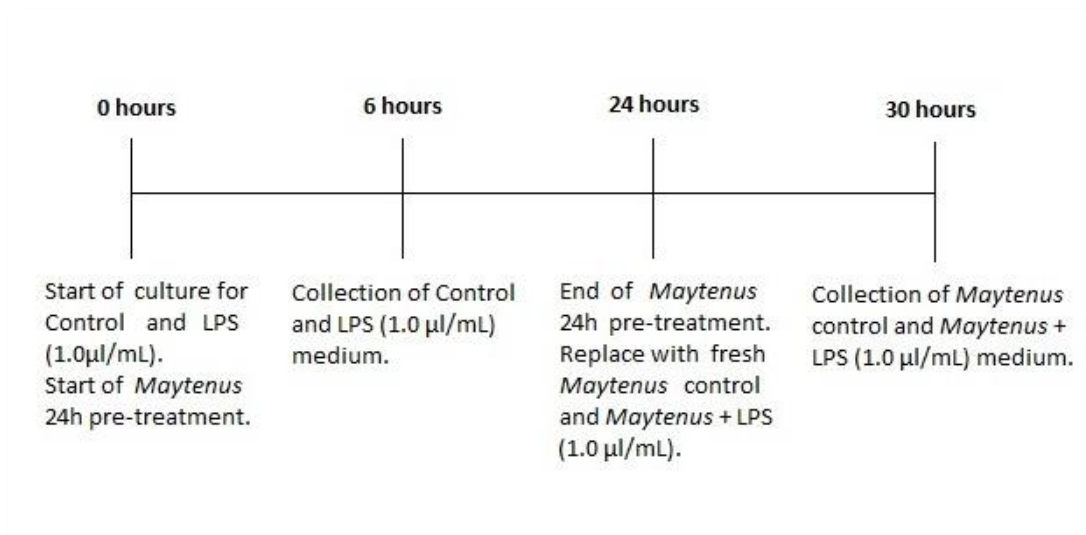


Figure 6.2. Time scale demonstrating the medium collection for the IL-10 investigation. The start of the culture for the control (media alone) and the LPS (1 µg/mL) groups was at 0h, as well as the start of the 24-hour pre-treatment with *M. ilicifolia* alone (100 µg/mL) in the *M. ilicifolia* control and in the *M. ilicifolia* + LPS wells. After 6 hours, 200 µl of media was collected from the control (media alone) and the LPS (1 µg/mL) culture wells. After 24h, the medium from the *M. ilicifolia* control and the *M. ilicifolia* + LPS wells was removed and replaced with *M. ilicifolia* alone (100 µg/mL) and with *M. ilicifolia* (100 µg/mL) + LPS (1 µg/mL). At 30 hours, 200 µl of media was collected from the *M. ilicifolia* control (100 µg/mL) and from the *M. ilicifolia* (100 µg/mL) + LPS (1 µg/mL) wells.

Finally, after periods of 24 or 48 hours, the explants were removed from the tissue culture, individually stored in 1.5 mL of RNALater at 4 °C for a period of 24 hours, removed from the RNALater and frozen at -20 °C until RNA-extraction. Once the explants were removed, the medium was collected and stored at -20°C until PGF_{2α} radioimmunoassays.

6.2.4 | Prostaglandin F_{2α} Radioimmunoassays

Radioimmunoassays were performed to quantify the PGF_{2α} production by explants after antigen challenge bacteria inoculation. Analysis compared the PGF_{2α} production between control and the different concentrations of LPS to inform the concentration that best induced uterine inflammation thereafter taken forwards to RNA extraction, RNA-Sequencing (RNA-Seq) and data analysis. All medium

samples were brought to room temperature and 150 µL of the medium from each triplicate culture treatment well was pooled. The pooled samples were then diluted in 0.05 M Tris buffer 1:200 and PGF_{2α} antisera diluted 1:16000. Medium samples were run in duplicate and the standard curve was run in triplicate as previously described in Chapter 3 and in Appendix 3 (Cheng *et al.*, 2001).

Briefly, the standard curve was prepared by making up eight standard concentrations (5, 2.5, 1, 0.5, 0.25, 0.10, 0.05 and 0.025 ng/mL) by dissolving the stock solution in 0.05 M Tris buffer. The standard, total binding, total count, buffer blank and test tubes were prepared, vortexed and incubated for 16-24 hours at 4 °C. The charcoal dextran solution (2% activated charcoal, 0.4% dextran) was added to all tubes, except total counts. Tubes were vortexed, incubated at 4 °C for 10 minutes and centrifuged at 1000-1500 x g. The supernatant was decanted into scintillation tubes, scintillation liquid was added and each tube was counted as counts per minute. The normalised percent bound for each sample was calculated and a standard curve was generated.

6.2.5 | Endometrial Expression of IL-10

Prior to performing the IL-10 ELISA, the medium samples from mares 3, 4 and 5 were allowed to return to room temperature. The technical triplicates from each treatment were pooled together and then diluted 1:2 and 1:10 using the diluent provided in the kit (EEIL10, Invitrogen, UK). The standards and the samples were measured in duplicate.

The endometrial expression of IL-10 was investigated using a commercially available ELISA kit following manufacturers' instructions. The detection range was

90 pg/mL to 25 ng/mL, and the sensitivity of the assay was 90 pg/mL. The plate was read using a microliter plate reader (iMark, Bio-Rad) at an absorbance of 450 nm.

6.2.6 | RNA Extraction and RNA-Sequencing

LPS 3 µg/mL was the treatment chosen to be taken to RNA-Seq. From all five mares providing explants for this experiment, total RNA was extracted from all technical replicates at all time points resulting in a total of 75 RNA samples. The Nanodrop 1000 Spectrophotometer (Thermo Scientific, UK) was used to check RNA concentrations and quality of each sample. The samples were also subjected to electrophoresis gel for RNA integrity assessment as previously described in Chapter 3.

Prior to constructing the libraries, equal concentrations of each technical replicate (duplicates for the “0 hours” samples and triplicates for the cultured “24 hours” and “48 hours” samples) were pooled into a single RNA sample to diminish oddities in a single replicate. The pooled samples had a final concentration of 1500 ng of RNA in a total volume of 50 µL. According to the manufacturer’s instructions, the Illumina TruSeq Stranded mRNA kit (20020594, Illumina) was used to prepare the dual-indexed next-generation sequencing libraries. After library construction, each library was individually quantified using an Epoch spectrophotometer (BioTek Ltd) and finally pooled again at equal concentrations. A Qubit fluorometer (Thermo Fisher Ltd) was used to quantify again the pooled DNA and agarose gel electrophoresis was used to determine the size of each library (average size of 300bp).

The pooled library was then diluted to 10 nM and sent to the Wales Gene Park (Institute of Medical Genetics, Cardiff University). Paired-ended reads in the format

of 2x75bp were performed on the Illumina HiSeq4000 platform at a final dilution of 8 pM. A first run was performed and the original pool was adjusted for a few underperforming samples by increasing the volume, re-quantifying and diluting them to 10 nM for transport to Cardiff.

6.2.7 | Data Processing and Gene Expression Analysis

Following RNA-Seq, a total of 25 pair-end raw reads were generated. For the quality check the reads were analysed using the FastQC software (version 0.11.2) and then the TopHat software (version 2.0.14) was used to map the reads to the equine reference genome (*Equus caballus*, EquCab2; GCA_000002305.1, Ensembl website). The total read counts for each one of the alignment files created by TopHat was retrieved using the equine annotation file (Ensembl website, version EquCab2.89). Table 6.2 describes each RNA-Seq sample.

The RNA-Seq analysis was carried out using the R/Bioconductor DESeq2 package. Pairwise analysis between the control and LPS groups were performed at 24 and at 48 hours, as well as a pairwise analysis of explants treated with LPS between 24 and 48 hours of treatment. Computer codes used in this chapter are shown in Appendix 6.2. Differentially expressed genes (DEGs) were then submitted to the Search Tool for the Retrieval of Interacting Genes/Proteins (STRING) database (Szklarczyk *et al.*, 2015) for retrieval of protein-protein interactions (PPI), network analysis and for the discovery of functional gene associations. The Kyoto Encyclopedia of Genes and Genomes (KEGG) pathways (Kanehisa and Goto, 2000) and the Protein families database (PFAM) (Bateman *et al.*, 2000) retrieved from STRING were discussed in more detail. PFAM is a protein family database, featuring literature references,

functional annotation and database links for each family (Bateman *et al.*, 2000; Bateman *et al.*, 2004).

Table 6.2. Summary of the 25 RNA-Sequencing samples.

Sample	Mare	Time point ^a	Treatment ^b	Total sequences Raw reads ^c	Mapped reads ^d	Alignment rate ^e	Total count ^f
1	1	0h	Fresh	17701562	16121060	90.2%	10141641
2	1	24h	Control	24846417	16743308	66.8%	15154964
3	1	24h	LPS	18398294	16701303	89.8%	11652793
4	1	48h	Control	13704434	12424768	89.7%	9032012
5	1	48h	LPS	19033058	17186376	89.5%	12316918
6	2	0h	Fresh	11852707	10722543	89.6%	6944685
7	2	24h	Control	17380573	15791770	90.0%	10855899
8	2	24h	LPS	17582079	16040102	90.4%	10729403
9	2	48h	Control	17677426	16145497	90.4%	10900574
10	2	48h	LPS	22268819	20305063	90.3%	13363555
11	3	0h	Fresh	14933482	13341562	88.4%	8412706
12	3	24h	Control	13993437	12549092	88.9%	8934190
13	3	24h	LPS	17951318	16022104	88.4%	10843436
14	3	48h	Control	18031924	16113863	88.5%	11177998
15	3	48h	LPS	20552807	18188787	87.7%	12589678
16	4	0h	Fresh	14692121	13114096	88.3%	9142711
17	4	24h	Control	20674149	18426927	88.1%	13465046
18	4	24h	LPS	20621888	18450725	88.5%	12985243
19	4	48h	Control	15338420	13611251	87.8%	9515124
20	4	48h	LPS	15006299	13341941	88.0%	9584447
21	5	0h	Fresh	13603818	12103539	88.2%	7724509
22	5	24h	Control	16669071	14994157	89.1%	10494651
23	5	24h	LPS	24389709	21883261	88.8%	15743688
24	5	48h	Control	18022900	16289994	89.4%	11567313
25	5	48h	LPS	17575401	15776466	88.7%	11408804

^a Specific time-points when explants were removed from culture.

^b Fresh samples were collected at the abattoir immediately after death.

^c Counts of the total number of sequences processed.

^d Number of reads mapped to the annotated equine genome.

^e Percentage of reads mapped to the annotated equine genome.

^f Counts of reads assigned to genomic features.

6.2.8 | Statistical Analysis

The SPSS statistical package (Version 23.0, IBM, USA) was used to perform the IL-10 data analysis. To assess IL-10 secretion between treatments a linear mixed model was used, with treatments (control, LPS 1 µg/mL, *M. ilicifolia* 100 µg/mL or *M.*

ilicifolia 100 µg/mL + LPS 1 µg/mL) set as fixed factors and horse as a random factor. Values were reported as the arithmetic mean \pm SEM for each treatment across horses. The results were classified as significant where $P < 0.05$.

Analysis of PGF_{2 α} secretion was also performed using SPSS. Descriptive statistics were expressed as the mean \pm standard error of the mean (SEM). PGF_{2 α} secretion concentrations were corrected as ng/mL per milligram of tissue and normalized by square root transformation. A linear mixed model was performed to compare PGF_{2 α} secretion over time and between control and treated explants, where mare were fitted as a random effect to control for variation in PGF_{2 α} secretion from explants collected from different animals. Time point and treatment were fitted as the repeated measures. Statistical significance was assumed when $P < 0.05$.

For the analysis of DEGs, a negative binomial distribution was used to perform the statistical analysis on the RNA-Seq data, performed by the R/Bioconductor DESeq2 package (Love *et al.*, 2014). The Benjamini-Hochberg (BH) false discovery rate (FDR) method (Benjamini and Hochberg, 1995) was used to correct the P value for multiple tests. Two tests were performed in total: between control (media alone) and LPS challenged explants at 24 hours, and from LPS challenged explants between 24 and 48 hours. Genes that had readings across all samples lower than 1000 were removed from the analysis. The genes were considered differentially expressed at an FDR of 0.05.

6.3 | Results

6.3.1 | Prostaglandin F_{2α} Secretion by Challenged Explants

The PGF_{2α} secretion from control explants (media alone) and explants treated with LPS 0.3 µg/mL, LPS 1.0 µg/mL and LPS 3.0 µg/mL are shown in Figure 6.3. The statistical analysis outcome for the LPS RIA analysis is that there was no significant difference between treatments at either 24 or at 48 hours. However, there was a time effect between 24 hours and 48 hours, meaning that the overall production of PGF_{2α} at 24 hours differs to the production at 48 hours.

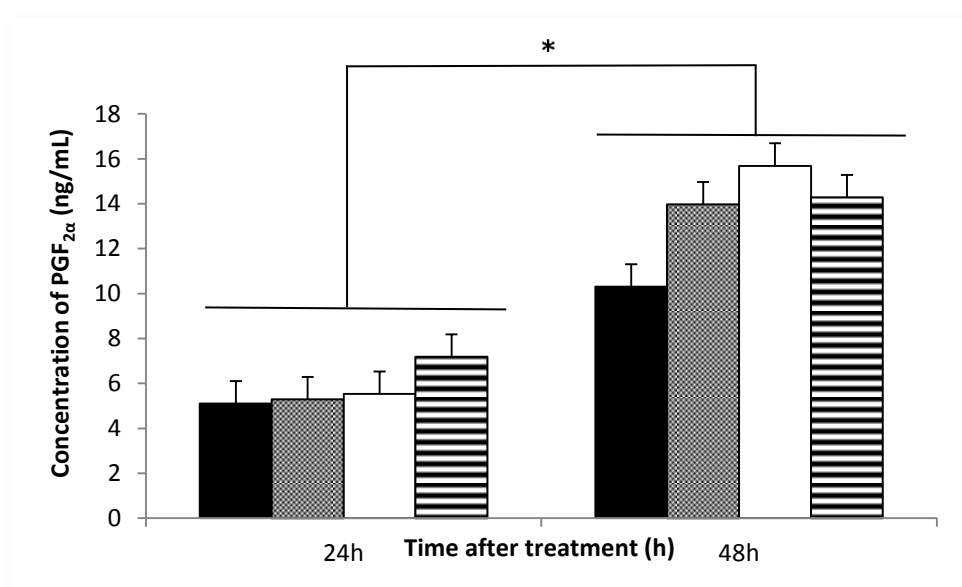


Figure 6.3. Secretion of PGF_{2α} (Mean ± SEM) from equine endometrial explants challenged with LPS. Explants were cultured in supplemented William's medium control (■), LPS 0.3 µg/mL (▨), LPS 1 µg/mL (□) and LPS 3 µg/mL (▤). After treatment, the PGF_{2α} concentrations were measured at 24 and 48 h. No significant difference was found between treatments at 24 h or at 48 h post-treatment. Values differ between 24 h and 48 h, * P < 0.001

6.3.2 | Endometrial Expression of IL-10 After LPS Inoculation

Interleukin-10 was expressed by cultured explants (Figure 6.4), however no significant differences in IL-10 production were found between the control, LPS 1.0

µg/mL treated explants, explants pre-treated with *M. ilicifolia* 100 µg/mL and *M. ilicifolia* (100 µg/mL) + LPS (1 µg/mL) at 6 hours.

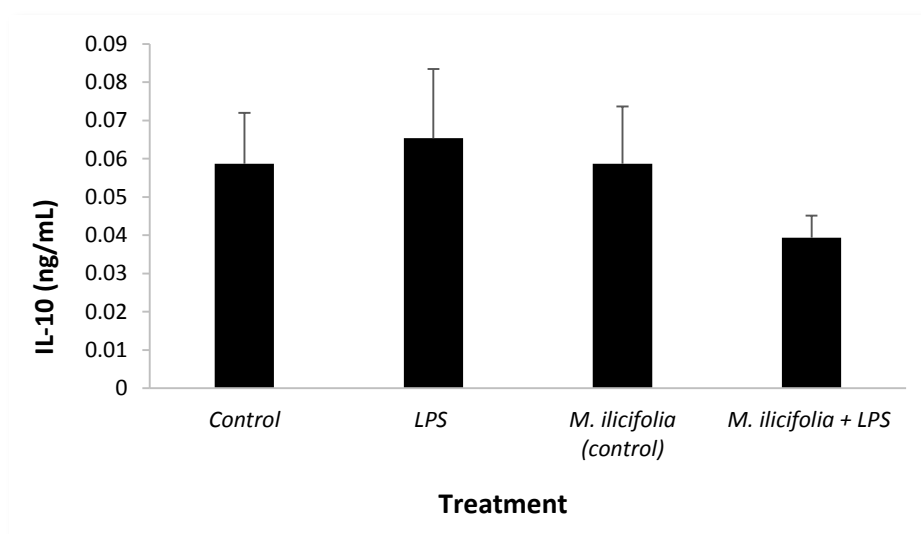


Figure 6.4. Interleukin-10 concentration (Mean ± SEM) of explants cultured in control media, challenged with LPS and pre-treated with *M. ilicifolia*. Control explants were cultured in media alone, treated with LPS, treated with LPS (1 µg/mL), pre-treated with *M. ilicifolia* (100 µg/mL) and *M. ilicifolia* (100 µg/mL) + LPS (1 µg/mL). After treatment, the IL-10 concentrations were measured after 6 hours. No significant difference was found between treatments.

6.3.3 | Gene Expression

The principal component analysis (PCA) plot, Figure 6.5 visually presents each sample in the data set, representing the effect of control (media alone) and LPS challenged explants over time, as well as the effect of explants collected at 0 hours on the count matrix. The cultured explants are clustered together separately from the 0 hours biopsies, as shown by the first component (PC1). Mare 1 (×) was the only horse where explants for the tissue culture were cultured in 4.25 mL of media instead of 3 mL like the other four mares (Mares 2, 3, 4 and 5). It is apparent from the figure that the gene count matrix of mare 1 (×) clustered together with the matrixes of the other mares. Taking into account the expected individual differences between biological replicates, the plot indicates that the gene expression was not altered by the amount of media used in the culture.

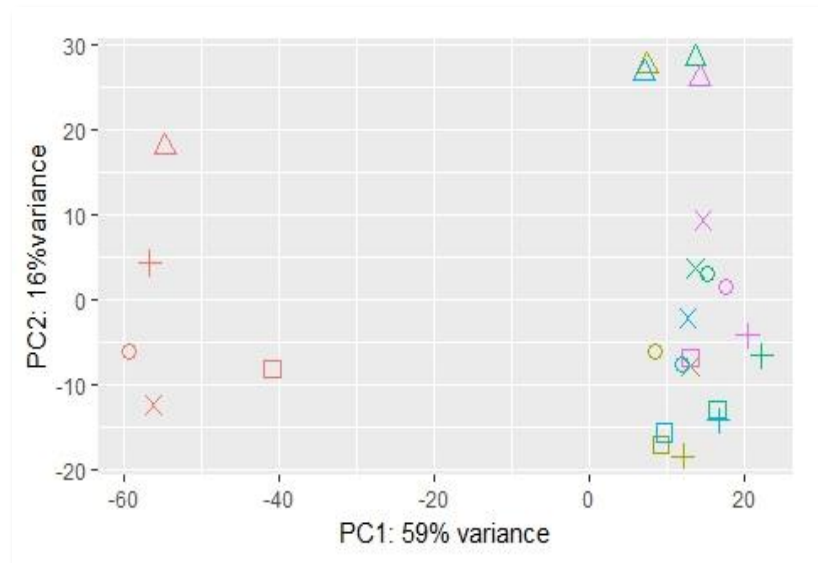


Figure 6.5. PCA plot of the RNA-Seq data. Biopsies taken at **0 hours**, and explants treated with **control (media alone) at 24 and 48 hours** or **treated with LPS (3 $\mu\text{g/mL}$) at 24 and at 48 hours**. Mares 1 (\times), 2 (\square), 3 (\circ), 4 (\triangle) and 5 ($+$). The plot displays each sample in the dataset, demonstrating a cluster for samples collected at **0 hours** and another cluster for the cultured samples (all other colours).

Changes in gene expression between control (media alone) explants and LPS challenged explants were compared using the DESeq2 package. The null hypothesis for each gene tested using DESeq2 was that there was no difference in its expression between the control (media alone) and LPS treated groups at 24 hours. The null hypothesis was rejected when the observed difference in expression of a gene was greater than expected by random chance (using an adjusted p-value of 0.05). At 24 hours, 11632 genes were found to be expressed, 2 of which were shown to be statistically significantly differentially up-regulated and 3 shown to be statistically significantly down regulated in the control relative to the LPS treated group, at an FDR of 0.05. The list of the 5 differentially expressed genes can be found in table 6.3.

Table 6.3. Summary of the differentially expressed genes between control and LPS challenged explants cultured for 24 hours sorted by p-value.

Mapped gene	Annotation ^a	Control 24h Counts ^b	LPS 24h Counts ^c	Bonferroni ^d
ENPP2	Ectonucleotide pyrophosphatase / phosphodiesterase 2	2071	636	2.11E-06
SOX13	SRY (sex determining region Y)-box 13	3679	2986	0.025
IRAK3	Interleukin-1 receptor-associated kinase 3	525	886	0.039
PLVAP	Plasmalemma vesicle associated protein	3832	2089	0.039
ZC3H12C	Zinc finger CCCH-type containing 12C	1377	1974	0.045

^a The protein coded by that specific gene.

^b The number of reads mapped to a specific gene from control explants.

^c The number of reads mapped to a specific gene from LPS-challenged explants.

^d Statistical correction for multiple comparisons.

The STRING functional enrichment analysis of the 5 DEGs identified at 24 hours between LPS and control explants in culture was performed using the 11632 total expressed genes as the statistical background. The statistical background analysis was set up using the list of the 11632 genes expressed in the analysis. The protein-protein interaction (PPI) network p-value was 1, meaning meaning that the list of genes was small (i.e. less than 5 or so) or that the list of 5 genes represented a random collection that is not well connected. As attested by STRING, this result does not determine that the genes are not biologically meaningful. For this reason, the genes found to be differentially expressed between control and LPS at 24 hours (Table 6.3) were individually assessed to determine the correlation of each one of them to LPS and inflammation.

The same was assumed for the analysis between 24 and 48 hours after LPS challenge. The null hypothesis for each gene tested using DESeq2 was that there was no difference in its expression between explants treated with LPS between after 24 and 48 hours. The null hypothesis was rejected when the observed difference in expression of a gene was greater than expected by random chance (using an adjusted p-value of 0.05). A total of 11632 genes were also found to be expressed, 66 of

which were shown to be statistically significantly differentially up-regulated and 1 shown to be statistically significantly down-regulated at 24 hours relative to 48 hours post-challenge, both at FDR of 0.05 with a $\text{Log}_2\text{FC} \geq \pm 2$. The STRING functional analysis of the DEGs identified between 24 and 48 hours from the LPS challenged explants was performed using the 11632 total expressed genes as the statistical background. The PPI p-value was 1.0^{-16} , indicating interaction enrichment between the proteins that are at least partially biologically connected as a group. The predicted STRING network was composed of 67 nodes and 200 edges.

The STRING enrichment analysis of all DEGs when comparing the transcriptome of explants treated with LPS at 24 and 48 hours returned a total of 3 enriched PFAM and 1 enriched KEGG pathway which are shown in more detail in table 6.4. The predicted STRING PPI network is illustrated in Figure 6.6, in which the enrichments featured in Table 6.4 are highlighted in different colours.

Table 6.4. Summary of the functional enrichments in the network retrieved by STRING between 24 and 48 hours after LPS challenge sorted by p-value.

Enrichments ^a	Pathway code ^b	Pathway description ^c	Count ^d	FDR p-value ^e
PFAM Protein Domains	PF00225	Kinesin motor domain	8	1.11×10^{-7}
KEGG Pathway	04110	Cell cycle	7	9.8×10^{-4}
PFAM Protein Domains	PF02984	Cyclin, C-terminal domain	4	0.002
PFAM Protein Domains	PF00134	Cyclin, N-terminal domain	4	0.012

^a Enrichments from either the KEGG or the PFAM Protein Domains/Families database.

^b Identification code from each pathway/database.

^c Description of each pathway from either KEGG or PFAM.

^d The number of genes involved in each pathway.

^e Over-represented p-value with false discovery rate statistical correction for multiple comparisons.

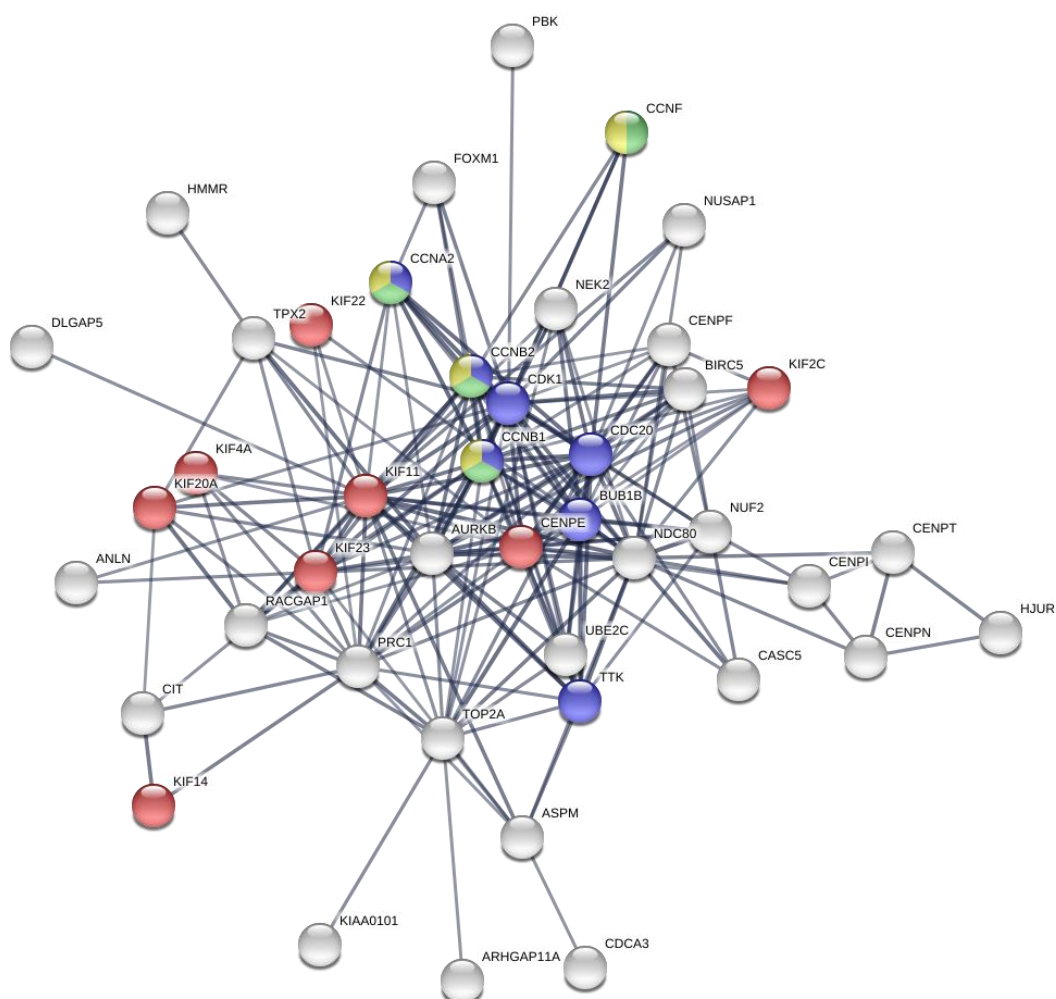


Figure 6.6. STRING predicted PPI network of the DEGs between 24 and 48 hours post LPS challenge in the tissue culture media. Blue nodes represent genes that belong to the KEGG “Cell cycle” pathway, red nodes represent genes that belong to the PFAM “Kinesin motor domain”, green nodes represent genes that belong to the PFAM “Cyclin, C-terminal domain” and yellow nodes represent genes that belong to the PFAM “Cyclin, N-terminal domain”. The interaction score between nodes was set to high confidence (0.7). Disconnected nodes are hidden in the network.

As shown in Table 6.4 the “Cell cycle” was the only significantly enriched KEGG pathway with an FDR p-value of 0.00098 and 7 genes involved: BUB1B (BUB1 Mitotic Checkpoint Serine/Threonine Kinase B), CCNA2 (Cyclin-A2), CCNB1 (Cyclin-B1), CCNB2 (Cyclin-B2), CDC20 (cell-division cycle protein 20), CDK1 (Cyclin-dependent kinase 1), and TTK (TTK protein kinase). These genes were up-regulated with a Log₂FC between 2.8 and 3.7. This list of genes involved in the “Cell cycle” pathway was fed to the “KEGG Color and Pathway Search” and the pathway is shown in Figure 6.7.

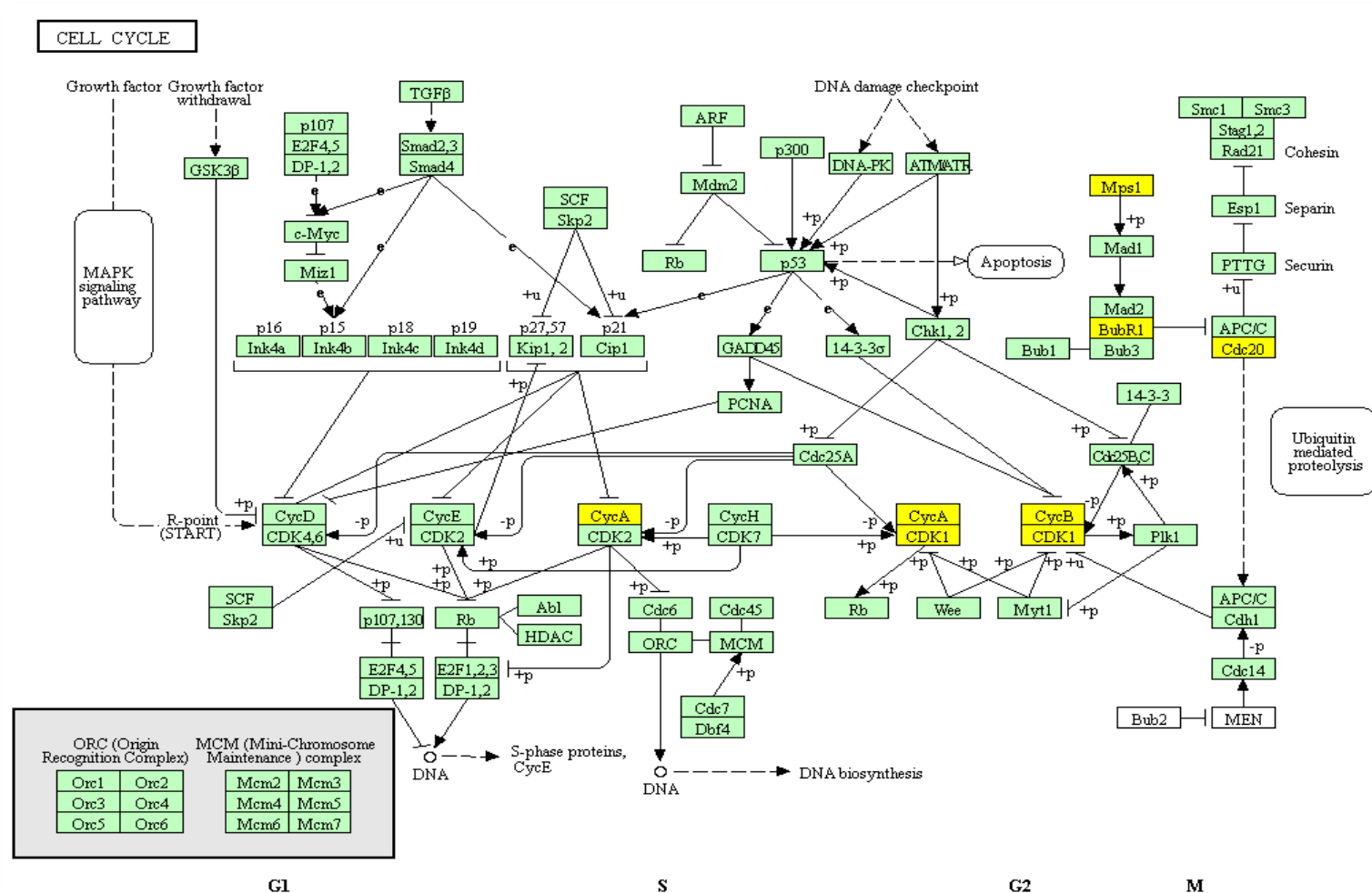


Figure 6.7. DEGs in the KEGG Cell cycle pathway between 24 and 48 hours after LPS challenge in the tissue culture media. Green boxes are genes in the equine transcriptome, but not differentially expressed. White boxes are genes not described as horse KO terms. Yellow boxes are DEGs. Image created using the KEGG Online “Search and Color Pathway” tool. G1 and G2 stand for gap phases 1 and 2, respectively. S stands for DNA synthesis phase and M for mitosis phase.

6.4 | Discussion

6.4.1 | Prostaglandin F_{2α} Secretion by Challenged Explants

There is a relatively small body of literature published on equine endometrial culture and biomarkers of inflammation. *In vivo*, neutrophils are an important process in inflammation and their presence in the endometrium is an indicator of inflammation (Katila *et al.*, 1990; Pycock and Allen, 1990; Kotilainen *et al.*, 1994; Zerbe *et al.*, 2003). The lack of peripheral circulation in the tissue culture makes it impossible to measure leucocyte infiltration into the endometrium. Consequently, finding other markers of inflammation such as prostaglandin F_{2α} production was needed (Nash *et al.*, 2010b).

Previous research findings using radioimmunoassay to determine the PGF_{2α} secretion by equine endometrial explants has already reported contrasting results between follicular and luteal phases and transitional season explants when challenged with 0.03 or 3.0 µg/mL LPS and with 10, 10³ and 10⁵ killed whole *S. zooepidemicus* (Nash *et al.*, 2008). Transitional season explants challenged with either LPS or *S. zooepidemicus* for 24 and 72 hours did secrete increased concentrations of PGF_{2α} when compared to control explants treated with medium alone, in a concentration-dependant manner. However, follicular and luteal explants did not significantly respond to treatment with LPS or *S. zooepidemicus* (Nash *et al.*, 2008). On the other hand, a more recent study demonstrated a PGF_{2α} response after challenging equine endometrial cultured explants with 3 µg/mL LPS (Nash *et al.*, 2018), and this is why PGF_{2α} was still used as a marker for explant functionality in the current study.

Nonetheless, the LPS RIA results of this study are similar to that first described using the equine endometrial culture model (Nash *et al.*, 2008). The time difference between 24 and 48 hours can somehow be attributed to the great difference between individuals, leading to similarities within subject over-time. Also, with the continuous LPS stimulation considering that the LPS remained in the tissue culture well, a continuous production of PGF_{2a} is expected to happen.

Based on the concentration used in previous studies (Nash *et al.*, 2018) and taking into account the concentration-dependent production of PGF_{2a} (Nash *et al.*, 2010b) the LPS 3 µg/mL was the one chosen to be taken forward to RNA extraction, RNA-Seq and transcriptomic analysis of up and down-regulated genes. Investigation using transcriptomic analysis was required to determine whether or not the explants challenged with inflammatory inoculants express genes related to the immune system and to inflammation pathways.

6.4.2 | Endometrial Expression of IL-10 After LPS Inoculation

The potential anti-inflammatory activities of *M. ilicifolia* in the equine endometrium was investigated *in vitro* in this pilot study by analysing the expression of IL-10 after LPS inoculation and after *M. ilicifolia* pre-treatment followed by LPS inoculation in endometrial explants. IL-10 is an anti-inflammatory cytokine that prevents damage to the host by regulating the inflammatory immune response to pathogens during infection and its analysis is important for the study of persistent endometritis (Fumuso *et al.*, 2006). The cultured explants expressed IL-10, however there was no significant difference in IL-10 expression between treatments.

One source of weakness in this study which could have affected the measurements of IL-10 was the number of horses (n=3). Further studies using more biological replicates might produce interesting results with a greater degree of accuracy when explants are challenged with LPS and pre-treated with *M. ilicifolia*. On the other hand, it appears that endometrial inflammation has not been induced properly, which leads to the hypothesis that LPS was not working for some reason. *E. coli* LPS is considered a potent pathogen-associated molecular pattern that is recognized by innate immune cells responsible for inflammatory responses (Tizard, 2013). Thus, LPS has been widely used by the research community to investigate immune responses both *in vivo* and *in vitro*. For example, it has already been demonstrated that the gene expression of IL-10 is up-regulated in mares following an experimentally induced endometritis using *E. coli* (Christoffersen *et al.*, 2012). However, previous studies have used either *E. coli*, killed spermatozoa or semen to induce endometritis (Fumuso *et al.*, 2006; Christoffersen *et al.*, 2012; Woodward and Troedsson, 2013). Therefore, a direct comparison between the results of the current study and published studies into equine endometritis are not possible.

6.4.3 | Gene Expression

The endometrial explant system was used to induce inflammation by LPS challenge in the culture medium to study the mechanisms underlying PMIE in mares at the level of gene expression. It is a surprising outcome that only 5 genes were shown to be differentially expressed when comparing the explants challenged with LPS and the control explants cultured in media alone for the period of 24 hours.

This study has identified the IRAK-3 gene to be up-regulated in the tissue explants after LPS treatment for a period of 24 hours. The IRAK3 is part of the IL-1 receptor

associated kinases (IRAK) and it is mainly expressed in cells of monomyeloic origin (Wesche *et al.*, 1999). Previous research findings into the IRAK family confirmed that their members are indeed involved in lipopolysaccharide signal transduction (Wesche *et al.*, 1999). It has already been reported by numerous studies that IRAK1, IRAK2 and IRAK4 are involved in the IL-1R1 and TLR signalling pathways (Kanakaraj *et al.*, 1998; Thomas *et al.*, 1999; Suzuki *et al.*, 2002; Suzuki *et al.*, 2003). IRAK-1 and IRAK-4 are positive TLR signal transducers and IRAK-1 and IRAK-2 take part in the activation of the NF- κ B transcription factor (O'Neill and Greene, 1998; Kobayashi *et al.*, 2002). IRAK-3 is induced by TLR stimulation, however, it negatively regulates the TLR signalling, being involved in the initiation of endotoxin tolerance. After persistent LPS stimulation, it has been demonstrated that IRAK-3 is indeed a key component in inducing LPS tolerance, maintaining the innate immune system homeostasis by negative regulating the TLR signalling (Kobayashi *et al.*, 2002).

Another study looked at the IRAK-3 expression after LPS stimulation in macrophages in cell culture (Lyroni *et al.*, 2017). It also supports the idea that IRAK-3 is involved in the mechanisms of endotoxin tolerance. It demonstrated that in the case of acute inflammation induced by LPS, IRAK-3 is induced within 24 hours of culture. However, during continuous LPS stimulation that occurred in that cell culture study, considering that the LPS stayed continuously in the cell culture medium, the transcriptional activation of IRAK-3 has been silenced after 24 hours to enable the cells to return to homeostasis and to be responsive (Lyroni *et al.*, 2017). It is suggested that this also happened in the current study as LPS was maintained in the medium where explants were cultured. IRAK might be induced by the LPS challenge, which in turn is dampening down the TLR pathway response so that a

large inflammatory response in healthy mares does not happen and therefore persistent inflammation is avoided to allow fertilisation to occur. Perhaps in susceptible mares the IRAK response does not lead to a dampening down of the TLR pathway and inflammation is free to persist. Nonetheless, not much is known about the transcriptional regulation of IRAK-3, therefore future studies are needed to determine how IRAK-3 interacts with other IRAK molecules and to better understand its role in inflammation (Zhou *et al.*, 2013; Lyroni *et al.*, 2017). Another hypothesis is that, as indicated by PGF_{2α}, the cultured explants did not respond to LPS challenge. This might explain why other members of the TLR pathway were not differentially expressed in this study.

The second up-regulated gene after LPS challenge at 24 hours was the ZC3H12C gene that encodes the Zinc Finger CCCH-Type containing 12C protein. To date, a study has demonstrated that the CCCH-zinc finger protein family participates in the macrophage activation (Liang *et al.*, 2008). A previous *in vitro* study showed that the inflammatory cytokine TNFα induces the expression of ZC3H12C in cultured endothelial cells. When overexpressed, ZC3H12C significantly inhibits the endothelial cell inflammatory response by attenuating the expression of chemokines such as MCP-1 (Monocyte chemoattractant protein-1), IL-8, VCAM-1 (Vascular cell adhesion protein 1), ICAM-1 (Intercellular adhesion molecule 1) and E-selectin (selectin cell adhesion molecule) as well as inhibiting the NF-κB signalling pathway (Liu *et al.*, 2013).

It is established that organisms do not benefit from uncontrolled inflammation and that it leads to tissue impairment, therefore negative feedback mechanisms usually take place to control inflammatory responses caused by pathogens (Liang *et al.*,

2008). IL-8 is a key chemokine in endometritis, attracting neutrophils to the uterus, which are the main effector cells of inflammation in endometritis (Fumuso *et al.*, 2006). Based on the previous research findings discussed above, if expression of ZC3H12C attenuated IL-8 in the healthy mares used in this study, it could mean that susceptible mares that do not upregulate this gene have a high IL-8 response and therefore neutrophil influx to the uterus, resulting in a massive persistent uterine inflammation. It is possible that ZC3H12C plays an anti-inflammatory role in the vascular endothelial cells *in vitro* (Liu *et al.*, 2013), however further research is needed to elucidate the mechanisms in which they regulate inflammation *in vivo* and *in vitro* for endometrial explants.

The ENPP2, also known as autotaxin, was down-regulated after the 24 hours LPS inoculation. It is responsible to convert extracellular lysophosphatidylcholine to lysophosphatidate (LPA), where the latter is linked to inflammatory pathways (Brindley *et al.*, 2013; Benesch *et al.*, 2014; Benesch *et al.*, 2015a). Injury and inflammation cause autotaxin to be produced, and its levels decrease with the resolution of tissue repair (Benesch *et al.*, 2014; Benesch *et al.*, 2015b). It is known that the healing cycle is disrupted by prolonged inflammation and a high autotaxin concentration leads to various inflammatory pathological conditions (Nikitopoulou *et al.*, 2012; Hozumi *et al.*, 2013; Benesch *et al.*, 2014; Benesch *et al.*, 2015a).

Therefore, a down-expression of autotaxin in healthy mares in this study suggests that the inflammation has already been resolved. It can then be hypothesised that mares susceptible to PMIE who do not down-regulate this gene have an intense and prolonged inflammatory response, leading to persistent uterine inflammation. Nonetheless, more research into the mechanism of autotoxin is needed, since it is

also involved in numerous metabolic pathways. It is important to understand whether a down-regulation of autotaxin is linked to metabolism or immunity (Knowlden and Georas, 2014).

The SOX13 gene was down-regulated after the 24 hours LPS inoculation. It is one of the members of the SOX family transcription factors that are related to development processes such as sex determination, cell proliferation, survival, differentiation and maturation in different cell lineages and also related to human genetic diseases (Wegner, 1999; Wang *et al.*, 2006; Lefebvre, 2010). It has been reported that SOX13 is linked with the emergence of gammadelta T cells in the thymus (Lefebvre, 2010). Gammadelta T cells can secrete pro-inflammatory cytokines such as IL-17, which plays a role in host defense against microorganisms and takes part during infection (Papotto *et al.*, 2017; Veldhoen, 2017). Therefore, a down-regulation of SOX13 in healthy mares means a lower emergency of gammadelta T cells and consequently a decrease in cytokine secretion. This happening at 24 hours after LPS challenge can suggest that inflammation has already been resolved by this time. On the other hand, PMIE susceptible mares might have an up-regulation of SOX13, leading to a higher emergency of gammadelta T cells and a consequent greater production of cytokines to tackle inflammation.

The PLVAP gene, also called PV-1, was also down-regulated after LPS challenge. It encodes the Plasmalemma Vesicle Associated Protein, which is a cell-specific protein related to transport across the endothelium. Therefore PLVAP is expressed by a subset of normal microvascular endothelial cells (ECs) creating trans-endothelial channels and fenestrae (Stan *et al.*, 2004; Niemela *et al.*, 2005). It has been suggested that PLPVAP might have a role in inflammation, specifically in the

leukocyte transendothelial migration (Keuschnigg *et al.*, 2009; Rantakari *et al.*, 2015). *In vitro* capillary flow assays demonstrated that PLPVAP contributes to the transcellular migration of leukocytes by diminishing the resistance through membrane fusion. Indeed, *in vivo* studies also showed that blockage of PLPVAP in a peritoneal inflammation reduced by approximately 85 % the migration of leukocytes overall, in special the neutrophil invasion was inhibited by 65 % (Keuschnigg *et al.*, 2009). A down-regulation of PLVAP in healthy mares in this study might suggest that susceptible mares who do not down-regulate this gene have an aggravated inflammatory response in the uterus by increasing leukocyte trafficking.

Between 24 and 48 hours after LPS inoculation, the differential expression analysis demonstrated an up-regulation of the cell cycle KEGG pathway (Table 6.4). The cell cycle is divided in DNA synthesis (S) and mitosis (M) phases, with two gap phases (G1 and G2) in the order G1/S/G2/M (Nurse, 2000; Rhind and Russell, 2012) as demonstrated in Figure 6.7. The progression through the cell cycle, in most cell types, is run by the interaction of numerous molecules such as cyclins, cyclin-activating kinases (CAKs), cyclin-dependent kinases (CDKs) and cyclin-dependent kinase inhibitors (CDKIs) (Sherr and Roberts, 1995; Tusell *et al.*, 2005). Within the cell cycle progression, cyclins and the CDKs classes of protein determine whether cells proceed through the cells cycles of cells endure in a state of arrest (Sherr, 1996; Meijer *et al.*, 1997; Tian *et al.*, 2007). Therefore, the enriched PFAM domains are also linked to the cell cycle KEGG pathway.

It has been demonstrated in a preliminary study that a selective cyclin-dependent kinase inhibitor significantly suppressed the expression of proinflammatory cytokines (Tian *et al.*, 2007), while another showed that cell cycle inhibition reduces

inflammatory responses after traumatic brain injury (Skovira *et al.*, 2016). The healthy pony mares used in the current study, known to be resistant to persistent uterine inflammation, were in the follicular phase of the oestrous cycle when immune responses are up-regulated. Therefore, it is thought that between 0 and 24 hours after LPS challenge the response was mounted, tackled inflammation and returned to normal by 24 hours. On the other hand, it is surprising that no immune genes were changed between 24 and 48 hours of LPS challenge, since it is known that most mares take up 48 hours after challenge to clear the uterine inflammation induced by semen and/or sperm. Therefore, it is also hypothesised that LPS was not working properly.

6.5 | Conclusion

In conclusion, this study provided preliminary information on the endometrial transcriptome modulation when explants are challenged with *E. coli* LPS *in vitro*. Surprisingly, there was no significant production of PGF_{2α} as a marker of inflammation following LPS challenge and explants showed very little difference in expression of genes related to inflammation when compared to the baseline set in Chapter 4.

Considering that the mares providing explants to this experiment were free of inflammation and thought to be resistant to persistent endometritis, the up-regulation of IRAK-3 suggests that during the first 24 hours of LPS inoculation, the endometrium was already resolving the inflammation and maintaining the innate immune system homeostasis by maybe producing tolerance to LPS. However, IRAK-3 was not up-regulated after 24 hours, agreeing with the result from previous *in vitro* research where LPS was maintained in the culture medium, that the

expression of IRAK-3 stops after 24 hours to allow the cells to be responsive again in case of a chronic explosion to LPS (Lyroni *et al.*, 2017). Similarly, the up-regulation of the ZC3H12C gene and the down-regulation of the ENPP2, SOX13 and PLPVAP genes after 24 hours of LPS inoculation lends further evidence to the hypothesis that by the end of the 24 hours the explants were already resolving the inflammation induced by LPS. The gene expression analysis between 24 and 48 hours after LPS inoculation retrieved a list of up-regulated genes related to the cell cycle. There is still limited knowledge regarding the linkage of cell cycle pathways, inflammation and endotoxin. However, this study suggests that by this time the inflammation caused by LPS was already resolved and that the cultured explants were again in homeostasis, therefore the only significant differentiated pathways were the ones related to the cell cycle.

These findings agree with the literature, where mares are considered resistant to PMIE when they clear the uterus of the normal transient inflammatory response within 48 hours after mating, sometimes at around 12-24 hours (LeBlanc *et al.*, 1994; Troedsson, 1999, 2006; Christoffersen *et al.*, 2012). Nonetheless, further research could focus on how the equine endometrial transcriptome is modulated after LPS challenge at earlier time points of inflammation such as 6 and 12 hours using the explant culture model described in this study. Using an earlier and broader range of time points after inflammation starts might shed more light on the inflammatory pathways expressed during endometritis before the inflammation is resolved. Further research could also study how the response is different in explants collected from susceptible mares. The five genes found to be over-expressed in this study, IRAK-3, ZC3H12C, ENPP2, SOX13 and PLPVAP might be interesting candidates to focus

upon when conducting future studies into LPS-induced persistent endometritis in mares.

CHAPTER 7

CHARACTERIZATION OF TRANSCRIPTOMIC PROFILES OF MARES RESISTANT AND SUSCEPTIBLE TO PMIE *IN VIVO* AND *EX VIVO*

7.1 | Introduction

A normal, transient uterine inflammation occurs in mares after natural mating or artificial insemination caused by many factors such as spermatozoa, seminal components, debris and bacteria (Troedsson *et al.*, 1999; Watson, 2000; Katila, 2001; Troedsson *et al.*, 2001a). This normal inflammation, known as mating-induced endometritis (MIE), is needed to cleanse the uterine environment and allow embryo survival (Troedsson, 2006; Troedsson and Woodward, 2016; Christoffersen and Troedsson, 2017). However, some mares fail to clear the MIE and it consequently becomes a persistent inflammation called persistent mating-induced endometritis (PMIE), causing subfertility in mares (Watson, 2000; Troedsson, 2006). Lower pregnancy rate in mares suffering from PMIE causes expensive losses to the horse breeding industry (Riddle *et al.*, 2007).

Based on their ability to clear uterine inflammation and infection, mares are classified as resistant or susceptible to PMIE. Mares are considered resistant to PMIE when they clear the uterus off the normal transient MIE within 36-48 hours post-challenge, while susceptible mares fail to clear inflammation and remain with intrauterine fluid after this period of time (Katila, 1995; Troedsson, 1999).

Traditionally, endometritis has been diagnosed based on mare's history, evidence of fluid within the uterine lumen during physical examination of cervix and vagina and laboratory diagnostic aids such as uterine culture, cytology and biopsy (LeBlanc and Causey, 2009). The uterine biopsy grading system (Kenney, 1978; Kenney and Doig, 1986) has been regularly used and proved to be an effective method to indicate the presence or absence of MIE and PMIE in mares (Troedsson *et al.*, 1993a; Fumuso *et al.*, 2003; Woodward *et al.*, 2012). However, these methods of diagnosis can only be

used after mating, when the inflammation is already present and may lead to infertility.

The endometrium is a mucous membrane, and the innate immune response is the main immunological response to inflammation along with myometrial contractions to mechanically clear the uterine environment (Troedsson, 2006; Christoffersen and Troedsson, 2017). Research has focused on the factors associated with resistance and susceptibility to PMIE in mares, demonstrating that cytokines contribute to the pathogenesis of persistent endometritis induced by mating or by bacterial inoculation (Fumuso *et al.*, 2003; Christoffersen *et al.*, 2010; Christoffersen *et al.*, 2012; Woodward *et al.*, 2013). It is also known that seminal plasma proteins modulate the innate immune response by up-regulating the expression of interleukin (IL) 8 and IL-1 β in susceptible mares, while this regulation does not happen in resistant mares (Fedorka *et al.*, 2016; Fedorka *et al.*, 2017).

However, the global gene expression underlying resistance before bacteria or semen reach the endometrium is still unclear. Therefore, the aim of this study was to identify differentially expressed genes (DEGs) between mares resistant and susceptible to PMIE before mating occurs, acting as a baseline for global transcriptome profile before a challenge has been applied to underlie the mechanisms involved in resistance and susceptibility.

7.2 | Materials and Methods

7.2.1 | Animals

Uteri from resistant native mares (n=3) in the follicular phase of the oestrous cycle were collected at an abattoir immediately after death. The age and reproductive

history of each mare were unknown. Biopsies from Finnhorse mares (n=3) thought to be susceptible to PMIE were collected during the follicular phase of the oestrous cycle. This procedure was performed at the Field Station for Equine Research, Resources Institute Finland approved by the National Animal Experiment Board Finland (Approval no. ESAVI/4961/04.10.06/2015).

7.2.2 | Sample Collection

Resistant (ex vivo) mares

Sample collection from native pony mares was performed following the protocol described in Chapter 3. Briefly, blood was collected directly from the jugular vein immediately post-mortem and stored at 4 °C for 24 hours, followed by blood serum separation by centrifugation and serum progesterone analysis to confirm the phase of the oestrous cycle at the time of the death. Records of criteria used in the abattoir to predict the stage of the oestrous cycle and serum progesterone concentrations for each animal are described in Table 7.1.

At the abattoir, cytology samples were collected with the aid of a cytobrush as previously described (Chapter 3), and all mares were free of uterine inflammation (neutrophil count < 2 per high power field). Immediately after death, biopsies were collected in duplicate from each uterus and stored in 1.5 mL of RNALater at 4 °C for a period of 24 hours, followed by RNALater removal and sample storage at -80 °C until RNA extraction. At the laboratory, a 1x1 cm² biopsy from the uterine body was taken and stored in 10 mL of Bouin's fixative liquid for a period of up to 6 months. Histology procedure was carried out as previously described (Chapter 3) and analysed by a Boarded Pathologist for pathological and/or degenerative endometrial

changes. Native pony mares were used as an example of PMIE resistant mares. The evidence is anecdotal, but in practice PMIE is very rarely observed in ponies; therefore, they are known to be resistant. Furthermore, all mares in this group were classified as Category I in the biopsy grading system (Appendix 7.1).

Susceptible (in vivo) mares

Paired endometrial biopsies were obtained from Finnhorse mares with a history of chronic endometritis and fluid accumulation but free of active inflammation the time of collection, from the Natural Resources Institute Finland, using a sterile biopsy instrument. Mares were classified as susceptible to PMIE based on their clinical history (Table 7.2).

Biopsies for RNA-Sequencing (RNA-Seq) were placed into 1.5 mL of RNALater immediately after collection for a period of 24 hours at 4 °C followed by RNALater removal and sample storage at -80 °C. Samples were posted to Aberystwyth University (Wales, United Kingdom) by airmail while frozen in dry ice. Biopsies for histopathologic analysis to confirm the susceptibility of mares collected at the same time were placed in formalin immediately after collection for a period of 2-4 weeks and then replaced by 70 % ethanol. Samples intended for histopathology analysis were sent to Aberystwyth University (Wales, United Kingdom) at room temperature via airmail. Histology procedure was performed as previously described (Chapter 3) and the pathological endometrial changes were analysed by a Boarded Pathologist (Appendix 7.1).

Table 7.1. Summary of resistant mares sampled at the abattoir. Information regarding ovarian structures, cervical analysis and serum progesterone concentration.

Mares	Ovaries ^a	Cervix ^b	Progesterone Concentration (ng/mL) ^c
1	One 41 mm x 32 mm follicle on left ovary. Small follicles (around 7 mm in diameter) on right ovary.	Cervix is pale in colour. Two fingers were passed through cervix	1.95
2	One small (10 mm in diameter) follicle on left ovary. One 33mm x 37 mm on right ovary.	Cervix is pale in colour. Three fingers were passed through cervix.	0.16
3	One 40mm in diameter follicle on right ovary. Smaller follicles (around 20 mm in diameter) on left ovary.	Cervix had a pink-pale colour and had an open appearance. Three fingers were passed through the cervix	0.21

^a Ultrasonographic measurements of ovaries.

^b Physical examination of cervix.

^c Serum progesterone analysis for confirmation of stage of the oestrous cycle.

Table 7.2. Clinical history of susceptible mares.

Mares	Clinical history
4	Born in 1999. Foaled 2009 and 2010 but did not conceive in 2006 and in 2010. Presence of cloudy uterine fluid during the follicular phase on 3 occasions in 2013. In 2014, presence of clear fluid (30 x 30 mm) during 3 follicular phases. In 2015, one occasion of cloudy fluid (15 x 70 mm) but no samples were taken for further analysis. Nothing remarkable in 2016 and 2017.
5	Born in 2000. Foaled 2010 and 2011. Did not conceive in 2014 (inseminated in 5 follicular phases, followed by 41 examinations). In 2014 there was the presence of cloudy fluid accumulations after artificial insemination (AI) in the second to fourth follicular phases. Uterine lavage and administration of oxytocin were performed in 3 follicular phases, but no swabs or cultures were done. Seven examinations and 2 AI were performed in 2015, with no accumulation of fluid. A total of 9 examinations were carried out in March 2017, followed by 3 AI in one follicular phase followed by increasing amounts and echogenicity of fluid. However, in August 2017 there was no fluid accumulation.
6	Born in 2003, but not used for breeding. Twenty-five examinations were carried out in 2011, where cervical bleeding was caused by a student and then cloudy fluid (60 x 80 mm) was present on one occasion after that. Six examinations were carried out in 2012, revealing a very tight cervix and clear fluid accumulations (25 x 30 mm) during one follicular phase. An intrauterine saline infusion in March 2013 led to cloudy fluid accumulation. Uterine lavage performed in April found neutrophils. Another uterine lavage with penicillin was performed in May and the content was clean, however, the cervix was extremely tight during the follicular phase. In 2014, an episode of endometritis was induced by a deep AI. No treatment was performed and no fluid accumulations happened from March to August. Six examinations were carried out in 2017 and fluid accumulation (maximum of 35 x 50 mm) was present once during one follicular phase and twice during the early luteal phase.

7.2.3 | RNA Extraction and RNA-Sequencing

Following the methods described in Chapter 3, total RNA was extracted from tissue harvested from all mares, resulting in a total of 6 RNA samples. The quality and concentration of each RNA sample were checked by Nanodrop spectrophotometer and RNA integrity was assessed by agarose gel electrophoresis as previously described. Each RNA sample was diluted in DNase/RNase-free water to a final concentration of 1500 ng of RNA in a total volume of 50 µL.

RNA samples were processed and sent to RNA-Seq. Briefly, dual-indexed next-generation sequencing libraries were prepared, quantified using an Epoch spectrophotometer and pooled at equal concentrations. Pooled libraries were quantified a second time using Qubit fluorometer and size determined via agarose gel electrophoresis, with an average of 300 base pairs (bp). Following a dilution to 10 nM, pooled libraries were sent to RNA-Seq in Wales Gene Park (Institute of Medical Genetics, Cardiff University). Pooled samples were paired-end sequenced in 2 x 75 bp format on an Illumina HiSeq4000 platform at a final dilution of 8 pM.

7.2.4 | Data Processing and Gene Expression Analysis

A total of 6 pair-ended raw reads were generated after RNA-Seq, shown in Table 7.3. As previously described in Chapter 3, the quality of the reads was checked using the FastQC software (version 0.11.2), followed by the use of the TopHat software (version 0.11.2) to map the reads to the equine reference genome (*Equus caballus*, EquCab2; GCA_000002305.1, Ensembl website). The equine annotation file (Ensembl website, version EquCab2.89) was used along with the FeatureCounts

package (version 1.5.2) to summarize the number of aligned reads per exon for each sample.

The R/Bioconductor DESeq2 package was used to perform the differential gene expression analysis between resistant and susceptible mares. Computer codes used in this chapter are shown in Appendix 7.2. The Ensembl gene ID's from the differentially expressed genes (DEGs) were submitted to the Search Tool for the Retrieval of Interacting Genes/Proteins (STRING) data base (Szklarczyk *et al.*, 2015) to retrieve the predicted protein-protein interactions (PPI) network analysis and enrichment discovery of Gene Ontology (GO) terms (Ashburner *et al.*, 2000) and Kyoto Encyclopedia of Genes and Genomes (KEGG) (Kanehisa and Goto, 2000) pathways.

Table 7.3. Summary of the 6 RNA-Sequencing samples.

Mare	Total sequences raw reads ^a	Mapped reads ^b	Alignment rate ^c	Total count ^d
1	14732999	13093630	88.0%	8189448
2	20944446	18583416	87.8%	12011433
3	17701562	16121060	90.2%	10141641
4	21859635	19667469	89%	13089310
5	16730252	15179851	90%	10096188
6	19196009	17395595	89.7%	12114955

^a A count of the total number of sequences processed.

^b Number of reads mapped to the annotated equine genome.

^c Percentage of concordant reads mapped to the annotated equine genome.

^d Counts of reads assigned to genomic features.

7.2.5 | Statistical Analysis

The analysis of DEGs was performed using the negative binominal distribution performed by the DESeq2 package (Love *et al.*, 2014). The differential gene expression between the resistant *ex vivo* relative to the susceptible *in vivo* samples

was performed. Differential expression was determined using the Benjamini-Hochberg (BH) false discovery rate (FDR) (Benjamini and Hochberg, 1995) method with an adjusted $P < 0.05$. Genes featuring less than 1000 reads across all samples were excluded from the enrichment analysis. DEGs were analysed with respect to KEGG pathways and GO terms.

7.3 | Results

The gene expression variation between samples was visually inspected based on principal component analysis (PCA) as shown in Figure 7.1. The PCA analysis confirmed that resistant mares cluster together, represented by the red colour. Susceptible mares are represented by the blue colour. Mares 4 and 5 cluster together while mare 6 shows a bigger variance. Mares 4 and 6 had their susceptibility to endometritis confirmed by the biopsy category III (Appendix 7.1), while mare 5 was classified in Category I.

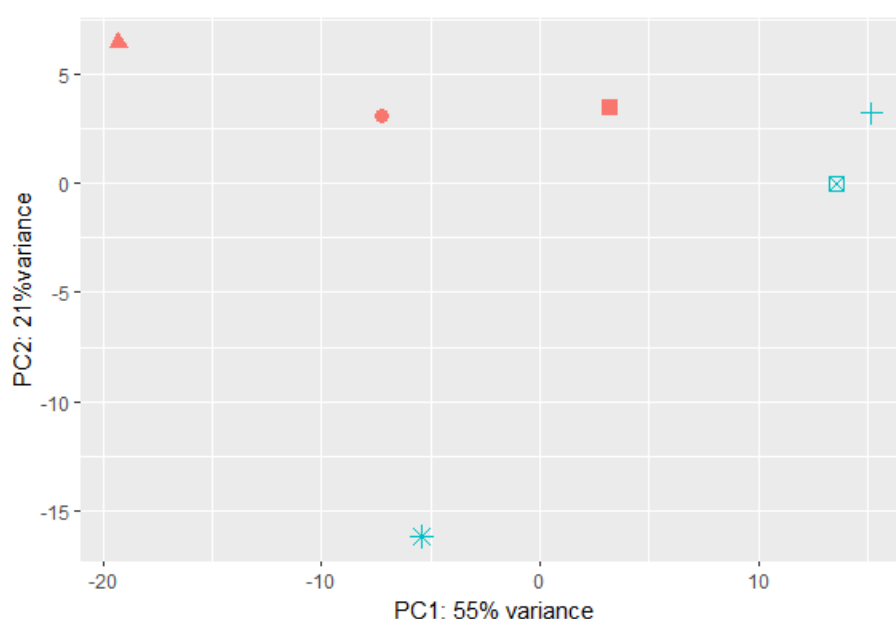


Figure 7.1. PCA plot of the gene expression profiles for the six mares analysed. The two colours represent biopsies from **susceptible** mares and **resistant** mares. Mares 1 (●), 2 (▲), 3 (■), 4 (⊠), 5 (+) and 6 (*).

The null hypothesis for each gene tested using DESeq2 was that there was no difference in its expression between PMIE resistant and susceptible groups before breeding. The null hypothesis was rejected when the difference in gene expression of a gene was greater than expected by random chance (using an adjusted p-value of 0.05).

A total of 17042 genes were found to be expressed, 56 of which were statistically significantly differentially up-regulated, and 122 genes were shown to be statistically significantly differentially down-regulated in the resistant relative to the susceptible group, at an FDR of 0.05. The STRING functional enrichment analysis of DEGs was performed using the 17042 total expressed genes as the statistical background. The PPI p-value was 1.4×10^{-4} , indicating that the genes are biologically connected as a group since the predicted network has significantly more interactions than expected when a similar size of random genes is analysed. The predicted STRING network was composed of 175 nodes and 159 edges.

The STRING enrichment analysis of all DEGs when comparing the transcriptome of resistant relative to the susceptible mares returned a total of 31 significantly enriched pathways were observed for the “molecular function” and “cellular component” GO categories (Appendix 7.3). The 10 most enriched GO terms are shown in more detail in Table 7.4. Also, a total of 6 significantly enriched KEGG pathways were observed, which are described in Table 7.5.

Table 7.4. Summary of the 10 most enriched GO terms. Comparing the transcriptome of resistant mares relative to the transcriptome of susceptible mares sorted by p-value. Table created using the STRING website.

GO Category ^a	Term name ^b	Description ^c	Count ^d	FDR p-value ^e
Cellular component	GO.0005737	Cytoplasm	10	8.86×10^{-6}
Cellular component	GO.0044464	Cell part	11	8.86×10^{-6}
Cellular component	GO.0005623	Cell	11	9.38×10^{-6}
Cellular component	GO.0005622	Intracellular	10	1.08×10^{-5}
Cellular component	GO.0005575	Cellular component	11	3.48×10^{-5}
Cellular component	GO.0016020	Membrane	8	6.80×10^{-5}
Cellular component	GO.0043226	Organelle	8	1.35×10^{-4}
Molecular function	GO.0003674	Molecular function	11	1.37×10^{-4}
Cellular component	GO.0044444	Cytoplasmic part	7	3.27×10^{-4}
Cellular component	GO.0043227	Membrane-bounded organelle	7	4.83×10^{-4}

^a GO domain (cellular component, biological process or molecular function).

^b Term associated with gene ontology biological processes.

^c Description of each GO category.

^d The number of genes involved in each biological process term.

^e Over-represented p-value with false discovery rate statistical correction for multiple comparisons.

Table 7.5. Summary of the 6 enriched KEGG pathways. Comparing the transcriptome of resistant mares relative to the transcriptome of susceptible mares sorted by p-value. Table created using the STRING website.

Pathway code ^a	Description ^b	Count ^c	FDR p-value ^d
05323	Rheumatoid arthritis	8	0.000
05168	Herpes simplex infection	10	0.002
01100	Metabolic pathways	26	0.006
05164	Influenza A	8	0.012
04145	Phagosome	7	0.029
05140	Leishmaniasis	5	0.029

^a KEGG pathway identification code.

^b Description of each KEGG pathway.

^c The number of genes involved in each pathway.

^d Over-represented p-value with false discovery rate statistical correction for multiple comparisons.

Although no enrichment of pathways related to pathogen recognition receptors, chemokines or antimicrobial peptides were observed, in isolation, genes related to the immune system were differentially expressed when comparing the transcriptome of resistant mares relative to susceptible mares. Genes coding for toll-like receptor (TLR4), chemokine (C-C) ligand family (CCL5), interferon regulatory factor (IRF7) and transcription factor (AP-1) were up-regulated in resistant mares in relation to susceptible mares, showing Log₂ fold changes (Log₂FC) between 1.3 and 2.9.

7.4 | Discussion

By analysing the gene expression profiles of each mare in the PCA plot (Figure 7.1), not all susceptible mares demonstrated expression profiles that could be clustered together. Mare 6 showed a considerable variation when compared to mares 4 and 5. Mare 6 has a clinical history of endometritis and showed a biopsy category III, confirming its susceptibility to PMIE. Mare 5 also has a clinical history of endometritis; however, it had a category I biopsy score. Kenney (1978) attests that improvement in the inflammatory status of the endometrium can happen as demonstrated by repeated biopsies. It is therefore hypothesised that the endometrium of mare 5 was classified as category I even though its clinical history attested its susceptibility to PMIE due to episodes of prolonged fluid accumulation after artificial insemination.

When comparing the transcriptome of resistant mares relative to the transcriptome of susceptible mares, a total of 179 genes were shown to be statistically significant differentially expressed. Cellular components and metabolic pathways were the two biological niches mostly retrieved from the enrichment analysis as previously shown in Tables 7.4 and 7.5. Nonetheless, this study aimed to understand how the gene expression modulates resistance and susceptibility to PMIE. Thus, each one of the four up-regulated DEGs related to the immune function was discussed in more detail.

The AP-1 is a family of transcript factors that participate in cell proliferation control, survival and death (Shaulian and Karin, 2001). However, many other stimuli such as serum, growth factor, tumour necrosis factor (TNF- α) and interleukin (IL) 1 can potently induce AP-1 activity (Lamph *et al.*, 1988; Ryder and Nathans, 1988; Brenner *et al.*, 1989; Muegge *et al.*, 1989). The AP-1 response to proinflammatory

cytokines such as TNF- α and IL-1 and toll-like receptors such as TLR4 suggest its involvement in inflammation and innate immune response (Grimm and Baeuerle, 1993; Chang and Karin, 2001; Shaulian and Karin, 2001). It is hypothesised that during an episode of MIE in resistant mares proinflammatory cytokines will induce AP-1 activity, which will then produce transcription factors and regulate gene expression related to inflammation to help them resolve MIE before it turns into PMIE.

Chemokines are involved in leukocyte chemotaxis and activation during inflammation (Tizard, 2013). However, besides acting during pathological conditions, chemokines are also involved in physiological conditions (Rossi and Zlotnik, 2000; Ning *et al.*, 2011). Therefore, it can be suggested that a physiological up-regulation of CCL5 in resistant mares compared to susceptible ones makes them more resistant to a persistent inflammatory response caused by semen and/or bacteria entering the uterus during breeding.

To date, there appears to exist only one study comparing the gene expression between resistant and susceptible mares before breeding but focusing on specific genes previously identified to be associated with acute endometritis (Marth *et al.*, 2018). It showed a higher expression of CCL2 in susceptible mares compared to resistant, but they did attest that presence of bacteria in some of the samples from PMIE susceptible mares might have increased the expression of some genes. Both CCL2 and CCL5 act in the immune context through their monocyte recruiting activities (Soria and Ben-Baruch, 2008). However, it has been shown that regulation of CCL5 expression is complex, involving a stimulus and also a tissue specific activation of transcription factors (Fessele *et al.*, 2001). Therefore, it is hypothesised

that a higher expression of CCL5 in the resistant compared to susceptible mares' endometrium makes them more resistant to a persistent inflammatory response, while the endometrium of susceptible mares is not able to express enough CCL5.

Toll-like receptors are pattern recognition receptors (TLRs), taking part in pathogen detection acting as the first step in the host's defence (Tizard, 2013). Lipopolysaccharides (LPS) from gram-negative bacteria such as *Escherichia coli* (*E. coli*) are recognized by TLR4, a transmembrane molecule (Chow *et al.*, 1999; Takeuchi *et al.*, 1999). Taking into account that *E. coli* is one of the most common microorganisms isolated from PMIE cases (Hughes and Loy, 1975), it can be hypothesised that resistant mares have a higher basal expression of TLR4 in order to quickly suppress the inflammation after breeding caused by invading gram-negative bacteria that can be deposited into the uterus during natural mating and in some cases, artificial insemination (Troedsson, 1999; Watson, 2000; Katila, 2001).

The current results are again in contrast with the recent findings of Marth *et al.* (2018) which found an up-regulation of TLR4 in susceptible mares compared to resistant mares. However, it included mares at different phases of the oestrous cycle in the analyses, and some of the susceptible mares showed bacteria in the uterus (Marth *et al.*, 2018). Instead of analysing the global gene expression in the equine endometrium, this study used quantitative real-time polymerase chain reaction to analyse specific genes previously identified to be linked to endometritis (Marth *et al.*, 2018). For experimental purposes, it is important to have similar methodologies to make comparisons and draw conclusions across studies. Therefore, the results of the current study might not be similar to those published due to different methodologies.

Interferon regulatory factors are involved in processes such as regulation of immune response, host defence, cytokine signalling and regulation of cell growth, specially regulation of immune cell differentiation and activation (Taniguchi *et al.*, 2001; Ning *et al.*, 2011). Interferon regulatory form 7 (IRF7), along with IRF3, is a key regulator of the type I interferon (IFN) comprised of IFN- α and - β , that play a role in both innate and adaptive immunity (Honda *et al.*, 2005). An inactive form of IRF7 is present in uninfected cells that, after being stimulated by different factors such as viral infections and TLRs, become phosphorylated and positively regulate other interferon-stimulated genes, participating in innate immunity (Honda *et al.*, 2005). Therefore, an up-regulation of IRF7 in resistant mares in relation to susceptible mares might contribute to homeostasis by preparing the uterine environment to resist infection and facilitate the healing process in case inflammation occurs.

7.5 | Conclusion

The biggest limitation of this study is the number of biological replicates for the susceptible group. The legislation in the United Kingdom is severely restricted and collecting biopsies from live mares in practice is difficult to obtain permissions for (both that of the mare owner and Home Office permissions). Thus, samples from Finland were used in this study where a population of research mares was available. Unfortunately, only three horses were available for sample collection. Moreover, it is difficult finding susceptible mares at the abattoir, since no information about their reproductive history is available.

Despite the enrichment analysis retrieving mostly metabolic and cellular pathways, specifically AP-1, CCL5, IRF7 and TLR4 genes provide an indication of immune responses when comparing resistant relative to susceptible mares. All samples used in the current study were collected before breeding. Therefore, all gene expression related to immunity is not a response to contamination and should represent the underlying endometrial immune homeostasis of resistant and susceptible mares. Thus, it is hypothesised that an over expression of immune genes by resistant mares means that they are able to physiologically prepare the uterus ahead of mating to tackle MIE caused by the introduction of foreign material in the uterus after breeding more efficiently than susceptible mares.

It is important to highlight that two different breeds of mares were used in this experiment, and genetic characterization is important to assign individuals to correct populations in order to assure breed integrity (Glowatzki-Mullis *et al.*, 2006). Therefore, the different genetic backgrounds of these two groups of mares could be the cause of the differences in gene expression seen when performing transcriptomic analysis. If further investigations in different populations with a bigger sample size using only one breed of mares retrieve the similar results, these genes can be used in the future as markers of resistance in mares before breeding.

In conclusion, the present study provides preliminary insights into measuring expression levels of genes linked to the immune system to better understand the mechanisms associated with resistance and susceptibility to PMIE in mares before breeding. An understanding of which genes regulate the delicate balance of resistance and susceptibility to PMIE is a promising approach for improved reproductive management. In future, understanding which genes are linked to PMIE

resistance and susceptibility will allow the appropriate classification of mares based on gene expression analysis of endometrial biopsies at the pre-breeding examination.

CHAPTER 8

GENERAL DISCUSSION

This thesis explored the use of an endometrial tissue culture system as a model to study the equine endometrium in combination with global gene expression analysis. The global endometrial gene expression throughout the oestrous cycle and anoestrous period, as well as the gene expression related to the innate immune system after bacterial challenge was analysed from *in vitro* cultured explants and *ex vivo* samples. This work also studied the *ex vivo* and the *in vivo* basal gene expression of resistant and susceptible mares before breeding.

One of the primary aims of this research project was to apply state-of-the-art RNA-Sequencing (RNA-Seq) technology to study the transcriptome of cultured endometrial explants to better understand the tissue culture system, which might be used in the future as a model to study the equine endometrium and more specifically, equine endometritis. RNA-Seq allows the quantification and identification of gene expression changes during different conditions, making it possible to classify normal developmental changes as well as illness and disease states (Wang *et al.*, 2009). RNA assessments have the potential to be used in the clinical diagnosis of different conditions (Wang *et al.*, 2009; Ozsolak and Milos, 2011).

Regarding the bioinformatics analysis, it is critical to choose the appropriate tool for the analysis of differentially expressed genes (DEGs) to ensure valid conclusions are drawn from a data set. Nonetheless, there is no optimal pipeline for the analysis of RNA-Seq data since there are many different applications and analysis scenarios in which this high-throughput technology can be used (Conesa *et al.*, 2016). The DESeq2 package (Love *et al.*, 2014) for the analysis of DEGs was chosen to be used for all RNA-Seq data created in this thesis as it can perform more complex analysis

such as multiple comparisons and analysis of time-series data (Conesa *et al.*, 2016). DESeq2 uses modelling to improve model performance under the negative binominal assumption of statistical analysis (Huang *et al.*, 2009; Love *et al.*, 2014). When compared to other software used for differential gene expression analysis such as edgeR, voom, SAMseq and Cuffdiff, DESeq2 showed a higher sensitivity, especially for small fold changes such as 2 or 3 (Love *et al.*, 2014; Zhou *et al.*, 2014).

All endometria from which explants were collected were carefully analysed, as previously described in Chapter 3, to ensure they were free of inflammation, both acute and chronic. The endometrial tissue culture was performed as previously described by Nash *et al.* (2008), but adopting the collection of intact explants using sterile punch biopsies according to Borges *et al.* (2012). Consistent with previous findings, the explants cultured in this piece of work appeared to be viable throughout the whole experimentation period since there was no alteration of their colour and appearance throughout the culture period of 72 hours (Nash *et al.*, 2008). It was decided to use the punch biopsy to collect intact explants rather than the mechanical tissue chopper to reduce releasing damage-associated molecular patterns (DAMPs) molecules after tissue disruption that happens when the tissue is mechanically chopped. The innate immune system can be modulated by DAMPs, thus triggering inflammation due to tissue damage (Borges *et al.*, 2012).

The first aim of the current work was to further investigate the explant tissue culture system by determining how the transcriptome of cultured explants is modulated once in culture and whether the transcriptome of cultured explants represents the transcriptome of a whole mare, to then use the culture system for future studies into equine endometritis. This work appears to be the first in the literature to sequence the

transcriptome of equine cultured endometrial explants at different time points and to investigate how the gene expression is modified once the explants are placed in culture. It was observed that there is an expected variation between the 0 hours *ex vivo* biopsies (collected at 0 hours, or as soon post-mortem as possible) compared to the *in vitro* explants cultured for a period of 24 hours (Chapter 4). The focus when studying the explant tissue culture at the global gene expression level was the innate immune genes' expression. This was done by comparing the 0 hours biopsies with the *in vitro* cultured explants at 24 hours followed by gene expression analysis between 24, 48 and 72 hours of culture.

The study established that the CCL2, CD40, IL1A, IL1B, IL23A, IL4R, IL6 and IL8 genes linked to the innate immunity were shown to be down-regulated (LogFC between -2.7 and -6) when comparing the transcriptome of the *ex vivo* 0 hours samples to the transcriptome of explants cultured for 24 hours. These genes were set as a baseline for future work involving inflammation of the endometrium when using the explant tissue culture system. The most likely explanation for this down-regulation in the *ex vivo* samples is that once the punch biopsies are collected from the endometrium and placed in the culture plate, there is a higher expression of inflammatory genes in the biopsies in relation to the whole mare. Even though intact explants were used in the current work, it is thought that impact to the innate immunity was caused to some extent when excising the biopsy from the tissue. The inflammatory responses from bovine cultured intact and chopped endometrium have already been compared, using control medium and medium challenged with *Escherichia coli* (*E. coli*) lipopolysaccharide (LPS) (Siegmund *et al.*, 2001; Borges *et al.*, 2012). Indeed, both intact explants and chopped endometrium showed an accumulation of interleukins, yet chopped tissue accumulated more IL-6, IL-8 and

IL-1 β than intact explants both in control medium and when challenged with LPS. It is expected that even intact explants might modulate the innate immunity; however, they have already been utilised in other research, *ex vivo* in rodents and *in vitro* in cows for the investigation of immunity and inflammation (Siegmund *et al.*, 2001; Borges *et al.*, 2012). Therefore, even though genes related to the innate immune system are expressed in cultured intact explants, the tissue culture system can still be validated in the future following further research and used as a model to study endometritis. If, after challenging with inflammatory stimulants, the expression of genes classified as the baseline is found to be higher, they may be indicative of a genuine innate immunity response to the inflammatory challenge itself, instead of a normally expected expression due to the removal of tissue from the intact endometrium. Indeed, after challenging explants with LPS (Chapter 5), expressed genes did not overlap with the ones set as a baseline here. This matter was discussed in more detail throughout the general discussion.

Between 24 hours and 48 hours of culture, there was a minimal change in gene expression (Chapter 4), which does not seem to interfere with the innate immunity. Nevertheless, based on the gene expression analysis, the explants showed altered transcriptomic profiles after 48 hours in culture. The greater expression of MMP13 at 72 hours of culture compared to 48 hours might be related to a compromised uterine environment as already reported in cows (Wathes *et al.*, 2011; Forde and Lonergan, 2012). Therefore, the transcriptomic analysis at 72 hours can bias the results of DEGs. This is in line with the findings of Borges *et al.* (2012), who found necrotic fragmentation of glands and stroma in bovine intact explants cultured after 48 hours. Thus, the explants for the subsequent experiments were only cultured for 24 and 48 hours.

The second aim of the thesis was to compare the global endometrial transcriptomic changes throughout the oestrous cycle and the anoestrous period from pony mares known to be resistant to persistent-mating induced endometritis (PMIE). The equine oestrous cycle takes place during the spring and summer and early autumn, and lasts an average of 21 days, comprising 5-7 days of follicular phase. The anoestrous phase takes place during the winter months and is characterized by a lack of ovarian activity (Aurich, 2011). Changes in ovarian hormones drive the morphology and molecular biology of reproductive organs throughout the oestrous cycle (Aurich, 2011; Marth *et al.*, 2015b). A better understanding of the cyclical physiological changes that happen in the equine endometrium during the different phases of the oestrous cycle might improve the understanding of inflammatory conditions and pathologies of the mare's reproductive tract.

The seasonal variability of gene expression throughout the oestrous cycles in mares (Chapter 5) supports previous findings that hormones change the physiological uterine environment (Gebhardt *et al.*, 2012; Marth *et al.*, 2015b). Based on the findings of the current work, it is possible to make a clear distinction between genes that are regulated during the follicular and luteal phases of the oestrous cycle. After 24 hours of culture, follicular phase explant gene expression related mainly to immune pathways when compared to the luteal phase of the oestrous cycle, with an up regulation of genes coding for interleukins (IL1A, IL23A, IL2RB and IL7R), chemokines (CXCL1, CXCL10 and CXCL14), tumour necrosis factor receptor (TNFRSF4), NF- κ B Inhibitor Alpha, an inhibin (INHABA) and follistatin (FST). During the follicular phase, when breeding occurs, the cervix is open enabling semen and often accompanying bacteria to enter the uterus. Thus, an up-regulation of innate immune genes will help tackle the intrusion of foreign material into the uterus

During the luteal phase, DEGs were mainly linked to molecular functions, biological processes and uterine functions, with an up-regulation of genes such as EDNRB, ESR1 and LEPR. Additionally, this research suggests the expression of genes linked to the innate immune system during the anoestrous period is higher when compared to the luteal phase, yet lower when compared to the follicular phase. This agrees with the hypothesis that during the luteal phase, high progesterone concentrations diminish the endometrial elimination of bacteria and/or semen, resulting in a lower uterine clearance (Evans *et al.*, 1986a; Watson *et al.*, 1987). It can be concluded that the expression of genes related to the innate immune system is greater during the follicular phase, followed by the anoestrous period and it is lowest during the luteal phase of the oestrous cycle during progesterone dominance.

The current study also showed an up-regulation of collagen genes during the anoestrous phase compared to the follicular and luteal phases. This contradicts recent findings where collagen genes were up-regulated during the follicular phase of the oestrous cycle in mares compared to the luteal phase (Marth *et al.*, 2015b). However, it is hard to compare results since the work from Marth *et al.* (2015b) did not study the gene expression during the anoestrous period. The higher collagen expression is a rather unexpected finding when studying the endometrial response during the anoestrous phase, and the current lack of information on the collagen content in the equine endometrium and also in other mammals make it difficult to theorise this finding.

Further research needs to be done to elucidate what the situation really is during the anoestrous period specifically, at the level of global gene expression using RNA-Seq. By collecting biopsies from susceptible and resistant mares during the anoestrous

period and comparing their transcriptomes might help finding the true picture about the anoestrous period in mares.

Unexpected outcomes, such as the “chemical carcinogenesis” KEGG pathway shown to be the only enriched pathway when comparing across the follicular and luteal phases at 48 hours, or the lower number of enriched pathways retrieved at 48 hours overall, might be linked to biases in the databases. Many pathways studies were based on human diseases, and they are included as results in other systems. Therefore, some retrieved pathways do not make much sense. Instead, the DEGs may be involved in another process not yet annotated. It has also been hypothesized that the analysis at 48 hours did not retrieve many enriched pathways, or the pathways were not related to the immune function or to the endometrial environment because the DEGs were taking part in pathways and processes that somehow overlapped, or because the list of genes was too general (Simillion *et al.*, 2017).

Moreover, the third aim of the thesis was to utilise the explant tissue culture to study equine endometrial inflammation, which can be mainly caused by bacterial infection and PMIE (Zent *et al.*, 1998; Troedsson, 1999; Causey, 2006; Woodward and Troedsson, 2013). The field of equine uterine inflammation is many years old, but little focus has been given to the global gene expression and most studies had used quantitative polymerase chain reaction (qPCR) to study a pre-selected, but limited number of genes thought to be related to endometritis (Fumuso *et al.*, 2003; Fumuso *et al.*, 2007; Nash *et al.*, 2010b; Christoffersen *et al.*, 2012; Woodward *et al.*, 2013). Only recently has there been a study using the RNA-Seq technology to investigate the endometrial gene expression related to inflammation after infecting mares with *E. coli*. The main up-regulated genes 3 hours after inoculation included toll-like

receptors 2 and 4, pro-inflammatory cytokines, chemokines and equine β -defensin 1 (Marth *et al.*, 2015a). The work conducted by Marth *et al.* (2015a) has only investigated the global gene expression during acute endometritis, at 6 hours post *E. coli* inoculation. However, it is already known that mating-induced endometritis (MIE) might take up to 36-48 hours to be cleared from the uterus. Therefore, by using the explant tissue culture, this thesis expanded the mentioned published work by looking at the global gene expression from explants after 24 and 48 hours of LPS challenge to better understand the mechanisms underlying the progression of MIE to PMIE.

Explants were cultured in control medium and in medium challenged with different concentrations of LPS (0.3 $\mu\text{g/mL}$, 1.0 $\mu\text{g/mL}$ or 3.0 $\mu\text{g/mL}$). Radioimmunoassays (RIA) were performed to quantify the prostaglandin $\text{F}_{2\alpha}$ ($\text{PGF}_{2\alpha}$) production by explants as a marker of inflammation to check whether the LPS was causing a response and to help refine the number of samples sent for transcriptomic analysis. However, no statistically significant difference was seen in $\text{PGF}_{2\alpha}$ production between treatments at either 24 or 48 hours. This result agrees with previous studies using the explant tissue culture, where explants at the follicular phase of the oestrous cycle did not significantly produce $\text{PGF}_{2\alpha}$ in response to challenge with LPS or *Streptococcus zooepidemicus* (Nash *et al.*, 2008). On the other hand, a more recent study using the same explant tissue culture has shown a $\text{PGF}_{2\alpha}$ response following challenge with 3 $\mu\text{g/mL}$ LPS in follicular stage explants, and this is why $\text{PGF}_{2\alpha}$ is still used as a marker for explant functionality (Nash *et al.*, 2018). Thus, since the main goal of the current work was to better understand the transcriptome of equine endometrium after antigen challenge, explants cultured in medium challenged with

LPS 3 µg/mL (instead of 0.3 or 1 µg/mL) were the ones chosen to be taken forward to RNA extraction, RNA-Seq and transcriptomic analysis (Chapter 6).

The enrichment analysis for DEGs did not retrieve many pathways related to the immune system after LPS challenge. A few isolated genes such as IRAK and ZC3H12C were shown to be up-regulated in cultured explants challenged with LPS for 24 hours when compared to explants cultured in media alone. On the other hand, the ENPP2, SOX13 and PLVAP genes were shown to be down-regulated after LPS challenge at 24 hours. None of these genes overlapped with the genes set as the baseline in Chapter 4, suggesting that the gene expression might be indeed related to the LPS challenge. Nonetheless, more genes related to immune responses were expected to be up-regulated after LPS challenge, which might suggest that the LPS was not working properly, in accordance with the lack of PGF_{2a} response. All uteri used in this experiment were collected from mares thought to be resistant to PMIE at the follicular phase of the oestrous cycle, when immune responses are up-regulated. Therefore, another hypothesis for this outcome is that between 0 and 24 hours the immune response was mounted and it was tackling inflammation induced by the LPS. Since the mares did not present acute or chronic endometritis, it is suggested that by the end of the 24 hours of challenge, the uterine immune system had already resolved most of the inflammation and it was bringing the uterine environment back to homeostasis. In the future, adding more time points to the explant tissue culture during challenge with LPS, such as 6 and 12 hours, might help shed light into the immune responses occurring in the endometrium before 24 hours. It would also be interesting to test explants from mares with active endometritis to study the global gene expression at different time points of the inflammation.

Finally, the fourth aim of the current work was to use RNA-Seq technology to study the transcriptome of PMIE resistant and susceptible mares before breeding, to better understand the innate differences in gene expression even before the endometrial environment is challenged with semen or bacteria. The majority of research conducted into MIE and PMIE focuses on immune changes after uterine challenge with semen and/or bacteria (Troedsson *et al.*, 1993c; Katila, 1995; Troedsson, 1999; Fumuso *et al.*, 2003; Christoffersen *et al.*, 2012; Marth *et al.*, 2015a). Notwithstanding this, this approach does not address the dearth of knowledge regarding any putative changes to endometrial homeostasis in susceptible or resistant mares before breeding. Advances in the understanding of how these two categories of mares differ in their uterine gene expression might shed light into the link between MIE and PMIE.

In the body of work detailed here, four genes have been identified as having the potential to distinguish mares between resistant and susceptible to PMIE before the uterine environment faces a challenge. PMIE resistant mares showed an up-regulation of TLR4, CCL5, IRF7 and AP-1 genes in relation to susceptible mares, which are genes linked to the immune response (Chapter 7).

The ability to distinguish between resistant and susceptible mares can have significant clinical implications in the breeding industry worldwide. This is the first study to look at the global gene expression between resistant and susceptible mares before breeding. Further transcriptomic analysis with a larger number of mares would be required to confirm the gene expression changes reported in this study. Nonetheless, in a field application technique, biopsies collected from broodmares as is routine during the pre-breeding period and can be utilised for RNA-Seq analysis;

there is thus potential for endometrial RNA-Seq analysis to be used as a screening method to classify mares likely to be resistant or susceptible to PMIE based on up or down-regulation of certain genes.

The utilisation of transcriptomics to better understand the equine endometrium and to identify potential genes for the identification of PMIE resistant and susceptible mares is novel and promising. However, there are a few limitations to this portion of work. Perhaps the most serious disadvantage of this study is that samples were collected from mares presented for euthanasia at a commercial abattoir and no background information about the animals was available. Since no metadata were available for each one of the mares used in this piece of work, it was not possible to divide them into homogeneous groups such as age, presence and/or absence of illness, type of management, etc. For this reason, a substantial variability in the specified outcome is expected. Thus, even though the results in gene expression might represent true differences, they can also be biased because of sampling variability. To balance this variability, a larger sample size is required (Biau *et al.*, 2008). Due to the difficulty in sample collection, the number of mares used in this study might be too small to account for all the variability in the data. Therefore, this study could be underpowered when it comes to statistical analysis. In statistics, the type II error is considered a “false negative”, when a null hypothesis that is false gets rejected, meaning that there is a fail to assert what is present (Steidl *et al.*, 1997; Akobeng, 2016). The risk of type II error increases as the power of a study decreases, which then also reduces the chances of detecting a difference when it exists (Biau *et al.*, 2008). For this reason, this study might have missed real results due to its high risk of type II errors.

Another point to consider is that accounting for the duration of sample collection plus the transportation of samples back to the laboratory a period of 7 hours elapsed. In addition, once in the laboratory uteri were dissected and punch biopsies were then collected, adding another hour until the tissue culture was set and running. There is a lack of research regarding the effects of time between collection and use of tissue samples derived from abattoirs. However, it has been demonstrated that the bacterial composition of sputum samples collected from human adults with respiratory infections changed after storage at room temperature for different intervals of time before samples were frozen (Cuthbertson *et al.*, 2014). It was showed that within the first hour of collection is the best window for sample storage/transportation at room temperature before freezing at -80 °C. However, the authors suggest that a window of 12 hours of collection is acceptable without significant differences in the bacterial composition in the case of sputum samples (Cuthbertson *et al.*, 2014). As regards this current study it is impossible to attest what could have occurred to the tissue at the level of gene expression in the period between sample collection and culture set up and how this could influence the results. These could be significant as after the uterus removal from the mare's body a cascade of reactions might occur due to many reasons such as the lack of blood circulation, differences in the mare's internal temperature compared to the outside room temperature and contact with the external environment. Taking this into consideration, specific gene expression patterns observed between the 0 hours' samples and the samples culture for up to 24 hours might be related not only to the effect of the culture itself, but also related to transcriptomic changes as a result of the long transportation time between uteri collection and the start of the tissue culture.

Another issue related to the methodology of the experiments in this thesis is that intact endometrial explants were used to set up a tissue culture. The tissue culture was chosen over alternative model systems such as epithelial and stromal cell cultures because the latter is one step behind in representing the uterus of a whole mare as it disrupts the endometrial architecture (Borges *et al.*, 2012). As previously described, the equine endometrial explants are composed of both epithelial and stromal cells (Nash *et al.*, 2008), however the proportion of these type of cells in each explant is unknown. For this reason, the heterogeneity of explants in terms of cell composition could not be assessed. It is known that the basal gene expression is different in cell types, as assessed by single-cell RNA-Seq analysis (Saliba *et al.*, 2014). Therefore, results in gene expression could have been modulated depending on the ratio between stromal and epithelial cells in the explants used in this thesis. For future studies it would be interesting to look at the gene expression of stromal and epithelial endometrial cells and perhaps compare the results with the results of the current thesis.

Handling RNA-Seq data is also challenging since there are many available tools available for each step of the analysis, but there is no standard protocol when it comes to data processing, differential analysis and functional pathway analysis. RNA-Seq is being used in many laboratories and tools for the analysis of such data are constantly being developed and improved (Williams *et al.*, 2014). Standardizing methods for experiment design, sample collection and RNA-Seq data analysis will provide the research community with powerful instruments to understand the biological implications of RNA-Seq results, as well as facilitate the comparison across different studies.

Furthermore, there is also the factor of biases in databases for the study of equine pathways which is a severe limitation when working with RNA-Seq data, which complicates the biological interpretation of sequence data. After analysing RNA-Seq data, the next step is to identify statistically enriched biological processes in the data through the analysis of biological pathways (Khatri *et al.*, 2012). Annotation inequality is a problem that is increasing over time (Haynes *et al.*, 2018). Good annotations are available for well-known processes; however, there is much to be discovered. For example, the protein-protein interaction networks in this thesis retrieved from the Search Tool for the Retrieval of Interacting Genes/Proteins (STRING) (Szklarczyk *et al.*, 2015) website reported genes with generally significant more connection than expected by random chance, suggesting that they are functional interacting units. However, not always the enrichment analysis linked these genes to known pathways, suggesting the possibility of unannotated processes that are being up or down-regulated. Nevertheless, the power of using transcriptomic analysis to comprehensively investigate the explant tissue culture and to better understand the global gene expression in the equine endometrium before and after challenge has been shown.

Conclusion

This work appears to be one of the firsts to use high-throughput analysis to study the equine endometrial environment before semen or bacterial inoculation, at the different stages of the oestrous cycle and after LPS inoculation. In studies of equine endometritis, the choice of sample is important. In fact, during the last 15 years, studies investigating the innate immune pathways in the equine endometrium after challenge with semen and bacteria used different protocols and different time points

for sampling (Fumuso *et al.*, 2003; Fumuso *et al.*, 2007; Christoffersen *et al.*, 2010; Nash *et al.*, 2010a; Nash *et al.*, 2010b; Christoffersen *et al.*, 2012; Woodward *et al.*, 2013). Thus, the comparison of results across studies is difficult and likely to be limited. There is a serious need for model systems where the main characteristics of the endometrium are preserved, to better understand the equine uterine function and innate immunity.

Despite its exploratory nature, this work investigated the use of the explant tissue culture system as a future model for studies of the equine endometrium at the level of the transcriptome as a standardized method to study endometritis in the mare. This study emphasized the complexity of interactions in the innate immune response in the equine endometrium under the effect of different hormones throughout the oestrous cycle, where innate immune genes exhibited increased expression during the follicular phase of the oestrous cycle when compared to the luteal phase and the anoestrous period. Also, a number of genes of potential interest were identified during bacterial challenge and also between resistant and susceptible mares before breeding.

The present thesis contributes to the knowledge in the field of *in vitro* research as well as in the field of equine endometritis, by providing evidence that the equine endometrial explant tissue culture can be used for further research into endometritis at the level of global gene expression and therefore, has important implications to help understanding fertility problems in mares. This study also provided important insights into gene expression to better understand the mechanisms linked to resistance and susceptibility to PMIE. This has a future application to clinical practice when the genes underlying resistance and susceptibility are fully elucidated,

by analysing the global gene expression of endometrial biopsies in order to classify mares into PMIE resistant and susceptible at the pre-breeding examination before challenge occurs.

REFERENCES

- Adams, G., Kastelic, J., Bergfelt, D., and Ginther, O. (1986). Effect of uterine inflammation and ultrasonically-detected uterine pathology on fertility in the mare. *Journal of reproduction and fertility. Supplement*, 35, 445-454.
- Akira, S. (2003). Mammalian Toll-like receptors. *Current Opinion in Immunology*, 15(1), 5-11.
- Akobeng, A. K. (2016). Understanding type I and type II errors, statistical power and sample size. *Acta Paediatr*, 105(6), 605-609.
- Albihn, A., Baverud, V., and Magnusson, U. (2003a). Uterine microbiology and antimicrobial susceptibility in isolated bacteria from mares with fertility problems. *Acta Vet Scand*, 44(3-4), 121-129.
- Albihn, A., Baverud, V., and Magnusson, U. (2003b). Uterine microbiology and antimicrobial susceptibility in isolated bacteria from mares with fertility problems. *Acta Veterinaria Scandinavica*, 44(3-4), 121-130.
- Alexander, S. L., and Irvine, C. H. G. (2011). FSH and LH. In A. O. McKinnon, E. L. Squires, W. E. Vaala, & D. D. Varner (Eds.), *Equine Reproduction* (2nd ed., pp. 1619-1630). Philadelphia, London: Wiley-Blackwell.
- Alghamdi, A., Foster, D., and Troedsson, M. (2004). Equine seminal plasma reduces sperm binding to polymorphonuclear neutrophils (PMNs) and improves the fertility of fresh semen inseminated into inflamed uteri. *Reproduction*, 127(5), 593-600.
- Allen, W. (1977). Artificial control of the mare's oestrous cycle. *Veterinary Record*, 100(4), 68-71.
- Allen, W. R., Brown, L., Wright, M., and Wilsher, S. (2007). Reproductive efficiency of Flatrace and National Hunt Thoroughbred mares and stallions in England. *Equine Vet J*, 39(5), 438-445.
- Anders, S., and Huber, W. (2010). Differential expression analysis for sequence count data. *Genome Biology*, 11(10), R106.
- Asbury, A., Halliwell, R., Foster, G., and Longino, S. (1980). Immunoglobulins in uterine secretions of mares with differing resistance to endometritis. *Theriogenology*, 14(4), 299-308.
- Asbury, A. C. (1986). Endometritis in the mare. In D. A. Morrow (Ed.), *Current Therapy in Theriogenology* (pp. 718-722). Philadelphia, USA: WB Saunders.
- Ashburner, M., Ball, C. A., Blake, J. A., Botstein, D., Butler, H., Cherry, J. M., Davis, A. P., Dolinski, K., Dwight, S. S., Eppig, J. T., Harris, M. A., Hill, D. P., Issel-Tarver, L., Kasarskis, A., Lewis, S., Matese, J. C., Richardson, J. E., Ringwald, M., Rubin, G. M., and Sherlock, G. (2000). Gene ontology: tool for the unification of biology. The Gene Ontology Consortium. *Nat Genet*, 25(1), 25-29.
- Atli, M. O., Kurar, E., Kayis, S. A., Aslan, S., Semacan, A., Celik, S., and Guzeloglu, A. (2010). Evaluation of genes involved in prostaglandin action in equine endometrium during estrous cycle and early pregnancy. *Animal reproduction science*, 122(1), 124-132.
- Aurich, C. (2011). Reproductive cycles of horses. *Anim Reprod Sci*, 124(3-4), 220-228.
- Aurich, J., and Aurich, C. (2006). Developments in European horse breeding and consequences for veterinarians in equine reproduction. *Reproduction in domestic animals*, 41(4), 275-279.
- Baker, C., and Kenney, R. (2007). Systematic approach to the diagnosis of the infertile or subfertile mare. In J. C. Samper, J. F. Pycoc, & A. O. McKinnon (Eds.), *Current Therapy in Equine Reproduction* (pp. 518-520). St. Louis, Missouri: St. Louis, Missouri : Elsevier Saunders.

- Baker, C. B., Little, T. V., and McDowell, K. J. (1993). The live foaling rate per cycle in mares. *Equine veterinary journal*, 25(S15), 28-30.
- Balbach, A. (1980). *A Flora Nacional na Medicina Doméstica* (11th ed.). São Paulo
- Ball, B. A., Little, T. V., Hillman, R. B., and Woods, G. L. (1986). Pregnancy rates at Days 2 and 14 and estimated embryonic loss rates prior to day 14 in normal and subfertile mares. *Theriogenology*, 26(5), 611-619.
- Bateman, A., Birney, E., Durbin, R., Eddy, S. R., Howe, K. L., and Sonnhammer, E. L. (2000). The Pfam protein families database. *Nucleic Acids Res*, 28(1), 263-266.
- Bateman, A., Coin, L., Durbin, R., Finn, R. D., Hollich, V., Griffiths-Jones, S., Khanna, A., Marshall, M., Moxon, S., Sonnhammer, E. L., Studholme, D. J., Yeats, C., and Eddy, S. R. (2004). The Pfam protein families database. *Nucleic Acids Res*, 32(Database issue), D138-141.
- Battut, I., Colchen, S., Fieni, F., Tainturier, D., and Bruyas, J. F. (1997). Success rates when attempting to nonsurgically collect equine embryos at 144, 156 or 168 hours after ovulation. *Equine Vet J Suppl*(25), 60-62.
- Bauersachs, S., Ulbrich, S. E., Gross, K., Schmidt, S. E., Meyer, H. H., Einspanier, R., Wenigerkind, H., Vermehren, M., Blum, H., Sinowatz, F., and Wolf, E. (2005). Gene expression profiling of bovine endometrium during the oestrous cycle: detection of molecular pathways involved in functional changes. *J Mol Endocrinol*, 34(3), 889-908.
- Benesch, M. G., Ko, Y. M., McMullen, T. P., and Brindley, D. N. (2014). Autotaxin in the crosshairs: taking aim at cancer and other inflammatory conditions. *FEBS Lett*, 588(16), 2712-2727.
- Benesch, M. G., Ko, Y. M., Tang, X., Dewald, J., Lopez-Campistrous, A., Zhao, Y. Y., Lai, R., Curtis, J. M., Brindley, D. N., and McMullen, T. P. (2015a). Autotaxin is an inflammatory mediator and therapeutic target in thyroid cancer. *Endocr Relat Cancer*, 22(4), 593-607.
- Benesch, M. G., Zhao, Y. Y., Curtis, J. M., McMullen, T. P., and Brindley, D. N. (2015b). Regulation of autotaxin expression and secretion by lysophosphatidate and sphingosine 1-phosphate. *J Lipid Res*, 56(6), 1134-1144.
- Benjamini, Y., and Hochberg, Y. (1995). Controlling the false discovery rate: a practical and powerful approach to multiple testing. *J Roy Stat Soc B*, 57.
- Bennett, D. G. (1987). Diagnosis and treatment of equine bacterial endometritis. *Journal of Equine Veterinary Science*, 7(6), 345-352.
- BETA. (2015). *British Equestrian Trade Association National Equestrian Survey* Retrieved from: <http://www.worldhorsewelfare.org/Removing-the-Blinkers#sthash.hJO5h9Yt.dpuf>
- Betteridge, K., Eaglesome, M., Mitchell, D., Flood, P., and Beriault, R. (1982). Development of horse embryos up to twenty two days after ovulation: observations on fresh specimens. *Journal of anatomy*, 135(Pt 1), 191.
- Beutler, B., Hoebe, K., Du, X., and Ulevitch, R. (2003). How we detect microbes and respond to them: the Toll-like receptors and their transducers. *Journal of leukocyte biology*, 74(4), 479-485.
- Biau, D. J., Kerneis, S., and Porcher, R. (2008). Statistics in brief: the importance of sample size in the planning and interpretation of medical research. *Clin Orthop Relat Res*, 466(9), 2282-2288.
- Blume-Jensen, P., Ronnstrand, L., Gout, I., Waterfield, M. D., and Heldin, C. H. (1994). Modulation of Kit/stem cell factor receptor-induced signaling by protein kinase C. *J Biol Chem*, 269(34), 21793-21802.
- Boraschi, D., and Tagliabue, A. (2013). The interleukin-1 receptor family. *Semin Immunol*, 25(6), 394-407.
- Borges, Á. M., Healey, G. D., and Sheldon, I. M. (2012). Explants of Intact Endometrium to Model Bovine Innate Immunity and Inflammation Ex Vivo. *American Journal of Reproductive Immunology*, 67(6), 526-539.

- Born, G. C. C. (2000). *Plantas medicinais da Mata Atlântica (Vale do Ribeira-SP)*. (Tese de Doutorado), Universidade de São Paulo, São Paulo.
- Bosh, K. A., Powell, D., Neibergs, J. S., Shelton, B., and Zent, W. (2009). Impact of reproductive efficiency over time and mare financial value on economic returns among Thoroughbred mares in central Kentucky. *Equine veterinary journal*, 41(9), 889-894.
- Brandt, G., and Manning, J. (1969). Improved uterine biopsy technics for diagnosing infertility in the mare. *Veterinary medicine, small animal clinician: VM, SAC*, 64(11), 977-983.
- Brenner, D. A., O'Hara, M., Angel, P., Chojkier, M., and Karin, M. (1989). Prolonged activation of jun and collagenase genes by tumour necrosis factor-alpha. *Nature*, 337(6208), 661-663.
- Bretzlaff, K. (1987). Rationale for Treatment of Endometritis in the Dairy Cow. *Veterinary Clinics of North America: Food Animal Practice*, 3(3), 593-607.
- Brindley, D. N., Lin, F.-T., and Tigyi, G. J. (2013). Role of the autotaxin-lysophosphatidate axis in cancer resistance to chemotherapy and radiotherapy. *Biochimica et biophysica acta*, 1831(1), 74-85.
- Brook, D. (1984). Uterine culture in mares. *Mod Vet Pract*, 65(5), A3-8.
- Cabrera, R. A., Dozier, B. L., and Duffy, D. M. (2006). Prostaglandin-endoperoxide synthase (PTGS1 and PTGS2) expression and prostaglandin production by normal monkey ovarian surface epithelium. *Fertil Steril*, 86(4 Suppl), 1088-1096.
- Cannon, J. G. (1998). Adaptive interactions between cytokines and the hypothalamic-pituitary-gonadal axis. *Ann N Y Acad Sci*, 856, 234-242.
- Card, C. (2005). Post-breeding inflammation and endometrial cytology in mares. *Theriogenology*, 64(3), 580-588.
- Carnevale, E., and Ginther, O. (1992). Relationships of age to uterine function and reproductive efficiency in mares. *Theriogenology*, 37(5), 1101-1115.
- Caslick, E. (1937). The vulva and the vulvo-vaginal orifice and its relation to genital health of the thoroughbred mare. *Cornell Vet*, 27(2), 178-187.
- Causey, R. C. (2006). Making sense of equine uterine infections: The many faces of physical clearance. *The Veterinary Journal*, 172(3), 405-421.
- Chang, L., and Karin, M. (2001). Mammalian MAP kinase signalling cascades. *Nature*, 410(6824), 37-40.
- Chelikani, P. K., Glimm, D. R., and Kennelly, J. J. (2003). Short communication: Tissue distribution of leptin and leptin receptor mRNA in the bovine. *J Dairy Sci*, 86(7), 2369-2372.
- Chen, G. Y., and Nuñez, G. (2010). Sterile inflammation: sensing and reacting to damage. *Nature reviews. Immunology*, 10(12), 826-837.
- Cheng, Z., Robinson, R. S., Pushpakumara, P. G., Mansbridge, R. J., and Wathes, D. C. (2001). Effect of dietary polyunsaturated fatty acids on uterine prostaglandin synthesis in the cow. *J Endocrinol*, 171(3), 463-473.
- Chilliard, Y., Bonnet, M., Delavaud, C., Faulconnier, Y., Leroux, C., Djiane, J., and Bocquier, F. (2001). Leptin in ruminants. Gene expression in adipose tissue and mammary gland, and regulation of plasma concentration. *Domest Anim Endocrinol*, 21(4), 271-295.
- Chow, J. C., Young, D. W., Golenbock, D. T., Christ, W. J., and Gusovsky, F. (1999). Toll-like receptor-4 mediates lipopolysaccharide-induced signal transduction. *Journal of Biological Chemistry*, 274(16), 10689-10692.
- Christoffersen, M., Baagoe, C. D., Jacobsen, S., Bojesen, A. M., Petersen, M. R., and Lehn-Jensen, H. (2010). Evaluation of the systemic acute phase response and endometrial gene expression of serum amyloid A and pro- and anti-inflammatory cytokines in mares with experimentally induced endometritis. *Vet Immunol Immunopathol*, 138(1-2), 95-105.
- Christoffersen, M., and Troedsson, M. (2017). Inflammation and fertility in the mare. *Reprod Domest Anim*, 52 Suppl 3, 14-20.

- Christoffersen, M., Woodward, E., Bojesen, A. M., Jacobsen, S., Petersen, M. R., Troedsson, M. H., and Lehn-Jensen, H. (2012). Inflammatory responses to induced infectious endometritis in mares resistant or susceptible to persistent endometritis. *BMC veterinary research*, 8(1), 41.
- Coelho, E. G. A., and Oliveira, D. A. A. (2008). Testes genéticos na equídeocultura. *Revista Brasileira de Zootecnia*(37), 202-205.
- Conesa, A., Madrigal, P., Tarazona, S., Gomez-Cabrero, D., Cervera, A., McPherson, A., Szczesniak, M. W., Gaffney, D. J., Elo, L. L., Zhang, X., and Mortazavi, A. (2016). A survey of best practices for RNA-seq data analysis. *Genome Biology*, 17, 13.
- Cronin, J. G., Turner, M. L., Goetze, L., Bryant, C. E., and Sheldon, I. M. (2012). Toll-like receptor 4 and MYD88-dependent signaling mechanisms of the innate immune system are essential for the response to lipopolysaccharide by epithelial and stromal cells of the bovine endometrium. *Biology of reproduction*, 86(2), 51, 51-59.
- Curry, T. E., Jr., and Osteen, K. G. (2003). The matrix metalloproteinase system: changes, regulation, and impact throughout the ovarian and uterine reproductive cycle. *Endocr Rev*, 24(4), 428-465.
- Cuthbertson, L., Rogers, G. B., Walker, A. W., Oliver, A., Hafiz, T., Hoffman, L. R., Carroll, M. P., Parkhill, J., Bruce, K. D., and van der Gast, C. J. (2014). Time between collection and storage significantly influences bacterial sequence composition in sputum samples from cystic fibrosis respiratory infections. *Journal of clinical microbiology*, 52(8), 3011-3016.
- Dahms, B. J., and Troedsson, M. H. T. (2002). *The effect of seminal plasma components on opsonisation and PMN-phagocytosis of equine spermatozoa* (Vol. 58).
- Dascanio, J. J. (2011). External Reproductive Anatomy In A. O. McKinnon, S. E. L., E. Vaala, & D. D. Varner (Eds.), *Equine Reproduction* (Vol. 2, pp. 1577-1581). Philadelphia, London: Wiley-Blackwell.
- Davies Morel, M. C. G. (2015). *Equine Reproductive Physiology, Breeding and Stud Management* (4th ed.). Oxfordshire: Wallingford : CABI
- de Winter, P. J. J., Verdonck, M., de Kruif, A., Devriese, L. A., and Haesebrouck, F. (1992). Endometritis and vaginal discharge in the sow. *Animal reproduction science*, 28(1), 51-58.
- Denu, J. M., and Dixon, J. E. (1998). Protein tyrosine phosphatases: mechanisms of catalysis and regulation. *Curr Opin Chem Biol*, 2(5), 633-641.
- Diel de Amorim, M., Gartley, C. J., Foster, R. A., Hill, A., Scholtz, E. L., Hayes, A., and Chenier, T. S. (2016). Comparison of Clinical Signs, Endometrial Culture, Endometrial Cytology, Uterine Low-Volume Lavage, and Uterine Biopsy and Combinations in the Diagnosis of Equine Endometritis. *Journal of Equine Veterinary Science*, 44, 54-61.
- Dunne, A., and O'Neill, L. A. (2003). The interleukin-1 receptor/Toll-like receptor superfamily: signal transduction during inflammation and host defense. *Sci STKE*, 2003(171), re3.
- Elhay, M., Newbold, A., Britton, A., Turley, P., Dowsett, K., and Walker, J. (2007). Suppression of behavioural and physiological oestrus in the mare by vaccination against GnRH. *Aust Vet J*, 85(1-2), 39-45.
- Evans, M., Hamer, J., Gason, L., Graham, C., Asbury, A., and Irvine, C. (1986a). Clearance of bacteria and non-antigenic markers following intra-uterine inoculation into maiden mares: effect of steroid hormone environment. *Theriogenology*, 26(1), 37-50.
- Evans, M., Hamer, J., Gason, L., and Irvine, C. (1986b). Factors affecting uterine clearance of inoculated materials in mares. *Journal of reproduction and fertility. Supplement*, 35, 327-334.
- Evans, M. J., and Irvine, C. (1975). Serum concentrations of FSH, LH and progesterone during the oestrous cycle and early pregnancy in the mare. *Journal of reproduction and fertility. Supplement*(23), 193-200.

- Fedorka, C., Woodward, E., Scoggin, K., Esteller-Vico, A., Squires, e., Ball, B., and Troedsson, M. (2016). The effect of cysteine-rich secretory protein-3 (CRISP-3) and lactoferrin on endometrial cytokine expression after breeding in the horse. *Journal of Equine Veterinary Science*, 48.
- Fedorka, C. E., Scoggin, K. E., Woodward, E. M., Squires, E. L., Ball, B. A., and Troedsson, M. (2017). The effect of select seminal plasma proteins on endometrial mRNA cytokine expression in mares susceptible to persistent mating-induced endometritis. *Reprod Domest Anim*, 52(1), 89-96.
- Fessele, S., Boehlk, S., Mojaat, A., Miyamoto, N. G., Werner, T., Nelson, E. L., Schlondorff, D., and Nelson, P. J. (2001). Molecular and in silico characterization of a promoter module and C/EBP element that mediate LPS-induced RANTES/CCL5 expression in monocytic cells. *Faseb j*, 15(3), 577-579.
- Fiala Rechsteiner, S., Pimentel, C. A., Steiger, K., Mattos, A. L. G., Gregory, R. M., and Mattos, R. (2002). *Effect of skim milk and seminal plasma uterine infusions in mares* (Vol. 58).
- Foley, J., Dann, P., Hong, J., Cosgrove, J., Dreyer, B., Rimm, D., Dunbar, M., Philbrick, W., and Wysolmerski, J. (2001). Parathyroid hormone-related protein maintains mammary epithelial fate and triggers nipple skin differentiation during embryonic breast development. *Development*, 128(4), 513-525.
- Forde, N., and Lonergan, P. (2012). Transcriptomic analysis of the bovine endometrium: what is required to establish uterine receptivity to implantation in cattle? *Journal of Reproduction and Development*, 58(2), 189-195.
- Freije, J. M., Diez-Itza, I., Balbin, M., Sanchez, L. M., Blasco, R., Tolivia, J., and Lopez-Otin, C. (1994). Molecular cloning and expression of collagenase-3, a novel human matrix metalloproteinase produced by breast carcinomas. *J Biol Chem*, 269(24), 16766-16773.
- Frontoso, R., De Carlo, E., Pasolini, M. P., van der Meulen, K., Pagnini, U., Iovane, G., and De Martino, L. (2008). Retrospective study of bacterial isolates and their antimicrobial susceptibilities in equine uteri during fertility problems. *Res Vet Sci*, 84(1), 1-6.
- Fumuso, E., Aguilar, J., Giguere, S., David, O., Wade, J., and Rogan, D. (2006). *Interleukin-8 (IL-8) and 10 (IL-10) mRNA transcriptions in the endometrium of normal mares and mares susceptible to persistent post-breeding endometritis*. Paper presented at the Animal reproduction science.
- Fumuso, E., Giguère, S., Wade, J., Rogan, D., Videla-Dorna, I., and Bowden, R. A. (2003). Endometrial IL-1 β , IL-6 and TNF- α , mRNA expression in mares resistant or susceptible to post-breeding endometritis: effects of estrous cycle, artificial insemination and immunomodulation. *Veterinary Immunology and Immunopathology*, 96(1), 31-41.
- Fumuso, E. A., Aguilar, J., Giguere, S., Rivulgo, M., Wade, J., and Rogan, D. (2007). Immune parameters in mares resistant and susceptible to persistent post-breeding endometritis: effects of immunomodulation. *Vet Immunol Immunopathol*, 118(1-2), 30-39.
- Gabriela, A. M., Cristóbal, F., Frederico, N., Emmanuel Dias, N., Laura, P., and Elmer, A. F. (2016). The impact of quality control in RNA-seq experiments. *Journal of Physics: Conference Series*, 705(1), 012003.
- Gebhardt, S., Merkl, M., Herbach, N., Wanke, R., Handler, J., and Bauersachs, S. (2012). Exploration of global gene expression changes during the estrous cycle in equine endometrium. *Biol Reprod*, 87(6), 136.
- Gentleman, R. C., Carey, V. J., Bates, D. M., Bolstad, B., Dettling, M., Dudoit, S., Ellis, B., Gautier, L., Ge, Y., Gentry, J., Hornik, K., Hothorn, T., Huber, W., Iacus, S., Irizarry, R., Leisch, F., Li, C., Maechler, M., Rossini, A. J., Sawitzki, G., Smith, C., Smyth, G., Tierney, L., Yang, J. Y., and Zhang, J. (2004). Bioconductor: open software development for computational biology and bioinformatics. *Genome Biol*, 5(10), R80.

- Ghanem, M. E., Tezuka, E., Devkota, B., Izaike, Y., and Osawa, T. (2015). Persistence of uterine bacterial infection, and its associations with endometritis and ovarian function in postpartum dairy cows. *The Journal of reproduction and development*, 61(1), 54-60.
- Ginther, O., Gastal, E., Gastal, M., and Beg, M. (2004). Seasonal influence on equine follicle dynamics. *Animal Reproduction*, 1, 31-44.
- Ginther, O. J. (1992). *Reproductive biology of the mare : basic and applied aspects* (2nd ed. ed.): Cross Plains, Wisconsin : Equiservices.
- Ginther, O. J., and Pierson, R. A. (1984). Ultrasonic evaluation of the reproductive tract of the mare: Ovaries. *Journal of Equine Veterinary Science*, 4(1), 11-16.
- Ginther, O. J., Utt, M. D., Bergfelt, D. R., and Beg, M. A. (2006). Controlling interrelationships of progesterone/LH and estradiol/LH in mares. *Anim Reprod Sci*, 95(1-2), 144-150.
- Glowatzki-Mullis, M. L., Muntwyler, J., Pfister, W., Marti, E., Rieder, S., Poncet, P. A., and Gaillard, C. (2006). Genetic diversity among horse populations with a special focus on the Franches-Montagnes breed. 37(1), 33-39.
- Gonçalves, R. W., Maia, T. L., Silva, E. S. P., Santos, D. C., Denucci, B. L., and Guedes, M. H. (2009). Análise da eficiência reprodutiva dos equinos (Analysis of reproductive efficiency in horses). *PUBVET*, 3(16).
- Gonzalez, F. G., and Di Stasi, L. C. (2002). Anti-ulcerogenic and analgesic activities of the leaves of *Wilbrandia ebracteata* in mice. *Phytomedicine*, 9(2), 125-134.
- Graham, J. K. (1996). Analysis of stallion semen and its relation to fertility. *Vet Clin North Am Equine Pract*, 12(1), 119-130.
- Green, K. A., and Lund, L. R. (2005). ECM degrading proteases and tissue remodelling in the mammary gland. *Bioessays*, 27(9), 894-903.
- Grimm, S., and Baeuerle, P. A. (1993). The inducible transcription factor NF-kappa B: structure-function relationship of its protein subunits. *Biochem J*, 290 (Pt 2)(Pt 2), 297-308.
- Harris, S. G., Padilla, J., Koumas, L., Ray, D., and Phipps, R. P. (2002). Prostaglandins as modulators of immunity. *Trends Immunol*, 23(3), 144-150.
- Hayden, M. S., and Ghosh, S. (2014). Regulation of NF-kappaB by TNF family cytokines. *Semin Immunol*, 26(3), 253-266.
- Haynes, W. A., Tomczak, A., and Khatri, P. (2018). Gene annotation bias impedes biomedical research. *Sci Rep*, 8(1), 1362.
- Hemberg, E., Lundeheim, N., and Einarsson, S. (2004). Reproductive Performance of Thoroughbred Mares in Sweden. *Reproduction in domestic animals*, 39(2), 81-85.
- Hemberg, E., Lundeheim, N., and Einarsson, S. (2005). Retrospective study on vulvar conformation in relation to endometrial cytology and fertility in thoroughbred mares. *Journal of Veterinary Medicine Series A*, 52(9), 474-477.
- Hens, J. R., and Wysolmerski, J. J. (2005). Key stages of mammary gland development: molecular mechanisms involved in the formation of the embryonic mammary gland. *Breast cancer research : BCR*, 7(5), 220-224.
- Herath, S., Lilly, S. T., Fischer, D. P., Williams, E. J., Dobson, H., Bryant, C. E., and Sheldon, I. M. (2009). Bacterial lipopolysaccharide induces an endocrine switch from prostaglandin F2alpha to prostaglandin E2 in bovine endometrium. *Endocrinology*, 150(4), 1912-1920.
- Honda, K., Yanai, H., Negishi, H., Asagiri, M., Sato, M., Mizutani, T., Shimada, N., Ohba, Y., Takaoka, A., Yoshida, N., and Taniguchi, T. (2005). IRF-7 is the master regulator of type-I interferon-dependent immune responses. *Nature*, 434(7034), 772-777.
- Hozumi, H., Hokari, R., Kurihara, C., Narimatsu, K., Sato, H., Sato, S., Ueda, T., Higashiyama, M., Okada, Y., Watanabe, C., Komoto, S., Tomita, K., Kawaguchi, A., Nagao, S., and Miura, S. (2013). Involvement of autotaxin/lysophospholipase D expression in intestinal vessels in aggravation of intestinal damage through lymphocyte migration. *Lab Invest*, 93(5), 508-519.

- Huang, D. W., Sherman, B. T., and Lempicki, R. A. (2009). Systematic and integrative analysis of large gene lists using DAVID bioinformatics resources. *Nat Protoc*, 4(1), 44-57.
- Hughes, J. (1980). Clinical examination and abnormalities in the mare. *Current Therapy in Theriogenology*, 706-721.
- Hughes, J. P., and Loy, R. G. (1975). The relation of infection to infertility in the mare and stallion. *Equine veterinary journal*, 7(3), 155-159.
- Hurtgen, J. P. (2006). Pathogenesis and treatment of endometritis in the mare: a review. *Theriogenology*, 66(3), 560-566.
- Hynes, R. O., and Zhao, Q. (2000). The evolution of cell adhesion. *J Cell Biol*, 150(2), F89-96.
- Irvine, C. H., and Alexander, S. L. (1997). Patterns of secretion of GnRH, LH and FSH during the postovulatory period in mares: mechanisms prolonging the LH surge. *J Reprod Fertil*, 109(2), 263-271.
- Itokawa, H., Shiota, O., Ikuta, H., Morita, H., Takeya, K., and Iitaka, Y. (1991). Triterpenes from *Maytenus ilicifolia*. *Phytochemistry*, 30(11), 3713-3716.
- Jones, D. A., Carlton, D. P., McIntyre, T. M., Zimmerman, G. A., and Prescott, S. M. (1993). Molecular cloning of human prostaglandin endoperoxide synthase type II and demonstration of expression in response to cytokines. *J Biol Chem*, 268(12), 9049-9054.
- Jones, S. M., and Troxel, T. R. (2006). Understanding reproductive physiology and anatomy of the mare. *University of Arkansas, Division of Agriculture, Research and Extension*. (FSA3039-PD-7-12RV), 1-4.
- Jorge, R. M., Leite, J. P., Oliveira, A. B., and Tagliati, C. A. (2004). Evaluation of antinociceptive, anti-inflammatory and antiulcerogenic activities of *Maytenus ilicifolia*. *J Ethnopharmacol*, 94(1), 93-100.
- Kanakaraj, P., Schafer, P. H., Cavender, D. E., Wu, Y., Ngo, K., Grealish, P. F., Wadsworth, S. A., Peterson, P. A., Siekierka, J. J., Harris, C. A., and Fung-Leung, W. P. (1998). Interleukin (IL)-1 receptor-associated kinase (IRAK) requirement for optimal induction of multiple IL-1 signaling pathways and IL-6 production. *J Exp Med*, 187(12), 2073-2079.
- Kanehisa, M., Furumichi, M., Tanabe, M., Sato, Y., and Morishima, K. (2017). KEGG: new perspectives on genomes, pathways, diseases and drugs. *Nucleic Acids Res*, 45(D1), D353-D361.
- Kanehisa, M., and Goto, S. (2000). KEGG: Kyoto Encyclopedia of Genes and Genomes. *Nucleic Acids Res*, 28(1), 27-30.
- Kanehisa, M., Sato, Y., Kawashima, M., Furumichi, M., and Tanabe, M. (2016). KEGG as a reference resource for gene and protein annotation. *Nucleic Acids Res*, 44(D1), D457-D462.
- Katila, T. (1995). Onset and duration of uterine inflammatory response of mares after insemination with fresh semen. *Biol Reprod Monogr*(1), 515-517.
- Katila, T. (1996). Uterine defence mechanisms in the mare. *Animal reproduction science*, 42(1), 197-204.
- Katila, T. (2001). Sperm-uterine interactions: a review. *Animal reproduction science*, 68(3), 267-272.
- Katila, T., Lock, T., Hoffmann, W., and Smith, A. (1990). Lysozyme, alkaline phosphatase and neutrophils in uterine secretions of mares with differing resistance to endometritis. *Theriogenology*, 33(3), 723-732.
- Kenney, R. (1978). Cyclic and pathologic changes of the mare endometrium as detected by biopsy, with a note on early embryonic death. *Journal of the American Veterinary Medical Association*, 172(3), 241-262.
- Kenney, R., and Doig, P. (1986). Equine endometrial biopsy. *Current Therapy in Theriogenology*, 2(3), 723-729.

- Keuschnigg, J., Henttinen, T., Auvinen, K., Karikoski, M., Salmi, M., and Jalkanen, S. (2009). The prototype endothelial marker PAL-E is a leukocyte trafficking molecule. *Blood*, 114(2), 478-484.
- Khatri, P., Sirota, M., and Butte, A. J. (2012). Ten years of pathway analysis: current approaches and outstanding challenges. *PLoS Computational Biology*, 8(2), e1002375.
- Kimbrell, D. A., and Beutler, B. (2001). The evolution and genetics of innate immunity. *Nat Rev Genet*, 2(4), 256-267.
- Knowlden, S., and Georas, S. N. (2014). The autotaxin-LPA axis emerges as a novel regulator of lymphocyte homing and inflammation. *J Immunol*, 192(3), 851-857.
- Knudsen, O. (1964). Endometrial cytology as a diagnostic aid in mares. *The Cornell veterinarian*, 54, 415-422.
- Kobayashi, K., Hernandez, L. D., Galan, J. E., Janeway, C. A., Jr., Medzhitov, R., and Flavell, R. A. (2002). IRAK-M is a negative regulator of Toll-like receptor signaling. *Cell*, 110(2), 191-202.
- Kotilainen, T., Huhtinen, M., and Katila, T. (1994). Sperm-induced leukocytosis in the equine uterus. *Theriogenology*, 41(3), 629-636.
- Krysko, D. V., Agostinis, P., Krysko, O., Garg, A. D., Bachert, C., Lambrecht, B. N., and Vandenabeele, P. (2011). Emerging role of damage-associated molecular patterns derived from mitochondria in inflammation. *Trends Immunol*, 32(4), 157-164.
- Lamph, W. W., Wamsley, P., Sassone-Corsi, P., and Verma, I. M. (1988). Induction of proto-oncogene JUN/AP-1 by serum and TPA. *Nature*, 334(6183), 629-631.
- LeBlanc, M., Asbury, A., and Lyle, S. (1989). Uterine clearance mechanisms during the early postovulatory period in mares. *American journal of veterinary research*, 50(6), 864-867.
- LeBlanc, M. M. (2011). Uterine Cytology. In A. O. McKinnon, E. L. Squires, E. Vaala, & D. D. Varner (Eds.), *Equine Reproduction* (pp. 1922-1928). Philadelphia, London: Wiley-Blackwell.
- LeBlanc, M. M., and Causey, R. C. (2009). Clinical and subclinical endometritis in the mare: both threats to fertility. *Reprod Domest Anim*, 44 Suppl 3, 10-22.
- LeBlanc, M. M., Neuwirth, L., Asbury, A. C., Tran, T., Mauragis, D., and Klapstein, E. (1994). Scintigraphic measurement of uterine clearance in normal mares and mares with recurrent endometritis. *Equine Vet J*, 26(2), 109-113.
- LeBlanc, M. M., Neuwirth, L., Jones, L., Cage, C., and Mauragis, D. (1998). Differences in uterine position of reproductively normal mares and those with delayed uterine clearance detected by scintigraphy. *Theriogenology*, 50(1), 49-54.
- LeBlanc, S. J., Duffield, T. F., Leslie, K. E., Bateman, K. G., Keefe, G. P., Walton, J. S., and Johnson, W. H. (2002). Defining and Diagnosing Postpartum Clinical Endometritis and its Impact on Reproductive Performance in Dairy Cows. *J Dairy Sci*, 85(9), 2223-2236.
- Lefebvre, V. (2010). The SoxD transcription factors--Sox5, Sox6, and Sox13--are key cell fate modulators. *Int J Biochem Cell Biol*, 42(3), 429-432.
- Leite, J. P., Rastrelli, L., Romussi, G., Oliveira, A. B., Vilegas, J. H., Vilegas, W., and Pizza, C. (2001). Isolation and HPLC quantitative analysis of flavonoid glycosides from Brazilian beverages (*Maytenus ilicifolia* and *M. aquifolium*). *J Agric Food Chem*, 49(8), 3796-3801.
- Levy, N., Kobayashi, S.-i., Roth, Z., Wolfenson, D., Miyamoto, A., and Meidan, R. (2000). Administration of Prostaglandin F2 α During the Early Bovine Luteal Phase Does Not Alter the Expression of ET-1 and of Its Type A Receptor: A Possible Cause for Corpus Luteum Refractoriness. *Biology of reproduction*, 63(2), 377-382.
- Ley, W. B. (2004). Anatomy and Physiology. In W. B. Ley (Ed.), *Broodmare Reproduction for the Equine Practitioner* (pp. 56-72). Jackson, WY: Teton NewMedia.
- Liang, J., Wang, J., Azfer, A., Song, W., Tromp, G., Kolattukudy, P. E., and Fu, M. (2008). A novel CCH-zinc finger protein family regulates proinflammatory activation of macrophages. *J Biol Chem*, 283(10), 6337-6346.

- Liu, I., Cheung, A., Walsh, E., and Ayin, S. (1986). The functional competence of uterine-derived polymorphonuclear neutrophils (PMN) from mares resistant and susceptible to chronic uterine infection: a sequential migration analysis. *Biology of reproduction*, 35(5), 1168-1174.
- Liu, I., and Troedsson, M. (2008). The diagnosis and treatment of endometritis in the mare: Yesterday and today. *Theriogenology*, 70(3), 415-420.
- Liu, L., Zhou, Z., Huang, S., Guo, Y., Fan, Y., Zhang, J., Zhang, J., Fu, M., and Chen, Y. E. (2013). Zc3h12c inhibits vascular inflammation by repressing NF-kappaB activation and pro-inflammatory gene expression in endothelial cells. *Biochem J*, 451(1), 55-60.
- Liu, X. L., Hu, X., Cai, W. X., Lu, W. W., and Zheng, L. W. (2016). *Effect of Granulocyte-Colony Stimulating Factor on Endothelial Cells and Osteoblasts* (Vol. 2016).
- Love, M. I., Huber, W., and Anders, S. (2014). Moderated estimation of fold change and dispersion for RNA-seq data with DESeq2. *Genome Biol*, 15(12), 550.
- Lyroni, K., Patsalos, A., Daskalaki, M. G., Doxaki, C., Soennichsen, B., Helms, M., Liapis, I., Zacharioudaki, V., Kampranis, S. C., and Tsatsanis, C. (2017). Epigenetic and Transcriptional Regulation of IRAK-M Expression in Macrophages. *J Immunol*, 198(3), 1297-1307.
- Ma, J., Chen, T., Mandelin, J., Ceponis, A., Miller, N. E., Hukkanen, M., Ma, G. F., and Kontinen, Y. T. (2003). Regulation of macrophage activation. *Cellular and Molecular Life Sciences CMLS*, 60(11), 2334-2346.
- Marth, C. D., Firestone, S. M., Hanlon, D., Glenton, L. Y., Browning, G. F., Young, N. D., and Krekeler, N. (2018). Innate immune genes in persistent mating-induced endometritis in horses. *Reprod Fertil Dev*, 30(3), 533-545.
- Marth, C. D., Young, N. D., Glenton, L. Y., Noden, D. M., Browning, G. F., and Krekeler, N. (2015a). Deep sequencing of the uterine immune response to bacteria during the equine oestrous cycle. *BMC genomics*, 16(1), 1.
- Marth, C. D., Young, N. D., Glenton, L. Y., Noden, D. M., Browning, G. F., and Krekeler, N. (2015b). Effect of ovarian hormones on the healthy equine uterus: a global gene expression analysis. *Reproduction, Fertility and Development*.
- Medzhitov, R., and Janeway, C. A., Jr. (1997). Innate immunity: the virtues of a nonclonal system of recognition. *Cell*, 91(3), 295-298.
- Meidan, R., Milvae, R. A., Weiss, S., Levy, N., and Friedman, A. (1999). Intraovarian regulation of luteolysis. *J Reprod Fertil Suppl*, 54, 217-228.
- Meijer, L., Borgne, A., Mulner, O., Chong, J. P., Blow, J. J., Inagaki, N., Inagaki, M., Delcros, J. G., and Moulinoux, J. P. (1997). Biochemical and cellular effects of roscovitine, a potent and selective inhibitor of the cyclin-dependent kinases cdc2, cdk2 and cdk5. *Eur J Biochem*, 243(1-2), 527-536.
- Metzker, M. L. (2010). Sequencing technologies—the next generation. *Nature Reviews Genetics*, 11(1), 31-46.
- Midwood, K. S., Hussenet, T., Langlois, B., and Orend, G. (2011). Advances in tenascin-C biology. *Cell Mol Life Sci*, 68(19), 3175-3199.
- Miro, J. (2012). Ovarian ultrasonography in the mare. *Reprod Domest Anim*, 47 Suppl 3, 30-33.
- Moon, S. Y., and Zheng, Y. (2003). Rho GTPase-activating proteins in cell regulation. *Trends Cell Biol*, 13(1), 13-22.
- Morresey, P. R. (2011). Oxytocin, Inhibin, Activin, Relaxin and Prolactin. In A. O. McKinnon, E. L. Squires, W. E. Vaala, & D. D. Varner (Eds.), *Equine Reproduction* (Vol. 2, pp. 1679-1686). Philadelphia, London: Wiley-Blackwell
- Morris, L. H., and Allen, W. R. (2002). Reproductive efficiency of intensively managed Thoroughbred mares in Newmarket. *Equine Vet J*, 34(1), 51-60.
- Muegge, K., Williams, T., Kant, J., Karin, M., Chiu, R., Schmidt, A., Siebenlist, U., Young, H., and Durum, S. (1989). Interleukin-1 costimulatory activity on the interleukin-2 promoter via AP-1. *Science*, 246(4927), 249-251.

- Murphy, G., and Docherty, A. J. (1992). The matrix metalloproteinases and their inhibitors. *Am J Respir Cell Mol Biol*, 7(2), 120-125.
- Mutz, K.-O., Heilkenbrinker, A., Lönne, M., Walter, J.-G., and Stahl, F. (2013). Transcriptome analysis using next-generation sequencing. *Current opinion in biotechnology*, 24(1), 22-30.
- Muzio, M., Ni, J., Feng, P., and Dixit, V. M. (1997). IRAK (Pelle) family member IRAK-2 and MyD88 as proximal mediators of IL-1 signaling. *Science*, 278(5343), 1612-1615.
- Nash, D., Lane, E., Herath, S., and Martin Sheldon, I. (2008). Endometrial explant culture for characterizing equine endometritis. *American Journal of Reproductive Immunology*, 59(2), 105-117.
- Nash, D., Sheldon, I., Herath, S., and Lane, E. (2010a). Markers of the uterine innate immune response of the mare. *Animal reproduction science*, 119(1), 31-39.
- Nash, D. M., Paddison, J., Davies Morel, M. C. G., and Barnea, E. R. (2018). Preimplantation factor modulates acute inflammatory responses of equine endometrium. *Vet Med Sci*, 4(4), 351-356.
- Nash, D. M., Sheldon, I. M., Herath, S., and Lane, E. (2010b). Endometrial explant culture to study the response of equine endometrium to insemination. *Reproduction in domestic animals*, 45(4), 670-676.
- Nathan, C. (2006). Neutrophils and immunity: challenges and opportunities. *Nature Reviews Immunology*, 6, 173.
- Neely, D., Kindahl, H., Stabenfeldt, G., Edqvist, L., and Hughes, J. (1979). Prostaglandin release patterns in the mare: physiological, pathophysiological, and therapeutic responses. *Journal of reproduction and fertility. Supplement*(27), 181.
- Niemela, H., Elima, K., Henttinen, T., Irjala, H., Salmi, M., and Jalkanen, S. (2005). Molecular identification of PAL-E, a widely used endothelial-cell marker. *Blood*, 106(10), 3405-3409.
- Nikitopoulou, I., Oikonomou, N., Karouzakis, E., Sevastou, I., Nikolaidou-Katsaridou, N., Zhao, Z., Mersinias, V., Armaka, M., Xu, Y., Masu, M., Mills, G. B., Gay, S., Kollias, G., and Aidinis, V. (2012). Autotaxin expression from synovial fibroblasts is essential for the pathogenesis of modeled arthritis. *J Exp Med*, 209(5), 925-933.
- Nikolakopoulos, E., and Watson, E. (1999). Uterine contractility is necessary for the clearance of intrauterine fluid but not bacteria after bacterial infusion in the mare. *Theriogenology*, 52(3), 413-423.
- Ning, S., Pagano, J. S., and Barber, G. N. (2011). IRF7: activation, regulation, modification and function. *Genes Immun*, 12(6), 399-414.
- Niranjan, B., Buluwela, L., Yant, J., Perusinghe, N., Atherton, A., Phippard, D., Dale, T., Gusterson, B., and Kamalati, T. (1995). HGF/SF: a potent cytokine for mammary growth, morphogenesis and development. *Development*, 121(9), 2897.
- Nishikawa, Y., Baba, T., and Imori, T. (1984). Effect of the estrous cycle on uterine infection induced by *Escherichia coli*. *Infection and immunity*, 43(2), 678-683.
- Nurse, P. (2000). A long twentieth century of the cell cycle and beyond. *Cell*, 100(1), 71-78.
- O'Neill, L. A., and Greene, C. (1998). Signal transduction pathways activated by the IL-1 receptor family: ancient signaling machinery in mammals, insects, and plants. *J Leukoc Biol*, 63(6), 650-657.
- Oliveira, M. G., Monteiro, M. G., Macaubas, C., Barbosa, V. P., and Carlini, E. A. (1991). Pharmacologic and toxicologic effects of two Maytenus species in laboratory animals. *J Ethnopharmacol*, 34(1), 29-41.
- Osborne, V. (1975). Factors influencing foaling percentages in Australian mares. *Journal of reproduction and fertility. Supplement*(23), 477-483.
- Ozsolak, F., and Milos, P. M. (2011). RNA sequencing: advances, challenges and opportunities. *Nature Reviews Genetics*, 12(2), 87-98.
- Papotto, P. H., Ribot, J. C., and Silva-Santos, B. (2017). IL-17(+) gammadelta T cells as kick-starters of inflammation. *Nat Immunol*, 18(6), 604-611.

- Penrod, L. V., Allen, R. E., Turner, J. L., Limesand, S. W., and Arns, M. J. (2013). Effects of oxytocin, lipopolysaccharide (LPS), and polyunsaturated fatty acids on prostaglandin secretion and gene expression in equine endometrial explant cultures. *Domest Anim Endocrinol*, 44(1), 46-55.
- Poltorak, A., He, X., Smirnova, I., Liu, M. Y., Van Huffel, C., Du, X., Birdwell, D., Alejos, E., Silva, M., Galanos, C., Freudenberg, M., Ricciardi-Castagnoli, P., Layton, B., and Beutler, B. (1998). Defective LPS signaling in C3H/HeJ and C57BL/10ScCr mice: mutations in Tlr4 gene. *Science*, 282(5396), 2085-2088.
- Pycock, J., and Newcombe, J. (1996). The relationship between intraluminal uterine fluid, endometritis, and pregnancy rate in the mare. *Equine practice (USA)*.
- Pycock, J. F., and Allen, W. E. (1990). Inflammatory components in uterine fluid from mares with experimentally induced bacterial endometritis. *Equine Vet J*, 22(6), 422-425.
- Ramadan, A. A., Johnson, G. L., 3rd, and Lewis, G. S. (1997). Regulation of uterine immune function during the estrous cycle and in response to infectious bacteria in sheep. *J Anim Sci*, 75(6), 1621-1632.
- Rantakari, P., Auvinen, K., Jappinen, N., Kapraali, M., Valtonen, J., Karikoski, M., Gerke, H., Iftakhar, E. K. I., Keuschnigg, J., Umemoto, E., Tohya, K., Miyasaka, M., Elima, K., Jalkanen, S., and Salmi, M. (2015). The endothelial protein PLVAP in lymphatics controls the entry of lymphocytes and antigens into lymph nodes. *Nat Immunol*, 16(4), 386-396.
- Raposo, C. G., Marin, A. P., and Baron, M. G. (2006). Colony-stimulating factors: clinical evidence for treatment and prophylaxis of chemotherapy-induced febrile neutropenia. *Clin Transl Oncol*, 8(10), 729-734.
- Rasmussen, C. D., Petersen, M. R., Bojesen, A. M., Pedersen, H. G., Lehn-Jensen, H., and Christoffersen, M. (2015). Equine Infectious Endometritis—Clinical and Subclinical Cases. *Journal of Equine Veterinary Science*, 35(2), 95-104.
- Reiswig, J. D., Threlfall, W. R., and Rosol, T. J. (1993). A comparison of endometrial biopsy, culture and cytology during oestrus and dioestrus in the horse. *Equine Vet J*, 25(3), 240-241.
- Rhind, N., and Russell, P. (2012). Signaling pathways that regulate cell division. *Cold Spring Harb Perspect Biol*, 4(10).
- Ricciotti, E., and FitzGerald, G. A. (2011). Prostaglandins and inflammation. *Arterioscler Thromb Vasc Biol*, 31(5), 986-1000.
- Riddle, W. T., LeBlanc, M. M., and Stromberg, A. J. (2007). Relationships between uterine culture, cytology and pregnancy rates in a Thoroughbred practice. *Theriogenology*, 68(3), 395-402.
- Roberts, A., Pimentel, H., Trapnell, C., and Pachter, L. (2011). Identification of novel transcripts in annotated genomes using RNA-Seq. *Bioinformatics*, 27(17), 2325-2329.
- Robertson, G., Hirst, M., Bainbridge, M., Bilenky, M., Zhao, Y., Zeng, T., Euskirchen, G., Bernier, B., Varhol, R., Delaney, A., Thiessen, N., Griffith, O. L., He, A., Marra, M., Snyder, M., and Jones, S. (2007). Genome-wide profiles of STAT1 DNA association using chromatin immunoprecipitation and massively parallel sequencing. *Nat Methods*, 4.
- Rodriguez-Pinon, M., Tasende, C., Casuriaga, D., Bielli, A., Genovese, P., and Garofalo, E. G. (2015). Collagen and matrix metalloproteinase-2 and -9 in the ewe cervix during the estrous cycle. *Theriogenology*, 84(5), 818-826.
- Roskoski, R., Jr. (2005). Signaling by Kit protein-tyrosine kinase--the stem cell factor receptor. *Biochem Biophys Res Commun*, 337(1), 1-13.
- Rossi, D., and Zlotnik, A. (2000). The biology of chemokines and their receptors. *Annu Rev Immunol*, 18, 217-242.
- Ryder, K., and Nathans, D. (1988). Induction of protooncogene c-jun by serum growth factors. *Proceedings of the National Academy of Sciences of the United States of America*, 85(22), 8464-8467.

- Saliba, A.-E., Westermann, A. J., Gorski, S. A., and Vogel, J. (2014). Single-cell RNA-seq: advances and future challenges. *Nucleic Acids Research*, 42(14), 8845-8860.
- Saut, J. P., Healey, G. D., Borges, A. M., and Sheldon, I. M. (2014). Ovarian steroids do not affect bovine endometrial cytokine or chemokine responses to *Escherichia coli* or LPS in vitro. *Reproduction*, 148(6), 593-606.
- Schlafer, D. (2007). Equine endometrial biopsy: Enhancement of clinical value by more extensive histopathology and application of new diagnostic techniques? *Theriogenology*, 68(3), 413-422.
- Schnare, M., Barton, G. M., Holt, A. C., Takeda, K., Akira, S., and Medzhitov, R. (2001). Toll-like receptors control activation of adaptive immune responses. *Nature immunology*, 2(10), 947-950.
- Sharp, D. C. (2011). Melatonin. In A. O. McKinnon, E. L. Squires, W. E. Vaala, & D. D. Varner (Eds.), *Equine Reproduction* (2nd ed., Vol. 1, pp. 1669-1678). Philadelphia, London Wiley-Blackwell.
- Shaulian, E., and Karin, M. (2001). AP-1 in cell proliferation and survival. *Oncogene*, 20(19), 2390-2400.
- Sherr, C. J. (1996). Cancer cell cycles. *Science*, 274(5293), 1672-1677.
- Sherr, C. J., and Roberts, J. M. (1995). Inhibitors of mammalian G1 cyclin-dependent kinases. *Genes Dev*, 9(10), 1149-1163.
- Shirota, O., Morita, H., Takeya, K., and Itokawa, H. (1994). Cytotoxic aromatic triterpenes from *Maytenus ilicifolia* and *Maytenus chuchuhuasca*. *J Nat Prod*, 57(12), 1675-1681.
- Siegmund, B., Lehr, H.-A., Fantuzzi, G., and Dinarello, C. A. (2001). IL-1 β -converting enzyme (caspase-1) in intestinal inflammation. *Proceedings of the National Academy of Sciences*, 98(23), 13249-13254.
- Silva, E., Leitão, S., Henriques, S., Kowalewski, M., Hoffmann, B., Ferreira-Dias, G., da Costa, L. L., and Mateus, L. (2010). Gene transcription of TLR2, TLR4, LPS ligands and prostaglandin synthesis enzymes are up-regulated in canine uteri with cystic endometrial hyperplasia-pyometra complex. *Journal of reproductive immunology*, 84(1), 66-74.
- Simillion, C., Liechti, R., Lischer, H. E. L., Ioannidis, V., and Bruggmann, R. (2017). Avoiding the pitfalls of gene set enrichment analysis with SetRank. *BMC Bioinformatics*, 18(1), 151-151.
- Sirois, J. (1994). Induction of prostaglandin endoperoxide synthase-2 by human chorionic gonadotropin in bovine preovulatory follicles in vivo. *Endocrinology*, 135(3), 841-848.
- Sirois, J., and Doré, M. (1997). The Late Induction of Prostaglandin G/H Synthase-2 in Equine Preovulatory Follicles Supports Its Role as a Determinant of the Ovulatory Process*. *Endocrinology*, 138(10), 4427-4434.
- Skovira, J. W., Wu, J., Matyas, J. J., Kumar, A., Hanscom, M., Kabadi, S. V., Fang, R., and Faden, A. I. (2016). Cell cycle inhibition reduces inflammatory responses, neuronal loss, and cognitive deficits induced by hypobaric exposure following traumatic brain injury. *J Neuroinflammation*, 13(1), 299.
- Snyder, D. A., Turner, D. D., Miller, K. F., Garcia, M. C., and Ginther, O. J. (1979). Follicular and gonadotrophic changes during transition from ovulatory to anovulatory seasons. *J Reprod Fertil Suppl*(27), 95-101.
- Soria, G., and Ben-Baruch, A. (2008). The inflammatory chemokines CCL2 and CCL5 in breast cancer. *Cancer Lett*, 267(2), 271-285.
- Sosa, C., Carriquiry, M., Chalar, C., Crespi, D., Sanguinetti, C., Cavestany, D., and Meikle, A. (2010). Endometrial expression of leptin receptor and members of the growth hormone-Insulin-like growth factor system throughout the estrous cycle in heifers. *Anim Reprod Sci*, 122(3-4), 208-214.
- Souza-Formigoni, M. L., Oliveira, M. G., Monteiro, M. G., da Silveira-Filho, N. G., Braz, S., and Carlini, E. A. (1991). Antiulcerogenic effects of two *Maytenus* species in laboratory animals. *J Ethnopharmacol*, 34(1), 21-27.

- Squires, E. L., McKinnon, A. O., and Shideler, R. K. (1988). Use of ultrasonography in reproductive management of mares. *Theriogenology*, 29(1), 55-70.
- Stan, R. V., Tkachenko, E., and Niesman, I. R. (2004). PV1 is a key structural component for the formation of the stomatal and fenestral diaphragms. *Mol Biol Cell*, 15(8), 3615-3630.
- Steidl, R. J., Hayes, J. P., and Schaubert, E. (1997). Statistical power analysis in wildlife research. *Journal of Wildlife Management*, 61(2), 270-279.
- Stout, T. A. E. (2011). Prostaglandins. In A. O. McKinnon, E. L. Squires, W. E. Vaala, & D. D. Varner (Eds.), *Equine Reproduction* (Vol. 2, pp. 1642-1647). Philadelphia, London: Wiley-Blackwell.
- Subramaniam, S., Stansberg, C., and Cunningham, C. (2004). The interleukin 1 receptor family. *Dev Comp Immunol*, 28(5), 415-428.
- Sullivan, J., and Pickett, B. (1975). Influence of ejaculation frequency of stallions on characteristics of semen and output of spermatozoa. *Journal of reproduction and fertility. Supplement*(23), 29-34.
- Suzuki, N., Chen, N. J., Millar, D. G., Suzuki, S., Horacek, T., Hara, H., Bouchard, D., Nakanishi, K., Penninger, J. M., Ohashi, P. S., and Yeh, W. C. (2003). IL-1 receptor-associated kinase 4 is essential for IL-18-mediated NK and Th1 cell responses. *J Immunol*, 170(8), 4031-4035.
- Suzuki, N., Suzuki, S., Duncan, G. S., Millar, D. G., Wada, T., Mirtsos, C., Takada, H., Wakeham, A., Itie, A., Li, S., Penninger, J. M., Wesche, H., Ohashi, P. S., Mak, T. W., and Yeh, W. C. (2002). Severe impairment of interleukin-1 and Toll-like receptor signalling in mice lacking IRAK-4. *Nature*, 416(6882), 750-756.
- Szklarczyk, D., Franceschini, A., Wyder, S., Forslund, K., Heller, D., Huerta-Cepas, J., Simonovic, M., Roth, A., Santos, A., Tsafou, K. P., Kuhn, M., Bork, P., Jensen, L. J., and von Mering, C. (2015). STRING v10: protein-protein interaction networks, integrated over the tree of life. *Nucleic Acids Res*, 43(Database issue), D447-452.
- Takeuchi, O., Hoshino, K., Kawai, T., Sanjo, H., Takada, H., Ogawa, T., Takeda, K., and Akira, S. (1999). Differential roles of TLR2 and TLR4 in recognition of gram-negative and gram-positive bacterial cell wall components. *Immunity*, 11(4), 443-451.
- Taniguchi, T., Ogasawara, K., Takaoka, A., and Tanaka, N. (2001). IRF family of transcription factors as regulators of host defense. *Annu Rev Immunol*, 19, 623-655.
- Tebar, M., de Jong, F. H., and Sanchez-Criado, J. E. (2000). Regulation of inhibin/activin subunits and follistatin mRNA expression in the rat pituitary at early estrus. *Life Sci*, 67(21), 2549-2562.
- Teichmann, S. A., and Chothia, C. (2000). Immunoglobulin superfamily proteins in *Caenorhabditis elegans*. *J Mol Biol*, 296(5), 1367-1383.
- Thomas, J. A., Allen, J. L., Tsen, M., Dubnicoff, T., Danao, J., Liao, X. C., Cao, Z., and Wasserman, S. A. (1999). Impaired cytokine signaling in mice lacking the IL-1 receptor-associated kinase. *J Immunol*, 163(2), 978-984.
- Tian, D. S., Xie, M. J., Yu, Z. Y., Zhang, Q., Wang, Y. H., Chen, B., Chen, C., and Wang, W. (2007). Cell cycle inhibition attenuates microglia induced inflammatory response and alleviates neuronal cell death after spinal cord injury in rats. *Brain Res*, 1135(1), 177-185.
- Tizard, I. R. (2013). *Veterinary Immunology* (9th ed. ed.). St. Louis, Mo.: Elsevier.
- Trapnell, C., Hendrickson, D. G., Sauvageau, M., Goff, L., Rinn, J. L., and Pachter, L. (2013). Differential analysis of gene regulation at transcript resolution with RNA-seq. *Nat Biotechnol*, 31(1), 46.
- Trapnell, C., Roberts, A., Goff, L., Pertea, G., Kim, D., Kelley, D. R., Pimentel, H., Salzberg, S. L., Rinn, J. L., and Pachter, L. (2012). Differential gene and transcript expression analysis of RNA-seq experiments with TopHat and Cufflinks. *Nat. Protocols*, 7(3), 562-578.
- Trapnell, C., Williams, B. A., Pertea, G., Mortazavi, A., Kwan, G., van Baren, M. J., Salzberg, S. L., Wold, B. J., and Pachter, L. (2010). Transcript assembly and

- quantification by RNA-Seq reveals unannotated transcripts and isoform switching during cell differentiation. *Nat Biotechnol*, 28(5), 511-515.
- Traub-Dargatz, J. L., Salman, M. D., and Voss, J. L. (1991). Medical problems of adult horses, as ranked by equine practitioners. *J Am Vet Med Assoc*, 198(10), 1745-1747.
- Troedsson, M. (1997). Therapeutic considerations for mating-induced endometritis. *Pferdeheilkunde*, 13(5), 516-520.
- Troedsson, M. (1999). Uterine clearance and resistance to persistent endometritis in the mare. *Theriogenology*, 52(3), 461-471.
- Troedsson, M. (2006). Breeding-induced endometritis in mares. *Veterinary Clinics of North America: Equine Practice*, 22(3), 705-712.
- Troedsson, M., Alghamdi, A., and Mattisen, J. (2002). Equine seminal plasma protects the fertility of spermatozoa in an inflamed uterine environment. *Theriogenology*, 58(2-4), 453-456.
- Troedsson, M., Lee, C., Franklin, R., and Crabo, B. (1999). The role of seminal plasma in post-breeding uterine inflammation. *Journal of reproduction and fertility. Supplement*(56), 341-349.
- Troedsson, M., and Liu, I. (1991). Uterine clearance of non-antigenic markers (51Cr) in response to a bacterial challenge in mares potentially susceptible and resistant to chronic uterine infections. *Journal of reproduction and fertility. Supplement*, 44, 283-288.
- Troedsson, M., Liu, I., Ing, M., Pascoe, J., and Thurmond, M. (1993a). Multiple site electromyography recordings of uterine activity following an intrauterine bacterial challenge in mares susceptible and resistant to chronic uterine infection. *Journal of reproduction and fertility*, 99(2), 307-313.
- Troedsson, M., Liu, I., and Thurmond, M. (1993b). Function of uterine and blood-derived polymorphonuclear neutrophils in mares susceptible and resistant to chronic uterine infection: phagocytosis and chemotaxis. *Biology of reproduction*, 49(3), 507-514.
- Troedsson, M., Liu, I., and Thurmond, M. (1993c). Immunoglobulin (IgG and IgA) and complement (C3) concentrations in uterine secretion following an intrauterine challenge of *Streptococcus zooepidemicus* in mares susceptible to versus resistant to chronic uterine infection. *Biology of reproduction*, 49(3), 502-506.
- Troedsson, M., Loset, K., Alghamdi, A., Dahms, B., and Crabo, B. (2001a). Interaction between equine semen and the endometrium: the inflammatory response to semen. *Animal reproduction science*, 68(3), 273-278.
- Troedsson, M. H., and Woodward, E. M. (2016). Our current understanding of the pathophysiology of equine endometritis with an emphasis on breeding-induced endometritis. *Reprod Biol*, 16(1), 8-12.
- Troedsson, M. H. T., Ababneh, M. M., Ohlgren, A. F., Madill, S., Vetscher, N., and Gregas, M. (2001b). Effect of periovulatory prostaglandin F2 α on pregnancy rates and luteal function in the mare. *Theriogenology*, 55(9), 1891-1899.
- Troedsson, M. H. T., and Ricketts, S. (2007). Fertility Expectations and Management for Optimal Fertility. In J. C. Samper, J. F. Pycoc, & A. O. McKinnon (Eds.), *Current Therapy in Equine Reproduction* (pp. 53-69). St. Louis, Missouri: St. Louis, Missouri : Elsevier Saunders.
- Tunon, A. M., Rodriguez-Martinez, H., Haglund, A., Albihn, A., Magnusson, U., and Einarsson, S. (1995). Ultrastructure of the secretory endometrium during oestrus in young maiden and foaled mares. *Equine Vet J*, 27(5), 382-388.
- Tusell, J. M., Saura, J., and Serratosa, J. (2005). Absence of the cell cycle inhibitor p21Cip1 reduces LPS-induced NO release and activation of the transcription factor NF-kappaB in mixed glial cultures. *Glia*, 49(1), 52-58.
- Ueno, N., Ling, N., Ying, S. Y., Esch, F., Shimasaki, S., and Guillemin, R. (1987). Isolation and partial characterization of follistatin: a single-chain Mr 35,000 monomeric protein that inhibits the release of follicle-stimulating hormone. *Proceedings of the National Academy of Sciences of the United States of America*, 84(23), 8282-8286.

- Underhill, D. M., and Ozinsky, A. (2002). Phagocytosis of microbes: complexity in action. *Annu Rev Immunol*, 20, 825-852.
- Vanderwall, D. K. (2011). Progesterone. In A. O. McKinnon, S. E. L., E. Vaala, & D. D. Varner (Eds.), *Equine Reproduction* (Vol. 2, pp. 1637-1641). Philadelphia, London: Wiley-Blackwell.
- Veldhoen, M. (2017). Interleukin 17 is a chief orchestrator of immunity. *Nat Immunol*, 18(6), 612-621.
- Wagener, K., Gabler, C., and Drillich, M. (2017). A review of the ongoing discussion about definition, diagnosis and pathomechanism of subclinical endometritis in dairy cows. *Theriogenology*, 94, 21-30.
- Wagner, B. (2006). Immunoglobulins and immunoglobulin genes of the horse. *Dev Comp Immunol*, 30(1-2), 155-164.
- Walton, K. L., Makanji, Y., and Harrison, C. A. (2012). New insights into the mechanisms of activin action and inhibition. *Mol Cell Endocrinol*, 359(1-2), 2-12.
- Wang, Y., Ristevski, S., and Harley, V. R. (2006). SOX13 exhibits a distinct spatial and temporal expression pattern during chondrogenesis, neurogenesis, and limb development. *J Histochem Cytochem*, 54(12), 1327-1333.
- Wang, Z., Gerstein, M., and Snyder, M. (2009). RNA-Seq: a revolutionary tool for transcriptomics. *Nature Reviews Genetics*, 10(1), 57-63.
- Warner, N., and Nunez, G. (2013). MyD88: a critical adaptor protein in innate immunity signal transduction. *J Immunol*, 190(1), 3-4.
- Wathes, D. C., Cheng, Z., Fenwick, M. A., Fitzpatrick, R., and Patton, J. (2011). Influence of energy balance on the somatotrophic axis and matrix metalloproteinase expression in the endometrium of the postpartum dairy cow. *Reproduction*, 141(2), 269-281.
- Watson, E. (1998). Reproduction. In T. Mair, S. Love, J. Schumacher, & E. Watson (Eds.), *Equine Medicine, Surgery and Reproduction* (pp. 278-309). London: London : W.B. Saunders.
- Watson, E., Pedersen, H. G., Thomson, S., and Fraser, H. (2000). Control of follicular development and luteal function in the mare: effects of a GnRH antagonist. *Theriogenology*, 54(4), 599-609.
- Watson, E., Stokes, C., David, J., and Bourne, F. (1987). Effect of ovarian hormones on promotion of bactericidal activity by uterine secretions of ovariectomized mares. *Journal of reproduction and fertility*, 79(2), 531-537.
- Watson, E. D. (2000). Post-breeding endometritis in the mare. *Animal reproduction science*, 60, 221-232.
- Weber, A., Wasiliew, P., and Kracht, M. (2010). Interleukin-1 (IL-1) pathway. *Sci Signal*, 3(105), cm1.
- Wegner, M. (1999). From head to toes: the multiple facets of Sox proteins. *Nucleic Acids Res*, 27(6), 1409-1420.
- Wesche, H., Gao, X., Li, X., Kirschning, C. J., Stark, G. R., and Cao, Z. (1999). IRAK-M is a novel member of the Pelle/interleukin-1 receptor-associated kinase (IRAK) family. *J Biol Chem*, 274(27), 19403-19410.
- Williams, A. G., Thomas, S., Wyman, S. K., and Holloway, A. K. (2014). RNA-seq Data: Challenges in and Recommendations for Experimental Design and Analysis. *Current protocols in human genetics*, 83, 11.13.11-11.13.20.
- Williamson, P., Dunning, A., O'Connor, J., and Penhale, W. (1983). Immunoglobulin levels, protein concentrations and alkaline phosphatase activity in uterine flushings from mares with endometritis. *Theriogenology*, 19(3), 441-448.
- Woessner, J. F., Jr. (1991). Matrix metalloproteinases and their inhibitors in connective tissue remodeling. *Faseb j*, 5(8), 2145-2154.
- Wonfor, R., Natoli, M., Parveen, I., Beckman, M., Nash, R., and Nash, D. (2017). Anti-inflammatory properties of an extract of *M. ilicifolia* in the human intestinal epithelial Caco-2 cell line. *J Ethnopharmacol*, 209, 283-287.
- Woodward, E., Christoffersen, M., Campos, J., Squires, E., and Troedsson, M. (2012). Susceptibility to persistent breeding-induced endometritis in the mare: relationship

- to endometrial biopsy score and age, and variations between seasons. *Theriogenology*, 78(3), 495-501.
- Woodward, E., and Troedsson, M. (2015). Inflammatory mechanisms of endometritis. *Equine veterinary journal*, 47(4), 384-389.
- Woodward, E. M., Christoffersen, M., Campos, J., Betancourt, A., Horohov, D., Scoggin, K. E., Squires, E. L., and Troedsson, M. H. (2013). Endometrial inflammatory markers of the early immune response in mares susceptible or resistant to persistent breeding-induced endometritis. *Reproduction*, 145(3), 289-296.
- Woodward, E. M., and Troedsson, M. H. (2013). Equine breeding-induced endometritis: a review. *Journal of Equine Veterinary Science*, 33(9), 673-682.
- Wouters, M. A., Rigoutsos, I., Chu, C. K., Feng, L. L., Sparrow, D. B., and Dunwoodie, S. L. (2005). Evolution of distinct EGF domains with specific functions. *Protein Sci*, 14(4), 1091-1103.
- Wright, M. F., Sayre, B., Keith Inskip, E., and Flores, J. A. (2001). Prostaglandin F2 α Regulation of the Bovine Corpus Luteum Endothelin System During the Early and Midluteal Phase1. *Biology of reproduction*, 65(6), 1710-1717.
- Zavy, M. T., Bazer, F. W., Sharp, D. C., Frank, M., and Thatcher, W. W. (1978). Uterine luminal prostaglandin F in cycling mares. *Prostaglandins*, 16(4), 643-650.
- Zent, W. W., Troedsson, M. H., and Xue, J.-L. (1998). *Postbreeding uterine fluid accumulation in a normal population of Thoroughbred mares: a field study*. Paper presented at the Proc Am Assoc Equine Pract.
- Zerbe, H., Schuberth, H. J., Engelke, F., Frank, J., Klug, E., and Leibold, W. (2003). Development and comparison of in vivo and in vitro models for endometritis in cows and mares. *Theriogenology*, 60(2), 209-223.
- Zheng, W., Jimenez-Linan, M., Rubin, B. S., and Halvorson, L. M. (2007). Anterior Pituitary Gene Expression with Reproductive Aging in the Female Rat1. *Biology of reproduction*, 76(6), 1091-1102.
- Zhou, H., Yu, M., Fukuda, K., Im, J., Yao, P., Cui, W., Bulek, K., Zepp, J., Wan, Y., Kim, T. W., Yin, W., Ma, V., Thomas, J., Gu, J., Wang, J. A., DiCorleto, P. E., Fox, P. L., Qin, J., and Li, X. (2013). IRAK-M mediates Toll-like receptor/IL-1R-induced NFkappaB activation and cytokine production. *Embo j*, 32(4), 583-596.
- Zhou, X., Lindsay, H., and Robinson, M. D. (2014). Robustly detecting differential expression in RNA sequencing data using observation weights. *Nucleic Acids Res*, 42(11), e91.

Appendix 3.1

Progesterone ELISA

The progesterone ELISA kit (EIA 1561, DRG Diagnostics) determined the progesterone concentration in blood serum. The kit contained one pre-treated 96 wells plate coated with anti-progesterone antibody, 7 standard vials ready to use in concentrations of 0; 0.3; 1.25; 2.5; 5; 15; 40 ng/mL, enzyme conjugate ready to use, substrate solution ready to use, stop solution ready to use and a 40 x concentrated wash solution. Thirty millilitres of 40x concentrated wash solution was diluted in 1170 mL deionized water. Reagents were allowed to reach room temperature before use and were mixed without foaming. Pregnant mare serum was used as a positive control, and male horse serum was used as a negative control.

The plate was snapped to the number of wells needed and secured in the holder. In duplicate, 25 μ L of standards, 25 μ L of samples and 25 μ L of controls were dispensed into wells and incubated for 5 minutes at room temperature. Two hundred microliters of enzyme conjugate were dispensed into each well and the plate was covered using a plate sealer cover. The plate was incubated on a rocker (Scientific Gyro rocker Stuart, Z316520, Sigma, UK) for 60 minutes at room temperature. Contents were shaken out, wells were washed with 400 μ L of diluted wash solution three times and wells were stroke sharply on absorbent paper. A volume of 200 μ L of substrate solution was dispensed into each well and the plate was covered again. The plate was incubated on a rocker for 15 minutes at room temperature in the dark. The reaction was stopped by adding 100 μ L of stop solution to each well.

Within 10 minutes of adding the stop solution, the plate was read. The absorbance of each well at 450 \pm 10 nm was determined using a plate reader (iMark Microplate Absorbance Reader, Bio-Rad, UK). The concentration (ng/mL) values for each standard, controls and samples were exported.

Appendix 3.2

Buffers and Reagents for Histology and Tissue Culture

Haematoxylin and Eosin for Histology

Harris Haematoxylin was made up by adding 1 g of haematoxylin (H9627, Sigma, UK) in 10 mL of absolute ethanol, and was then added to a previously dissolved 20 g of aluminium potassium sulphate (11443713, Fisher, UK) in 200 mL of warm distilled water. The mixture was brought to boil and 0.5 g of mercuric oxide (203793, Sigma, UK) was added. The solution was rapidly cooled and 4 mL of acetic acid was added to improve nuclear selectivity. Alcoholic Eosin was made up by adding 1 g of eosin (E4009, Sigma, UK) in 100 mL 70 % ethanol.

Epidermal Growth Factor Stock

A vial of 50 µg Epidermal Growth Factor (10605-HNAE-250, Life Technologies, UK) was reconstituted by adding 1000 µL of sterile water, resulting in a final concentration of 50 µg/mL. The solution was stored in 100 µL aliquots at -20 °C.

Neomycin and Streptomycin Stock

A 10 mg/mL stock solution of neomycin trisulfate salt hydrate (N6386, Sigma, UK) and streptomycin sulfate salt (S6501, Sigma, UK) was prepared. By using a high precision balance, 1 g of neomycin and 1 g of streptomycin were weighed into a beaker. Distilled water was added to the beaker until the final weight was 100 g. The solution was stirred until the powder was completely dissolved and then filtered through a 0,22 µg filter. The solution was stored in 5 mL aliquots at -20°C.

Appendix 3.3

Prostaglandin F_{2α} Radioimmunoassay

Chemicals and Reagents

Tris Buffer (0.05M)

One gram of gelatin (440454B, BDH) was dissolved in 200 mL distilled water by stirring at 50 °C. To this 0.2 g sodium azide (S-8032, Sigma, UK), 6.61 g Tris HCl (T-3253, Sigma, UK), 0.97 g Tris base (T-1503, Sigma, UK) were added and solution was made up to 1 L with distilled water. The pH was adjusted to 7.4 by adding 1 M HCl or 10 % NaOH when necessary.

Dextran-coated charcoal suspension

In 190 mL distilled water 0.8 g dextran (3190, Sigma, UK) was dissolved and stirred for 20 minutes. To this, 4.0 g of activated charcoal (C404053, Fisher, UK) was added and the suspension was stirred for approximately 20 minutes. The suspension was made up to 200 mL with distilled water and stored at 4 °C for up to 14 days. The suspension was thoroughly stirred before each use.

Tracer

To achieve the working concentration of 10000-12000 counts per minute (cpm) per mL, 10 µL PGF_{2α} tracer (NET433250UC, Perkin Elmer, UK) was added into 1990 µL Tris buffer. The tracer solution was read as cpm to find the final concentration. If the concentration was lower than the 10000-12000 cpm expected, more tracer was added to it until the solution reached the final working concentration.

Antiserum

A standard dilution of antiserum was performed to discover which solution produces 30 % binding of tracer when non-radioactive PGF_{2α} is present. Firstly, a 1:100 dilution of antiserum was made up by adding 100 µL antiserum to 9900 µL Tris buffer and aliquots were stored at -20 °C. A 1:2 serial dilution of the 1:100 diluted antiserum was then performed. Five hundred microliters of tris buffer were added to

8 different tubes. From the 1:100 diluted antiserum, 500 μ L was taken and added to the next tube and mixed by pipetting, giving a 1:2000 dilution. This procedure was repeated for each tube in sequence, by removing 500 μ L each time to perform a serial dilution. The final concentrations of antiserum were: 1:1000, 1:2000, 1:8000, 1:16000, 1:32000, 1:64000, 1:128000, 1:256000. Antisera were a kind gift from Professor N Poyser (University of Edinburgh, Edinburgh, Scotland, UK) and Professor Claire Wathes (Royal Veterinary College, London, UK).

PGF_{2 α} Standards

A 1 mg/mL stock solution was made up by adding 1 mL absolute ethanol to a 1 mg vial of PGF_{2 α} (P0314-1MG, Sigma, UK). A 1 μ g/mL standard solution was made up by adding 100 μ L of 1 mg/mL solution to 99.9 mL tris buffer and aliquots were stored at -20 °C until needed. A 2 mL of 10 ng/mL standard solution was performed by adding 20 μ L of 1 μ g/mL solution to 1980 μ L tris buffer (1:100 dilution). The standards were made up in tubes as per table and were kept at 4 °C for up to 15 days. One standard curve was needed for each centrifugation.

Standard Concentration (ng/mL)	Volume of 10 ng/mL standard (μ L)	Volume of Tris Buffer (μ L)
5 (1:2)	500	500
2.50 (1:4)	250	750
1.00 (1:10)	100	900
0.50 (1:20)	50	950
0.25 (1:40)	25	975
0.10 (1:100)	10	990
0.05 (1:200)	5	995
0.025 (1:400)	2.5	997.5

Assay Procedure

Each standard/sample was run in triplicate. Tubes (11778908, Fisher, UK) were TC (total count), NSB (Buffer blank), TB (total binding), Std (standard), QC (quality check) and Tests (sample), and volumes of each reagent were added as per crib sheet.

Reagents	TC	NSB	TB	Std	QC	Tests
Standards	-	-	-	100 µl	-	-
Sample	-	-	-	-	100 µl	100 µl
Buffer	500 µl	300 µl	200 µl	100 µl	100 µl	100 µl
Antiserum	-	-	100 µl	100 µl	100 µl	100 µl
Tracer	100 µl	100 µl	100 µl	100 µl	100 µl	100 µl

Tubes were vortexed and incubated at 4 °C for 16-24 hours. Two hundred microliters of charcoal dextran solution were added to each tube except total count. Tubes were vortexed, incubated for 10 mins at 4 °C and centrifuged at 1000-1500 g at 4 °C. Supernatant was decanted into labelled 6 mL scintillation tubes (E1412-7000, Star Lab, UK), 4 mL of scintillation liquid (1200-436, Optiphase HiSafe, Perkin Elmer, UK) was added to each tube and tubes were shaken to mix throughout. Count as counts per minute (cpm) for 2 mins was performed for each tube.

Calculation

Normalised percent bound for each standard/sample was gained with the following equation:

$$\%B/B_0 = \frac{(standard\ or\ sample\ cpm - NSB\ cpm)}{(B_0\ cpm - NSB\ cpm)} \times 100\%$$

A standard curve was generated by plotting the normalised percent bound as a function of the log₁₀ PGF_{2α} concentrations.

Appendix 3.4

RNA Extraction

The GeneJET RNA purification kit (K0731, GeneJET RNA Purification Kit, Thermo Scientific, UK) was used to purify total RNA cultured tissue. The kit contained Proteinase K, Lysis buffer, Wash buffer 1 concentrated, wash buffer 2 concentrated, nuclease-free water, GeneJET RNA purification columns pre-assembled with collection tubes, 2 mL collection tubes and 1.5 mL collection tubes. Components were stored at room temperature and proteinase K was stored at -20 °C after being opened.

Fifty millilitres of 96-100 % ethanol was added to Wash Buffer 1, and 170 mL of ethanol was added to Wash Buffer 2. The required amount of Lysis buffer was supplemented with 20 µl β-mercaptoethanol (M6250, Sigma, UK) for each 1 mL volume of Lysis buffer. Proteinase K was diluted by adding 10 µl to 590 µL of TE buffer (10 mM Tris HCl, pH 8.0, 1 mM EDTA).

Up to 30 mg of fresh or frozen tissue was placed in a safe lock tube (0030123328, Fisher, UK) containing 300 µL of supplemented lysis buffer and a stainless steel bead (69989, 5mm, Qiagen, UK). The tissue was immediately disrupted using a rotor-stator homogenizer (TissueLyser LT, 85600, Qiagen, UK) until the suspension was uniform. Tubes containing the lysate and the beads were centrifuged for 2 minutes at 12000 x g to pellet any cell debris. Supernatant was transferred to another RNA/DNase free tube (11598252, Fisher, UK). Six hundred microliters of diluted Proteinase K was added to each tube, vortexed and incubated at 15-25 °C for 10 minutes. After incubation, tubes were centrifuged for 10 min at $\geq 12000 \times g$ and supernatant was transferred into a new RNase-free microcentrifuge tube. Four hundred and fifty microliters of ethanol (96-100%) were added to each tube and mixed by pipetting.

Up to 700 µL of lysate was transferred to the GeneJET RNA Purification Column inserted in a collection tube. The column was centrifuged for 1 min at 12000 x g. The flow-through was discarded and the purification column was placed back in the collection tube. This procedure was repeated until all lysate was transferred into the column and centrifuged, then the collection tube containing the flow-through solution

was discarded. The RNA purification column was placed into a new 2 mL collection tube. Seven hundred microliters of wash buffer 1 (supplemented with ethanol) were added to the RNA purification column and centrifuged for 1 min at 12000 x g. The flow-through was discarded and the purification column was placed back into the collection tube. Six hundred microliters of wash buffer 2 (supplemented with ethanol) were added into the RNA purification column and centrifuged for 1 min at 12000 x g. The flow-through was discarded and the purification column was placed back into the collection tube. Two hundred and fifty microliters of wash buffer 2 (supplemented with ethanol) were added to the purification column and centrifuged for 2 min at 12000 x g. If residual solution was seen in the purification column, the collection tube was emptied and the column was centrifuged again for 1 min at maximum speed. Finally, the collection tube containing the flow-through solution was discarded and the purification column was transferred to a sterile 1.5 mL RNA-se free micro centrifuge tube. A hundred microliter of nuclease/rnase-free water was added to the centre of the RNA purification column membrane and centrifuged for 1 min at 12000 x g to elute RNA. The purification column was discarded and the extracted RNA was stored at -80 °C until use.

Appendix 3.5

Computer code

Quality check, mapping the reads to the reference genome and total counts of RNA-Sequencing data

Quality control of raw reads

```
> module load fastqc/0.11.2
> fastqc -o ../output_folder -t 4 --extract <rawfastq_forward_read>.fq
> fastqc -o ../output_folder -t 4 --extract <rawfastq_reverse_read>.fq
```

Map reads to the reference genome

```
# TopHat requires Bowtie to map the reads to the reference genome
# Bowtie needs the genome to be indexed
```

```
> module load bowtie/2.2.3
```

```
# -f specifies that the genome is in fasta format file
# INDEX is the prefix chosen to all files that will be written by
Bowtie
```

```
> bowtie2-build -f <genome>.fa <genome>.INDEX
```

```
> module load tophat/2.0.14
> module load samtools/0.1.19
```

```
# tophat -p 8 -G <annotationfile>.gtf -o ../output_directory
<genome.INDEX> <rawfastq_forward_read>.fq <rawfastq_reverse_read>.fq
```

```
> tophat -p 8 -G annotationfile.gtf -o ../output_directory genome.INDEX
sample1_R1.fastq sample2_R2.fastq
```

FeatureCounts

```
> module load subread/1.5.2
```

```
# featureCounts -p <for paired reads> -t <specifies feature in
annotation file> -g <specifies attribute type in annotation file>
-a <annotation_file> -o <output_file> input_file1 [input_file2] ...
```

```
> featureCounts -p -t exon -g gene_id -a annotationfile.gtf -o outputfile
sample1.bam sample2.bam sample3.bam ...
```

Appendix 4.1

Kenney Classification of Mares Providing Endometrial Explants in Chapter 4

Mares	Histology report ^b	Kenney classification
1	Medium epithelium. Stratum compactum examined, no pathologic findings noted. Stratum spongiosum showed difuse grade 1 fibrosis.	I
2	Medium epithelium. Stratum compactum showed lymphocyte focal infiltration grade 1. Stratum spongiosum examined, no pathologic findings noted.	I
3	Medium epithelium. Stratum compactum examined, no pathologic findings noted. Stratum spongiosum showed focal cystic glands grade 1.	I
4	Tall epithelium. Stratum compactum showed diffuse gland atrophy grade 1. Stratum spongiosum showed diffuse gland atrophy grade 2, multifocal cystic glands grade 3 with inspissated contents, fibrosis periglandular grade 3 and lymphocyte infiltration grade 1.	II
5	Tall epithelium. Stratum compactum showed lymphocyte infiltration grade 1. Stratum spongiosum showed focal cystic glands grade 1.	I
6	Medium epithelium. Stratum compactum showed lymphocyte infiltration grade 1, macrophage and erythrophagocytes infiltration grade 2. Stratum spongiosum showed lymphocyte infiltration grade 1, macrophage and erythrophagocytes infiltration grade 2 and siderocyte infiltration grade 1.	I
7	Tall epithelium. Stratum compactum showed focal lymphocyte infiltration grade 1. Stratum spongiosum examined, no pathologic findings noted.	I
8	Stratum compactum showed infiltration of macrophages and erythrophagocytes grade 3. Stratum spoingiosum showed focal cystic glands grade 1, focal periglandular fibrosis grade 1 and infiltration of macrophages and erythrophagocytes grade 1.	I

^a Grade 1 = minimal/very few/very small. Grade 2 = slight/few/small. Grade 3 = moderate/moderate number/moderate size. Grade 4 = marked/many/large.

Appendix 4.2

Computer Codes used in Chapter 4

Trimmomatic script for each sample

```
> module load java/jdk1.7.0_40

# java -jar <path to trimmomatic jar> paired-end PE [-threads
<threads>] [-phred33 | -phred64] <input_forward_read>.fq
<input_reverse_read>.fq <output_forward_paired>.fq
<output_forward_unpaired>.fq <output_reverse_paired>.fq
<output_reverse_unpaired>.fq

> java -jar ../trimmomatic/0.33/trimmomatic-0.33.jar PE -threads 2
-phred33 sample1_R1.fastq sample1_R2.fastq sample1_R1_trim.p.fastq
sample1_R1_trim.unp.fastq sample1_R2_trim.p.fastq
sample1_R2_trim.unp.fastq ILLUMINACLIP:/cm/shared/apps/trimmomatic/
0.33/adapters/TruSeq3-PE-2.fa:2:30:10 LEADING:30 TRAILING:30
SLIDINGWINDOW:4:30 MINLEN:100 HEADCROP:10
```

Tuxedo analysis

Cufflinks

```
> module load cufflinks/2.2.1

# for each sample
# -p -o <output_directory> <sample_accepted_hits>.bam
> cufflinks -p 6 -o ../sample1_output_directory sample1_accepted_hits.bam
> cufflinks -p 6 -o ../sample2_output_directory sample2_accepted_hits.bam
...
> cufflinks -p 6 -o ../sample2_output_directory
sample32_accepted_hits.bam

# create a file called assemblies.txt that lists the assembly file
created by TopHat for each sample. The file should contain the following
lines:
../sample1/transcripts.gtf
../sample2/transcripts.gtf
../sample3/transcripts.gtf
...
../sample32/transcripts.gtf

# run cuffmerge on all assemblies to create a single merged
transcriptome annotation

> cuffmerge -o ../output_folder_merged -g annotation.gtf -s genome.fasta
-p 8 assemblies.txt
```

Cuffdiff sample to sample analysis

```
> module load cufflinks/2.2.1

# -o <output_directory> -b <genome>.fa -L <labels> -u <cuffmerge>.gtf
<sample1_acceptedhits>.bam <sample2_acceptedhits>.bam ...

> cuffdiff -o ../output_directory -b genome.fasta -p 8 -L \
M1_0h,M1_24h,M1_48h,M1_72h,M2_0h,M2_24h,M2_48h,M2_72h,M3_0h,M3_24h,M3_4
8h,M3_72h,M4_0h,M4_24h,M4_48h,M4_72h,M5_0h,M5_24h,M5_48h,M5_72h,M6_0h,M
6_24h,M6_48h,M6_72h,M7_0h,M7_24h,M7_48h,M7_72h,M8_0h,M8_24h,M8_48h,M8_7
2h -u merged.gtf sample1_accepted_hits.bam \

sample2_accepted_hits.bam sample3_accepted_hits.bam ... \
sample32_accepted_hits.bam
```

Cuffdiff time-point analysis

```
> module load cufflinks/2.2.1

# -o <output_directory> -b <genome>.fa -L <labels> -u <cuffmerge>.gtf

> cuffdiff -o ../output_directory -b genome.fasta -p 8 -L
Time0h,Time24h,Time48h,Time72h -u merged.gtf \
sample1_accepted_hits.bam,sample5_accepted_hits.bam,sample9_accepted_hi
ts.bam,sample13_accepted_hits.bam,sample21_accepted_hits.bam,sample29_a
ccepted_hits.bam \
sample2_accepted_hits.bam,sample6_accepted_hits.bam,sample10_accepted_h
its.bam,sample14_accepted_hits.bam,sample22_accepted_hits.bam,sample30_
accepted_hits.bam \
sample3_accepted_hits.bam,sample7_accepted_hits.bam,sample11_accepted_h
its.bam,sample15_accepted_hits.bam,sample23_accepted_hits.bam,sample31_
accepted_hits.bam \
sample3_accepted_hits.bam,sample7_accepted_hits.bam,sample11_accepted_h
its.bam,sample15_accepted_hits.bam,sample23_accepted_hits.bam,sample31_
accepted_hits.bam \
```

DESeq2 analysis

```
# load package to summarize bam files
> library(GenomicAlignments)

# put bam files together in a list
bamfilelist <-c("sample1.bam", "sample2.bam", "sample3.bam, ...
sample28.bam")

#BamFileList from Rsamtools provides an R interface to BAM files
> library(Rsamtools)
> bamfiles <- BamFileList(bamfilelist)

# use annotation file with the function makeTxDbFromGFF from
GenomicFeatures
# list of exons grouped by gene for counting read/fragments
> library(GenomicFeatures)
> txdb <- makeTxDbFromGFF("annotationfile.gtf", format="gtf")
```

```

# produce a GRangesList of all the exons grouped by gene
> ebg <- exonsBy(txdb, by="gene")

# summarizeOverlaps from GenomicAlignment counts the fragments/reads
and produces a SummarizedExperiment object 'se'
> se <- summarizeOverlaps(features=ebg, reads=bamfiles,
                           mode="Union",
                           singleEnd=FALSE,
                           ignore.strand=TRUE,
                           fragments=TRUE )

# metadata file created in excel (info about the experiment)
> sampleTable <- read.csv("exp1_metadata.csv")

# assign the sampleTable as the colData of the summarized experiment by
converting it into a DataFrame
> colData(se) <- DataFrame(sampleTable)
> colData(se)
DataFrame with 28 rows and 3 columns
      sample timepoint horse
      <factor>   <factor> <factor>
1 sample1.bam,control0h,1
2 sample2.bam,time24h,1
3 sample3.bam,time48h,1
4 sample4.bam,time72h,1
5 sample5.bam,control0h,2
6 sample6.bam,time24h,2
7 sample7.bam,time48h,2
8 sample8.bam,time72h,2
9 sample9.bam,control0h,3
10 sample10.bam,time24h,3
11 sample11.bam,time48h,3
12 sample12.bam,time72h,3
13 sample13.bam,control0h,4
14 sample14.bam,time24h,4
15 sample15.bam,time48h,4
16 sample16.bam,time72h,4
17 sample17.bam,control0h,5
18 sample18.bam,time24h,5
19 sample19.bam,time48h,5
20 sample20.bam,time72h,5
21 sample21.bam,control0h,6
22 sample22.bam,time24h,6
23 sample23.bam,time48h,6
24 sample24.bam,time72h,6
25 sample25.bam,control0h,7
26 sample26.bam,time24h,7
27 sample27.bam,time48h,7
28 sample28.bam,time72h,7

# DESeq2 - differential analysis
# SummarizedExperiment 'se' created before will be used for DESeq2
# nbinomLRT() function to test for the significance of multiple
coefficients at once
> library(DESeq2)
> ddsLRT <- DESeqDataSet(se, design = ~ horse + timepoint)
> ddsLRT <- estimateSizeFactors(ddsLRT)
> ddsLRT <- estimateDispersions(ddsLRT)
> ddsLRT <- nbinomLRT(ddsLRT, reduced = ~ horse)
> resLRTA <- results(ddsLRT)
> summary(resLRT)
> write.csv(resLRT, "resLRTExp1.csv")

# dispersion-mean plot
> plotDispEsts(ddsLRT, main="Estimation of dispersion", sub="For
Likelihood ratio test object")

# calc of size factors
> sizeFactors(dds)

```



```

# normalize data to produce PCA plot
> rld <- rlog(ddsLRT, blind=FALSE)
> pcaData <- plotPCA(rld, intgroup = c("timepoint", "horse"),
returnData = TRUE)
> percentVar <- round(100 * attr(pcaData, "percentVar"))
> library("ggplot2")
> ggplot(pcaData, aes(x = PC1, y = PC2, color = timepoint, shape =
horse)) + geom_point(size = 3) + xlab(paste0("PC1: ", percentVar[1], "%
variance")) + ylab(paste0("PC2: ", percentVar[2], "%variance")) +
coord_fixed() + scale_shape_manual(values=seq(0, 8))

#DESeq2 analysis of normal data

> dds <- DESeqDataSet(se, design = ~ horse + timepoint)
> dds <- DESeq(dds)
> resultsNames(dds)
> plotDispEsts(dds, main="Estimation of dispersion", sub="For DESeq2
object")

#'contrast' argument to extract comparisons of different levels
# contrast = c('factorName','numeratorLevel','denominatorLevel')
> res_0hand24h <- results(dds, contrast=c("timepoint", "control0h",
"time24h"))
> res_24hand48h <- results(dds, contrast=c("timepoint", "time24h",
"time48h"))
> res_48hand72h <- results(dds, contrast=c("timepoint", "time48h",
"time72h"))

# save and export
> write.csv(res_0hand24h, "resWH5A_0hand24h.csv")
> write.csv(res_24hand48h, "resWH5A_24hand48h.csv")
> write.csv(res_48hand72h, "resWH5A_48hand72h.csv")

```

Appendix 4.3

List of all significantly enriched GO terms in Chapter 4 between 0 hours (control) and 72 hours – Cuffdiff results

Enrichment term	Term name	Gene count	FDR p-value
GOTERM_CC_DIRECT	GO:0070062~extracellular exosome	644	4.17×10^{-41}
GOTERM_CC_DIRECT	GO:0005925~focal adhesion	130	2.71×10^{-19}
GOTERM_CC_DIRECT	GO:0005737~cytoplasm	598	9.30×10^{-12}
GOTERM_CC_DIRECT	GO:0009897~external side of plasma membrane	68	3.73×10^{-10}
GOTERM_BP_DIRECT	GO:0007229~integrin-mediated signaling pathway	36	2.00×10^{-8}
GOTERM_BP_DIRECT	GO:0007155~cell adhesion	56	1.12×10^{-7}
GOTERM_BP_DIRECT	GO:0030335~positive regulation of cell migration	52	1.10×10^{-6}
GOTERM_CC_DIRECT	GO:0009986~cell surface	101	2.54×10^{-6}
GOTERM_CC_DIRECT	GO:0008305~integrin complex	16	9.44×10^{-6}
GOTERM_BP_DIRECT	GO:0001525~angiogenesis	44	4.70×10^{-5}
GOTERM_CC_DIRECT	GO:0045121~membrane raft	40	8.66×10^{-5}
GOTERM_MF_DIRECT	GO:0005524~ATP binding	276	9.12×10^{-5}
GOTERM_MF_DIRECT	GO:0005509~calcium ion binding	148	1.49×10^{-4}
GOTERM_BP_DIRECT	GO:0008284~positive regulation of cell proliferation	73	5.32×10^{-4}
GOTERM_CC_DIRECT	GO:0005829~cytosol	218	5.99×10^{-4}
GOTERM_CC_DIRECT	GO:0005783~endoplasmic reticulum	120	8.15×10^{-4}
GOTERM_CC_DIRECT	GO:0030027~lamellipodium	41	8.26×10^{-4}
GOTERM_BP_DIRECT	GO:0008285~negative regulation of cell proliferation	70	8.81×10^{-4}
GOTERM_BP_DIRECT	GO:0030198~extracellular matrix organization	31	0.001
GOTERM_CC_DIRECT	GO:0005634~nucleus	486	0.002
GOTERM_CC_DIRECT	GO:0005615~extracellular space	210	0.002
GOTERM_BP_DIRECT	GO:0008360~regulation of cell shape	40	0.003
GOTERM_BP_DIRECT	GO:0010628~positive regulation of gene expression	48	0.004
GOTERM_CC_DIRECT	GO:0005911~cell-cell junction	40	0.004
GOTERM_CC_DIRECT	GO:0005604~basement membrane	23	0.008
GOTERM_BP_DIRECT	GO:0034446~substrate adhesion-dependent cell spreading	19	0.009
GOTERM_BP_DIRECT	GO:0007160~cell-matrix adhesion	27	0.010
GOTERM_BP_DIRECT	GO:0033138~positive regulation of peptidyl-serine phosphorylation	27	0.010
GOTERM_BP_DIRECT	GO:0045766~positive regulation of angiogenesis	31	0.010
GOTERM_BP_DIRECT	GO:0048146~positive regulation of fibroblast proliferation	20	0.010

GOTERM_BP_DIRECT	GO:0043066~negative regulation of apoptotic process	66	0.011
GOTERM_MF_DIRECT	GO:0008201~heparin binding	35	0.013
GOTERM_BP_DIRECT	GO:0030155~regulation of cell adhesion	18	0.015
GOTERM_BP_DIRECT	GO:0043065~positive regulation of apoptotic process	45	0.018
GOTERM_BP_DIRECT	GO:0006954~inflammatory response	60	0.024
GOTERM_CC_DIRECT	GO:0048471~perinuclear region of cytoplasm	86	0.026
GOTERM_MF_DIRECT	GO:0046872~metal ion binding	186	0.027
GOTERM_MF_DIRECT	GO:0005178~integrin binding	12	0.029
GOTERM_BP_DIRECT	GO:0030154~cell differentiation	43	0.032
GOTERM_CC_DIRECT	GO:0005578~proteinaceous extracellular matrix	51	0.032
GOTERM_CC_DIRECT	GO:0043209~myelin sheath	46	0.036
GOTERM_BP_DIRECT	GO:0043123~positive regulation of I-kappaB kinase/NF-kappaB signaling	45	0.037
GOTERM_CC_DIRECT	GO:0001772~immunological synapse	17	0.038
GOTERM_BP_DIRECT	GO:0032496~response to lipopolysaccharide	30	0.043
GOTERM_CC_DIRECT	GO:0031012~extracellular matrix	33	0.046
GOTERM_BP_DIRECT	GO:0048008~platelet-derived growth factor receptor signaling pathway	14	0.049

Appendix 4.4

Clusters between 0 hours (control) and 72 hours

Annotation Cluster 1 - Enrichment Score: 5.99				
Category	Term	Count	PValue	FDR
UP_KEYWORDS	Integrin	19	9.93×10^{-9}	0.000
INTERPRO	IPR013649:Integrin alpha-2	14	7.54×10^{-7}	0.001
INTERPRO	IPR000413:Integrin alpha chain	14	7.54×10^{-7}	0.001
INTERPRO	IPR018184:Integrin alpha chain, C-terminal cytoplasmic region, conserved site	13	1.07×10^{-6}	0.002
INTERPRO	IPR013519:Integrin alpha beta-propellor	14	1.99×10^{-6}	0.004
INTERPRO	IPR013517:FG-GAP repeat	13	7.60×10^{-6}	0.014
SMART	SM00191:Int_alpha	14	1.38×10^{-5}	0.020

Annotation Cluster 2 - Enrichment Score: 4.06				
Category	Term	Count	PValue	FDR
UP_KEYWORDS	EGF-like domain	38	1.97E-05	0.026
INTERPRO	IPR001881:EGF-like calcium-binding	37	4.17E-05	0.075
INTERPRO	IPR000152:EGF-type aspartate/asparagine hydroxylation site	31	5.53E-05	0.099
SMART	SM00179:EGF_CA	37	0.002	1.731

Annotation Cluster 3- Enrichment Score: 3.66				
Category	Term	Count	PValue	FDR
INTERPRO	IPR008266:Tyrosine-protein kinase, active site	32	3.44E-05	0.062
INTERPRO	IPR020635:Tyrosine-protein kinase, catalytic domain	29	4.83E-05	0.087
INTERPRO	IPR001245:Serine-threonine/tyrosine-protein kinase catalytic domain	39	4.63E-04	0.830
UP_KEYWORDS	Tyrosine-protein kinase	25	7.85E-04	1.042
SMART	SM00219:TyrKc	29	8.74E-04	1.256

Annotation Cluster 4 - Enrichment Score: 3.49				
Category	Term	Count	PValue	FDR
INTERPRO	IPR003599:Immunoglobulin subtype	76	2.64E-05	0.047
INTERPRO	IPR007110:Immunoglobulin-like domain	95	3.03E-04	0.543
SMART	SM00409:IG	76	0.004119	5.790

Annotation Cluster 5 - Enrichment Score: 3.26				
Category	Term	Count	PValue	FDR
INTERPRO	IPR008936:Rho GTPase activation protein	29	8.39E-05	0.151
INTERPRO	IPR000198:Rho GTPase-activating protein domain	22	6.25E-04	1.118
SMART	SM00324:RhoGAP	22	0.003	4.630

Annotation Cluster 6 - Enrichment Score: 2.64				
Category	Term	Count	PValue	FDR
INTERPRO	IPR000387:Protein-tyrosine/Dual specificity phosphatase	26	4.42E-04	0.793
INTERPRO	IPR003595:Protein-tyrosine phosphatase, catalytic	21	0.00	2.326
INTERPRO	IPR016130:Protein-tyrosine phosphatase, active site	21	0.005	8.797
SMART	SM00404:PTPc_motif	21	0.009	12.949

Annotation Cluster 7 - Enrichment Score: 2.48				
Category	Term	Count	PValue	FDR
INTERPRO	IPR002172:Low-density lipoprotein (LDL) receptor class A repeat	17	0.001	2.374
INTERPRO	IPR023415:Low-density lipoprotein (LDL) receptor class A, conserved site	14	0.002	4.291
SMART	SM00192:LDLa	16	0.011	15.034

Annotation Cluster 8 - Enrichment Score: 2.34				
Category	Term	Count	PValue	FDR
UP_KEYWORDS	ANK repeat	48	0.002	2.343
INTERPRO	IPR002110:Ankyrin repeat	49	0.005	8.346
INTERPRO	IPR020683:Ankyrin repeat-containing domain	49	0.011	18.191

Annotation Cluster 9 - Enrichment Score: 2.25				
Category	Term	Count	PValue	FDR
INTERPRO	IPR002073:3'5'-cyclic nucleotide phosphodiesterase, catalytic domain	11	0.002	3.307
INTERPRO	IPR023088:3'5'-cyclic nucleotide phosphodiesterase	10	0.003	5.775
INTERPRO	IPR023174:3'5'-cyclic nucleotide phosphodiesterase, conserved site	10	0.005	8.702
INTERPRO	IPR003607:HD/PDEase domain	9	0.033	45.393

Annotation Cluster 10 - Enrichment Score: 1.96				
Category	Term	Count	PValue	FDR
INTERPRO	IPR025660:Cysteine peptidase, histidine active site	7	0.004	6.572
INTERPRO	IPR000668:Peptidase C1A, papain C-terminal	7	0.012	19.418
INTERPRO	IPR013128:Peptidase C1A, papain	7	0.012	19.418
SMART	SM00645:Pept_C1	7	0.027	32.254

Annotation Cluster 11 - Enrichment Score: 1.94				
Category	Term	Count	PValue	FDR
INTERPRO	IPR020728:Apoptosis regulator, Bcl-2, BH3 motif, conserved site	5	0.005	7.938
INTERPRO	IPR020717:Apoptosis regulator, Bcl-2, BH1 motif, conserved site	5	0.012	19.203
INTERPRO	IPR026298:Blc2 family	6	0.013	20.667
GOTERM_MF	GO:0046982~protein heterodimerization activity	8	0.013	19.247
INTERPRO	IPR002475:Bcl2-like	6	0.022	32.737

Annotation Cluster 12 - Enrichment Score: 1.61				
Category	Term	Count	PValue	FDR
GOTERM_BP	GO:0048846~axon extension involved in axon guidance	5	0.016	26.309
GOTERM_BP	GO:0097490~sympathetic neuron projection extension	4	0.026	39.350
GOTERM_BP	GO:0097491~sympathetic neuron projection guidance	4	0.026	39.350
GOTERM_BP	GO:0036486~ventral trunk neural crest cell migration	4	0.026	39.350
GOTERM_BP	GO:0061549~sympathetic ganglion development	5	0.031	45.511

Annotation Cluster 13 - Enrichment Score: 1.50				
Category	Term	Count	PValue	FDR
INTERPRO	IPR016161:Aldehyde/histidinol dehydrogenase	8	0.031	43.672
INTERPRO	IPR015590:Aldehyde dehydrogenase domain	8	0.031	43.672
INTERPRO	IPR016162:Aldehyde dehydrogenase, N-terminal	8	0.031	43.672
INTERPRO	IPR016163:Aldehyde dehydrogenase, C-terminal	8	0.031	43.672

Annotation Cluster 14 - Enrichment Score: 1.49				
Category	Term	Count	PValue	FDR
INTERPRO	IPR000426:Proteasome, alpha-subunit, N-terminal domain	5	0.024	34.894
GOTERM_CC	GO:0019773~proteasome core complex, alpha-subunit complex	5	0.027	34.494
INTERPRO	IPR023332:Proteasome A-type subunit	5	0.040	52.444
SMART	SM00948:SM00948	5	0.042	46.103

Annotation Cluster 15 - Enrichment Score: 1.48				
Category	Term	Count	PValue	FDR
GOTERM_MF	GO:0004740~pyruvate dehydrogenase (acetyl-transferring) kinase activity	4	0.023	31.537
GOTERM_BP	GO:0010510~regulation of acetyl-CoA biosynthetic process from pyruvate	4	0.026	39.350
INTERPRO	IPR005467:Signal transduction histidine kinase, core	4	0.044	55.796
INTERPRO	IPR018955:Branched-chain alpha-ketoacid dehydrogenase kinase/Pyruvate dehydrogenase kinase, N-terminal	4	0.044	55.796

Annotation Cluster 16 - Enrichment Score: 1.47				
Category	Term	Count	PValue	FDR
INTERPRO	IPR012896:Integrin beta subunit, tail	5	0.024	34.894
INTERPRO	IPR002369:Integrin beta subunit, N-terminal	5	0.040	52.444
SMART	SM01242:SM01242	5	0.042	46.103

Annotation Cluster 17 - Enrichment Score: 1.46				
Category	Term	Count	PValue	FDR
INTERPRO	IPR020422: Dual specificity phosphatase, subgroup, catalytic domain	11	0.026	38.217
INTERPRO	IPR024950: Dual specificity phosphatase	10	0.034	45.921
INTERPRO	IPR000340: Dual specificity phosphatase, catalytic domain	12	0.049	59.184

Annotation Cluster 18 - Enrichment Score: 1.43				
Category	Term	Count	PValue	FDR
GOTERM_MF	GO:0008865~fructokinase activity	4	0.023	31.537
GOTERM_MF	GO:0019158~mannokinase activity	4	0.023	31.537
INTERPRO	IPR019807: Hexokinase, conserved site	4	0.044	55.796
INTERPRO	IPR022672: Hexokinase, N-terminal	4	0.044	55.796
INTERPRO	IPR001312: Hexokinase	4	0.044	55.796
INTERPRO	IPR022673: Hexokinase, C-terminal	4	0.044	55.796

Annotation Cluster 19 - Enrichment Score: 1.39				
Category	Term	Count	PValue	FDR
INTERPRO	IPR026791: Deducator of cytokinesis	5	0.040	52.444
INTERPRO	IPR027007: DHR-1 domain	5	0.040	52.444
INTERPRO	IPR027357: DHR-2 domain	5	0.040	52.444
INTERPRO	IPR010703: Deducator of cytokinesis C-terminal	5	0.040	52.444

Appendix 4.5

**List of all significantly enriched KEGG pathways and GO terms in Chapter 4
when comparing the 0 hours (control) relative to 24 hours associated with
Log₂FC ≥2 at an FDR of 0.05 sorted by p-value – DESeq2 results**

Enrichment term	Term name	Description	Gene count	FDR p-value
KEGG pathway	4610	Complement and coagulation cascades	24	6.92 x 10 ⁻¹⁵
Cell component	GO.0005576	extracellular region	24	5.94 x 10 ⁻¹¹
KEGG pathway	4640	Hematopoietic cell lineage	19	7.03 x 10 ⁻¹¹
Cell component	GO.0044421	extracellular region part	20	1.33E x 10 ⁻¹¹
KEGG pathway	4060	Cytokine-cytokine receptor interaction	29	1.69 x 10 ⁻⁹
Cell component	GO.0005575	cellular_component	33	2.65 x 10 ⁻⁹
KEGG pathway	4151	PI3K-Akt signaling pathway	49	1.92 x 10 ⁻⁸
Biological Process	GO.0008150	biological_process	33	2.10 x 10 ⁻⁸
KEGG pathway	4512	ECM-receptor interaction	22	6.55 x 10 ⁻⁸
Biological Process	GO.0044699	single-organism process	29	6.84 x 10 ⁻⁸
Biological Process	GO.0006950	response to stress	18	6.84 x 10 ⁻⁸
Biological Process	GO.0006952	defense response	15	6.84 x 10 ⁻⁸
Cell component	GO.0005615	extracellular space	14	3.32 x 10 ⁻⁷
KEGG pathway	10	Glycolysis / Gluconeogenesis	17	3.62 x 10 ⁻⁷
KEGG pathway	4066	HIF-1 signaling pathway	23	9.44 x 10 ⁻⁷
Biological Process	GO.0050896	response to stimulus	19	2.04 x 10 ⁻⁷
Biological Process	GO.0006954	inflammatory response	11	2.04 x 10 ⁻⁷
KEGG pathway	5020	Prion diseases	12	6.34 x 10 ⁻⁷
KEGG pathway	4668	TNF signaling pathway	24	6.72 x 10 ⁻⁶
Molecular Function	GO.0003674	molecular_function	27	9.18 x 10 ⁻⁶
Molecular Function	GO.0043167	ion binding	18	9.18 x 10 ⁻⁶
Molecular Function	GO.0005488	binding	21	1.01 x 10 ⁻⁵
KEGG pathway	4510	Focal adhesion	33	1.06 x 10 ⁻⁵
KEGG pathway	5200	Pathways in cancer	42	2.71 x 10 ⁻⁵
Molecular Function	GO.0070011	peptidase activity, acting on L-amino acid peptides	6	2.96 x 10 ⁻⁵
KEGG pathway	5206	MicroRNAs in cancer	25	3.38 x 10 ⁻⁵
Biological Process	GO.0009987	cellular process	24	4.86 x 10 ⁻⁵
KEGG pathway	5144	Malaria	11	6.12 x 10 ⁻⁵
Biological Process	GO.0044763	single-organism cellular process	21	0.000
Biological Process	GO.0050789	regulation of biological process	18	0.000
Biological Process	GO.0044707	single-multicellular organism process	14	0.000
Biological Process	GO.0065008	regulation of biological quality	13	0.000
Molecular Function	GO.0046872	metal ion binding	12	0.000
KEGG pathway	5222	Small cell lung cancer	18	0.000
KEGG pathway	4630	Jak-STAT signaling pathway	20	0.000
KEGG pathway	5202	Transcriptional misregulation in cancer	24	0.000

Biological Process	GO.0002376	immune system process	11	0.000
Biological Process	GO.0044238	primary metabolic process	18	0.000
Biological Process	GO.0065007	biological regulation	18	0.000
Biological Process	GO.0006953	acute-phase response	6	0.000
KEGG pathway	1120	Microbial metabolism in diverse environments	24	0.000
Biological Process	GO.0006629	lipid metabolic process	7	0.000
KEGG pathway	1230	Biosynthesis of amino acids	15	0.000
KEGG pathway	5323	Rheumatoid arthritis	15	0.000
Biological Process	GO.0044710	single-organism metabolic process	15	0.000
Biological Process	GO.0071704	organic substance metabolic process	18	0.000
KEGG pathway	5150	Staphylococcus aureus infection	9	0.000
Biological Process	GO.0006508	proteolysis	6	0.001
KEGG pathway	5146	Amoebiasis	17	0.001
KEGG pathway	5219	Bladder cancer	10	0.002
KEGG pathway	5322	Systemic lupus erythematosus	10	0.002
Biological Process	GO.0008152	metabolic process	19	0.002
Biological Process	GO.0051239	regulation of multicellular organismal process	10	0.002
Biological Process	GO.0006955	immune response	8	0.002
KEGG pathway	5133	Pertussis	13	0.002
Molecular Function	GO.0004175	endopeptidase activity	4	0.003
KEGG pathway	5414	Dilated cardiomyopathy	12	0.003
Cell component	GO.0005623	cell	20	0.003
Molecular Function	GO.0003824	catalytic activity	14	0.003
Molecular Function	GO.0005509	calcium ion binding	5	0.003
Cell component	GO.0005622	intracellular	18	0.003
Biological Process	GO.0050794	regulation of cellular process	14	0.003
KEGG pathway	140	Steroid hormone biosynthesis	6	0.004
Molecular Function	GO.0046914	transition metal ion binding	7	0.004
Cell component	GO.0044464	cell part	19	0.004
KEGG pathway	4015	Rap1 signaling pathway	25	0.004
KEGG pathway	5134	Legionellosis	11	0.004
KEGG pathway	5410	Hypertrophic cardiomyopathy (HCM)	11	0.004
KEGG pathway	5205	Proteoglycans in cancer	26	0.005
Biological Process	GO.0051716	cellular response to stimulus	11	0.005
KEGG pathway	51	Fructose and mannose metabolism	8	0.005
KEGG pathway	4064	NF-kappa B signaling pathway	14	0.005
KEGG pathway	4976	Bile secretion	10	0.005
Biological Process	GO.0048518	positive regulation of biological process	11	0.007
Cell component	GO.0044424	intracellular part	17	0.007
Biological Process	GO.0048522	positive regulation of cellular process	10	0.008
Biological Process	GO.0032787	monocarboxylic acid metabolic process	5	0.008
Cell component	GO.0005737	cytoplasm	16	0.008
Molecular Function	GO.1901681	sulfur compound binding	4	0.009

Biological Process	GO.0042221	response to chemical	10	0.009
Biological Process	GO.0044767	single-organism developmental process	10	0.009
KEGG pathway	5142	Chagas disease (American trypanosomiasis)	15	0.010
KEGG pathway	5143	African trypanosomiasis	6	0.010
KEGG pathway	1200	Carbon metabolism	16	0.010
Biological Process	GO.0042592	homeostatic process	8	0.010
Molecular Function	GO.0008270	zinc ion binding	5	0.013
Biological Process	GO.0048856	anatomical structure development	9	0.014
KEGG pathway	4080	Neuroactive ligand-receptor interaction	11	0.017
Biological Process	GO.0043436	oxoacid metabolic process	6	0.017
Molecular Function	GO.0004222	metalloendopeptidase activity	3	0.018
KEGG pathway	4014	Ras signaling pathway	23	0.019
KEGG pathway	4913	Ovarian steroidogenesis	7	0.019
Biological Process	GO.0009056	catabolic process	7	0.021
KEGG pathway	4380	Osteoclast differentiation	15	0.021
Cell component	GO.0012505	endomembrane system	7	0.022
Biological Process	GO.0048731	system development	8	0.031
Biological Process	GO.0070887	cellular response to chemical stimulus	8	0.031
Biological Process	GO.0001516	prostaglandin biosynthetic process	3	0.031
Biological Process	GO.0030574	collagen catabolic process	3	0.031
Biological Process	GO.0051781	positive regulation of cell division	4	0.032
KEGG pathway	4115	p53 signaling pathway	11	0.033
Biological Process	GO.0048583	regulation of response to stimulus	8	0.033
Cell component	GO.0044425	membrane part	11	0.034
Biological Process	GO.0051336	regulation of hydrolase activity	5	0.034
Biological Process	GO.0098542	defense response to other organism	5	0.034
Biological Process	GO.0009605	response to external stimulus	7	0.037
Biological Process	GO.0048513	organ development	7	0.037
Molecular Function	GO.0005539	glycosaminoglycan binding	4	0.039
KEGG pathway	5145	Toxoplasmosis	15	0.040
Biological Process	GO.0007275	multicellular organismal development	8	0.041
KEGG pathway	5412	Arrhythmogenic right ventricular cardiomyopathy (ARVC)	9	0.042
KEGG pathway	524	Butirosin and neomycin biosynthesis	2	0.044
KEGG pathway	4672	Intestinal immune network for IgA production	6	0.047
Cell component	GO.0043226	organelle	13	0.050
Cell component	GO.0016020	membrane	12	0.050
Cell component	GO.0071944	cell periphery	8	0.05

Appendix 5.1

Kenney Classification of Mares Providing Endometrial Explants in Chapter 5

Mares	Histology report ^b	Kenney classification
1	Medium epithelium. Stratum compactum examined, no pathologic findings noted. Stratum spongiosum showed diffuse grade 1 fibrosis.	I
2	Medium epithelium. Stratum compactum showed lymphocyte focal infiltration grade 1. Stratum spongiosum examined, no pathologic findings noted.	I
3	Tall epithelium. Stratum compactum showed diffuse gland atrophy grade 1. Stratum spongiosum showed diffuse gland atrophy grade 2, multifocal cystic glands grade 3 with inspissated contents, fibrosis periglandular grade 3 and lymphocyte infiltration grade 1.	II
4	Medium epithelium. Stratum compactum showed lymphocyte infiltration grade 1, macrophage and erythrophagocytes infiltration grade 2. Stratum spongiosum showed lymphocyte infiltration grade 1, macrophage and erythrophagocytes infiltration grade 2 and siderocyte infiltration grade 1.	I
5	Tall epithelium. Stratum compactum showed focal lymphocyte infiltration grade 1. Stratum spongiosum examined, no pathologic findings noted.	I
6	Tall epithelium. Stratum compactum showed focal lymphocyte infiltration grade 1. Stratum spongiosum showed focal cystic glands grade 1 and local lymphocyte infiltration grade 1.	I
7	Medium epithelium. Stratum compactum examined, no pathological findings noted. Stratum spongiosum showed multifocal cystic glands with inspissated contents grade 1.	I
8	Low epithelium. Stratum compactum showed siderocyte infiltration grade 1. Stratum spongiosum examined, no pathologic findings noted.	I
9	Low epithelium. Stratum compactum examined, no pathologic findings noted. Stratum spongiosum showed focal cystic glands grade 1	I

	with inspissated contents and epithelial hyperplasia and cystic glands grade 1.	
10	Low epithelium. Stratum compactum examined, no pathologic findings noted. Stratum spongiosum showed focal cystic glands grade 1 with inspissated contents and epithelial hyperplasia.	I
11	No tissue available for examination.	-
12	Low epithelium. Stratum compactum showed lymphocyte infiltration grade 1. Stratum spongiosum showed focal cystic glands grade 1.	I
13	Low epithelium. Stratum compactum examined, no pathologic findings noted. Stratum spongiosum showed multifocal cystic glands grade 2 with inspissated contents, epithelial hyperplasia and focal cystic glands grade 1.	I
14	Low epithelium. Stratum compactum examined, no pathologic findings noted. Stratum spongiosum showed multifocal cystic glands grade 1 with inspissated contents and lymphocyte infiltration grade 1.	I
15	No tissue available for examination.	-
16	Low epithelium. Stratum compactum examined, no pathologic findings noted. Stratum spongiosum showed multifocal cystic glands grade 2 with inspissated contents and periglandular fibrosis grade 2.	II
17	Low epithelium. No pathologic findings.	I
18	Low epithelium. Stratum compactum showed siderocyte infiltration grade 1. Stratum spongiosum showed multifocal cystic glands grade 2 with inspissated contents and infiltration of siderocytes grade 2.	I

^a Grade 1 = minimal/very few/very small. Grade 2 = slight/few/small. Grade 3 = moderate/moderate number/moderate size. Grade 4 = marked/many/large.

Appendix 5.2

Computer Code used in Chapter 5

DESeq2 analysis

```
# load package to summarize bam files
> library(GenomicAlignments)

# put bam files together in a list
bamfilelist <- c("sample1.bam", "sample2.bam", "sample3.bam", ...
sample50.bam")

# BamFileList from Rsamtools provides an R interface to BAM files
> library(Rsamtools)
> bamfiles <- BamFileList(bamfilelist)

# use annotation file with the function makeTxDbFromGFF from
GenomicFeatures
# list of exons grouped by gene for counting read/fragments
> library(GenomicFeatures)
> txdb <- makeTxDbFromGFF("annotationfile.gtf", format="gtf")

# produce a GRangesList of all the exons grouped by gene
> ebg <- exonsBy(txdb, by="gene")

# summarizeOverlaps from GenomicAlignment counts the fragments/reads
and produces a SummarizedExperiment object 'se'
> se <- summarizeOverlaps(features=ebg, reads=bamfiles,
                        mode="Union",
                        singleEnd=FALSE,
                        ignore.strand=TRUE,
                        fragments=TRUE )

# metadata file created in excel (info about the experiment)
> sampleTable <- read.csv("exp2_metadata.csv")

# assign the sampleTable as the colData of the summarized experiment by
converting it into a DataFrame
> colData(se) <- DataFrame(sampleTable)
> colData(se)
DataFrame with 50 rows and 5 columns
sample,phase,horse,timepoint,horse.n
1 sample_1.bam,follicular,1,0h,1
2 sample_2.bam,follicular,1,24h,1
3 sample_3.bam,follicular,1,48h,1
4 sample_4.bam,follicular,2,0h,2
5 sample_6.bam,follicular,2,48h,2
6 sample_10.bam,follicular,3,0h,3
7 sample_11.bam,follicular,3,24h,3
8 sample_12.bam,follicular,3,48h,3
9 sample_13.bam,follicular,4,0h,4
10 sample_14.bam,follicular,4,24h,4
11 sample_15.bam,follicular,4,48h,4
12 sample_16.bam,follicular,5,0h,5
13 sample_17.bam,follicular,5,24h,5
14 sample_18.bam,follicular,5,48h,5
15 sample_55.bam,follicular,6,0h,6
16 sample_56.bam,follicular,6,24h,6
17 sample_58.bam,follicular,6,48h,6
18 sample_22.bam,luteal,8,0h,1
19 sample_23.bam,luteal,8,24h,1
20 sample_24.bam,luteal,8,48h,1
21 sample_25.bam,luteal,9,0h,2
22 sample_26.bam,luteal,9,24h,2
```

```

23 sample_27.bam,luteal,9,48h,2
24 sample_28.bam,luteal,10,0h,3
25 sample_29.bam,luteal,10,24h,3
26 sample_30.bam,luteal,10,48h,3
27 sample_31.bam,luteal,11,0h,4
28 sample_32.bam,luteal,11,24h,4
29 sample_33.bam,luteal,11,48h,4
30 sample_34.bam,luteal,12,0h,5
31 sample_35.bam,luteal,12,24h,5
32 sample_36.bam,luteal,121D,48h,5
33 sample_37.bam,anoestrous,13,0h,1
34 sample_38.bam,anoestrous,13,24h,1
35 sample_39.bam,anoestrous,13,48h,1
36 sample_40.bam,anoestrous,14,0h,2
37 sample_41.bam,anoestrous,14,24h,2
38 sample_42.bam,anoestrous,14,48h,2
39 sample_43.bam,anoestrous,15,0h,3
40 sample_44.bam,anoestrous,15,24h,3
41 sample_45.bam,anoestrous,15,48h,3
42 sample_46.bam,anoestrous,16,0h,4
43 sample_47.bam,anoestrous,16,24h,4
44 sample_48.bam,anoestrous,16,48h,4
45 sample_49.bam,anoestrous,17,0h,5
46 sample_50.bam,anoestrous,17,24h,5
47 sample_51.bam,anoestrous,17,48h,5
48 sample_52.bam,anoestrous,18,0h,6
49 sample_53.bam,anoestrous,18,24h,6
50 sample_54.bam,anoestrous,18,48h,6

# DESeq2 - differential analysis
# SummarizedExperiment 'se' created before will be used for DESeq2
> library(DESeq2)
> dds_matrix <- DESeqDataSet(se, design = ~ phase + timepoint +
phase:timepoint)
> dds_matrix <- DESeq(dds_matrix)
> resultsNames(dds_matrix)

# reassign DESeqDataSet a design of ~ grp + grp:ind.n + grp:cnd
# this new design will result in the following model matrix
# exp2_matrix2 <- model.matrix(~ phase + phase:horse.n +
phase:timepoint, colData)
> exp2_matrix2 <- model.matrix(~ phase + phase:horse.n +
phase:timepoint, colData)
> dds_matrix2 <- DESeq(dds_matrix, full=exp2_matrix2, betaPrior=F)

#'contrast' argument to extract comparisons of different levels
# contrast = c('factorName','numeratorLevel','denominatorLevel')
> res_follicular_luteal_24h_matrix2 <- results(dds_matrix2,
contrast=list("phasefollicular.timepoint24h","phaseluteal.timepoint24h"
))

> res_follicular_luteal_48h_matrix2 <- results(dds_matrix2,
contrast=list("phasefollicular.timepoint48h","phaseluteal.timepoint48h"
))

> res_follicular_anoestrous_24h_matrix2 <- results(dds_matrix2,
contrast=list("phasefollicular.timepoint24h","phaseanoestrous.timepoint
24h"))
> res_follicular_anoestrous_48h_matrix2 <- results(dds_matrix2,
contrast=list("phasefollicular.timepoint48h","phaseanoestrous.timepoint
48h"))

> res_luteal_anoestrous_24h_matrix2 <- results(dds_matrix2,
contrast=list("phaseluteal.timepoint24h","phaseanoestrous.timepoint24h"
))
> res_luteal_anoestrous_48h_matrix2 <- results(dds_matrix2,
contrast=list("phaseluteal.timepoint48h","phaseanoestrous.timepoint48h"
))

```

```

#writing files for results
> write.csv(res_follicular_luteal_24h_matrix2,
"res_follicular_luteal_24h_matrix2.csv")
> write.csv(res_follicular_luteal_48h_matrix2,
"res_follicular_luteal_48h_matrix2.csv")

> write.csv(res_follicular_anoestrous_24h_matrix2,
"res_follicular_anoestrous_24h_matrix2.csv")
> write.csv(res_follicular_anoestrous_48h_matrix2,
"res_follicular_anoestrous_48h_matrix2.csv")

> write.csv(res_luteal_anoestrous_24h_matrix2,
"res_luteal_anoestrous_24h_matrix2.csv")
> write.csv(res_luteal_anoestrous_48h_matrix2,
"res_luteal_anoestrous_48h_matrix2.csv")

# dispersion-mean plots
> plotDispEsts(dds_matrix2, main="Estimation of dispersion for
dds_matrix2", sub="For DESeq2 object")

# calc of size factors
> sizeFactors(dds_matrix2)

# normalize data to produce PCA plot
> rld_matrix2 <- rlog(dds_matrix2, blind=FALSE)

> pcaData_rld_matrix2 <- plotPCA(rld_matrix2, intgroup = c("timepoint",
"horse", "phase"), returnData = TRUE)
percentVar <- round(100 * attr(pcaData_rld_matrix2, "percentVar"))

> library("ggplot2")
> ggplot(pcaData_rld_matrix2, aes(x = PC1, y = PC2, color = phase,
shape = timepoint)) + geom_point(size = 3) + xlab(paste0("PC1: ",
percentVar[1], "% variance")) + ylab(paste0("PC2: ", percentVar[2],
"%variance")) + coord_fixed() + scale_shape_manual(values=seq(0, 20))

```

Appendix 5.3

List of all significantly enriched GO terms in Chapter 5 when comparing the follicular and luteal phase groups at 24 hours associated with $\text{Log}_2\text{FC} \geq 2$ at an FDR of 0.05 sorted by p-value

GO Category	Term name	Description	Count	FDR p-value
Cellular component	GO.0005575	Cellular component	13	4.10×10^{-6}
Biological process	GO.0044707	Single-multicellular organism process	8	8.04×10^{-5}
Cellular component	GO.0005576	Extracellular region	8	1.49×10^{-4}
Molecular function	GO.0003674	Molecular function	11	2.37×10^{-4}
Molecular function	GO.0005488	Binding	9	2.37×10^{-4}
Molecular function	GO.0046914	Transition metal ion binding	5	2.37×10^{-4}
Biological process	GO.0044699	Single-organism process	10	7.80×10^{-4}
Biological process	GO.0050794	Regulation of cellular process	8	7.80×10^{-4}
Molecular function	GO.0046872	Metal ion binding	6	8.51×10^{-4}
Biological process	GO.0008150	Biological process	10	0.002
Biological process	GO.0044767	single-organism developmental process	6	0.002
Biological process	GO.0065008	regulation of biological quality	6	0.002
Biological process	GO.0050896	response to stimulus	7	0.002
Biological process	GO.0048518	positive regulation of biological process	6	0.002
Biological process	GO.0051716	cellular response to stimulus	6	0.002
Cellular component	GO.0044421	extracellular region part	6	0.003
Biological process	GO.0002376	immune system process	5	0.005
Biological process	GO.0048731	system development	5	0.005
Biological process	GO.0006357	regulation of transcription from RNA polymerase II promoter	4	0.006
Biological process	GO.0007275	multicellular organismal development	5	0.007
Molecular function	GO.0038023	signaling receptor activity	3	0.008
Biological process	GO.0009987	cellular process	8	0.008
Biological process	GO.0048522	positive regulation of cellular process	5	0.008
Biological process	GO.0065007	biological regulation	7	0.008
Biological process	GO.0042221	response to chemical	5	0.009
Biological process	GO.0006954	inflammatory response	4	0.009
Molecular function	GO.0008270	zinc ion binding	3	0.011
Biological process	GO.0003008	system process	3	0.013
Biological process	GO.0044763	single-organism cellular process	7	0.016
Biological process	GO.0001660	fever generation	2	0.018
Biological process	GO.0006950	response to stress	5	0.018
Biological process	GO.0008217	regulation of blood pressure	2	0.018
Biological process	GO.0033554	cellular response to stress	3	0.018
Biological process	GO.0048513	organ development	4	0.018
Molecular function	GO.0004222	metalloendopeptidase activity	2	0.020
Molecular function	GO.0016209	antioxidant activity	2	0.020
Molecular function	GO.0005515	protein binding	3	0.029
Biological process	GO.0045893	positive regulation of transcription, DNA-templated	3	0.030
Biological process	GO.0051094	positive regulation of developmental process	3	0.030
Biological process	GO.0048583	regulation of response to stimulus	4	0.031
Biological process	GO.0002244	hematopoietic progenitor cell differentiation	2	0.034
Biological process	GO.0030574	collagen catabolic process	2	0.034
Biological process	GO.0045639	positive regulation of myeloid cell differentiation	2	0.034
Cellular component	GO.0005623	cell	7	0.037
Cellular component	GO.0005615	extracellular space	4	0.037
Biological process	GO.0008152	metabolic process	6	0.049
Cellular component	GO.0005886	plasma membrane	4	0.050
Cellular component	GO.0071944	cell periphery	4	0.050

Appendix 5.4

List of all significantly enriched GO terms in Chapter 5 when comparing the follicular and anoestrous phase groups at 24 hours associated with $\text{Log}_2\text{FC} \geq 2$ at an FDR of 0.05 sorted by p-value

GO Category	Term name	Description	Count	FDR p-value
Biological process	GO.0044699	Single-organism process	9	5.71×10^{-5}
Biological process	GO.0008150	Biological process	9	1.12×10^{-4}
Molecular function	GO.0003674	Molecular function	8	2.29×10^{-4}
Molecular function	GO.0005488	Binding	7	2.29×10^{-4}
Cellular component	GO.0005575	Cellular component	8	4.8×10^{-4}
Biological process	GO.0042221	Response to chemical	5	9.52×10^{-4}
Biological process	GO.0048871	Multicellular organismal homeostasis	3	9.52×10^{-4}
Biological process	GO.0050794	Regulation of cellular process	6	9.52×10^{-4}
Biological process	GO.0050896	Response to stimulus	6	9.52×10^{-4}
Cellular component	GO.0044421	Extracellular region part	5	0.001
Biological process	GO.0009987	Cellular process	7	0.002
Biological process	GO.0051716	Cellular response to stimulus	5	0.002
Biological process	GO.0006950	Response to stress	5	0.002
Biological process	GO.0006953	Acute-phase response	3	0.003
Cellular component	GO.0005576	Extracellular region	5	0.003
Cellular component	GO.0005615	Extracellular space	4	0.003
Cellular component	GO.0005623	Cell	6	0.003
Biological process	GO.0044763	Single-organism cellular process	6	0.004
Biological process	GO.0006952	Defense response	4	0.005
Molecular function	GO.0043167	Ion binding	5	0.006
Biological process	GO.0001660	Fever generation	2	0.008
Biological process	GO.0065008	Regulation of biological quality	4	0.011
Molecular function	GO.0046914	Transition metal ion binding	3	0.016
Biological process	GO.0044707	Single-multicellular organism process	4	0.019
Biological process	GO.0006955	Immune response	3	0.024
Cellular component	GO.0044464	Cell part	5	0.024
Biological process	GO.0008152	Metabolic process	5	0.029
Biological process	GO.0044700	Single organism signaling	3	0.036
Biological process	GO.0044710	Single-organism metabolic process	4	0.037
Biological process	GO.0007154	Cell communication	3	0.043

Appendix 5.5

List of all significantly enriched GO terms in Chapter 5 when comparing the luteal and anoestrous phase groups at 48 hours associated with Log₂FC ≥2 at an FDR of 0.05 sorted by p-value

GO Category	Term name	Description	Count	FDR p-value
Biological process	GO.0051716	Cellular response to stimulus	9	0.005
Cellular component	GO.0005615	Extracellular space	7	0.005
Cellular component	GO.0012505	Endomembrane system	6	0.005
Cellular component	GO.0005576	Extracellular region	9	0.006
Cellular component	GO.0044421	Extracellular region part	8	0.006
Biological process	GO.0006508	Proteolysis	4	0.022
Biological process	GO.0009887	Organ morphogenesis	4	0.022
Biological process	GO.0009987	Cellular process	12	0.022
Biological process	GO.0032501	Multicellular organismal process	8	0.022
Biological process	GO.0044767	Single-organism developmental process	7	0.022
Biological process	GO.0048705	Skeletal system morphogenesis	3	0.022
Biological process	GO.0048856	Anatomical structure development	7	0.022
Biological process	GO.0060349	Bone orphogenesis	3	0.022
Biological process	GO.0065008	Regulation of biological quality	7	0.022
Cellular component	GO.0005623	Cell	11	0.024
Cellular component	GO.0005575	Cellular component	12	0.025
Cellular component	GO.0005886	Plasma membrane	6	0.025
Cellular component	GO.0071944	Cell periphery	6	0.025
Biological process	GO.0002376	Immune system process	6	0.027
Biological process	GO.0022412	Cellular process involved in reproduction in multicellular organism	3	0.027
Biological process	GO.0045637	Regulation of myeloid cell differentiation	3	0.027
Biological process	GO.0048731	System development	6	0.027
Biological process	GO.0060348	Bone development	3	0.027
Biological process	GO.0044707	Single-multicellular organism process	7	0.033
Biological process	GO.0007275	Multicellular organismal development	6	0.036
Cellular component	GO.0044464	Cell part	10	0.037
Biological process	GO.0050896	Response to stimulus	8	0.041
Biological process	GO.0008150	Biological process	12	0.045
Biological process	GO.0044699	Single-organism process	11	0.045
Biological process	GO.0048522	Positive regulation of cellular process	6	0.045
Biological process	GO.0001501	Skeletal system development	3	0.046

Appendix 6.1

Kenney Classification of Mares Providing Endometrial Explants in Chapter 6

Mares	Histology report ^b	Kenney classification
1	Tall epithelium. Stratum compactum showed focal lymphocyte infiltrate grade 1. Stratum spongiosum showed focal cystic glands grade 1 and local lymphocyte infiltration grade 1.	I
2	Medium epithelium. Stratum compactum showed lymphocyte and siderocyte infiltrate grade I. Stratum spongiosum showed focal cystic glands grade 1, epithelial hyperplasia grade 1, periglandular fibrosis grade 1 and siderocyte grade 2.	I
3	Medium epithelium. Stratum compactum examined, no pathologic findings noted. Stratum spongiosum showed focal cystic glands grade 1 with inspissated contents.	I
4	Tall epithelium. Stratum compactum showed lymphocyte infiltration grade 1. Stratum spongiosum examined, no pathologic findings noted.	I
5	Tall epithelium. Stratum compactum showed multifocal cystic glands grade 2 with inspissated contents. Stratum spongiosum showed periglandular fibrosis grade 2.	II

^a Grade 1 = minimal/very few/very small. Grade 2 = slight/few/small. Grade 3 = moderate/moderate number/moderate size. Grade 4 = marked/many/large.

Appendix 6.2

Computer Code used in Chapter 6

```
# load package to summarize bam files

> library(GenomicAlignments)

# put bam files together in a list
bamfilelist <- c("sample1.bam", "sample2.bam", "sample3.bam, ...
sample25.bam")

# BamFileList from Rsamtools provides an R interface to BAM files
> library(Rsamtools)
> bamfiles <- BamFileList(bamfilelist)

# use annotation file with the function makeTxDbFromGFF from
GenomicFeatures
# list of exons grouped by gene for counting read/fragments
> library(GenomicFeatures)
> txdb <- makeTxDbFromGFF("annotationfile.gtf", format="gtf")

# produce a GRangesList of all the exons grouped by gene
> ebg <- exonsBy(txdb, by="gene")

# summarizeOverlaps from GenomicAlignment counts the fragments/reads
and produces a SummarizedExperiment object 'se'
> se <- summarizeOverlaps(features=ebg, reads=bamfiles,
                           mode="Union",
                           singleEnd=FALSE,
                           ignore.strand=TRUE,
                           fragments=TRUE )

# metadata file created in excel (info about the experiment)
> sampleTable <- read.csv("exp3_metadata.csv")

# assign the sampleTable as the colData of the summarized experiment by
converting it into a DataFrame
> colData(se) <- DataFrame(sampleTable)
> colData(se)
DataFrame with 25 rows and 3 columns
  sample_id treatment horse_id
  <factor>   <factor> <factor>
1 sample1.bam,alive_0h,1
2 sample_2.bam,control_24h,1
3 sample_3.bam,LPS_24h,1
4 sample_4.bam,control_48h,1
5 sample_5.bam,LPS_48h,1
6 sample_6.bam,alive_0h,2
7 sample_7.bam,control_24h,2
8 sample_8.bam,LPS_24h,2
9 sample_9.bam,control_48h,2
10 sample_10.bam,LPS_48h,2
11 sample_11.bam,alive_0h,3
12 sample_12.bam,control_24h,3
13 sample_13.bam,LPS_24h,3
14 sample_14.bam,control_48h,3
15 sample_15.bam,LPS_48h,3
16 sample_16.bam,alive_0h,4
17 sample_17.bam,control_24h,4
18 sample_18.bam,LPS_24h,4
19 sample_19.bam,control_48h,4
20 sample_20.bam,LPS_48h,4
```

```

21 sample_21.bam,alive_0h,5
22 sample_22.bam,control_24h,5
23 sample_23.bam,LPS_24h,5
24 sample_24.bam,control_48h,5
25 sample_25.bam,LPS_48h,5

# DESeq2 - differential analysis
# SummarizedExperiment 'se' created before will be used for DESeq2
> dds <- DESeqDataSet(se, design = ~ horse + treatment)
> dds <- DESeq(dds)
> resultsNames(dds)

#'contrast' argument to extract comparisons of different levels
# contrast = c('factorName','numeratorLevel','denominatorLevel')
> res_exp3_control24h_LPS24h <- results(dds_exp3,
contrast=c("treatment", "control_24h", "LPS_24h"))
> res_exp3_LPS24h_LPS48h <- results(dds_exp3, contrast=c("treatment",
"LPS_24h", "LPS_48h"))

#save and export
> write.csv(res_exp3_control24h_LPS24h,
"res_exp3_control24h_LPS24h.csv")
> write.csv(res_exp3_LPS24h_LPS48h, "res_exp3_LPS24h_LPS48h.csv")

# normalize data to produce PCA plot
> rld <- rlog(dds, blind=FALSE)
> pcaData <- plotPCA(rld, intgroup = c("treatment", "horse_id"),
returnData = TRUE)
> percentVar <- round(100 * attr(pcaData, "percentVar"))
> library("ggplot2")
> ggplot(pcaData, aes(x = PC1, y = PC2, color = treatment, shape =
horse_id)) + geom_point(size = 3) + xlab(paste0("PC1: ", percentVar[1],
"% variance")) + ylab(paste0("PC2: ", percentVar[2], "%variance")) +
coord_fixed() + scale_shape_manual(values=seq(0, 8))

```

Appendix 7.1

Kenney classification of mares providing biopsies in Chapter 7

Mares	Histology report ^a	Kenney classification
1	Medium epithelium. Stratum compactum examined, but no pathologic findings noted. Stratum spongiosum showed diffuse fibrosis grade 1.	I
2	Medium epithelium. Stratum compactum showed focal lymphocyte infiltration grade 1. Stratum spongiosum examined, but no pathologic findings noted.	I
3	Tall epithelium. Stratum compactum showed focal infiltration of lymphocytes grade 1. Stratum spongiosum showed focal cystic glands grade 1 and focal lymphocyte infiltrate grade 1.	I
4	Medium epithelium. Stratum compactum showed diffuse gland atrophy grade 2 and focal lymphocyte infiltration grade 1. Stratum spongiosum showed diffuse gland atrophy grade 2, multifocal cystic glands with inspissated contents grade 3, epithelial hyperplasia of cystic glands grade 1, periglandular fibrosis grade 2 and focal haemorrhage grade 2.	III
5	Medium epithelium. Stratum compactum showed diffuse gland atrophy grade 4. Stratum spongiosum showed diffuse gland atrophy grade 4 and lymphocyte infiltration grade 1.	I
6	Tall epithelium. Stratum compactum showed diffuse gland atrophy grade 3, cystic glands grade 2 and focal haemorrhage grade 1. Stratum spongiosum showed diffuse gland atrophy grade 3, multifocal cystic glands grade 3 with inspissated contents and epithelial hyperplasia grade 3.	III

^a Grade 1 = minimal/very few/very small. Grade 2 = slight/few/small. Grade 3 = moderate/moderate number/moderate size. Grade 4 = marked/many/large.

Appendix 7.2

Computer Code used in Chapter 7

```
# load package to summarize bam files
> library(GenomicAlignments)

# put bam files together in a list
bamfilelist <-c("sample1.bam", "sample2.bam", "sample3.bam",
"sample4.bam", "sample5.bam", "sample6.bam", )

#BamFileList from Rsamtools provides an R interface to BAM files
> library(Rsamtools)
> bamfiles <- BamFileList(bamfilelist)

# use annotation file with the function makeTxDbFromGFF from
GenomicFeatures
# list of exons grouped by gene for counting read/fragments
> library(GenomicFeatures)
> txdb <- makeTxDbFromGFF("annotationfile.gtf", format="gtf")

# produce a GRangesList of all the exons grouped by gene
> ebg <- exonsBy(txdb, by="gene")

# summarizeOverlaps from GenomicAlignment counts the fragments/reads
and produces a SummarizedExperiment object 'se'
> se <- summarizeOverlaps(features=ebg, reads=bamfiles,
                           mode="Union",
                           singleEnd=FALSE,
                           ignore.strand=TRUE,
                           fragments=TRUE )

# metadata file created in excel (info about the experiment)
> sampleTable <- read.csv("exp4_metadata.csv")

# assign the sampleTable as the colData of the summarized experiment by
converting it into a DataFrame
> colData(se) <- DataFrame(sampleTable)
> colData(se)
DataFrame with 6 rows and 3 columns
      sample    tissue    mare
  <factor> <factor> <integer>
1 sample_1.bam ex_vivo      1
2 sample_2.bam ex_vivo      2
3 sample_3.bam ex_vivo      3
4 sample_4.bam in_vivo      4
5 sample_5.bam in_vivo      5
6 sample_6.bam in_vivo      6

# DESeq2 - differential analysis
# SummarizedExperiment 'se' created before will be used for DESeq2
> library(DESeq2)
> dds <- DESeqDataSet(se, design = ~ tissue)
> dds <- DESeq(dds)
> resultsNames(dds)

# dispersion-mean plot
> plotDispEsts(dds, main="Estimation of dispersion", sub="For DESeq2
object")
```

```

#'contrast' argument to extract comparisons of different levels
# contrast = c('factorName','numeratorLevel','denominatorLevel')
> res <- results(dds_exp4_1A1B7B, contrast=c("tissue", "ex_vivo",
"in_vivo"))

#save and export
> write.csv(res,"res_exp4.csv")

# normalize data to produce PCA plot
> rld<- rlog(dds, blind=FALSE)
> pcaData <- plotPCA(rld_, intgroup = c("tissue", "mare"), returnData =
TRUE)
percentVar <- round(100 * attr(pcaData, "percentVar"))
> library("ggplot2")
> ggplot(pcaData, aes(x = PC1, y = PC2, colour = tissue, shape = mare))
+ geom_point(size =3) + xlab(paste0("PC1: ", percentVar[1], "%
variance")) + ylab(paste0("PC2: ", percentVar[2], "%variance")) +
coord_fixed()

```


Appendix 7.3

List of all significantly enriched GO terms in Chapter 7 when comparing the transcriptome of resistant mares relative to the transcriptome of susceptible mares at an FDR of 0.05 sorted by p-value

GO Category ^a	Term name ^b	Description ^c	Count ^e	FDR p-value ^f
Cellular component	GO.0005737	Cytoplasm	10	8.86×10^{-6}
Cellular component	GO.0044464	Cell part	11	8.86×10^{-6}
Cellular component	GO.0005623	Cell	11	9.38×10^{-6}
Cellular component	GO.0005622	Intracellular	10	1.08×10^{-5}
Cellular component	GO.0005575	Cellular component	11	3.48×10^{-5}
Cellular component	GO.0016020	Membrane	8	6.80×10^{-5}
Cellular component	GO.0043226	Organelle	8	1.35×10^{-4}
Molecular function	GO.0003674	Molecular function	11	1.37×10^{-4}
Cellular component	GO.0044444	Cytoplasmic part	7	3.27×10^{-4}
Cellular component	GO.0043227	Membrane-bounded organelle	7	4.83×10^{-4}
Cellular component	GO.0043229	Intracellular organelle	7	7.54×10^{-4}
Cellular component	GO.0098796	Membrane protein complex	4	7.54×10^{-4}
Cellular component	GO.0044429	Mitochondrial part	4	0.002
Molecular function	GO.0003824	Catalytic activity	7	0.002
Cellular component	GO.0043231	Intracellular membrane-bounded organelle	6	0.002
Cellular component	GO.0044446	Intracellular organelle part	5	0.002
Cellular component	GO.0031090	Organelle membrane	4	0.003
Cellular component	GO.0005739	Mitochondrion	4	0.003
cellular component	GO.0016021	Integral component of membrane	5	0.003
Cellular component	GO.0070469	Respiratory chain	3	0.004
Molecular function	GO.0008137	NADH dehydrogenase (ubiquinone) activity	3	0.005
Molecular function	GO.0098772	Molecular function regulator	4	0.005
Cellular component	GO.0031966	Mitochondrial membrane	3	0.007
Molecular function	GO.0016491	Oxidoreductase activity	4	0.008
Cellular component	GO.0005740	Mitochondrial envelope	3	0.009
Cellular component	GO.0005886	Plasma membrane	4	0.010
Cellular component	GO.0071944	Cell periphery	4	0.011
Cellular component	GO.0005747	Mitochondrial respiratory chain complex I	2	0.017
Cellular component	GO.0005746	Mitochondrial respiratory chain	2	0.023
Cellular component	GO.0005743	Mitochondrial inner membrane	2	0.032
Molecular function	GO.0030234	Enzyme regulator activity	3	0.037